Secretory markers of dense-core vesicles in Alzheimer's disease

Neus Barranco Muñoz

Memòria presentada per Neus Barranco Muñoz per a optar al grau de

Doctora en Biomedicina per la Universitat de Barcelona

SECRETORY MARKERS OF DENSE-CORE VESICLES IN ALZHEIMER'S DISEASE

Programa de Doctorat en Biomedicina

Febrer 2016 – Gener 2020

Neus Barranco Muñoz
Doctoranda

Dr. Fernando Aguado Tomás
Director de Tesi

“Thresholds don’t exist in terms of our bodies.
Our speed and strength depend on our body, but the real thresholds,
those that make us give up or continue the struggle,
those that enable us to fulfil our dreams,
depend not on our bodies but on our minds and the hunger we feel
to turn dreams into reality.”

— Kilian Jornet —

“The finish line is just the beginning of a whole new race.”

— Unknown —

AGRAÏMENTS

A escassos dies d'iniciar el final d'aquesta bonica etapa, miro enrere i me n'adono de la sort que he tingut, durant tots aquests anys, d'haver estat envoltada de persones meravelloses que, d'una manera o d'una altra, han resultat ser imprescindibles per al desenvolupament d'aquesta tesi i sense les quals aquest projecte no hauria vist mai la llum. A totes vosaltres, moltes gràcies de tot cor.

En primer lugar, muchas gracias Fernando por confiar en mí y concederme la oportunidad de formar parte de este equipo, que se ha convertido en mi pequeña segunda familia. Hace ya más de seis años que decidiste apostar por un par de estudiantes del Grado de Biomedicina, Paula y Neus, para realizar el TFG. Normalmente solías decidir un único estudiante de Grado, nos comentaste, pero ese año nos elegiste a las dos y este pequeño gesto marcó para mí una gran diferencia. A pesar de mis dudas, y tras finalizar también el TFM, volviste a depositar tu confianza en mí de nuevo, esta vez para llevar a cabo algo mucho más importante: la tesis doctoral. Pese a las dificultades y los obstáculos que he ido encontrando a lo largo de esta "carrera de fondo", tus consejos siempre me han ayudado a ver las cosas de otro modo y a hacerlo todo mucho más llevadero: cada día ha sido realmente un aprendizaje para mí. Entre otras muchísimas cosas, he aprendido a trabajar con rigor, a no conformarme, a buscar alternativas, a razonar, a discutir, a valorar el esfuerzo, a reconocer el trabajo bien hecho y, sobre todo, a disfrutar de cada pequeño pasito o de cada gran zancada a lo largo de este recorrido. Gracias además por los muchos y muy agradables y divertidos momentos dentro y fuera del laboratorio. Guardo recuerdos especialmente buenos de los viajes de congreso a Copenhague, Alicante, Berlín y, más recientemente, Santiago: aviones con sobrepeso de 1000kg, jazz en Cristiania, zamburiñas exquisitas, Tivoli, paellas riquísimas, museos, y un largo etcétera. Por último, gracias también por tu dedicación i tu paciencia, sobre todo en los pocos momentos intensos en qué el camino se ha hecho ligeramente cuesta arriba, al fin y al cabo, esto suele ocurrir en las mejores familias, ¿verdad?

Muchísimas gracias Irene, por todo, por tanto. Nada de esto habría sido posible sin ti. Además de ser la mejor compañera de laboratorio del mundo, has sido y sigues siendo un apoyo fundamental y una gran inspiración para mí. Recuerdo tu primer día, la ilusión con la que empezaste, con la que sigues trabajando hoy y que transmites a tu alrededor sin darte cuenta. Fuiste mi primera estudiante de "prácticum" y es curioso ver cómo, después de todo, la aprendiz se ha convertido en maestra y la maestra en aprendiz. Me siento súper orgullosa de poder decir que hemos crecido juntas a lo largo

de estos años, no sólo como investigadoras sino también como personas. Gracias por todos los buenos momentos que hemos vivido, dentro y fuera del laboratorio. Las risas, los desayunos, las birras, las bravas (del Rellotge), los bailes, las fiestas (y las Biofestes), las barbacoas, los cumpleaños, los congresos, los viajes… ¡ojalá podamos compartir muchos más! Gracias también por estar ahí en los momentos más críticos, de llantos, de decepciones, de heridas de guerra, de deadlines, de páginas en blanco y de capítulos que parecía no se iban a cerrar nunca pero que al final, poco a poco, se han ido cerrando. Pronto empezarás la recta final y, aunque ya no estaré en el laboratorio, me tendrás a tu lado para cualquier cosa. ¡No te imaginas cuánto te voy a echar de menos!

Quiero dar también las gracias a otro miembro muy importante de nuestra pequeña familia investigadora. Virginia: has sido una buenísima compañera y un gran referente para mí desde el primer momento. Tuviste la paciencia de enseñarme, cuando era aún una estudiante de Grado, el ABC del laboratorio, desde las técnicas más generales hasta los detalles más particulares, que sentarían la base para todo lo que necesitaría posteriormente. Fue un placer trabajar mano a mano y codo con codo, organizarnos juntas, compartir conocimientos, experiencias y momentos únicos. Mil gracias, de verdad, por todo. Es increíble la energía que desprendes. Aún hoy, a pesar de la distancia, siempre con una sonrisa, dispuesta a echar un cable, ¡o a mandar una tarta en avión si hace falta! Además de dejar huella en el laboratorio, la has dejado en nuestras vidas para siempre.

Moltíssimes gràcies Paula, per haver aparegut i haver-te quedat a la meva vida. Recordo perfectament el nostre primer dia al Laboratori 1, el 20 de febrer del 2014, un parell de “topos” desorientades, nervioses, però molt felices i motivades. Quan tot just ens coneixíem de vista, qui ens hauria dit que acabaríem sent tant essencials l’una per l’altra? Vam iniciar el camí com a investigadores juntes al laboratori i des de llavors, hem sigut inseparables tot i els centenars de quilòmetres que hi ha hagut en algunes ocasions entre nosaltres. Gràcies per ser a l’altra banda del telèfon o a l’altra banda de la taula quan més ho he necessitat; sempre m’has entès millor que ningú. M’has ensenyat a relativitzar, a ser optimista, a actuar, a lluitar i a tirar endavant, costi el que costi. Has estat i continues sent un pilar imprescindible sense el qual m’hauria estat extremadament difícil tancar aquesta etapa. Ves pensant en quin racó del mon voldràs que ens prenem els gin-tònics de la victòria!

Durant aquests anys, heu passat pel nostre grup d'investigació i heu format part d'aquesta família una bona colla de "pràcticums" de Grau i Màster. Me'n recordo de totes i tots, i us agraeixo sincerament les vostres ganes d'aprendre, la il·lusió, les forces per seguir endavant que m'heu transmès i tota l'ajuda que m'heu proporcionat, que ha estat molta. Hi ha un trosset de tots i cadascun de vosaltres en aquesta tesi. Ha estat un plaer treballar junts, formar-vos i, alhora, formar-me any rere any al vostre costat. Ho heu fet sempre tot molt fàcil! Carla, Joanot, Eva i Fèlix, moltes gràcies especialment per les bones estones compartides entre *westerns,* cultius, exosomes i sinaptosomes. Roger, el meu *runner* preferit, gràcies per ensenyar-me que els límits no existeixen i que, si treballes fort i dones tot el que tens, els resultats i les línies de meta arriben, tant en la ciència com en el *running*. Lourdes, la meva eivissenca bonica, gràcies per haver estat l'alegria del laboratori durant aquests dos últims anys. Sempre riallera, feliç, música, llum. Els matins ja no són el mateix sense el Kanka sonant de fons amb les teves segones veus brillant per damunt. Mònica, la meva petita i valenta *realfooder*, et miro i em veig a mi mateixa sis anys enrere, no ho puc evitar! En només un any t'has guanyat un raconet del meu cor i has estat una peça clau durant aquest temps: moltes, moltes gràcies, de debò.

Agrair-vos també a totes i tots els integrants, permanents i transitoris, de l'altra gran família que viu al Laboratori 1 el suport que m'heu donat i els bons moments que hem compartit, dins i fora del laboratori. Ha estat un plaer immens treballar al vostre costat. En especial, moltes gràcies Carme i Ester per aconsellar-me i ajudar-me sempre que ho he necessitat i per les bones estones de riures i més riures al menjador. Jordi, gràcies per la teva ajuda incondicional, sempre disposat a donar un cop de mà i a buscar la millor solució per a qualsevol problema. Rubén, María, Luke, Kira, Aída y Rilda, muchas gracias a todos por vuestro apoyo y por el buen ambiente de trabajo que habéis instaurado en el laboratorio a lo largo de estos años. Caru y Jon, nada de esto habría sido lo mismo sin vosotros. Gracias Caru, mi alicantino favorito, por ser mi particular fuente de buen rollo, locuras, piropos, sustos, cotilleos, risas, birras y bailoteos. Eskerrik asko Jon, por estar ahí todos estos años, por sacarme una sonrisa cuando más lo he necesitado, por tus "ni te rayes" en momentos de crisis y por ser el mejor compañero del mundo (de laboratorio y de *swing*). Milesker por todos los buenos ratos que hemos compartido, que no han sido pocos: los jueves en el Rellotge y en *Ballaswing*, las Biofestes, los cafés, las barbacoas, los viajes a Euskadi y Zaragoza y, por supuesto, la Behobia-San Sebastián.

Moltíssimes gràcies també a tots els altres membres del Departament de Biologia Cel·lular. Heu fet del departament una segona llar, per a mi. Moltes gràcies Mercè pels teus valuosíssims consells i ànims, i gràcies també per portar-nos cada setmana les nous més bones del món. Gràcies també Yoli, Mariajosé i Susana per la vostra professionalitat i dedicació, sempre a punt per solucionar qualsevol entrebanc. Agrair-vos també als companys i companyes del Laboratori 2, especialment Marina, Sergi, Marc, Alejo i Ana, tot el vostre suport, els consells, els reactius cedits, les penes i les moltes, moltes alegries compartides. Sou els millors companys de tesi que hauria pogut tenir!

Aida, Alba, Anna, Eli, Jesusa i Lidia, ja fa quasi 10 anys que compartim l'amistat, a banda de l'entusiasme per la ciència. Els nostres camins es van creuar el setembre de 2010 en una aula de la Facultat de Biologia i, des de llavors, hem crescut juntes com a dones i com a investigadores. És un orgull comptar amb talents com els vostres dins les meves amistats. Fortes, lluitadores, valentes, divertides, amables, increïbles, sou tot un referent per a mi. Gràcies a totes, de tot cor, pel vostre suport incondicional. Moltes gràcies Aida per les quedades inter-departamentals d'emergència que li han salvat la vida a aquesta tesi en més d'una ocasió. Lidia, gràcies per ensenyar-me que amb constància i dedicació, més tard o més d'hora, tot acaba sortint. Mil gràcies Alba per tots els "cafès-olés" compartits i les abraçades tant necessàries sempre. Les tres heu estat imprescindibles durant aquests anys i, especialment, en aquest *sprint* final d'etapa.

No voldria acabar sense fer menció als amics i amigues de la colla de Cardedeu: heu estat tots aquests anys al meu costat i heu "patit" aquesta tesi quasi tant com jo. Moltíssimes gràcies per animar-me dia a dia a seguir i per "obligar-me" a descansar quan tocava. Moltes gràcies a les nenes i al Rubén de *Retraining* per les nits de boxa, abdominals i riures, heu estat clau aquests darrers mesos. Gràcies també Sunyi i Helen per la vostra vitalitat i energia, que es contagien.

Finalment, agrair-vos també a tota la meva família pel suport incondicional que m'heu donat sempre. Papa, mama i Paula, moltes gràcies per tot el que heu fet per mi, si he arribat fins aquí ha estat gràcies a vosaltres. Per últim, moltes gràcies Josep per ser el millor company de viatge que hauria pogut tenir, per confiar en mi, per ser al meu costat, per la teva infinita paciència, per demostrar-me que puc aconseguir tot el que em proposi i per ensenyar-me que cada dia té una raó per ser un gran dia.

PREFACE

The present dissertation is the result of experimental work performed in the Intercellular Communication Laboratory at the Department for Cell Biology, Physiology and Immunology of the Faculty of Biology (University of Barcelona), under the careful supervision and guidance of Dr. Fernando Aguado Tomás. The study was initially supported by an FI-DGR scholarship from the Catalan Government (Agència de Gestió d'Ajuts Universitaris i de Recerca) and ultimately by an FPU grant from the Spanish Government (Ministerio de Educación, Cultura y Deporte).

ABSTRACT

The regulated secretory pathway is a hallmark of professional secretory cells as neurons and endocrine cells. Significant peptidergic neurotransmitters as hormones, neurotrophins and growth factors are targeted to dense-core vesicles (DCVs) and released after stimulation. DCV secretory markers include granins, carboxypeptidases and proprotein convertases and constitute DCV molecular machinery. In addition to their important intracellular roles in sorting, trafficking and processing of peptidergic cargos, extracellular neurotrophic functions have been proposed for certain DCV markers. Of note, variations in some members of the granin family such as chromogranin A (CgA) have been described in the brain and cerebrospinal fluid (CSF) of Alzheimer's disease (AD) patients. However, other abundant DCV secretory proteins as the granin SgIII, the enzyme convertase CPE and the proprotein convertases PC1 and PC2, have been poorly studied in AD. Hence, we have analyzed alterations in the secretory markers of DCVs in the brain and CSF of AD patients and in the 5xFAD mouse model of familial AD. As a major finding of the present dissertation, DCV secretory markers accumulate in dystrophic neurites and granulovacuolar degeneration bodies, two prominent neuropathological features of AD. Moreover, DCV secretory proteins markedly decay in the CSF of AD patients, correlating with neurodegeneration and cognitive decline. Furthermore, secretory markers of DCV initially increase and later decrease in the hippocampi and age-dependently decline in the CSF of 5xFAD mice. Additionally, since reactive astrogliosis is a common feature of neurodegenerative diseases, understanding the mechanisms underlying gliotransmission under control and proinflammatory conditions is fundamental. Here we have shown that astrocyte peptidergic secretory vesicles are heterogeneous and display variable release rates in response to Ca^{2+}-mediated stimulation, which are modulated in proinflammatory-treated astrocytes *in vitro* and in a neuroinflammation model *in situ*. Besides, unstimulated release of astrocyte secretory proteins *in vitro* is independent of intrinsic Ca^{2+} oscillations but critically depends on intracellular Ca^{2+}. Altogether, since neurotransmission and gliotransmission are clearly affected in AD, our results suggest that alterations in the regulated secretory pathway of neurons and astrocytes may participate in underlying pathological mechanisms and propose DCV secretory markers as candidate biomarkers for AD.

RESUM

Mitjançant la via de secreció regulada de neurones i cèl·lules endocrines, hormones, neurotrofines i altres missatgers peptídics importants pel funcionament del sistema nerviós són internalitzats en vesícules de centre dens (VCD) i alliberats per exocitosi en resposta a estímuls. La maquinària molecular de les VCD inclou granines i enzims processadors (carboxipeptidases i convertases) que s'encarreguen de dirigir i processar els missatgers peptídics a les VCD. Aquests components de les VCD són solubles i se secreten, amb els altres transmissors peptídics, a l'espai extracel·lular, on alguns desenvolupen funcions neurotròfiques rellevants. Proteïnes de la família de les granines, com la cromogranina A, han estat tradicionalment relacionades amb malaltia d'Alzheimer (MA), on s'han trobat alterades al cervell i al líquid cefalorraquidi (LCR) de pacients. No obstant, altres marcadors de les VCD molt abundants com la secretogranina III, la carboxipeptidasa E i les convertases PC1 i PC2 han estat poc estudiats en el context de la MA. Així, hem analitzat alteracions dels marcadors de VCD al cervell i al LCR de pacients de la MA i de ratolins 5xFAD, un model animal transgènic per a la MA familiar. Les proteïnes marcadores de VCD s'acumulen a les neurites distròfiques i als cossos de degeneració granulovacuolar, mentre els seus nivells disminueixen al LCR dels pacients de la MA, on correlacionen amb neurodegeneració i declivi cognitiu. A més, es troben inicialment augmentades i finalment disminuïdes a l'hipocamp dels ratolins 5xFAD, on també disminueixen progressivament al LCR amb l'edat. Atès que l'astrogliosi és present en malalties neurodegeneratives, és important l'estudi de la gliotransmissió tant en situacions control com de neuroinflamació. Així, mitjançant el tractament proinflamatori d'astròcits *in vitro* i un model de neuroinflamació *in situ* hem determinat que la secreció peptidèrgica dels astròcits sota estimulació és variable i moderada i que, en absència d'estímul, la seva alta taxa d'alliberació és independent d'oscil·lacions espontànies però dependent de calci intracel·lular. En resum, les alteracions de la via de secreció regulada de neurones i astròcits podrien participar en la progressió de la malaltia i, per això, proposem les proteïnes marcadores de VCD com a biomarcadors candidats per a la MA.

TABLE OF CONTENTS

LIST OF FIGURES

LIST OF TABLES

LIST OF ABBREVIATIONS

7B2	Neuroendocrine protein 7B2
Aβ	Amyloid beta peptide
ACSF	Artificial cerebrospinal fluid
AD	Alzheimer's disease
AMPAR	2-Amino-3-(3-hydroxy-5-methyl-isoxazol-4-yl) propanoic acid receptor
ANP	Atrial natriuretic peptide
APOE	Apolipoprotein E
APP	Amyloid precursor protein
ATP	Adenosine tri-phosphate
BACE	β-secretase
BAPTA	1,2-bis o-aminophenoxy ethane-N,N,N′,N′-tetraacetic acid
BBB	Blood-brain barrier
BDNF	Brain-derived neurotrophic factor
CDR	Clinical dementia rating
CgA	Chromogranin A
CgB	Chromogranin B
CHMP2B	Charged multivesicular body protein 2 B
CHX	Cycloheximide
CK1δ	Casein kinase 1 isoform delta
CNS	Central nervous system
CPE	Carboxypeptidase E
CSF	Cerebrospinal fluid
CysC	Cystatin C
DCV	Dense-core vesicle
EAAT	Excitatory amino acid transporter
ER	Endoplasmic reticulum
FAD	Familial Alzheimer's disease
GABA	Gamma-aminobutyric acid
GFAP	Glial fibrillary acidic protein

GVD	Granulovacuolar degeneration
HCX	H^+/Ca^{2+} exchanger
Iba1	Ionized calcium binding adapter molecule 1
IFNγ	Interferon gamma
IgM	Immunoglobulin M
IL-1β	Interleukin 1 beta
IP3R	Inositol tri-phosphate receptor
KAR	Kainic acid receptor
KR	Kiss-and-run
KS	Kiss-and-stay
LAMP1	Lysosomal-associated membrane protein 1
LCN2	Lipocalin 2
LDCV	Large dense-core vesicle
LPS	Lipopolysaccharide
MCI	Mild cognitive impairment
MCU	Mitochondrial Ca^{2+} uniporters
mGluR	Metabotropic glutamate receptor
MMSE	Mini-mental state examination
MPTP	Mitochondrial permeability transition pore
MRI	Magnetic resonance imaging
NCX	Na^+/Ca^{2+} exchanger
NFL	Neurofilament light chain
NFT	Neurofibrillary tangle
NMDAR	N-methyl-D-aspartic acid receptor
NPY	Neuropeptide Y
PBS	Phosphate-buffered saline
PC1/3	Proprotein convertase 1/3
PC2	Proprotein convertase 2
PET	Positron emission tomography
PLC	Phospholipase C
POMC	Proopiomelanocortin

ProSAAS	Proprotein convertase 1 inhibitor
PSD-95	Postsynaptic density protein 95
PSEN1	Presenilin 1
P-tau	Phosphorylated-tau protein
SAD	Sporadic Alzheimer's disease
SEM	Standard error mean
SERCA	Sarco-endoplasmic reticulum Ca^{2+}-ATPase
SgII	Secretogranin II
SgIII	Secretogranin III
SNARE	Soluble n-ethylmaleimide-sensitive factor attachment protein receptor
SNAP-25	Synaptosome-associated protein 25
SOCC	Store-operated Ca^{2+} channel
SV	Synaptic vesicle
Syp	Synaptophysin
TEM	Transmission electron microscopy
TG	Thapsigargin
TGN	Trans-Golgi network
TLR	Toll-like receptor
TNFα	Tumor Necrosis Factor alpha
T-tau	Total-tau protein
VAMP	Vesicle associated membrane protein
VGAT	Vesicular GABA transporter
VGCC	Voltage-gated Ca^{2+} channel
VGLUT	Vesicular glutamate transporter
VNUT	Vesicular nucleotide transporter
WT	Wild type

INTRODUCTION

INTRODUCTION

1. Communication in the nervous system

1.1. Neurotransmission: synaptic vesicles and dense-core vesicles

Receiving, processing and integrating information from external (environment) and internal (organism itself) stimuli and generating appropriate reactions is the main role of the nervous system. Fundamental features of the nervous system are analogous in the vast majority of pluricellular animals despite the existence of different complexity levels (Emes and Grant, 2012). Basically, to coordinate responses to received stimuli, cells of the nervous system (neurons and glial cells) communicate with each other via chemical or electrical signals in a process known as neurotransmission (Pereda, 2014).

Classically, a synapse has been defined as a structure that enables functional communication between two neurons. Chemical synapses (Figure 1A) are mediated by small clear vesicles of 30-50nm known as synaptic vesicles (SVs), which contain neurotransmitters and are secreted from the presynaptic neuron in response to a stimulation (Jahn and Südhof, 1994; Qu et al., 2009). Released neurotransmitters travel through the synaptic cleft and interact with specific receptors of the postsynaptic neuron (Lin and Scheller, 2000). In electrical synapses (Figure 1B), though, neurotransmitters are not required: the nerve impulse is directly transmitted by gap junctions (Connors and Long, 2004). However, a mixed synaptic transmission exists, where communication via both chemical and electrical signals coexists in the same neuron (Cachope and Pereda, 2012).

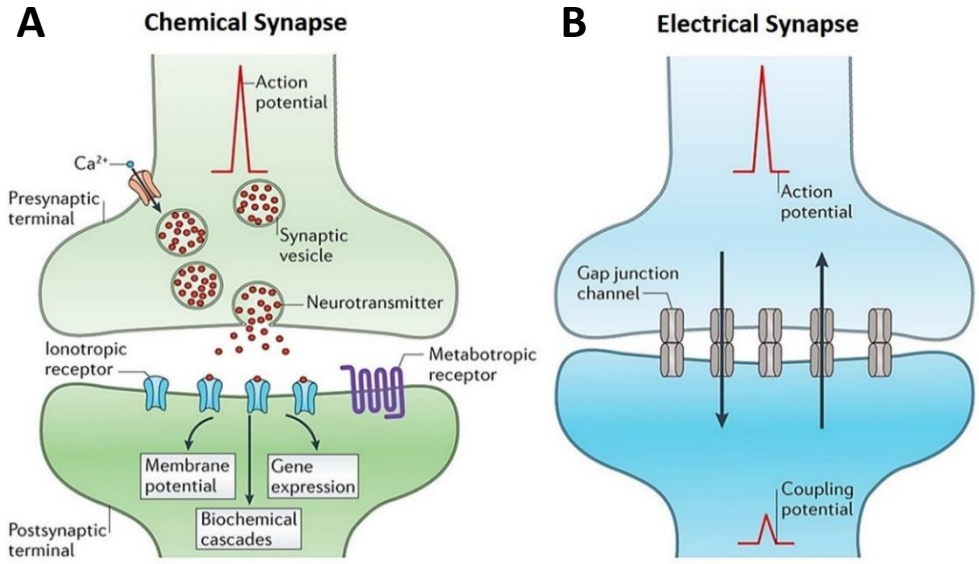

Figure 1. Different modalities of synaptic transmission: chemical (A) and electrical (B) synapses (Pereda, 2014).

In the vertebrate central nervous system (CNS) electrical synapses exist mostly provisionally preceding the establishment of definitive chemical synapses (Ovsepian, 2017). Thus, chemical transmission is predominant and is capable of undergoing structural changes under determinate conditions (Citri and Malenka, 2008). Processes that modify cerebral function by means of experience-derived neuronal activity are known as synaptic plasticity and are crucial for neuronal circuits early development and adult NS optimal functioning (Bennett and Zukin, 2004). Even though gap junction-based synapses are structurally simpler than chemical synapses, both play a key role in neuronal circuitry remodelling (Curti and O'Brien, 2016).

In chemical synapses, several consecutive steps constitute the life cycle of SVs (Figure 2A). SV associated proteins are synthesised at the soma (step 1) and transported to the neuron terminal (step 2), where neurotransmitters must be actively transported into the vesicle (step 3). SVs are then tethered to the cytoskeleton (step 4), mobilized (step 5) and docked (step 6) to the active zone. Subsequently, SVs undergo adenosine tri-phosphate (ATP)-dependent priming (step 7), which ultimately makes them competent for Ca^{2+}-evoked opening of the fusion-pore to release neurotransmitters (step 8) and recycle (steps 9 and 10) (Lin and Scheller, 2000; Südhof, 2004).

Low-molecular-weight neurotransmitters (i.e. amino acids) as glutamate (excitatory) or gamma-aminobutyric acid (GABA; inhibitory) are internalized into SVs and released from the presynaptic terminal by an action potential (Bak et al., 2006; Katz and Miledi, 1969). Exocytosis of SVs occurs due to a massive Ca^{2+} entrance into the nerve terminal through Ca^{2+} channels opened by an action potential. Importantly, not every action potential triggers the release of SVs but only a 10-20% of them efficiently evoke secretion (Goda and Südhof, 1997).

A single active zone of a small hippocampal synapse enables the docking of approximately 10 vesicles, which are found in a pool of SVs known as the ready-releasable pool. Additionally, two other SV pools exist: the recycling pool (16 SVs) and the reserve pool (240 SVs) (Gan and Watanabe, 2018). The number of SVs secreted has been determined according to a certain release probability which depends on the increased intracellular Ca^{2+} concentration (Katz and Miledi, 1969; Stevens, 2003). However, a recent study has demonstrated that it is actually the size of the ready-releasable pool the responsible of regulating the amount of released SVs, upstream of vesicle release probability (Vaden et al., 2019).

Multiple proteins constitute the molecular machinery of synaptic transmission. Transporters are needed to actively internalize neurotransmitters into SVs, such as vesicular glutamate transporter (VGLUT) or vesicular GABA transporter (VGAT) (Hackett and Ueda, 2015). Release sites are organized by scaffolding proteins (e.g. Bassoon and Piccolo) whereas tethering proteins (e.g. Munc 13, Munc 18 and myosin V) gather docking and release machineries (Figure 2B).

SV docking and fusion are arbitrated by SNARE (soluble N-ethylmaleimide-sensitive factor attachment protein receptor) complex proteins: synaptobrevin/vesicle-associated membrane protein (VAMP), the most abundant SV membrane protein, together with synaptosome-associated protein 25 (SNAP-25) and Syntaxin-1, found in the plasma membrane. Synaptophysin (Syp), the second most abundant SV protein, is crucial for synaptobrevin recruitment during endocytosis (Gordon et al., 2016). Fusion of SVs also depends on members of the synaptotagmin family, which act as Ca^{2+} sensors and interact with SNARE proteins (Gramlich and Klyachko, 2019).

Neurotransmitter receptors are mostly found in postsynaptic membranes. In glutamatergic synapses, both metabotropic (mGluR) and ionotropic receptors (2-Amino-3-(3-hydroxy-5-methyl-isoxazol-4-yl)propanoic acid – AMPAR, kainic acid – KAR and N-methyl-D-aspartic acid – NMDAR) exist (Niswender and Conn, 2010; Traynelis et al., 2010). GABAergic synapses display ionotropic (GABA-A/C) and metabotropic (GABA-B) receptors, as well (Jembrek and Vlainic, 2015).

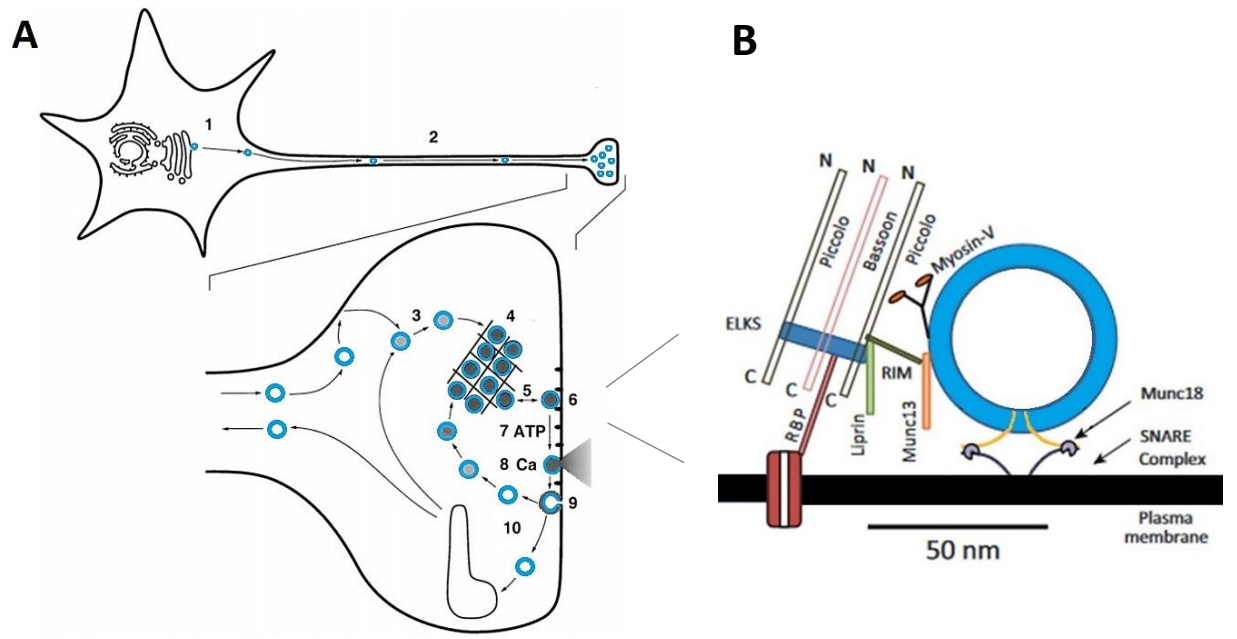

Figure 2. Life cycle of SVs (A) and molecules responsible of SV tethering, docking and fusion at release sites in the active zone (B). Modified from Lin and Scheller (2000) and Gramlich and Klyachko (2019), respectively.

Apart from receptors and ion channels, vertebrate postsynaptic densities comprise an extremely complex and conserved proteome which includes numerous proteins with key functions (e.g. adhesion, scaffolding, signalling) such as Homer and postsynaptic density protein 95 (PSD-95) (Kim and Sheng, 2004). These proteins are organized in complexes and supercomplexes which include receptors, channels and enzymes. Growing evidence suggests that synapse diversity may be the result of the differential distribution of these super molecular machines (Frank and Grant, 2017).

After fusion of SVs and release of neurotransmitters, an endocytic recycling process occurs from the plasma membrane of the presynaptic neuron. The ultimate purpose of SV recycling is reusing components of the membrane to obtain newly refilled and fusion-competent SVs ready for a new cycle of exocytosis (Rizzoli, 2014). Four main mechanisms of SV recycling and exocytosis-endocytosis coupling have been described (Figure 3):

A. Clathrin-dependent endocytosis: after full fusion of SVs with the plasma membrane, a clathrin coat is formed and SVs are endocytosed. New SVs are formed far from the release site and subsequently reacidified and refilled with neurotransmitters directly or indirectly (through endosomal structures) (Südhof, 2004; Watanabe, 2015). The process of clathrin recruitment can be slow (when it requires *de novo* formation) or fast (when evolving from preformed clathrin-coated pits). Therefore, clathrin-mediated endocytosis functions both gradually or rapidly, depending on recruitment speed (Yuan et al., 2015; Zhu et al., 2009). Fast endocytosis is especially relevant during intense stimulation when exocytosis is sustained in time (Kawasaki et al., 2011; Yuan et al., 2015).

B. Kiss-and-run (KR): fusion of SVs with the plasma membrane occurs in a transient manner with the subsequent closure of the fusion pore. SVs undergo an undocking process and are locally recycled and refilled with neurotransmitters (Alabi and Tsien, 2013; Fesce et al., 1994). KR is a relatively fast (1-2s) recycling mechanism present in a significant percentage of releasing events (Van Kempen et al., 2011; Park et al., 2012; Zhang et al., 2009). A particular type of KR is the Kiss-and-stay (KS) mechanism, where fusion of SVs is partial and vesicular structures are retained at the release site (An and Zenisek, 2004; Rizzoli and Jahn, 2007; Taraska et al., 2003). In KS fusion pores are larger (20-150nm compared to KR 10nm) and SVs remain docked at the active zone to be reacidified and replenished with neurotransmitters (Liang et al., 2017).

C. Activity bulk endocytosis: after full fusion of multiple SVs and multivesicular exocytosis (homotypical fusion of vesicles with each other before fusion with the plasma membrane) internalization of great-sized endocytic vesicles occurs by means of cavernous invaginations of the plasma membrane (Wen et al., 2012; Wu and Wu, 2007). SVs are regenerated from endosomes via clathrin-dependent or independent pathways (Watanabe and Boucrot, 2017).

D. Ultrafast endocytosis and endosomal sorting: SVs fully fuse with the plasma membrane and are rapidly endocytosed after 50 to 100ms not as intact vesicles, but as greater invaginations. Precisely because no integral SVs are retrieved, this mechanism must be independent of KR endocytosis. Besides, it is 200x faster than clathrin-dependent recycling mechanisms, which suggests that it is a pathway ultimately destined to the rapid restoration of the membrane surface. Regeneration of synaptic vesicles is mediated by clathrin at endosomes (Gan and Watanabe, 2018; Watanabe et al., 2013).

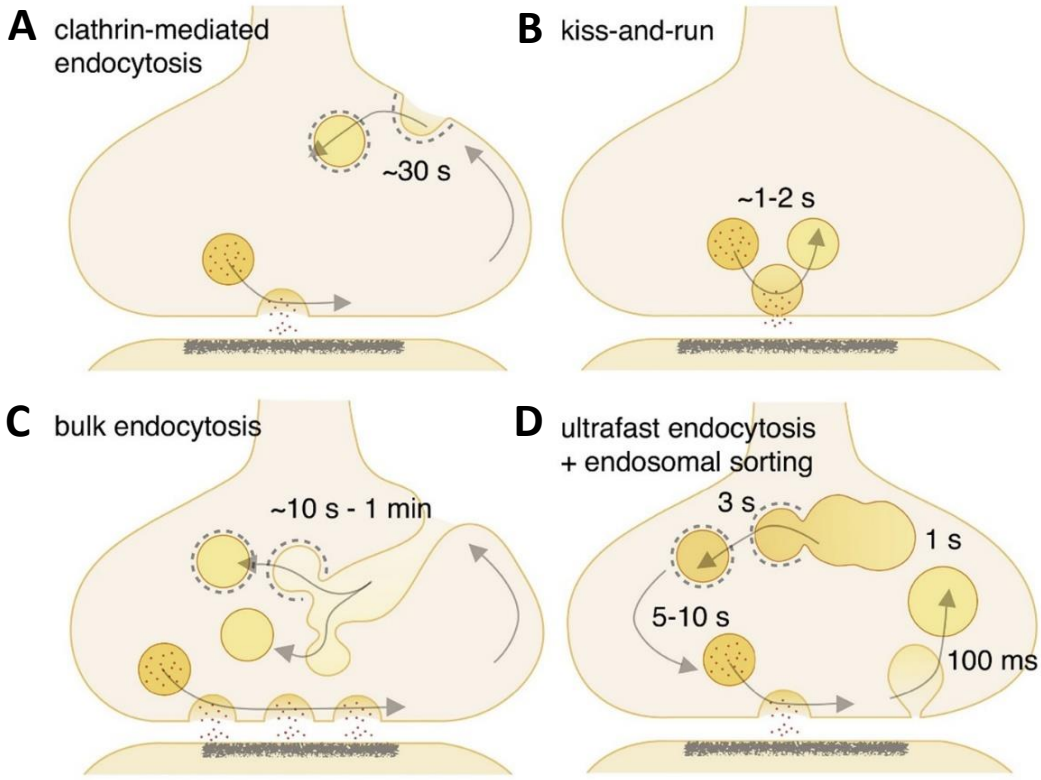

Figure 3. Main mechanisms of SV recycling and exocytosis-endocytosis coupling: clathrin-mediated endocytosis (A), kiss-and-run (B), bulk endocytosis (C) and ultrafast endocytosis and endosomal sorting (D). Modified from Watanabe and Boucrot (2017).

In addition to fast amino acid neurotransmission, a slower peptidergic transmission exists in neurons which is also present in endocrine and neuroendocrine cells (Ng and Tang, 2016). Neuropeptide transmitters are small peptides which coexist in neurons with classical SV neurotransmitters (Hökfelt et al., 2000). Both neurotransmission systems are essential but display different features (Figure 4). Specifically, distinct distribution, vesicle dimensions and molecular structures may be responsible of the different transmission velocities, although SNARE proteins and regulation systems are equivalent in both types of transmission (Kreutzberger et al., 2019).

Hormones, growth factors, neurotrophins and other neuropeptide transmitters are sorted into secretory granules (dense-core vesicles (DCVs) or large-dense core vesicles (LDCVs), in neurons), stored in the cytoplasm and released following stimulation (Vázquez-Martínez et al., 2012). Even though neuropeptides are present in most neurons, some of them are produced only in discrete areas of the brain (e.g. orexin) while others are synthesized in many regions (e.g. neuropeptide Y – NPY and brain derived neurotrophic factor – BDNF) (Lipska et al., 2001; van den Pol, 2012). Differences in localization may be explained by the variety of functions that neurotrophins and neuropeptides exert, as they are key modulators of neurogenesis, synaptic plasticity and neuronal activity (Malva et al., 2012; Park and Poo, 2013; Zaben and Gray, 2013).

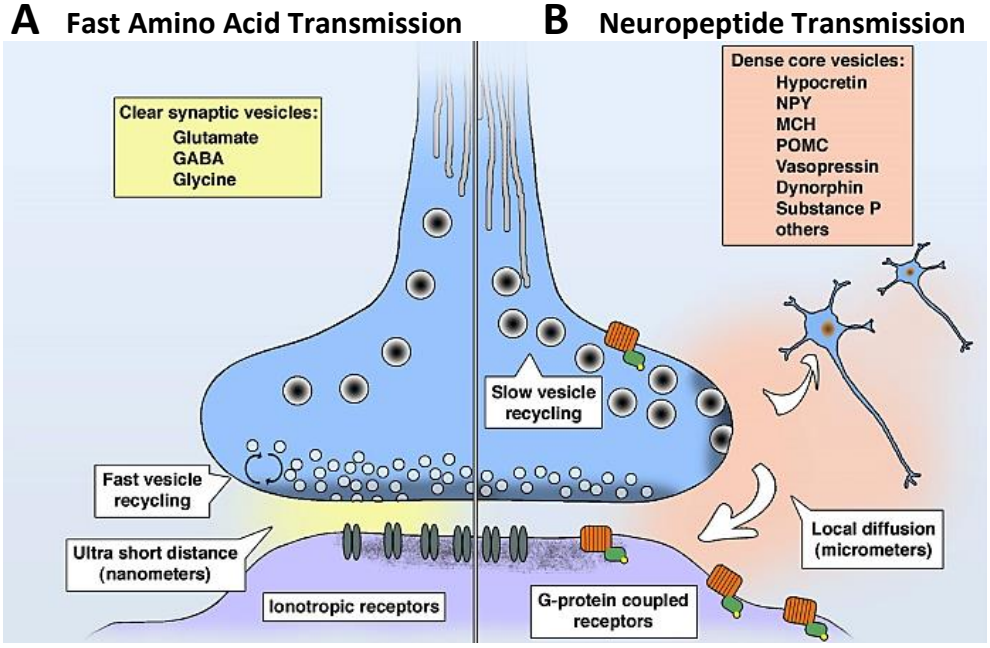

Figure 4. Main characteristics and differences of fast amino acid transmission (A) and slower neuropeptide transmission (B). Modified from Van den Pol (2012).

Although in fast neurotransmission amino acid transmitters are mainly synthesized at release sites, neuropeptides are generally synthesized at the soma from mRNAs (Comeras et al., 2019). Afterwards, peptidergic transmitters are targeted to the endoplasmic reticulum (ER) and delivered via coat protein complex II coated vesicles to the Golgi apparatus (Kurokawa and Nakano, 2019) to finally be sorted in the trans-Golgi network (TGN) into immature DCVs. Before release, DCVs undergo a maturation process which is clathrin-mediated and involves biochemical and biophysical processes (e.g. lumen acidification, protein aggregation, vesicle fusion and membrane remodelling) (Bonnemaison et al., 2013; Tooze and Tooze, 1986).

DCVs migrate to the periphery, where they can be intracellularly reserved for a long time before being released in a stimulation dependent manner (e.g. K+-evoked depolarization) (Kim et al., 2006; Lim et al., 2017). However, a basal secretion of DCVs exists at a low rate even in the lack of stimuli (Alvarez de Toledo et al., 1993; Zhang et al., 2017). Like in SV exocytosis, DCV secretion relies on a series of steps arbitrated by several factors which include proteins of the SNARE complex. Mature DCVs undergo docking and priming processes that bring them together to the plasma membrane in preparation for Ca^{2+}-evoked release (Rizo and Xu, 2015).

On average, from two to three DCVs are found at synapses but, differently from SV release, neuropeptide secretion is not only limited to the synapse and DCVs can also be released from extra-synaptic locations (Matsuda et al., 2009). Even though DCVs are distributed similarly in axons and dendrites they are preferentially released at axons, where release probability ranges from 1% to 6% depending on the type of stimulus (Persoon et al., 2018). Besides, repetitive and more prolonged stimulation is required for fusion of DCVs in comparison with SVs release (Balkowiec and Katz, 2002; Frischknecht et al., 2008).

After fusion of DCVs, released neuropeptides preferentially act on metabotropic receptors (i.e. G protein-coupled receptors) either in excitatory or inhibitory manners (Nusbaum et al., 2017). Even though the predominant location of neuropeptide action is relatively close to the presynaptic neuron, given the high affinity of these receptors for peptidergic transmitters they can easily diffuse and travel longer distances than amino acid transmitters (Alpár et al., 2019). For instance, while NPY effect is usually near to the release site, targets for hormones such as leptin and ghrelin are typically distant (Sternson, 2013).

Transmembrane DCV proteins endocytosis mechanisms are relatively slower phenomena (seconds) compared to DCV fusion (Bauer et al., 2004; Eliasson et al., 1996). Transmembrane proteins which have been integrated to the plasma membrane during DCV fusion are retrieved and internalized via endosomes. Interestingly, endosomal structures may then interconnect either with the TGN (incorporating membrane material to form new DCVs) or with immature DCVs (contributing to their maturation by means of membrane remodelling) (Wasmeier et al., 2005). Numerous DCV membrane proteins are also found in other endosomal and lysosomal compartments, which suggests that different routes may be taken when recycling. Thus, endosomal recycling represents a crossroad between the regulated secretory pathway and the endocytic route (Ang et al., 2004).

It must be considered, however, that release of DCVs in endocrine cells differs from release in neurons in some aspects (Bulgari et al., 2019). Regarding localization, neuronal DCVs are considerably smaller (100nm compared to 300-1000nm diameter) which enables them to access axons and dendritic boutons (Merighi, 2018). But precisely because of their reduced size, neuronal DCVs are not capable of forming great fusion pores as neuroendocrine DCVs (Shin et al., 2018). Thus, KR and KS (i.e. cavicapture) recycling mechanisms have been described for neuronal DCVs as well. In fact, reuptake of DCVs after fusion by cavicapture processes is mediated by dynamin-1 and appears to be independent of classical endocytosis (Liang et al., 2017; Tsuboi et al., 2004; Wong et al., 2015).

Different neuropeptides can be stored together (i.e. coexist) in the same individual DCV (Merighi, 2009; Salio et al., 2007). As seen in Figure 5A, newly generated DCVs emerge from the TGN containing one kind of neuropeptide and homotypically fuse with other immature DCVs which store different cargoes, creating greater DCVs in a process orchestrated by the conserved coiled-coil protein 1 (Cattin-Ortolá et al., 2017). Although different neuropeptides already coexist in the resulting DCVs, they still cannot be considered as mature due to their greater size, which will be reduced following condensation once in the terminal (Bonnemaison et al., 2013). Co-stored neuropeptides may then be released together (i.e. non-selectively) or separate (i.e. selectively) via numerous cycles of cavicapture until DCVs are completely empty (Merighi, 2018).

It is also during DCV maturation when neuropeptides, which are typically synthesized as inactive long precursors, are enzymatically processed into shorter biologically active transmitters (Lin and Salton, 2013). After beginning at the TGN, where explicit molecular signals promote packaging of cargoes (Topalidou et al., 2016), the processing continues inside the vesicles, where proteins involved in DCV biogenesis and neuropeptide processing reside (Kögel and Gerdes, 2010).

The machinery in charge of aggregating and processing neuropeptides inside of DCVs (Figure 5B) are members of the granin family (chromogranin A – CgA, chromogranin B – CgB, secretogranin II – SgII and secretogranin III – SgIII), processing enzymes (carboxypeptidase E – CPE) and prohormone convertases 1/3 and 2 – PC1/3 and PC2) (Arnaoutova et al., 2003; Beuret et al., 2004). These components are also sorted into DCVs, activated by processing enzymes and, given their soluble nature, released with the other DCV cargoes after fusion (Bartolomucci et al., 2011).

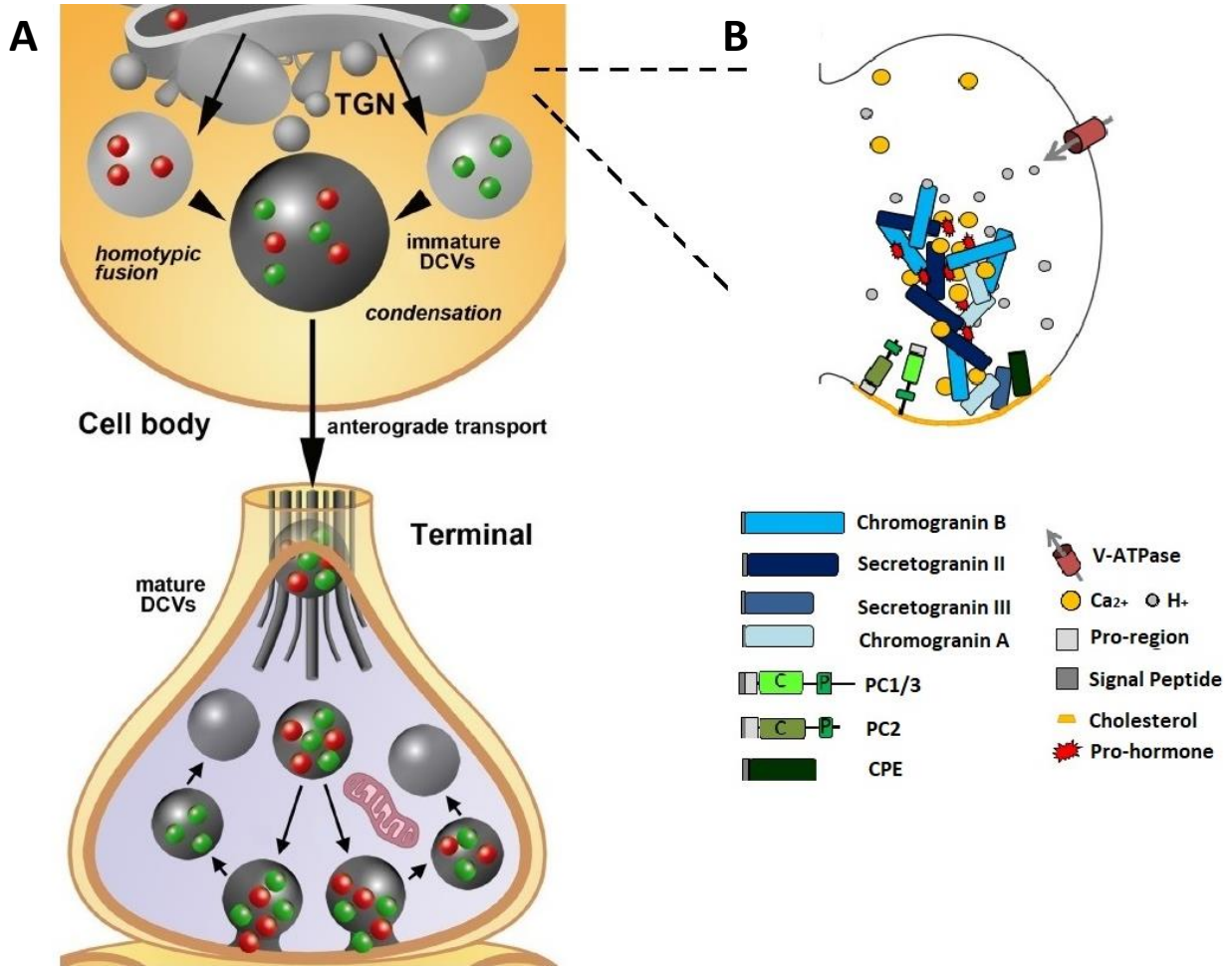

Figure 5. Biogenesis, filling, maturation, transport and release (A) and molecular components (B) of DCVs. Modified from Merighi (2018) and Bonnemaison, Eipper and Mains (2013), respectively.

Members of the chromogranin/secretogranin family are the most abundant DCV components (Taupenot et al., 2003). Due to their capacity of binding Ca^{2+} and forming aggregates, chromogranins are essential for DCV biogenesis (Courel et al., 2010). So much so that the lack of CgA and CgB has been determined to cause alterations in content and release of DCVs in chromaffin cells (Díaz-Vera et al., 2012).

To exclude the entrance of constitutive secretory proteins to the regulated pathway, insoluble aggregation of DCV precursor proteins starts at the TGN (Hummer et al., 2017). Early aggregates are then transferred into immature DCVs where further compaction occurs due to the aggregation role of granins. In cholesterol-rich membrane platforms, prohormones in premature aggregates are then transferred to the neighbouring processing enzymes which process them into smaller and mature fragments (Ji et al., 2017). In turn, processed mature hormones are incorporated to the neighbouring premature aggregates (Hosaka and Watanabe, 2010) (Figure 6).

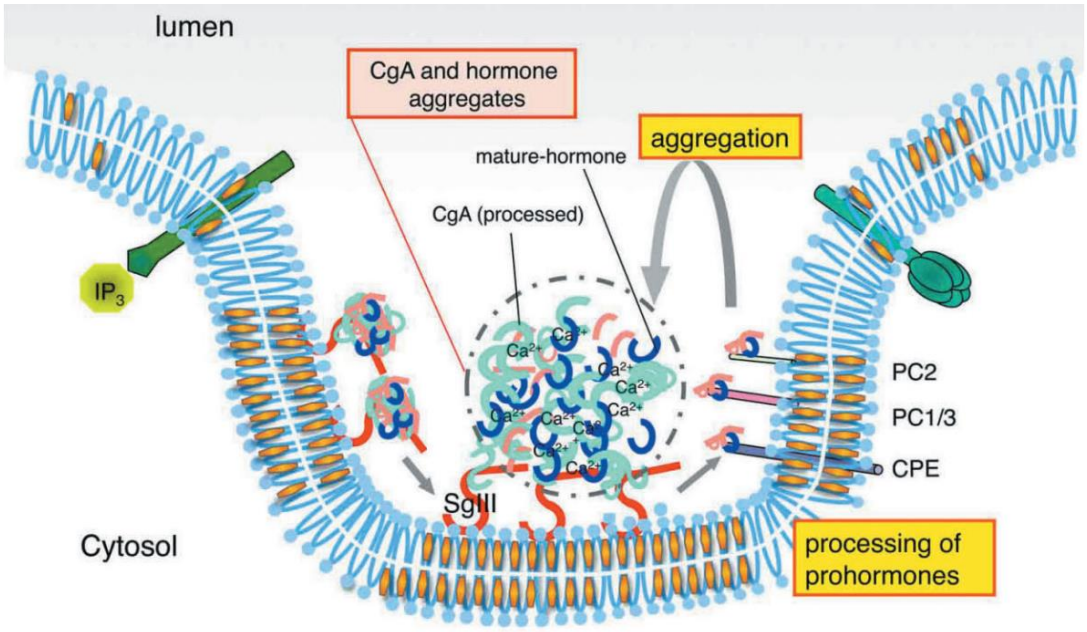

Figure 6. Processes and molecules implicated in DCV biogenesis. Modified from Hosaka and Watanabe (2010).

Granins are also proteolytically processed to become active and exert their biological effects either in autocrine, paracrine or endocrine ways once released (Montero-Hadjadje et al., 2008). In addition to SgII and SgIII, which are also key participants of DCV biogenesis, other members of the secretogranin family are secretogranin V (also known as neuroendocrine protein 7B2), secretogranin VI and the proprotein convertase 1 inhibitor (proSAAS) (Bartolomucci et al., 2011).

One of the enzymes in charge of processing propeptides into mature hormones and neuropeptides is the exopeptidase CPE (Ji et al., 2017). As a carboxypeptidase, CPE acts removing carboxyterminal arginine or lysine amino acids from neuropeptides previously cleaved by endopeptidases (Cawley et al., 2012). CPE has been also implicated in processes such as sorting of secretory proteins destined to the regulated pathway and in neurotrophic functions (Cheng et al., 2014). BDNF is one of the neuropeptides sorted to DCVs by CPE and, in turn, CPE is essential for BDNF signalling in the hippocampus (Xiao et al., 2017). Additionally, CPE is implicated in dendrite arborization and neuronal migration (Liang et al., 2018).

Neuropeptides destined to the regulated secretory pathway display a signal peptide which is only present in the pre-protein form. After its cleavage, the resulting protein is still a precursor (i.e. pro-protein), which is further cleaved by endoproteases to eliminate the N-terminal pro-domain and become an active and mature protein ready to be released (Vázquez-Martínez et al., 2012). In some cases, however, both mature and precursor proteins can be secreted and act on their receptors promoting different functional effects (Bartkowska et al., 2010).

The main endoproteolytic processing enzymes are prohormone convertases (PCs), which constitute a family of nine calcium-dependent endoproteases: furin, PC1/3, PC2, PACE4, PC5/6, PC7/8, SKI-1 and PCSK9 (Klein-Szanto and Bassi, 2017). Except for the two last, all of them cleave at the C-terminal end of sequences containing arginine or lysine residues (Lee et al., 2004). PCs generally display a signal peptide (N-terminal), a pro-region, a catalytic domain, a P-region and a C-terminal domain (Pickett et al., 2013). PC1 and PC2 are exclusively expressed in neurons and endocrine cells and are targeted to the regulated secretory pathway by a sorting signal located in their c-terminal region (Dikeakos et al., 2009).

PC1 is activated in the ER by autocatalysis of its pro-region (Zhou and Lindberg, 1994) and it is involved in the activation of many prohormones and proneuropeptides as glucagon, insulin, enkephalin, proopiomelanocortin (POMC) and NPY (Pickett et al., 2013). The activity of PC1 can be regulated by autoinhibition (i.e. mediated either by the pro-region or the C-terminal domain) or inhibition mediated by the granin proSAAS (Lee et al., 2004). The absence of PC1 has been related to impaired neuropeptide processing which can lead to a wide range of metabolic diseases (e.g. obesity, hypogonadism, hypoadrenalism) (Artenstein and Opal, 2011).

PC2 participates in the processing and maturation of insulin, corticotropin, melanocyte-stimulating hormones, β-endorphin, somatostatin and POMC (Zhan et al., 2009). Differently from the other PCs, PC2 does not undergo initial autocatalysis in the ER to become active (Seidah et al., 2008). However, PC2 activation requires the binding of the chaperone 7B2, which is at the same time a potent PC2 inhibitor (Jarvela et al., 2018). The lack of PC2 can give rise to alterations related to hypoglycemia and growth retardation (Klein-Szanto and Bassi, 2017).

The relevance of neuropeptide transmitters and DCV molecular machinery in maintaining metabolic and homeostatic balances has been evidenced thus far. Interestingly, neuropeptide role in the regulation of these processes seems to be less decisive and much more modulatory, i.e. based on adjusting synaptic activity (Comeras et al., 2019). Furthermore, in some brain regions, synaptic modulation has been determined as the main function of neuropeptide release, even though neuropeptide actions are generally not limited to it (van den Pol, 2012).

Neuropeptide modulation of neuronal activity occurs in the presynaptic terminal by regulating neurotransmitter release (Nusbaum and Blitz, 2012) (Figure 7). There are neuropeptide receptors located on axon terminals of glutamatergic and GABAergic neurons, indicating that neuropeptides mediate direct actions at the terminal level (Willis, 2006). Such receptors, usually metabotropic, activate second messengers that finally alter transmitter release (de Jong and Verhage, 2009).

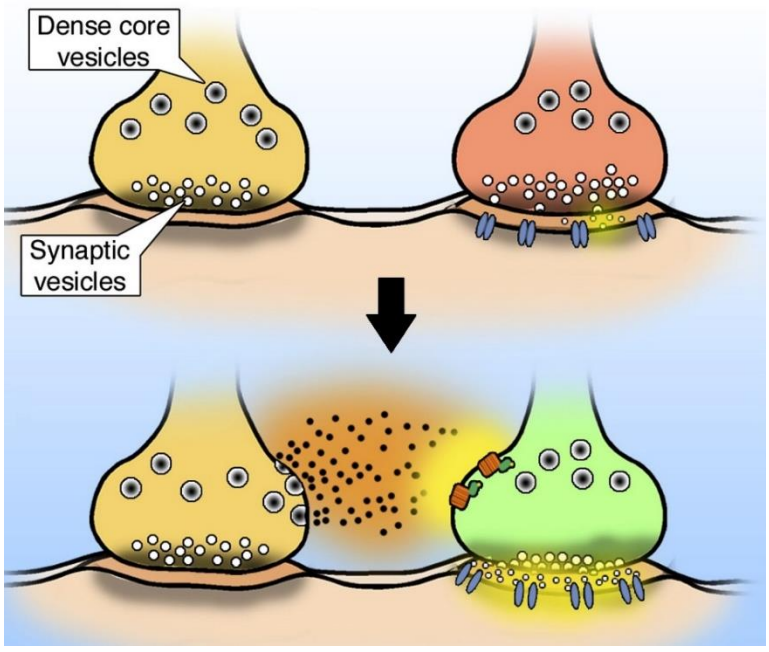

Figure 7. Presynaptic modulation of classic neurotransmitter release. Modified from van den Pol (2012).

Delivered neurotransmitters may originate from a peptidergic presynaptic terminal (i.e. external messengers) or from the postsynaptic terminal itself (i.e. retrograde-feedback messengers) (Regehr et al., 2009). Moreover, presynaptic modulation can be positive and promote secretion (e.g. hypocretin and glucagon-like peptide 1) or negative and cause a reduction of release (e.g. NPY, somatostatin and dynorphin) (Colmers et al., 1988; Fu et al., 2004; López-Huerta et al., 2012).

Small amino acid neurotransmitters and neuropeptide transmitters largely coexist in the same neurons all over the NS, which results in a great communication flexibility: co-transmission provides additional mechanisms of variable neuromodulation (Nusbaum et al., 2017). In fact, neurons that secrete both classical and peptidergic transmitters exert key functions in receptor modulation, gene expression and trophic sustenance (Vaaga et al., 2014). Different targets can be modified by one, the other or both co-transmitters and, by affecting different receptors, the same transmitter can modify diverse targets (Ren et al., 2011).

Another important neuropeptide mediated- modulation mechanism lies in their inactivation by extracellular peptidases (Isaac et al., 2009). In detail, a particular kind of circuit may be influenced differently by neuropeptide transmitters depending on the concrete action of peptidases (Wood and Nusbaum, 2002). Furthermore, due to neuropeptide capacity of diffusing and traveling long distances, the inhibiting role of peptidases may not be restricted to locations close to release sites (Nässel, 2009).

Precisely because of these diffusion properties, peptidergic transmitters facilitate communication between distant cerebral regions (Alpár et al., 2019; Comeras et al., 2019). Since the cerebrospinal fluid (CSF) directly interacts with the cerebral extracellular space, released transmitters may diffuse into the CSF, thus revealing the biochemical changes occurring in the CNS (Johanson et al., 2008). In addition, two other mechanisms have been described for neuropeptide release into the CSF (Figure 8): direct release (A) and amplification release (B). In the first one, neurons may release neuropeptides directly at the ventricular surface whilst, in the second one, synapses formed with ependymal cells may cause the latter to amplify the signal (Alpár et al., 2018; Noble et al., 2018).

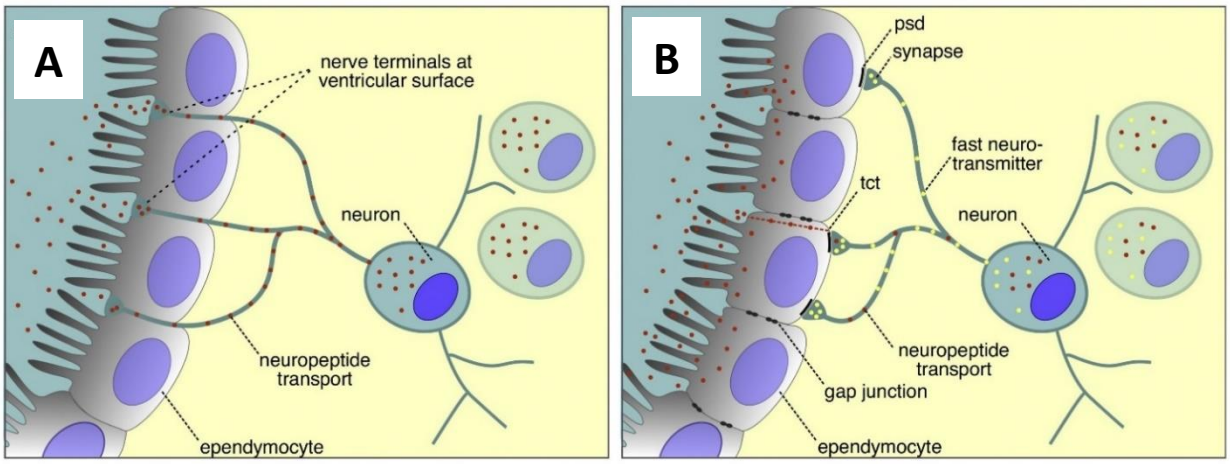

Figure 8. Direct (A) and amplification (B) mechanisms of neuropeptide diffusion via CSF. Modified from Alpár *et al.* (2019).

The features of peptidergic secretion described thus far in the present work come from studies generally conducted in rodents. In fact, the regulated secretory pathway has been poorly investigated in human neurons until recently, when the use of human induced pluripotent stem cells has shed some light into the matter (Hook et al., 2014; Merkle et al., 2015).

According to a recent study conducted in induced pluripotent stem cells, human DCV main characteristics are similar to the previously described in rodents. In particular, human DCV trafficking dynamics (i.e. faster in axons than in dendrites), secretion efficiency (i.e. low and intensity-demanding), SNARE and Ca^{2+} dependencies are consistent with rodent studies (van de Bospoort et al., 2012; Emperador Melero et al., 2017; Farina et al., 2015; Kwinter et al., 2009; De Wit et al., 2009). Furthermore, differences in maturation timings between peptidergic and classical neurotransmission have been described, being DCVs released at highest levels when there is a little SV secretion yet (Emperador Melero et al., 2017).

1.2. Gliotransmission

Traditionally, neuroscience has focused on the study of neurons to decipher and comprehend the mysteries of the brain. However, to really understand the functioning of such a complex organ, the role of glial cells could not be further underestimated. In the previous years, great advances have been made regarding glia and their communication with neurons (Perea et al., 2014). Even though glial cells were originally underrated to a mere agglutination role, today it is widely accepted that they participate in many other cerebral functions (i.e. homeostasis, metabolism, neurotransmission) (Allen and Barres, 2009; Souza et al., 2019).

Glial cells can be classified into macroglia (constituted by astrocytes and oligodendrocytes) and microglia, all of them in continuous communication with neurons in order to achieve their functional purposes (Zeng et al., 2018). Astrocytes are the most numerous kind of glial cell found in the CNS and they represent the most adaptable and multifunctional type of glia (Bass et al., 1971; Zorec et al., 2016). Curiously, astrocytes (i.e. astroglia) owe their name to their star-shaped morphology (Kimelberg and Nedergaard, 2010), whereby they can also be classified into different subtypes: protoplasmatic and fibrous (Tabata, 2015).

Protoplasmatic astrocytes display a greater number of branches than the fibrous ones, and they are found in grey or white matter, respectively (Lanjakornsiripan et al., 2018). It is precisely due to such branches and ramifications that astrocytes contact with synapses and blood vessels to perform key energetic functions (Schwarz et al., 2017). Noteworthily, the main processes attributed to astroglia are actually carried out by protoplasmatic astrocytes, whereas the role of fibrous astrocytes is still not entirely understood (Souza et al., 2019; Tabata, 2015).

Astrocyte important functions include ion homeostasis, neurotransmitter removal, regulation of energy and metabolism at synapses, preservation of the blood brain barrier (BBB) and secretion of gliotransmitters (i.e. transmitters and modulators as glutamate, D-serine, ATP; neurotrophins and peptides as NPY, BDNF, atrial natriuretic peptide – ANP) (Bonansco et al., 2011; Mathiisen et al., 2010; Simard and Nedergaard, 2004; Zorec et al., 2016). Besides, astrocytes communicate with each other via a gap-junctions, which enable them to work together as a glial network or syncytium and to carry out processes as ion buffering or elimination of toxins (Giaume and Liu, 2012; Ma et al., 2016).

Beyond the clearance of neurotransmitters and ions, astrocytes are active participants of synaptic transmission thus integrating and controlling synaptic processes (Perea et al., 2009). A bidirectional intercommunication exists between astroglia and neurons at the synaptic level, which has been termed as tripartite synapse (Volterra and Bezzi, 2002). According to the tripartite synapse model, astrocytes are considered to be the third constitutive element of synapses, surrounding presynaptic and postsynaptic terminals (Figure 9) (Halassa et al., 2007). It is proposed that secreted neurotransmitters are recognised by astrocyte metabotropic receptors, which trigger an increase in intracellular Ca^{2+} and the subsequent release of gliotransmitters (Santello et al., 2012).

However, since the first studies of astrocyte secretion were published, great controversy has been elicited regarding gliotransmission Ca^{2+}-dependence and its functional implications *in vivo*. It seems that, even though astrocyte transmission is not limited to, it is mostly mediated by Ca^{2+} (Savtchouk and Volterra, 2018). Multiple evidences indicate that astrocytes are able to release molecules through many mechanisms, some dependent and other independent of Ca^{2+} signalling. Different frequencies, cellular locations and origins of Ca^{2+} transients will trigger diverse specific responses, such as gliotransmitter vesicular or non-vesicular release (Bazargani and Attwell, 2016; Verkhratsky et al., 2016).

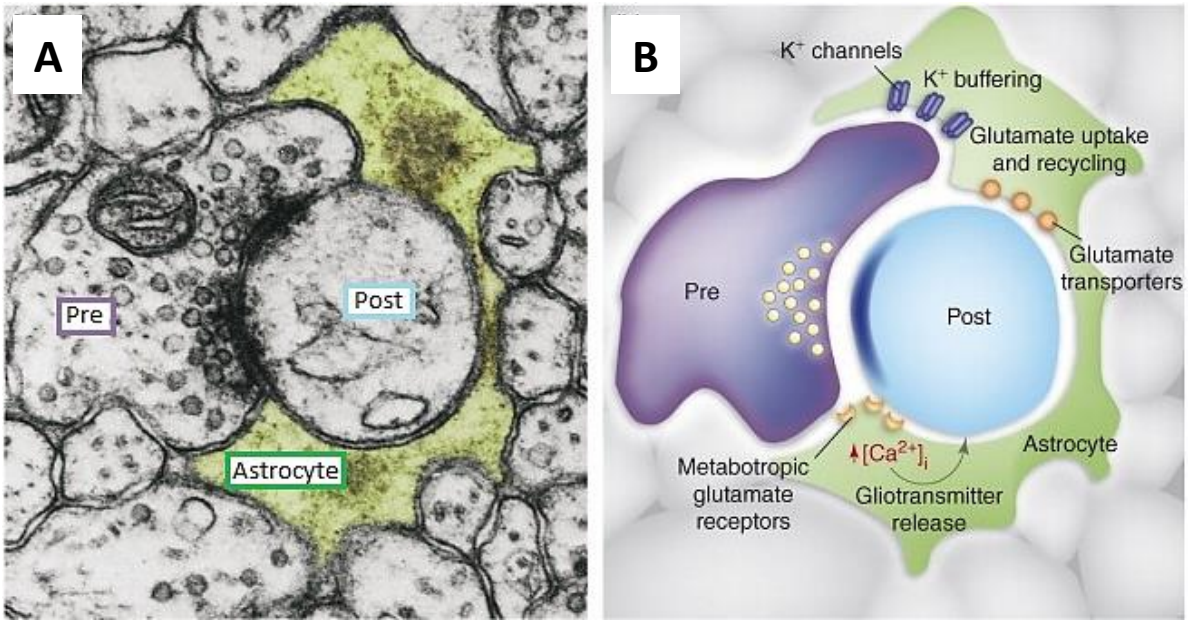

Figure 9. Electron micrograph (A) and representative schema (B) of a tripartite synapse. Modified from Halassa, Fellin and Haydon (2007).

Regarding non-vesicular neurotransmitter release, two main processes exist in astrocytes: channel-mediated diffusion and transporter-dependent extrusion (Verkhratsky et al., 2016). Glutamate and ATP are released by diffusion via anionic channels, connexins and P2X7 receptors (Liu et al., 2006; Scemes et al., 2007; Suadicani et al., 2006). Otherwise, astrocyte GABA secretion is operated by the GABA-transporter 3 with inversed functioning (Unichenko et al., 2012). Glutamate, though, may also be released by antiporter transport proteins as the cysteine/glutamate antiporter (Fiacco and McCarthy, 2018).

Glutamate release from astrocytes ultimately modulates neuronal networks locally or distantly (Matos et al., 2018). However, after being taken up, it is not only destined to gliotransmission (Souza et al., 2019). Glutamate may enter the glutamate-glutamine cycle, an ATP-consuming and astrocyte-exclusive reaction that transforms glutamate into glutamine, which is released to ensure fast glutamate regeneration in neurons (Tani et al., 2014). Moreover, glutamate is used to synthesize and release glutathione, which is a crucial anti-redox unevenness defender (Dringen and Hirrlinger, 2003). Lastly, glutamate may undergo oxidative degradation to become pyruvate, thus resulting in another lactate supply for neurons (Anderson and Swanson, 2000).

Interestingly, glutamate secretion in astrocytes occurs from vesicular exocytosis, as well (Guček et al., 2012). In fact, astrocytes display different vesicles whereby amino acid and peptidergic transmitters can be released in a Ca^{2+} dependent manner (Verkhratsky et al., 2016). Amino acid transmitters, such as glutamate and D-serine, are stored and released in small and clear vesicles similar to neuronal synaptic vesicles (i.e. synaptic-like micro vesicles – SLMVs). Neuropeptides as BDNF and ANP are incorporated and secreted in larger vesicles that resemble neuronal DCVs (i.e. DCV-like) (Calegari et al., 1999; Parpura and Zorec, 2010).

Besides SLMVs and DCVs, other releasable vesicular organelles are found in astrocytes. Astrocytic lysosomes, for instance, may act as secretory lysosomes and release their content (e.g. proteolytic enzymes and ATP) following stimulation (Li et al., 2008; Verderio et al., 2012). Moreover, endocytosis of extracellular components into recycling vesicles and their following release occur in astrocytes as well, which are crucial processes that contribute to CSF composition and functioning of the glymphatic system (Thrane et al., 2014; Vardjan et al., 2014).

Diverse Ca^{2+} sources exist in astrocytes that contribute to vesicular secretion. Extracellular Ca^{2+} entrance via store-operated Ca^{2+} channels (SOCCs) and voltage-gated Ca^{2+} channels (VGCCs), participate in astrocyte vesicular release (Sakuragi et al., 2017; Yaguchi and Nishizaki, 2010). However, increases in intracellular Ca^{2+} promoting astrocyte exocytosis are mainly caused by the efflux of Ca^{2+} ions from internal stores as the ER and mitochondria (Parpura et al., 2011). That is, astrocytes sensing of synaptic and extrasynaptic signals cause local intracellular Ca^{2+} elevations which are further amplified by Ca^{2+}-mediated receptor activation and subsequent Ca^{2+} efflux from internal stores (Figure 10) (Semyanov, 2019).

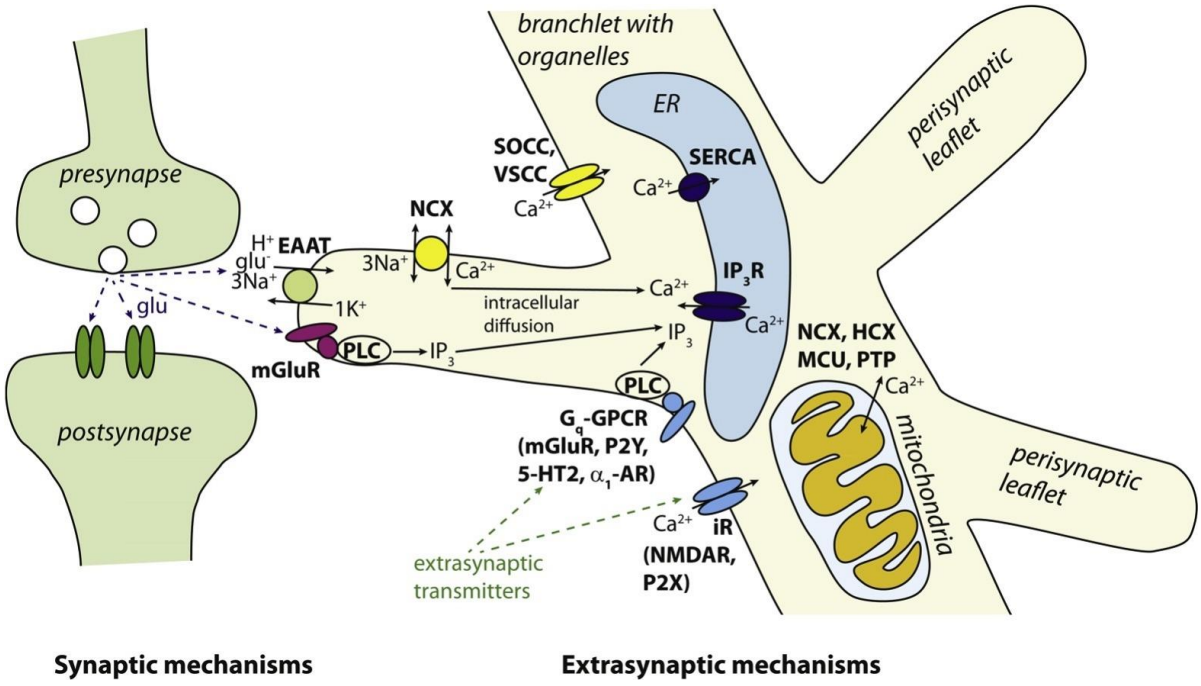

Figure 10. Synaptic and extrasynaptic activity mechanisms for signal sensing and Ca^{2+} amplification in astrocytes. Extracted from Semyanov (2019).

Ca^{2+} enters the ER via the sarco-endoplasmic reticulum Ca^{2+}-ATPase (SERCA), whereas it exits the ER due to activation of ER receptors as ryanodine receptors and inositol tri-phosphate receptors (IP3R) (Hua et al., 2004). After Ca^{2+} elevation at micromolar concentrations, Ca^{+2} ions are internalized in mitochondria via mitochondrial Ca^{2+} uniporters (MCUs) (Williams et al., 2013). Nanomolar Ca^{2+} concentrations, however, cause the entrance of Ca^{2+} into mitochondria via H^+/Ca^{2+} exchangers (HCXs) (Santo-Domingo and Demaurex, 2010). Ca^{+2} efflux from mitochondria is mediated by mitochondrial permeability transition pores (MPTPs) and Na^+/Ca^{2+} exchangers (NCXs) (Rizzuto et al., 2012).

Two main mechanisms mediate astrocyte sensing of synaptic signals and amplification of local Ca^{2+} increases. Firstly, astrocytic synaptic branches uptake glutamate via excitatory amino acid transporters (EAAT), which cause an increase in Na^{+} (Danbolt, 2001). In turn, excess of Na^{+} must be removed in exchange with Ca^{2+} via NCX inverse functioning, thus causing Ca^{2+} local increases (Kirischuk et al., 2016). Secondly, synaptic glutamate interacts with metabotropic receptors at astrocyte membranes which activate phospholipase C (PLC) and the subsequent increase of IP3. As IP3R agonists, both Ca^{2+} and IP3 promote Ca^{2+} release from the ER (Sherwood et al., 2017).

Extrasynaptic mechanisms of signal sensing and Ca^{2+} amplification exist in astrocytes, as well. Neurotransmitters and gliotransmitters diffuse far from synaptic sites thus becoming extrasynaptic signals which target astrocyte receptors (both metabotropic and ionotropic) (Araque et al., 2014). Glutamate and ATP ionotropic receptors (i.e. NMDAR and P2XR, respectively) cause direct Ca^{2+} influx from the extracellular space when activated by extrasynaptic glutamate or ATP (Palygin et al., 2010). Otherwise, activation of metabotropic receptors for glutamate, ATP, serotonin and adrenoreceptors (i.e. mGluR, P2Y, 5-HT2 and α1-AR, respectively) cause the subsequent production of IP3, which promotes Ca^{2+} release from the ER (Kirischuk, 1996; Kirischuk et al., 1995; Porter and McCarthy, 1995).

In addition to Ca^{2+}-mediated Ca^{2+} release mechanisms, astrocytes display intrinsic Ca^{2+} oscillations that arise independently of external signals (Aguado et al., 2002; Nett et al., 2002; Oheim et al., 2018). Spontaneous Ca^{+2} fluctuations diverge in time and size, are found in small astrocyte microdomains and occur both *in vitro* and *in situ* (Sun et al., 2014). Mechanisms participating in astrocyte spontaneous Ca^{2+} events include IP3R-dependent spontaneous efflux from ER, Ca^{2+} entrance via the plasma membrane and opening of mitochondrial MTPs (Agarwal et al., 2017; Aguado et al., 2002; Berridge et al., 2003; Pankratov and Lalo, 2014; Rungta et al., 2016).

Astrocyte regulated secretion relies on multiple proteins that constitute the molecular machinery of gliotransmission (Bohmbach et al., 2016; Paco et al., 2009). As in neurons, synaptotagmin proteins act as Ca^{2+} sensors of astrocyte vesicular secretion (Zhang et al., 2004). Astrocytic synaptotagmin isoforms include synaptotagmins 4, 5, 7 and 11 whereas neuronal synaptotagmins 1 and 2 are apparently absent in astrocytes (Mittelsteadt et al., 2009; Wilhelm et al., 2004). In turn, some variations exist regarding astrocytic and neuronal SNARE isoforms (Guček et al., 2012).

In particular, VAMP2 and syntaxin-1 are found both in neurons and astrocytes, even though VAMP3 is additionally expressed in many astrocytes (Bergersen and Gundersen, 2009; Paco et al., 2009). After interacting with syntaxin-1 and VAMP2, SNAP23 (astrocytic equivalent of the neuronal SNAP25) maintains vesicles tethered for longer times (Montana et al., 2009). Both astrocyte SLMVs and DCVs may display VAMP2 or VAMP3 in vesicle membranes (Verkhratsky et al., 2016). Differently, VAMP7 (or tetanus neurotoxin insensitive-VAMP) is the vesicular SNARE responsible of astrocyte secretory lysosome fusion (Verderio et al., 2012).

Other important astrocyte secretion machinery includes vesicular neurotransmitter transporters as VGLUT, VGAT, vesicular nucleotide transporter (VNUT) and D-serine transporter, which are key for the entrance of glutamate, GABA, ATP and D-serine into SLMVs, respectively (Bezzi et al., 2004; Blakely and Edwards, 2012; Martineau et al., 2013). As in neurons, astrocytic DCVs rely on members of the secretogranin family as SgII and SgIII for cargo concentration and vesicle biogenesis (Calegari et al., 1999; Paco et al., 2009, 2010).

Each astrocytic secretory organelle has specific Ca^{2+} requirements to achieve fusion. For instance, slow and constrained Ca^{2+} increases are needed for secretory lysosomes to fusion, whereas secretion of SLMVs is associated to Ca^{2+} spikes (Li et al., 2008; Verderio et al., 2012). Vesicle trafficking is also differently affected by determined Ca^{2+} levels in astrocytes. SLMVs containing glutamate move faster when intracellular Ca^{2+} levels rise, whilst trafficking of secretory lysosomes and DCVs decelerate (Potokar et al., 2010; Stenovec et al., 2007).

Astrocytic exocytosis has been determined to happen in a much slower timescale than neurons (usually <0.5ms) (Südhof, 2012); that is, a considerable delay (generally > 1min) exists between intracellular Ca^{2+} increase and secretion (Vardjan et al., 2016). In detail, SLMVs positive for VGLUT markers fuse hundreds of milliseconds after Ca^{2+} rises (Bezzi et al., 2004). Secretion of astrocyte DCVs occurs around minutes after stimulation (Paco et al., 2009; Prada et al., 2011; Ramamoorthy and Whim, 2008), in the same manner than for secretory lysosomes (Li et al., 2008). The most significant characteristic features of astrocyte vesicular secretory organelles described thus far are summarized in Table 1.

	SLMVs	DCVs	Secretory Lysosomes
Size (nm)	30 – 100	100 – 600	300 – 500
Appearance	Clear, lucent	Dense-core	Not so dense
Vesicle formation	Plasma membrane recycling vesicles	Golgi apparatus-nascent vesicles	Lysosomal organelles with LAMP1 and cathepsin D
Molecular machinery	VGLUT	SgII SgIII	VNUT
Fusion machinery (vesicle SNAREs)	VAMP2 VAMP3	VAMP2 VAMP3	VAMP7
Stimulation to fusion delay	> 100ms	> 1min	> 1min
Released transmitters	Glutamate D-serine ATP	BDNF ANP NPY ATP	ATP Cathepsin B Proteolytic Enzymes

Table 1. Characteristic features of astrocyte SLMVs, DCVs and secretory lysosomes. Modified from Guček, Vardjan and Zorec (2012) and Verkhratsky *et al.* (2016).

Important peptide transmitters as BDNF, NPY and ANP are synthesized in astrocytes and released following regulated stimulation in DCVs (Calegari et al., 1999; Krzan et al., 2003; Paco et al., 2009; Ramamoorthy and Whim, 2008). Such transmitters exert key physiological functions as synapse modulation and regulation of neurotransmitter availability and recycling at synapses (Verkhratsky et al., 2016). BDNF, for instance, is a strong controller of synaptic plasticity (Poo, 2001), NPY is a potent regulator of neuronal proliferation and growing of vascular tissue (Geloso et al., 2015) and ANP regulates brain blood and salt intake (Potter et al., 2009).

Astrocyte secretion of peptidergic transmitters as neuropeptides and hormones is also crucial for the regulation of other important neuroendocrine physiological functions as metabolism, fluid homeostasis, circadian rhythms and reproduction (MacDonald et al., 2019). Besides, as constitutive elements of the BBB, astrocytes are not only direct targets but also regulators of circulating hormones and peptides throughout the CNS (Abbott et al., 2006).

1.3. Neurotransmission and gliosecretion in brain pathologies

Understanding the physiological mechanisms of regulated secretion is key to comprehend the dysregulations in neurotransmission and gliotransmission that occur in many cerebral disorders (Verkhratsky et al., 2017; Volk et al., 2015). Alterations of classical and peptidergic transmission have been evidenced in several brain diseases as ischemia, epilepsy, schizophrenia, autism, cognitive impairment and other neurological and neurodegenerative diseases (Hynd et al., 2004; Meyer-Lindenberg et al., 2011; Sah and Geracioti, 2013).

Neurotransmission and synaptic plasticity are strongly affected by the immune system (Limanaqi et al., 2019). Glial cells trigger variable responses after brain damage, which are known as reactive gliosis (Burda and Sofroniew, 2014). Even though astrogliosis has been traditionally considered detrimental, several findings have shown that interfering astrogliosis can aggravate the progression of the damage (Nobuta et al., 2012; Okada et al., 2006). In fact, two different types of reactive astrocytes have been described: A1 astrocytes, which are harmful to synapses, and A2 astrocytes, which are considered to be protective (Liddelow et al., 2017).

Astrocyte reactivity is acknowledged as the expression of intermediate filament proteins as glial fibrillary acidic protein (GFAP) increases (Pekny et al., 2014). Moreover, overexpression of other proteins as lipocalin 2 (LCN2) have been reported in reactive astrogliosis (Zamanian et al., 2012). In addition to morphological changes, reactive astrocytes also undergo variations in the secretion of immunomodulators (Waschek, 2013). Vesicle delivery is affected in reactive astrocytes and alterations in gliotransmission (i.e. release of cytokines, amino acids, peptidergic transmitters and growth factors) has been linked to the pathological mechanisms of several brain disorders (Allan and Rothwell, 2001; Brosseron et al., 2018; Halassa et al., 2007).

According to a biological model of astrocyte activation, astrocyte activity may range from hypoactive to hyperactive stages, being the physiological states at the middle (Figure 11). Hypoactive astrocytes display decreased gliotransmission and NMDAR activity, whilst in hyperactivated astroglia increased Ca^{2+} fluctuation frequencies, gliotransmission and NMDAR functioning are exhibited (Halassa et al., 2007). Therefore, imbalances caused by astrocyte hypoactivation have been related to disorders as schizophrenia whereas hyperactive astroglia has been linked to pathologies as epilepsy (Rajkowska et al., 2002; Tian et al., 2005).

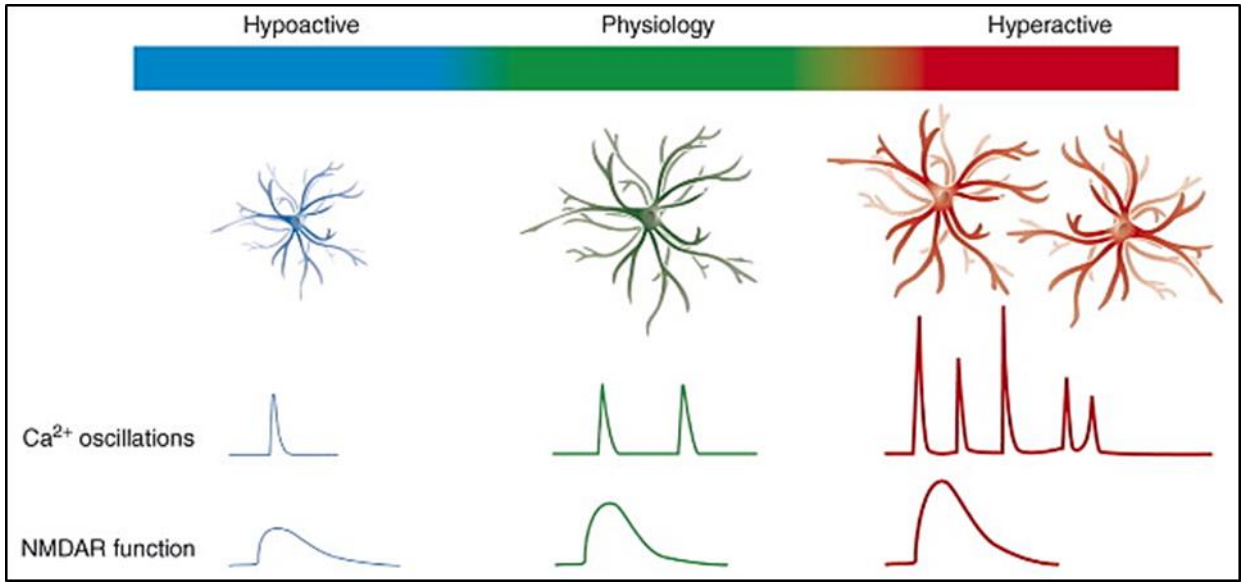

Figure 11. Activation spectrum of astrocytes in physiological and pathological states. Extracted from Halassa, Fellin and Haydon (2007).

In neurodegenerative diseases, besides reactive astrogliosis, another profound alteration occurs in astrocytes which is known as astrodegeneration and is evidenced as astrocyte aberrant homeostatic functioning and atrophy (Scuderi et al., 2013). Both reactive and atrophic profiles may coexist in time and cerebral region in normal aging and dementia indicating that when atrophy prevails over reactivity, progression of neurological deficits is promoted (Olabarria et al., 2010; Yeh et al., 2011). Besides, abnormal Ca^{2+} dynamics is evidenced in astrocytes located at prefrontal and entorhinal cortical regions, which may contribute to the susceptibility of these specific areas to neurodegeneration (Verkhratsky, 2019).

Alterations in Ca^{2+} signalling and, subsequently, in neurotransmitter release have been described in neurons in the context of neurodegenerative diseases, as well (Mattson and Chan, 2003; Moreth et al., 2013). In fact, disturbances in glutamate neurotransmission may be related to the pathological processes occurring in neurodegenerative disorders (Hynd et al., 2004). Other characteristic features of neurodegeneration include aggregation and accumulation of disease-related proteins, lysosomal and autophagy disfunction and abnormal mitochondrial functioning (Katsnelson et al., 2016). Altogether, intercellular communication processes in the brain are clearly affected in neurodegenerative diseases and represent an important target not only for therapeutic interventions but also to further comprehend the pathological mechanisms underlying disease.

2. Alzheimer's disease

2.1. Epidemiology and physiopathology

Alzheimer's disease (AD) is the most prevalent neurodegenerative disorder and the most frequent cause of dementia worldwide (Wolters and Ikram, 2018). Currently, 50 million people are suffering from dementia: AD-dementia representing around two thirds of the cases and the other third being due to vascular dementia, mixed dementia or dementia with Lewy bodies or frontotemporal degeneration (Alzheimer's Disease International, 2018). With annual costs of hundreds of billion dollars, AD has an enormous impact on society and economy (Deb et al., 2017).

AD primarily affects the cerebral cortex, causing cognitive dysfunction and memory loss (Sun et al., 2018). Core AD histopathological hallmarks are extracellular amyloid-β (Aβ) plaques and intracellular aggregates of hyperphosphorylated tau protein (i.e. neurofibrillary tangles – NFTs) (Selkoe and Hardy, 2016). Other AD pathological features include gliosis (Acosta et al., 2017), neuronal degeneration (Kamat et al., 2016) and granulovacuolar degeneration (GVD) bodies (i.e. membrane-bound vacuoles that accumulate in tauopathies) (Wiersma et al., 2019). In addition, synaptic dysfunction and synapse loss are early events occurring in AD pathogenesis which, together with impaired hippocampal neurogenesis, may contribute to the initiation of the cognitive impairment (Moreno-Jiménez et al., 2019; Tönnies and Trushina, 2017).

According to diagnostic criteria, AD can be divided into diverse clinical stages, i.e. preclinical AD, mild cognitive impairment (MCI) and AD dementia (McKhann et al., 2011), which may be prolonged in time more than decades (Morris, 2005). In spite of all the scientific advances, early clinical diagnosis is still difficult, considering the comorbidities and lack of entire correlation between histological alterations and clinical symptoms (Hyman et al., 2012). Besides, while imaging techniques provide information about amyloid deposition in patients, other pathological hallmarks of AD as synapse loss, gliosis and GVD are tough to quantify *in vivo* (Hane et al., 2017).

In the past 20 years, really few from hundreds of AD drugs have been approved, being solely useful for symptom management (Alzheimer's Association, 2018). Thus, in the coming years, research on disease-modifying drugs together with new early intervention and prevention strategies will be crucial and will represent a huge challenge for science (Long and Holtzman, 2019).

2.2. Hypotheses on the etiopathogenesis

AD is a complex disease with multifactorial triggering causes that can be grouped into genetic (70%) and environmental (30%) (Dorszewska et al., 2016). Genetic factors include hereditary or spontaneous mutations in genes associated with the amyloid precursor protein (APP), accounting for familial AD (FAD) or sporadic AD (SAD), respectively (Campion et al., 2016). Genes responsible for early-onset FAD are primarily APP itself and proteins associated with APP processing, as presenilin 1 (PSEN1) and presenilin 2 (PSEN2) (Lanoiselée et al., 2017). Otherwise, age, chromosomal sex and apolipoprotein E (APOE) are well-established risk factors for late-onset SAD (Riedel et al., 2016).

APOE is released in the brain principally by astrocytes (followed by microglia and neurons) and, as a protein of the cholesterol metabolism, it exerts key functions for synapse formation and maintenance (Xu et al., 2006). Three APOE isoforms exist in humans, which influence synaptic proteins as PSD-95 and Syp specifically (APOEε4 > APOEε3 > APOEε2) (Love et al., 2006). Besides, carrying a single copy or two copies of APOEε4 is associated with 3-fold or 12-fold greater AD risk, respectively (Holtzman et al., 2011). In AD patients, APOEε4 is linked to an earlier onset and a faster disease progression (Agosta et al., 2009) while most of late-onset AD cases are associated with double APOEε3 carriers (Wolfe et al., 2019).

Based on a great number of scientific evidences several theories have been postulated on the etiopathogenesis of AD, among which the following represent the two major hypotheses (Sochocka et al., 2017): the “amyloid cascade hypothesis” (Hardy and Allsop, 1991) and the “inflammation hypothesis of AD” (Krstic and Knuesel, 2013).

According to the amyloid cascade hypothesis, an increase in the levels of Aβ is an initiating event in AD (Selkoe and Hardy, 2016). An incorrect processing of APP into the Aβ-peptide in the brain induces an imbalance between the production and clearance of Aβ, raising the relative levels of the most self-aggregating forms of the peptide, which results in the formation of aberrant Aβ-plaques that will lead to neuronal degeneration, dementia and eventually death (Hardy and Selkoe, 2002).

APP is a membrane protein processed by three proteases known as "secretases" (α, β and γ-secretases) due to the secretion that undergo their cleaved substrates (Haass, 2004). β-secretase is also known as BACE and the γ-secretase complex includes PSEN1 and PSEN2 as its catalytic subunit (Haass and Selkoe, 2007). Two main APP processing pathways exist: the amyloidogenic pathway (promotes Aβ production) and the anti-amyloidogenic pathway (avoids Aβ formation).

In the anti-amyloidogenic processing of APP (Figure 12A), α-secretase activity followed by γ-secretase finally results in the liberation of a truncated Aβ peptide called P3, which is irrelevant to the pathology (Haass *et al.*, 2012). In the amyloidogenic pathway (Figure 12B), production of Aβ occurs by the combined activity of β and γ-secretases. BACE-mediated processing liberates a large truncated peptide which corresponds to the ectodomain of APP (APPsβ) together with a carboxyterminal portion (βAPP CTF), which is subsequently cleaved via γ-secretase activity (Selkoe and Hardy, 2016). Consequently, generated Aβ is released extracellularly and may reach fluids as plasma or CSF (Haass *et al.*, 2012).

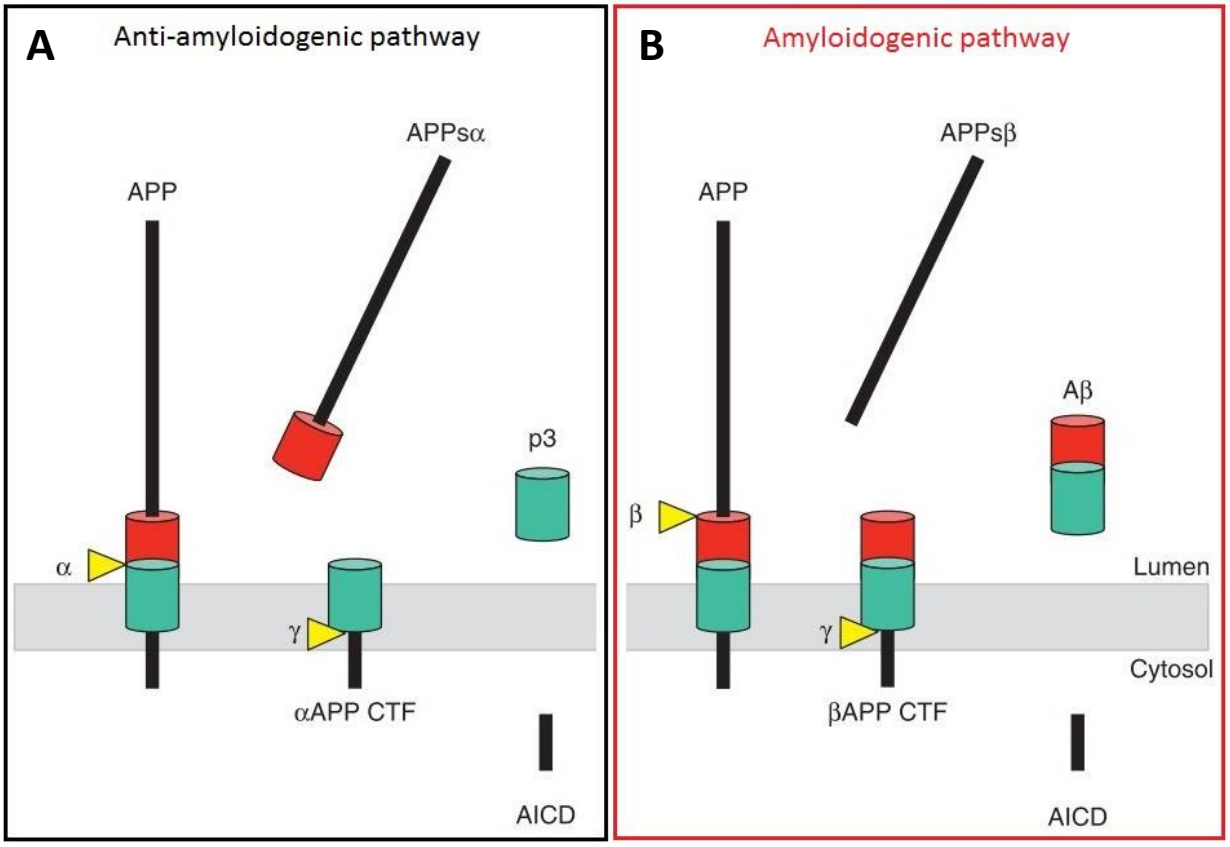

Figure 12. APP proteolytic processing via the anti-amyloidogenic (A) and the amyloidogenic (B) pathways. Modified from (Haass et al., 2012)

Mutations in APP may lead to early-onset FAD by means of two different mechanisms: rising the general production of all Aβ forms (e.g. APP mutations surrounding the β cleavage location and APP duplications) or generating Aβ species as Aβ42 and Aβ43, which are much more susceptible of aggregation (e.g. mutations within the Aβ sequence in APP) (Lanoiselée et al., 2017). Differently, all the diverse mutations in presenilins seem to decrease cleavage processivity, rising the relative production of larger aggregation-prone Aβ forms, which is suggested to occur in some SAD cases, as well (Szaruga et al., 2015).

The connection between the Aβ deposition and the tau pathology is not completely understood (Israel et al., 2012). Diverse evidences point towards the requirement of Aβ-plaques for the development of the tauopathy in AD (Long and Holtzman, 2019). In fact, human studies have determined that the progression of the tau pathology from the entorhinal cortex to the neocortex does not occur when the Aβ accumulation is missing (Pontecorvo et al., 2019; Wang et al., 2016a). Besides, live imaging techniques of amyloid and tau pathologies performed longitudinally in AD patients have evidenced that Aβ deposition levels predict the beginning of the tauopathy which, in turn, predicts the decline of cognitive functions (Hanseeuw et al., 2019).

The original amyloid cascade hypothesis has been ampliated with the lately proposed theory of "the cellular phase of AD" (De Strooper and Karran, 2016). According to this hypothesis, AD pathology pre-symptomatically begins with the Aβ deposition and the tauopathy (i.e. biochemical phase), which are initially well-tolerated alterations until cellular homeostasis is gradually disrupted (i.e. cellular phase) prompting the development of cognitive symptoms (i.e. clinical phase) (Salta and De Strooper, 2017). Thereby, the disease would only be clinically acknowledged whenever cellular homeostatic functions and physiological processes stop working appropriately.

During the cellular phase, the impairment of the neurovascular unit together with alterations in calcium signalling and neurotransmission drive the dysfunction of neuronal and glial activity which ultimately lead to neurodegeneration and cognitive impairment (Long and Holtzman, 2019). Diverse factors may promote the cellular phase of AD, including impaired glucose metabolism and mitochondrial dysfunction, which are both early events in AD pathology (Caldwell et al., 2015; Habeck et al., 2012). Mitochondrial dysfunction is especially relevant as it seems to be pivotal for the onset of neuroinflammation (Pugazhenthi, 2017).

In fact, inflammatory responses strongly correlate with the onset and progression of AD in humans (Van Eldik et al., 2016). As postulated in the inflammation hypothesis of AD (Figure 13), chronic inflammation and ageing-derived cellular stress affect the cytoskeleton structural integrity and alter the axonal transport, which may drive accumulation of APP and formation of NFTs (Krstic and Knuesel, 2013).

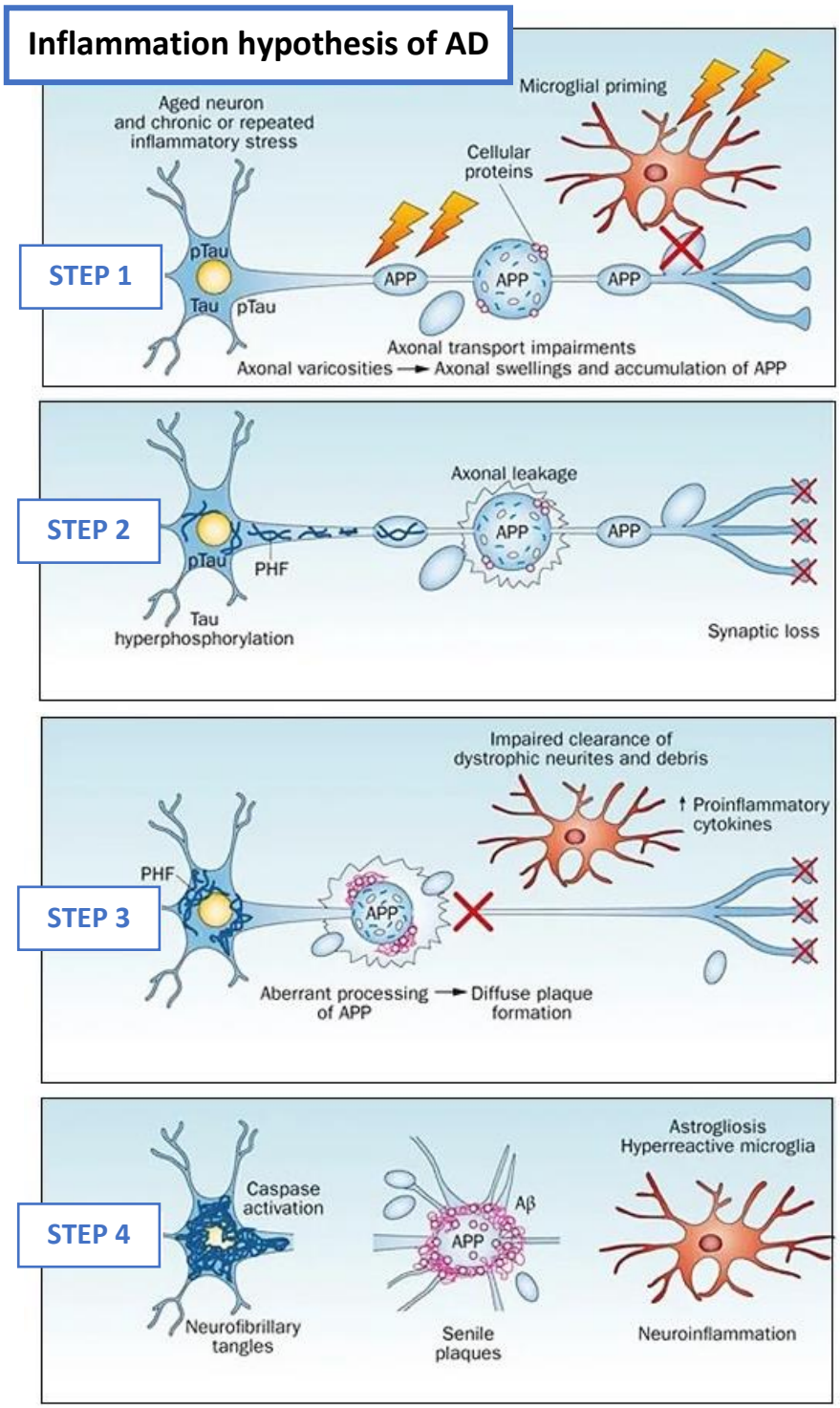

Figure 13. The inflammation hypothesis of late-onset AD. Modified from Krstic and Knuesel (2013).

According to this model, cellular stress associated with neuronal ageing would trigger the development of axonal varicosities that are extruded and eliminated by neighbouring glial cells (Doehner et al., 2012). During chronic inflammation (due to infection, disease or ageing), hyperphosphorylated tau damages axonal transport (Kanaan et al., 2011) and stress-driven APP accumulates in larger axonal protuberances together with mitochondria and other organelles (step 1) (Shahpasand et al., 2012). This situation would also prepare microglia for the immune tasks that may consequently occur (Krstic et al., 2012).

Consequently, impairment of axonal transport may drive the destabilization of synapses (with the subsequent synapse loss), the development of paired helical filaments (i.e. precursor forms of NFTs) in dystrophic neurites and axonal leakage (step 2) (Iijima-Ando et al., 2012; Xiao et al., 2011). Then, inappropriate functioning of hyperreactive surrounding microglial cells may lead to alterations in the clearance of dystrophic neurites and to the production of neurotoxic proinflammatory conditions (step 3) (Krstic and Knuesel, 2013). Lastly, axonal loss together with the neighbouring proinflammatory signals would drive the development of NFTs and the subsequent neuronal death (step 4) (Kocherhans et al., 2010).

Neuronal modulatory signals keep microglial functions in a controlled silent homeostatic status, which is altered in neurodegenerative diseases (Sheridan and Murphy, 2013). As aforementioned, dysregulations in this homeostatic microglial phenotype promote a shift into an hyperreactive inflammatory state which would contribute to the spreading of the tauopathy (Bolós *et al*., 2016). Besides, due to their close relationship with Aβ accumulations, microglial cells are crucial mediators of AD progression (Condello *et al*., 2015). Thus, not only Aβ has an effect in neurons (i.e. pre-conditioning the synaptic pathology) but also it triggers gradual alterations in microglia that induce and accelerate onset and disease progression (Simon *et al*., 2019).

Astrogliosis is another clear hallmark of AD pathology, especially around Aβ plaques (Acosta *et al*., 2017). In fact, Aβ promotes the activation of both astroglia and microglia, which occurs early in the progression of AD, even before the formation of Aβ plaques (Ahmad *et al*., 2019). Augmented production of proinflammatory cytokines results in increased oxidative stress, which mediates synaptic dyshomeostasis (Avila-Muñoz and Arias, 2014). Importantly, it has been evidenced that oxidative stress promotes tau pathology and synapse dysfunction in AD (Kamat *et al*., 2016).

Another core feature of AD pathogenesis is the loss of neurons in diverse cerebral regions, which starts during the preclinical phase of AD (i.e. before the formation of Aβ depositions and NFTs) and correlates with the cognitive manifestations (Long and Holtzman, 2019). The proposed mechanism of neuronal death in AD involves Aβ and NFT-mediated activation of caspases, which drive mitochondrial damage and activation of downstream effectors that ultimately lead to the apoptotic death of cells (Ribe et al., 2008).

Even though neuronal loss is mainly detrimental, selective neuronal death in AD has been proven to be beneficial against Aβ-mediated injury and cognitive impairment (Coelho et al., 2018). Several stress factors as impaired neuronal activity, synapse and energy metabolism affect each neuron differently and favour fitness variances between neurons (Coelho and Moreno, 2019).

Neuronal networks can be reorganized during neuronal damage, as dysfunctional neurons result more harmful for the circuit than the elimination of them from the circuit itself (Kim and Kim, 2016; Yaron and Schuldiner, 2016). Thus, the "neuronal competition hypothesis of AD" (Figure 14) postulates that individuals displaying effective neuronal competition mechanisms may be at lower risk of suffering from AD than those with a less efficient system (Coelho and Moreno, 2019).

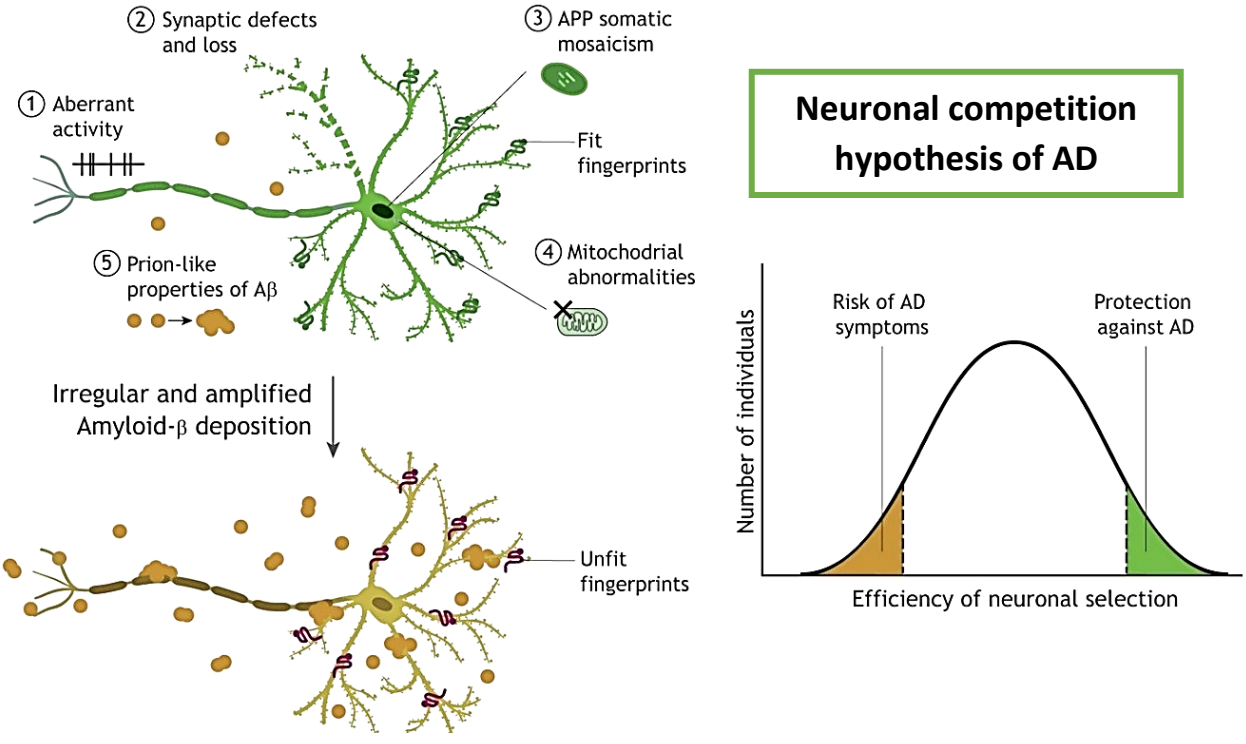

Figure 14. The neuronal competition hypothesis of AD. Modified from Coelho and Moreno (2019).

2.3. Animal models

It is nowadays widely accepted that AD starts many years before the manifestation of clinical symptoms but the study of such pathological early features is still difficult (Sperling et al., 2011). Investigating AD in animal models is key to ensure a better understanding of AD physiopathology, especially at initial stages of the disease (Nilsen et al., 2012). The use of genetically modified animal models facilitates the study of AD triggering factors, disease progression, therapeutics and biomarkers (Sasaguri et al., 2017). Additionally, several non-transgenic inducible animal models for AD have also been developed (Chen et al., 2013; Höglund et al., 2020; Lahmy et al., 2013).

The perfect transgenic model has to imitate several aspects of the human pathology, which should include the involvement of analogous cells and structures, similar causation origin and time course progression (Sosa et al., 2012). Moreover, an appropriate AD model should enable the study of cognitive functions as learning and memory, the application of brain imaging techniques and the examination of body fluids (i.e. blood and CSF) (Do Carmo and Cuello, 2013). Since the creation of the first effective transgenic mouse model of AD (Games et al., 1995), several useful mouse models have been defined (Dietrich et al., 2018). Most of them are based in genes involved in the familial type of AD (i.e. APP, PSEN1 and PSEN2) and display diverse features of AD pathology as Aβ depositions, inflammation and, in some cases, tau phosphorylation and behavioural impairments (Esquerda-Canals et al., 2017).

After the first mouse models of AD, which were based in APP mutations (Games *et al*., 1995; Hsiao *et al*., 1996), several other APP models were developed, presenting either one or two mutations in APP (e.g. APP Swedish mutation in the APP23 model or both APP swedish and Indiana mutations in the J20 model) (Sasaguri et al., 2017). First models, however, nedeed high APP overexpression to acomplish plaque formation and displayed no taupathology (Dietrich et al., 2018). As mouse models obtained exclusively with presenilin mutated genes exhibited increased levels of Aβ42 but lacked amyloid plaques, models combining APP and PSEN1 transgenes were developed. These models, such as APP/PS1 and 5xFAD mice, presented an earlier onset and a faster disease progression than monogenic lines (Esquerda-Canals et al., 2017).

In detail, the 5xFAD mouse model combines APP Swedish, Florida and London mutations with two PSEN1 mutations (M146V and L286V) and develops a rapid amyloidosis exhibiting Aβ depositions from 2 months of age, followed by significant extracellular Aβ plaques from 3 months (Dietrich et al., 2018; Oakley et al., 2006). Early cognitive alterations have been described in this model at 6-7 months of age (Lee et al., 2019), whereas greater cognitive impairment is evidenced at 9-10 months (Schneider et al., 2014), coinciding with synaptic degeneration and neuronal loss (Esquerda-Canals et al., 2017; Oakley et al., 2006; Spangenberg et al., 2016). Given the early neuropathological alterations and the subsequent functional and behavioral disorders, 5xFAD mice are considered a very suitable model to study AD (Gurel et al., 2018; Schneider et al., 2014).

Since mutations in tau are absent in 5xFAD mice, neurofibrillary tangle pathology is not evidenced in this model (Oakley et al., 2006; Stancu et al., 2014). To overcome this limitation, researchers developed triple transgenic models combining mutations in APP, PSEN and tau, such as the 3xTg-AD mouse model, which develop tauopathy in addition to the amyloid pathology (Oddo et al., 2003). However, even though mouse models may not display every single feature of AD, as might be the lack of tau pathology in several transgenic mice (Israel et al., 2012), they are still crucial for 1) comprehending interactions between genetic factors and the Aβ accumulation, 2) identifying new therapeutic targets and 3) evaluating effects of disease-modifying strategies on clinical symptoms recapitulation (Ribe et al., 2008).

Rat models for AD have been developed as well, which exhibit several advantages compared to mice: their larger body enable the application of difficult surgical procedures, they are physiologically closer to humans and display a more complex behavioural profile (Do Carmo and Cuello, 2013). A significant transgenic rat model for AD is the TgF344-AD model, which carries mutations in APP and PS1, develops progressive Aβ accumulation from 6 months of age and seems to display tau pathology from 16 months (Cohen et al., 2013). However, in other similar transgenic rat models with APP/PS1 mutations, amyloid pathology but no tau pathology have been described (Flood et al., 2009; Leon et al., 2010).

2.4. Biomarkers

Up-to-date, confirmative diagnosis of AD is only attainable post-mortem and extensive research is being done to find biomarkers that contribute to earlier detection (Lashley et al., 2018). Suitable AD biomarkers must be quantifiable indicators that enable evaluation of disease progression (Hane et al., 2017). AD biomarkers can be classified according to diverse research strategies or contexts of use as onset prediction, risk stratification, diagnosis, prognosis and drug-response monitoring (Molinuevo et al., 2018). The most well-established AD biomarkers include image biomarkers and fluid biomarkers (i.e. CSF and blood biomarkers) (Lewczuk et al., 2017).

Regarding image biomarkers, magnetic resonance imaging (MRI), X-ray ultrasound, positron emission tomography (PET) and single photon emission computed tomography are frequently used for diagnosis (Prescott, 2013). For instance, MRI is employed to assess AD-derived brain structural alterations, as atrophy in temporal and parietal regions, which correlate with cognitive impairment (Frisoni et al., 2010). Otherwise, fluorodeoxyglucose-PET technology enables the tracking of low glucose metabolism, which has been associated with reduced synaptic activity, whereas amyloid-PET imaging facilitates the recognition of Aβ plaques *in vivo* (Falgàs et al., 2019).

Blood biomarkers are highly advantageous indicators compared to imaging and CSF biomarkers, since they are less invasive and more cost and time-effective (Lista et al., 2013). Even though the search for appropriate blood AD biomarkers has been difficult, as many of the alterations encountered reflect systemic changes rather than brain alterations (Lewczuk et al., 2017), a correlation between plasma Aβ levels and brain Aβ load has been recently evidenced (Nakamura et al., 2018). In relation to tau pathology, the detection of t-tau or p-tau in neuron-derived blood exosomes seems to enhance accuracy for tau as a blood biomarker (Fiandaca et al., 2015).

As CSF directly interacts with the brain and reflects its biochemical alterations, CSF AD biomarkers may offer a clearer perspective into the several features of AD pathogenesis (Dhiman et al., 2019). Three core CSF biomarkers for AD have been stablished: decreased Aβ42 and increased total-tau protein (t-tau) and phosphorylated-tau (p-tau) (Figure 15) (Blennow and Zetterberg, 2018). CSF Aβ42 inversely correlates with cerebral Aβ accumulation (Ashton et al., 2018), whereas p-tau indicates the levels of tau that is phosphorylated and t-tau provides information about the severity of AD neurodegeneration, even though is not a disease-specific marker (Sato et al., 2018).

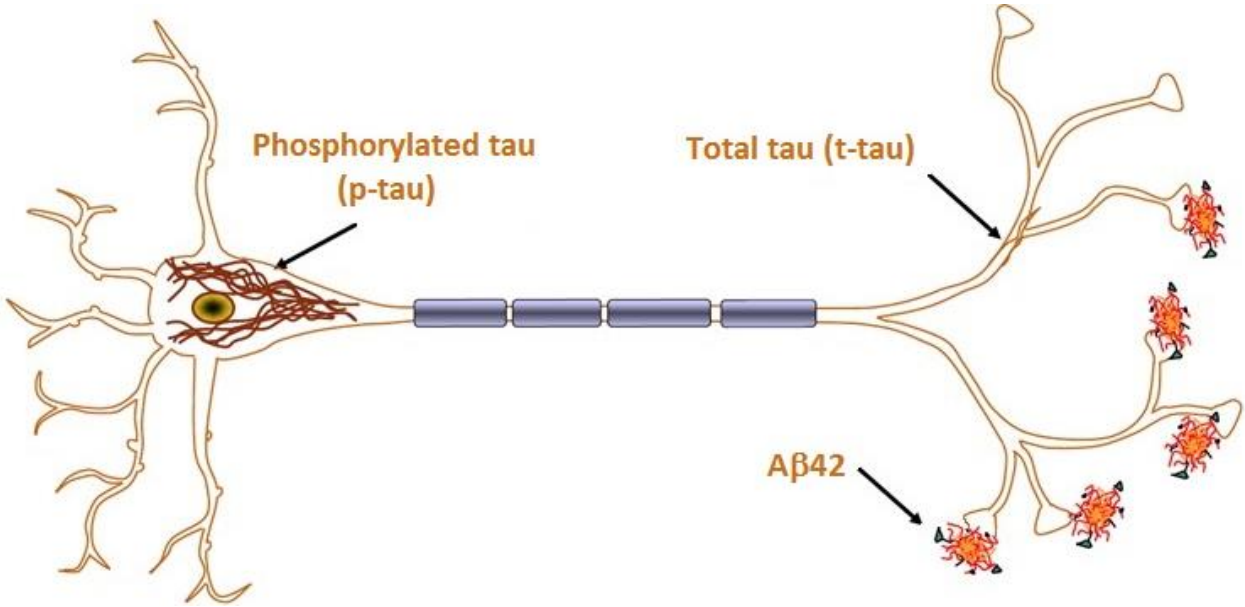

Figure 15. Core CSF biomarkers for AD. Modified from Blennow and Zetterberg (2018).

The combination of these three core CSF biomarkers markers is specific for identifying an individual with preclinical AD (Dubois, 2018). Consequently, according to CSF biomarker profile and neuropathological criteria, diverse phases of AD have been defined (Dubois, 2018; Hane et al., 2017): in preclinical AD, in spite of being cognitively normal, individuals already display altered CSF core AD biomarkers; then, in the prodromal stage of AD, patients display a mild cognitive impairment (MCI) together with alterations in the CSF biomarker profile, which are also present in the AD-dementia phase, when cognitive functions are extremely affected.

The severity of dementia can be measured using several approaches, as is the Clinical Dementia Rating (CDR) (Morris, 1997), which assesses the grade of dysfunction in patients according to exercises that test memory, orientation, problem solving and daily-life activities. With a CDR result of 0 individuals are considered cognitively normal while scores of 0.5, 1, 2 and 3 represent questionable, mild, moderate and severe dementia, respectively (Long and Holtzman, 2019). CDR is a highly effective and extensively used method, but it requires the collection of a great quantity of data from patients and informants. Thus, other easier-performing tests as the Mini-Mental State Examination (MMSE) are being used as an alternative indicator for dementia staging in AD. MMSE score equivalence with CDR is: 30 for cognitively normal, 26 – 29 for questionable, 21 – 25 for mild, 11 – 20 for moderate and 0 – 10 for severe dementia (Perneczky et al., 2006).

The major AD pathological hallmarks develop differently during the course of the disease (Figure 16). Levels of the diverse biomarkers vary before (CDR = 0) and after the onset (CDR = 0.5) and progressive decline (CDR = 1 – 3) of cognition (Long and Holtzman, 2019). Initially, preclinical AD is well established by an early Aβ accumulation, which is evidenced by a decrease in CSF and plasma levels of Aβ42 and augmented signalling on amyloid-PET (Counts et al., 2017).

Simultaneously, neuroinflammatory alterations (i.e. astrocyte and microglia activation) are revealed (Ahmad *et al.*, 2019), which are later followed by the development of the tauopathy from medial cerebral regions to the neocortex, evidenced by an increase in CSF p-tau levels (Dhiman et al., 2019). Synaptic alterations and neuronal loss begin with the advance of the tau pathology and may be determined by image analysis of hippocampal and cortical structures (Scheff et al., 2006, 2007). Of note, a correlation exists between the onset and development of cognitive decline with tau and hippocampal volume but not with the Aβ load (Long and Holtzman, 2019).

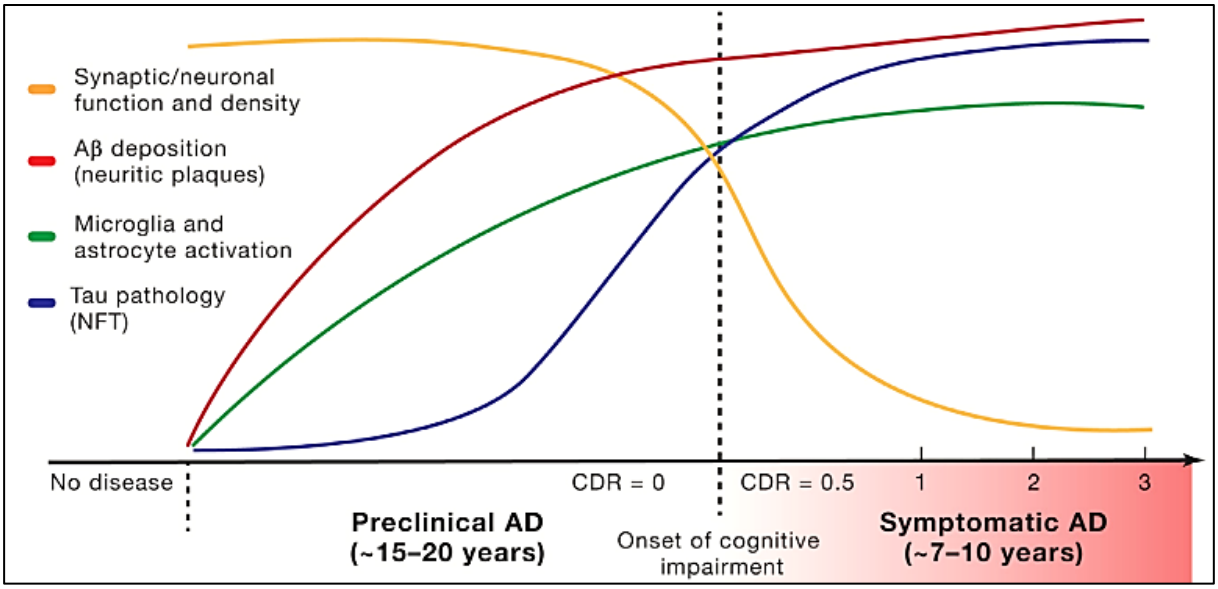

Figure 16. Time course development of major AD pathological events. Extracted from Long and Holtzman (2019).

In preclinical AD subjects are cognitively normal yet already display impaired core CSF biomarkers and such alterations are maintained during the whole course of the disease (i.e. from preclinical to prodromal and AD-dementia) (Dubois B. 2018). Hence, there is an urgent need for new CSF biomarkers that change during the course of the disease, in order to enhance diagnostic precision and to identify further abnormalities involved in AD pathogenesis (Blennow et al., 2010; Molinuevo et al., 2018; Vinters, 2015).

Accordingly, changes in CSF levels of several molecules related to the amyloid pathology have been investigated in the search for complementary AD biomarkers. For instance, CSF levels of the inhibitor of cysteine proteases Cystatin C (CysC), which is a secretory protein that has been reported to bind Aβ (Ghidoni et al., 2011), are significantly reduced in AD patients (Fagan and Perrin, 2012). CysC is also reduced in the CSF of patients with dementia with Lewy bodies (Maetzler et al., 2010), which makes the decrease in CSF CysC consistent across diseases coursing with amyloid pathology (Mathews and Levy, 2016).

In addition to amyloid pathology and tauopathy, neuroinflammation and synapse loss are associated with AD and correlate with the cognitive decline (Condello et al., 2015; Selkoe, 2002). Thus, CSF biomarkers for these alterations may be valuable for monitoring disease prognosis and the grade of cognitive impairment (Duits et al., 2018). Glial activation has been associated with neuronal dysfunction and changes in synaptic plasticity in AD and, consequently, the identification of CSF biomarkers for glial activation has gained interest (Lashley et al., 2018). In fact, several studies have reported increased CSF levels of diverse astrocyte and microglia markers as YKL-40, TREM2 and CD14 (Guo et al., 2009; Heslegrave et al., 2016; Kester et al., 2015). However, as astrogliosis is a common feature in other neurodegenerative diseases, glial associated CSF biomarkers are generally not sensitive and specific enough to be suitable for direct use in clinical diagnosis (Brosseron et al., 2018).

Regarding biomarkers for synaptic degeneration, neurogranin has been proposed as a CSF biomarker for synapse loss associated with AD, as its concentration is increased in AD patients (Hellwig *et al*., 2015). Similarly, other candidate markers for synapse dysfunction have been suggested, as SNAP25 and synaptotagmin 2 (Bereczki *et al*., 2018; Brinkmalm *et al*., 2014). Nevertheless, further studies are required to validate candidate biomarkers as many have been identified by means of high throughput techniques (Lashley *et al*., 2018). Given the severity of AD, the search for new biomarkers is especially needed, not only as a method of improving therapeutic strategies but also to better understand and track disease physiopathology and development in patients.

It is of particular interest to find accurate and specific markers that correlate with synapse loss and cognitive impairment. Although changes in the nonpeptidic secretory pathways have been evidenced in AD, the impact of the disease on peptide secretion has been poorly studied. Thus, considering synaptic dysfunction and synapse loss as key events in AD pathogenesis, an impairment of the peptidergic regulated secretion may be suggested in AD, as well. In fact, granins have been proposed as potential CSF biomarkers for neuronal disorders including AD (Bartolomucci et al., 2010). Additionally, previous investigations in our laboratory have demonstrated that SgIII and CPE are abnormally accumulated in both neurons and reactive astrocytes in the cerebral cortex of AD patients (Plá et al., 2013).

Therefore, a major hypothesis in this study is that peptidergic transmission is altered in AD. Consequently, the main goal of this dissertation has been investigating alterations in the secretory markers of DCVs in the cerebral cortex and CSF of patients and animal models of AD.

OBJECTIVES

OBJECTIVES

The ultimate aim of this dissertation is to analyze alterations in the secretory markers of dense-core vesicles in the cerebral cortex and cerebrospinal fluid of patients and animal models of Alzheimer's disease.

It is the object of this study to fulfill the subsequent specific objectives:

1. To study astrocyte peptidergic secretion dependence on intracellular Ca^{2+} under control and proinflammatory conditions.

2. To examine alterations of DCV secretory markers in the brain and CSF of AD patients, as novel disease biomarkers.

3. To investigate changes in the levels of secretory proteins in the cerebral cortex and CSF of the 5xFAD mouse model for familial AD.

MATERIALS AND METHODS

MATERIALS AND METHODS

Animals. CD1 mice were acquired from the Laboratory Animal Service of the University of Barcelona to obtain astrocyte cultures, acute brain slices, brain histological sections and CSF. Neuroinflammation was induced in CD1 mice by intraperitoneal injection of lipopolysaccharide (LPS) (Sigma-Aldrich, Diesenhofen, Germany) at a dose of 5 mg LPS/kg of body weight. LPS was dissolved in saline to a concentration of 0.4 mg LPS/mL and injected mice were kept for 48h before the obtention of acute brain slices to perform secretion assays. Control mice (sham-injected) were injected with a volume of saline equally proportional to their weight. Additionally, 3, 6 and 12-month-old male 5xFAD transgenic mice (reference 006554, Jackson Laboratory) and their non-transgenic wild type (WT) littermates were used to obtain CSF, synaptosomes, brain tissue homogenates and histological sections. These specific ages were selected according to neuropathological staging of 5xFAD mice (Oakley et al., 2006). The 5xFAD mouse colony was maintained under the supervision of Dr. Teresa Fernández (Universidad Rey Juan Carlos, Madrid). Identification of the genotype was done by polymerase chain reaction according to Jackson Laboratory conditions. Mice were specific-pathogen-free and were housed together up to five mice per cage with controlled environment (22–25°C, 50% humidity and a 12-hour light/dark cycles).

Astrocyte primary cultures. Cerebral cortex from CD1 mice at the postnatal stage 2 were dissected and subjected to 0.25% trypsin and 0.01% DNase. Cells were seeded in flasks and grown in high-glucose Dulbecco's Modified Eagle's Medium and F-12 (1:1) supplemented with 10% fetal bovine serum, 10 mM HEPES and penicillin/streptomycin at 37ºC and 5% CO_2. At confluence (10-12 days), flasks were shaken overnight and cells were rinsed. Detached cells were sub-cultured on poly-D-lysine coated culture plates and coverslips. As previously described, our cultures were principally composed by astrocytes (around 92%) yet contained a minor percentage of microglia (around 5%), immature oligodendrocytes (around 3%) and were virtually devoid of neuronal cells (Paco et al., 2009). Astrocyte enriched glial cultures were maintained for 10-11 days in vitro. To acquire an enhanced activated phenotype, cultured astrocytes were treated with a cocktail of proinflammatory cytokines (TNFα, IFNβ and IL-1β) from PreproTech (Rocky Hill, NJ, USA) at a final concentration of 20ng/mL for 24h. Secretion experiments were performed right after.

Acute brain slices. Obtention of acute brain slices was performed as previously described (Aguado et al., 2002; Plá et al., 2017), with minor modifications. Briefly, adult CD1 male mice (sham and LPS-injected) were decapitated and their brains were rapidly removed and immersed in cold artificial cerebrospinal fluid (ACSF) (120mM NaCl, 3mM KCl, 10mM D-glucose, 26mM $NaHCO_3$, 2.25mM NaH_2PO_4 and 8mM $MgSO_4$) bubbled with 95% O_2 and 5% CO_2, where they were cut into 300µm-thickness horizontal slices with a vibratome (Pelco Vibratome Sectioning System™, Ted Pella, Redding, CA, USA). After a 2-3h stabilization in ACSF supplemented with 2mM $CaCl_2$, each slice was placed separately in a 12-well plate with ACSF and secretion experiments were performed right after. Slices were always preserved in oxygenated ACSF.

Secretion assays. Unstimulated secretion in astrocytes was studied in different times ranging from 30min to 24h. To study Ca^{2+} dependence during secretion 7.5µM cycloheximide, 100µM 1,2-bis o-aminophenoxy ethane-N,N,N′,N′-tetraacetic acid (BAPTA)-AM and 1µM thapsigargin were added to cultured astrocytes. Astrocyte regulated secretion was assessed 10min after the addition of 1µM ionomycin to the culture media. Secretion experiments in acute brain slices were performed in 55mM KCl and 68mM NaCl ACSF. Secretory proteins in the media were precipitated with trichloroacetic acid and were analyzed by western blot.

Live calcium imaging. Intracellular Ca^{+2} levels in astrocyte cultures were visualized with the membrane-permeant acetoxymethyl ester of fluo-3 AM dissolved in 1:1 w/v dimethyl sulfoxide with 0.001% pluronic acid. Cells were incubated with a 2µM solution of fluo-3 AM in Dulbecco's modified eagle medium for 30min and then washed. Recordings of Ca^{+2} changes were imaged in a ZEISS LSM 880 confocal laser scanning microscope (Carl Zeiss Microscopy GmbH, Jena, Germany) with a 60x water-immersion objective at 37ºC and 5% CO_2. Fluo-3 fluorescence images were collected at 3s intervals (4 frames were averaged for each time point) at a single excitation wavelength (514nm) during periods of 10 to 30min.

Mouse hippocampal and cortical homogenates. Dissected cerebral cortices and hippocampi of 3, 6 and 12-month-old WT and 5xFAD mice (n=6/group) were sonicated 2 times during 30s using an ultrasonic probe in pH 7.4 ice-cold lysis buffer containing 50mM Tris–HCl, 150mM NaCl, 5mM $MgCl_2$, 1mM EGTA and protease inhibitor cocktail (Roche Diagnostics, Indianapolis, IN, USA). Protein concentrations were determined using the Pierce BCA Protein Assay Kit (Thermo Fisher Scientific, Waltham, MA, USA) and samples were analyzed by western blot.

Synaptosome preparation from mouse brains. Synaptosomal fractions were obtained from 3, 6 and 12-month-old WT and 5xFAD mouse brains (n=3-6/group) as previously described (Carmona et al., 2003), with minor modifications. Cerebral cortex and hippocampus were homogenized separately in 1ml of ice-cold 0.32M sucrose buffer with a Teflon/glass homogenizer. Homogenization was performed with 10 strokes at 600rpm. Homogenates were centrifuged at 3000xg and 4ºC for 2min and supernatants followed a centrifugation at 14000xg and 4ºC for 12min. Pellets were resuspended in ice-cold 0.32M sucrose buffer and transferred to ultracentrifuge tubes containing a discontinuous Ficoll gradient of 5%, 9% and 12% (vol/ vol) and centrifuged at 22500rpm and 4ºC for 35min in a Beckman Coulter Optima L-90K ultracentrifuge (Beckman Coulter Inc, Brea, CA, USA). After centrifugation, interfaces containing synaptosomes (9% Ficoll fractions) were obtained, resuspended in phosphate-buffered saline (PBS) and centrifuged at 14000xg and 4ºC for 12min. Subsequent pellets were resuspended in PBS with 1% Triton X-100 and 1% protease inhibitor cocktail. Protein concentrations were determined using the Pierce BCA Protein Assay Kit (Thermo Fisher Scientific, Waltham, MA, USA) and samples were analyzed by western blot.

Synaptosome preparation for transmission electron microscopy (TEM). Synaptosomes were resuspended in 55μL of cold 0.1M PBS, aliquoted (50μg) and centrifuged 2min at 14000xg. The pellet was fixed adding 500μL of a solution with 2.5% glutaraldehyde and 2% paraformaldehyde. Fixation was done at 14,000xg and 10ºC for 50min. The pellet was washed with cold PBS at 14000xg and 10ºC for 5min, repeating this step 3 times. The fixed pellet was dehydrated using acetone and infiltrated with eponate-12 resin without catalyst using mixes of 1:3,1:1 and 3:1 of eponate: acetone. Ultrathin slices were visualized with a JEOL J1010 80kV transmission electron microscope (JEOL Ltd, Tokyo, JA).

Release experiments from live synaptosome preparations. Obtained synaptosomes were resuspended in 100μL of cold pH 7.4 Krebs-HEPES medium containing 147mM NaCl, 3mM KCl, 10mM D-glucose, 1.5mM $CaCl_2$, 1.5mM $MgSO_4$ and 20mM HEPES. Then, 400μL of Krebs-HEPES buffer at 37ºC were added and samples were shaken during 5min at 300rpm. Afterwards, 100μL of 37ºC Krebs-HEPES buffer with the presence or absence of stimuli were added, depending on experiment conditions. Stimuli consisted in Krebs-HEPES medium supplemented with 330mM KCl. Then, samples were shaken at 300rpm for 5min to allow secretion. To finish the release experiment, samples were centrifuged 1min at 4ºC and 14000xg and supernatants were separated into new tubes, while pellets were resuspended in 25μL of lysis solution. To analyze secreted proteins by western blot, proteins in the supernatants were precipitated using trichloroacetic acid.

Murine CSF isolation. CSF was extracted from the cisterna magna compartment of CD1 mice (for preliminary analyses) and from 3, 6 and 12-month-old WT and 5xFAD mice (n=8-13/group) as previously described (DeMattos et al., 2002), with slight modification. Mice were anesthetized with ketamine/xylazine (100mg/kg:10mg/kg) and immobilized in a stereotaxic frame under a dissecting microscope. An incision was preformed from the skull to the thorax and skin and musculature were removed until meninges covering the cisterna magna were visible. Tissue above the cisterna magna was removed and the adjacent area was cleaned of any blood residue using a cotton swab. A borosilicate narrow capillary was used to puncture the arachnoid membrane covering the cistern. CSF instantly flowed out into the capillary because of pressure differences. CSF resulting volumes (3-12µL) were then transferred into Eppendorf tubes and visually inspected for possible blood contamination. Only visible clear CSF samples were considered for analysis. In addition, clear samples were immediately centrifuged 1.5min at 16000xg and 4ºC to remove any possible blood or cellular residue.

Human brain tissues and CSF samples. 7 non-AD and 7 AD (Braak V-VI) post-mortem human brain samples were provided by Dr. Isidre Ferrer from the Institute of Neuropathology Brain Bank IDIBELL at Hospital Universitari de Bellvitge (Bellvitge, Spain). Biopsied CSF samples were provided by Dr. Albert Lleó from the Hospital de la Santa Creu i Sant Pau (Barcelona, Spain) and were collected by lumbar puncture from living diseased AD patients (n=33) and from living healthy controls (n=33). This study was approved by the local ethic committee and it was carried out in accordance with the Declaration of Helsinki. All patients (or their nearest relatives) and controls gave informed consent to participate in the study. Extensive clinical, neuropsychological, magnetic resonance imaging and molecular examinations were performed in all subjects. Centrifugation at 4°C for 10min at 2000×g and storage of 500µL aliquots in polypropylene tubes at −80 °C were accomplished within 1h after collection. All AD patients fulfilled clinical criteria for probable AD according to the revised NIA-AA criteria (McKhann et al., 2011) and had a CSF biomarker profile consisting of decreased Aβ42 levels together with high t-tau and p-tau levels measured by immunoassays (Innogenetics, Ghent, Belgium), indicating high likelihood of being due to AD. The cut-off values used to define the study AD cohort were 550pg/mL for Aβ42, 350pg/mL for t-tau, and 70pg/mL for p-tau. The control group was defined according to the following criteria: objective cognitive performance within the normal range (performance within 1.5SD) in all tests from a specific test battery, clinical dementia rating scale score of 0, no significant psychiatric symptoms or previous neurological disease, and a non-pathological CSF biomarker profile. AD and control groups were well matched for age at the time of CSF collection.

Immunohistochemistry and immunocytochemistry. Right after CSF extraction, animals were transcardially perfused with a 4% paraformaldehyde solution and brains were removed from skull, post-fixed for 4h and cryoprotected in a 30% sucrose solution. Afterwards, brains were frozen and histological sections of 40µm were obtained using a Leica CM 3050 S cryostat (Leica Biosystems, Wetzlar, Germany). Brain sections were incubated in blocking solution 1h at RT. Incubation with primary antibodies was carried out overnight at 4°C. Cells were fixed in 4% paraformaldehyde in PBS 0.1M, washed in PBS and then pre-incubated for 1h in blocking solution. Incubation with primary antibodies was done overnight at 4ºC. Tissues and cells were incubated 1h at RT with fluorochrome-conjugated secondary antibodies (Alexa Fluor Secondary Antibodies, Thermo Fisher Scientific, Waltham, MA, USA). Preparations were visualized in a ZEISS LSM 880 Confocal Laser Scanning Microscope (Carl Zeiss Microscopy GmbH, Jena, Germany).

SDS-PAGE and western blotting. Cell media, lysates and media from release experiments in acute brain slices, as well as synaptosomes, synaptosomal release and CSF samples from WT and 5xFAD animals and human CSF, were electrophoresed in SDS-PAGE gels. Analyses of brain homogenates from both human and animal samples were performed in Criterion™ TGX (Tris-Glycine extended) Stain-Free™ precast gels from Bio-Rad Laboratories, which include trihalo compounds that allow rapid fluorescent detection of proteins with the Gel Doc™ EZ imaging systems (Bio-Rad Laboratories, Hercules, CA, USA). Proteins were transferred to polyvinylidene difluoride immobilization membranes, stained with Ponceau-S staining or visualized in the Gel Doc™ EZ imaging systems, blocked for 1h, incubated with primary antibodies overnight at 4ºC and 1h with horseradish peroxidase-conjugated secondary antibodies from Dako (Agilent Technologies Inc, Santa Clara, CA, USA). Bound antibodies were visualized with Clarity Western ECL Substrate (Bio-Rad Laboratories, Hercules, CA, USA). Blot images were captured with a scanner and densitometric values were obtained using ImageJ® software.

Primary antibodies. Antibodies used in the different experiments are listed in the table below.

Antibody	Company/Source	Reference
β-actin	Sigma-Aldrich (Diesenhofen, Germany)	A3854
Aβ	DAKO Agilent Technologies (Santa Clara, CA, USA)	M0872
APP	Abcam (Cambridge, UK)	ab2072
AT8	Innogenetics (Gent, Belgium)	90206
CgA	Abcam (Cambridge, UK)	ab15160

Antibody	Company/Source	Reference
CgB	Santa Cruz Biotechnology (Heidelberg, Germany)	sc-1489
CHMP2B	R&D Systems (Minneapolis, MN, USA)	MAB7509
CK1δ	R&D Systems (Minneapolis, MN, USA)	AF4568
CPE	BD Transduction Laboratories (San Jose, CA, USA)	610758
CPE	GeneTex (Irvine, CA, USA)	GTX11044
CPE	R&D Systems (Minneapolis, MN, USA)	AF3587
CysC	EMD Millipore (Burlington, MA, USA)	ABC20
GAPDH	EMD Millipore (Burlington, MA, USA)	MAB374
GFAP	EMD Millipore (Burlington, MA, USA)	MAB360
Iba1	GeneTex (Irvine, CA, USA)	GTX100042
IgM (human)	Jackson Immuno Research (Cambridgeshire, UK)	709-035-073
IgM (mouse)	Jackson Immuno Research (Cambridgeshire, UK)	715-035-140
LAMP1	Developmental Studies Hybridoma Bank (University of Iowa, Iowa, USA)	H4A3-c
LCN2	R&D Systems (Minneapolis, MN, USA)	AF1857
NFL	Cell Signalling Technology (Leiden, The Netherlands)	2835S
PC1	Abcam (Cambridge, UK)	ab3532
PC1	Thermo Fisher Scientific (Waltham, MA, USA)	PA1-057
PC1	Cell Signalling Technology (Leiden, The Netherlands)	11914S
PC2	Dr. Iris Lindberg (Maryland, BA, USA)	18BF
PC2	GeneTex (Irvine, CA, USA)	GTX23533
PC2	R&D Systems (Minneapolis, MN, USA)	AF6018
PSD-95	Thermo Fisher Scientific (Waltham, MA, USA)	MA1-046
SgIII	Sigma-Aldrich (Diesenhofen, Germany)	HPA006880
Syp	DAKO Agilent Technologies (Santa Clara, CA, USA)	M 0776

Table 2. List of used primary antibodies.

Statistical analysis. Quantitative data were statistically analyzed using GraphPad Prism 6.01® software (GraphPad Software, CA, USA). Non-parametric analysis of data was performed using a Kruskal-Wallis test followed by Dunn's multiple comparisons test. For two-group categorical variables non-parametric analysis was performed using a two-tailed Mann-Whitney test. All data are presented as the standard error mean (SEM). Significance was set at $p < 0.05$. Correlations of measured values were examined using the Spearman correlation coefficient. A significance cutoff of $p \leq 0.0019$ based on Bonferroni correction was applied.

RESULTS

RESULTS

1. Intracellular Ca^{2+}-dependence of astrocyte peptidergic secretion

In the regulated secretory pathway, proteins and peptides are secreted to the extracellular space in response to certain stimuli (i.e. increases in intracellular Ca^{2+}). Even though this route has been very well characterized in neurons and endocrine cells, its presence and role in astroglia is controversial, considering astrocyte non-excitable nature. Besides, while SV release have been extensively studied in astroglial cells, DCV secretion from astrocytes has been scarcely investigated.

In previous research from our laboratory, astrocytes were determined to specifically synthesize CPE and SgIII, two DCV secretory markers that belong to the regulated secretory pathway (Plá et al., 2017). In detail, DCV-contained proteins, mainly SgIII and CPE, were expressed in astrocytes in a lesser extent than in neurons and displayed variable release in response to increases in intracellular Ca^{2+} (Paco et al., 2010; Plá et al., 2017).

The current section of the present dissertation aims to further comprehend astrocyte peptidergic secretion and its Ca^{2+}-dependence, both under release-stimulation and non-stimulation conditions. Thus, secretion experiments *in situ* and *in vitro* were performed to analyze the release of endogenous astrocyte secretory proteins as DCV-markers (i.e. CPE and SgIII) and other astrocyte-released proteins as is the extracellular inhibitor of lysosomal cysteine proteases Cystatin C (CysC).

Understanding the mechanisms of fundamental astrocytic processes as peptidergic secretion is crucial, since alterations in Ca^{2+} signalling and gliotransmitter release have been described in neurodegenerative diseases as AD (Mattson and Chan, 2003; Moreth et al., 2013; Verkhratsky, 2019). Moreover, reactive astrogliosis has been associated to AD synaptic dysfunction (Brosseron et al., 2018; Van Eldik et al., 2016). Hence, we investigated the expression and release mechanisms of astrocyte secretory proteins in two models likely promoting reactive astrogliosis, both *in situ* (in an LPS-induced neuroinflammation mouse model) and *in vitro* (in cultured astrocytes treated with proinflammatory cytokines).

Release of astrocyte secretory proteins in LPS-induced neuroinflammation *in situ*

As formerly described, CPE and SgIII were detected in pyramidal neurons and astroglial cell bodies and processes in mouse cortical brain regions (Plá et al., 2013). Additional immunohistochemistry analyses revealed high expression levels of the protein convertases PC1 and PC2 in neurons of mouse cortical and hippocampal brain sections. However, expression of these protein convertases in astrocytes was not evidenced (data not shown). As seen in Figure 17A, PC2 was found mainly in pyramidal neurons and interneurons of the hippocampal CA1 region, whereas SgIII and CysC were also detected in astroglial-like cells. Astrocyte identity was corroborated with double immunolabeling with GFAP (data not shown).

To obtain a reactive astrocytic phenotype, an experimental mouse model of neuroinflammation was induced by intraperitoneal injection of lipopolysaccharide (LPS) derived from gram negative bacteria, as performed in similar studies (Aslankoc et al., 2018; Erickson and Banks, 2011; Gasparotto et al., 2017). Toll-like receptors (TLRs), a group of germline-encoded receptors from the innate immune system, mediate the effects of LPS (Takeda and Akira, 2004; Triantafilou and Triantafilou, 2002). In particular, LPS specifically binds to TLR4, whose expression is clear in microglia and remains under debate in astrocytes. Hence, astrocyte activation in the LPS-induced neuroinflammation model would be indirectly mediated by microglial signaling (Chakravarty and Herkenham, 2005; Lehnardt et al., 2003).

Glial reactivity in mouse brains after LPS injection was confirmed with peroxidase immunohistochemistry analyses of GFAP and ionized calcium binding adapter molecule 1 (Iba1), which are typically overexpressed in reactive astrocytes and microglia, respectively (Haim et al., 2015; Imai and Kohsaka, 2002; Suter et al., 2007). In LPS-injected mouse brains, GFAP immunoreactivity was markedly increased in astroglial cells after 48h, compared to sham-injected mice (Figure 17B). Similar results were obtained for Iba1 immunolabeling (data not shown).

To further validate the neuroinflammation model, expression of the secretory protein Lipocalin 2 (LCN2), an iron siderophore binding protein, was assessed in both control and LPS-injected mouse brains. LCN2 has been described as a marker of reactive astrocytic response in several studies performed in different brain injury models, including neuroinflammation (Jang et al., 2013; Jin et al., 2014; Lee et al., 2009; Naudé et al., 2012).

LCN2 was broadly overexpressed in glial-like cells of the cerebral cortex, behaving as an inflammatory acute phase protein. Double immunofluorescence labeling with GFAP identified astrocytes as the main cell type expressing LCN2 after 48h of LPS injection (Figure 17B). Constitutive LCN2 expression was observed in the choroid plexus, whereas acute expression of LCN2 was evidenced in endothelial cells and in the neuropil as a diffuse staining likely attributed to astrocytic branches (data not shown). LCN2 expression was negligible in microglia and neurons (not shown).

Besides, being determined as an endogenous astrocyte-specific secretory protein, LCN2 could be a useful tool for assessing the peptidergic regulated secretion in astrocytes *in situ*. Secretion experiments were then carried out in acute mouse brain slices 48h after LPS and saline (sham) injection, using KCl as a secretagogue, which induced intracellular Ca^{2+} increase in neurons and, indirectly, in astrocytes. As epithelial cells of the choroid plexus also displayed LCN2, this brain structure was removed from slices before secretion assays, in order to avoid interferences.

KCl-evoked release of CPE, LCN2 and CysC in the same acute brain slices from 48h control (sham) and LPS-treated mice was analyzed by western blot (Figure 17C). Control slices displayed a stimulated release of the DCV-protein CPE ($p = 0.004$) of around 600% compared to basal secretion (100%), which similarly occurred in LPS slices (665% evoked release, $p < 0.001$). CysC stimulated release did not show relevant variations compared to basal secretion, both in control and LPS slices ($p = 0.14$ and $p = 0.57$, respectively). Not surprisingly, LCN2 was not detected in the secretion media from control slices, as its expression in control tissue was extremely low. In 48h LPS-treated slices, however, LCN2 displayed KCl-evoked secretion (155%, $p = 0.03$), even though its stimulation degree was markedly lower than it was for CPE.

Because CPE and CysC were expressed in both astrocytes and neurons, their presence in the media from acute brain slices could have these two possible cellular origins. Besides, their differential responses to KCl-evoked release indicated the presence of a heterogeneity of peptidergic vesicles in both neurons and astrocytes. Additionally, our results suggested the existence of an astrocytic regulated secretion of LCN2 from acute brain slices *in situ*, in a mouse model of LPS-induced neuroinflammation. However, further experiments *in vitro* were required to specifically study astrocyte regulated secretion in a context devoid of neuronal cells, both in untreated and proinflammatory-treated astrocytes.

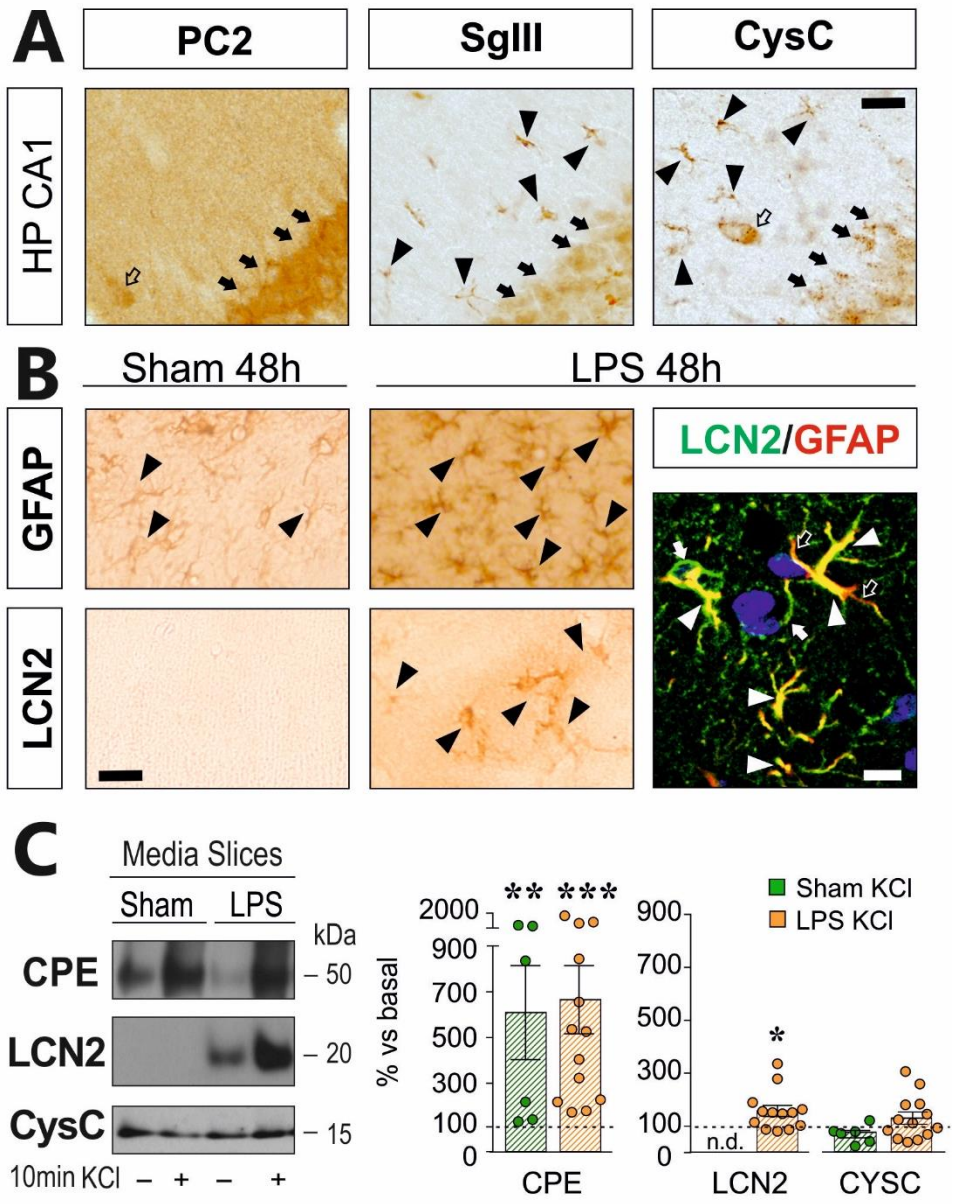

Figure 17. Astrocyte secretory proteins in LPS-induced neuroinflammation *in situ*. A. In peroxidase immunohistochemical analyses of mouse control hippocampal (HP) CA1 region PC2 is found mainly in pyramidal neurons (arrows) and interneurons (open-arrows), whereas SgIII and CysC are evidenced also in astroglial-like cells (arrow-heads). B. In LPS-injected mouse brains, GFAP and LCN2 are overexpressed in astroglial-like cells (black arrow-heads) after 48h. Astrocyte identity of LCN2+ (arrows; green) cells is confirmed in double immunolabeling with GFAP (empty-arrows; red). Arrow-heads show colocalization in yellow. C. Representative western blots (left) and summarizing graphs (right) of KCl-evoked release of CPE, LCN2 and CysC in the same acute brain slices from control (sham) and 48h LPS-treated mice. CPE secretion is evoked by KCl, both in control and LPS slices, whereas CysC stimulated release is maintained compared to basal secretion. LCN2 is not detected (n.d.) in the media from control slices. In the media from 48h LPS-treated slices, however, LCN2 is significantly increased in KCl-evoked release, even though its stimulation degree is markedly lower than for CPE. Data are presented as the mean ± SEM. Statistically significant difference is calculated using a two-tailed Mann-Whitney test. * indicates p-value < 0.05, ** indicate p-value < 0.01 and *** indicate p-value < 0.001. Scale bars in µm: A, 20; B, left, 15; right, 10.

Heterogeneity of exocytic peptidergic vesicles in astrocytes *in vitro*

To further investigate expression and release mechanisms of astrocyte secretory proteins *in vitro*, astroglial primary cultures were obtained from early postnatal mice. Besides, to acquire an enhanced astrocyte-activated phenotype, cultured astrocytes were treated with a cocktail of proinflammatory cytokines (i.e. TNFα, IFNβ and IL-1β) at a final concentration of 20ng/mL for 24h, as similarly performed in other studies (Von Boyen et al., 2004).

Immunocytochemical analyses revealed that astrocyte secretory proteins such as CPE, SgIII, LCN2 and CysC were distributed heterogeneously in diverse vesicle subtypes. Confocal immunofluorescence images displayed a poor colocalization of the DCV-contained peptides CPE and SgIII, thus evidencing the existence of differential DCV populations (Plá et al., 2017). Similarly, CysC displayed a markedly low colocalization degree with both CPE and SgIII (data not shown). Of note, double labeling of LCN2 and CysC revealed a colocalization of around 30% (Figures 18C and 18D), while LCN2 did not colocalize neither with CPE nor with SgIII (data not shown), indicating that they were located in different subcellular compartments.

To further characterize the different vesicle subpopulations, double immunofluorescence analyses were performed between secretory proteins and the lysosome-associated membrane protein 1 (LAMP1) (Figures 18A and 18B). Not SgIII neither CPE (not shown) colocalized with LAMP1, which was expected given the DCV nature of SgIII and CPE-containing vesicles. Otherwise, both LCN2 and CysC (not shown) -containing vesicles were positively stained for LAMP1, both showing a 28% of colocalization with the lysosomal marker, respectively (Figure 18D). These results were consistent with previous studies evidencing CysC in endosomal/lysosomal compartments (Deng et al., 2001; Lee et al., 2006).

Ca^{2+}-mediated release of secretory proteins is enhanced in proinflammatory-treated astrocytes

In previous research, DCV-contained proteins (i.e. CPE, SgIII, PC1, PC2) were typically secreted in cultured neurons in response to a depolarizing stimulus as KCl (Plá et al., 2017). Besides, CPE and SgIII were released in unstimulated conditions in astrocytic cells *in vitro* (Paco et al., 2010). However, in KCl-evoked conditions there was no significant increase in the release of SgIII and CPE in astrocytes, according to their non-excitable nature compared to neurons, and ionomycin-mediated stimulation enhanced the release of CPE but not of SgIII (Plá et al., 2017).

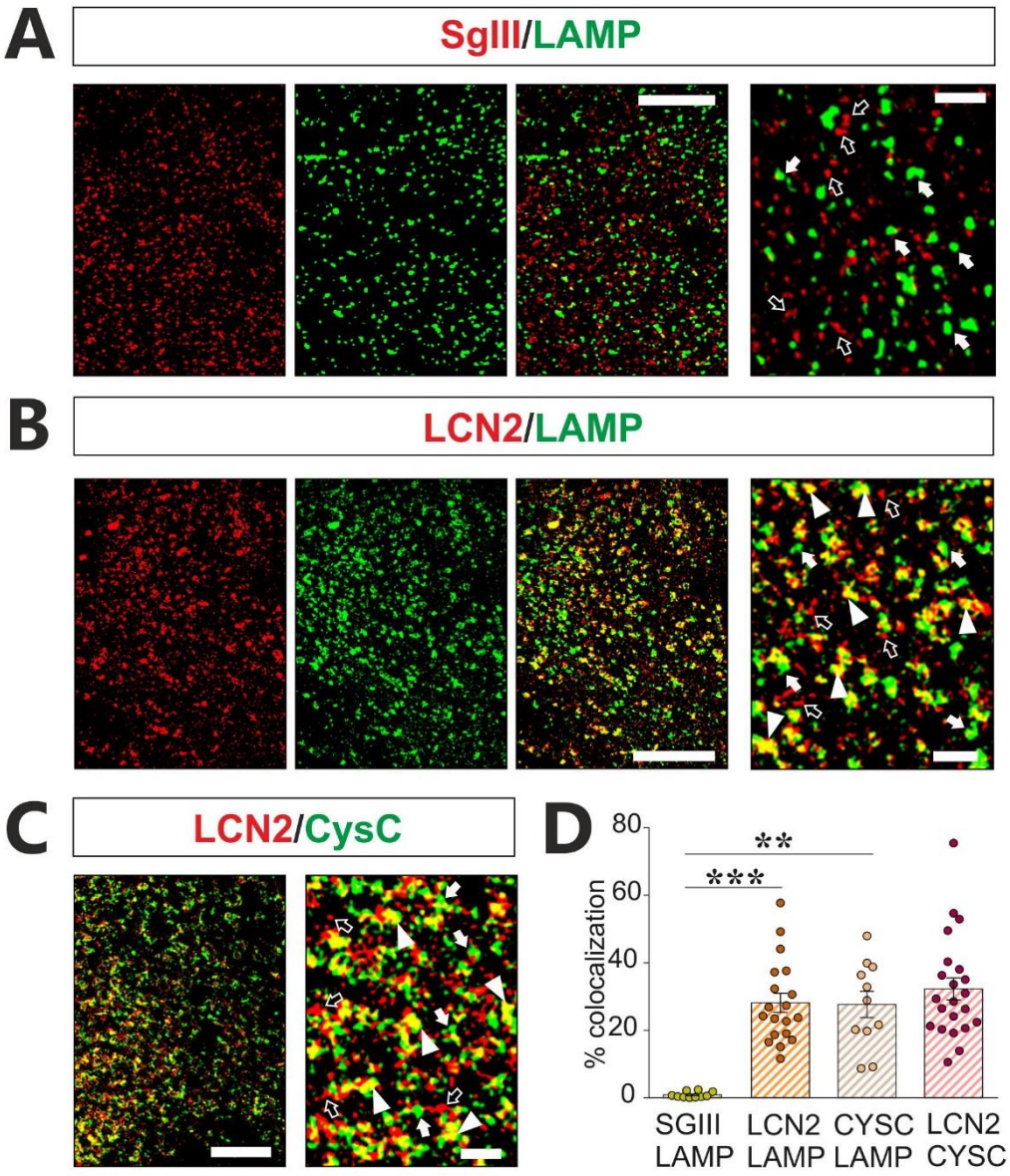

Figure 18. Heterogeneity of exocytic peptidergic vesicles in astrocytes *in vitro*. Double labeling of LCN2 (red; empty-arrows) and CysC (green; arrows) reveals a 32% of colocalization (yellow; arrow-heads) in cultured astrocytes. Colocalization of both LCN2 (28%; red) and CysC (28%; not shown) -containing vesicles with LAMP1 (green) are shown, differently from SgIII whose colocalization with LAMP1 is virtually null (0.86%; red). Scale bars in µm: A left, 13; A right, 4; B left, 17, B right 4; C left, 17; C right, 4. Data are presented as the mean ± SEM. Statistically significant difference is calculated using a Kruskal-Wallis test followed by Dunn's multiple comparisons test (D). ** indicate p-value < 0.01 and *** indicate p-value < 0.001.

To further study the release mechanisms of astrocyte peptidergic vesicles, additional secretion experiments were carried out in untreated and proinflammatory-treated astrocyte primary cultures, devoid of neuronal cells. After the addition of 1µM ionomycin for 10min, extracellular media were collected and concentrated and secretory proteins were evaluated by immunoblotting.

In untreated astrocytes (Figure 19A), release of CPE was significantly increased in response to ionomycin stimulation (210%, p = 0.03), whereas evoked release for LCN2 and CysC did not reach statistical significance (133%, p = 0.63 and 131%, p = 0.71, respectively). All proteins exhibited a substantially high basal release and their intracellular levels were invariable. In some cases, there was a low but consistent expression of LCN2 in control astrocytes, which presumably varied according to the intrinsic activation-state of astrocytes *in vitro*. Consequently, due to such low expression rates, LCN2 was not detected in the media from 10min basal release neither in the liberated content after 10min ionomycin stimulation in untreated astrocytes (data not shown).

Otherwise, after 24h of proinflammatory treatment, LCN2 was highly overexpressed compared to untreated cultured astrocytes. Under proinflammatory conditions, release of all analyzed secretory proteins was significantly increased following Ca^{2+}-mediated stimulation caused by ionomycin. CPE stimulated release was similar (259%, p = 0.0035) to the observed in untreated astrocytes. However, unlike in untreated astrocytes, LCN2 and CysC displayed an evoked release under proinflammatory treatment (200%, p = 0.0028 and 260%, p = 0.0076, respectively). Of note, LCN2 displayed high rates of basal release and was apparently less affected by extracellular Ca^{2+} entry in comparison to DCV-contained proteins as CPE (Figure 19B).

In conclusion, only CPE but no CysC was released in a stimulated manner in untreated cultured astrocytes. As LCN2 expression in astrocytes *in vitro* was very low and variable from culture to culture, it was under detection limits in the release media. Interestingly, in proinflammatory-treated astrocytes, all analyzed DCV (CPE) and lysosomal (LCN2 and CysC) -related proteins were released in response to intracellular Ca^{2+} increases caused by the ionophore ionomycin. However, release of LCN2 was apparently less influenced by extracellular Ca^{2+} entry than the secretion of DCV subpopulations containing CPE. Finally, in both control and activated astrocytes, relatively high rates of secretory protein basal (unstimulated) release were evidenced.

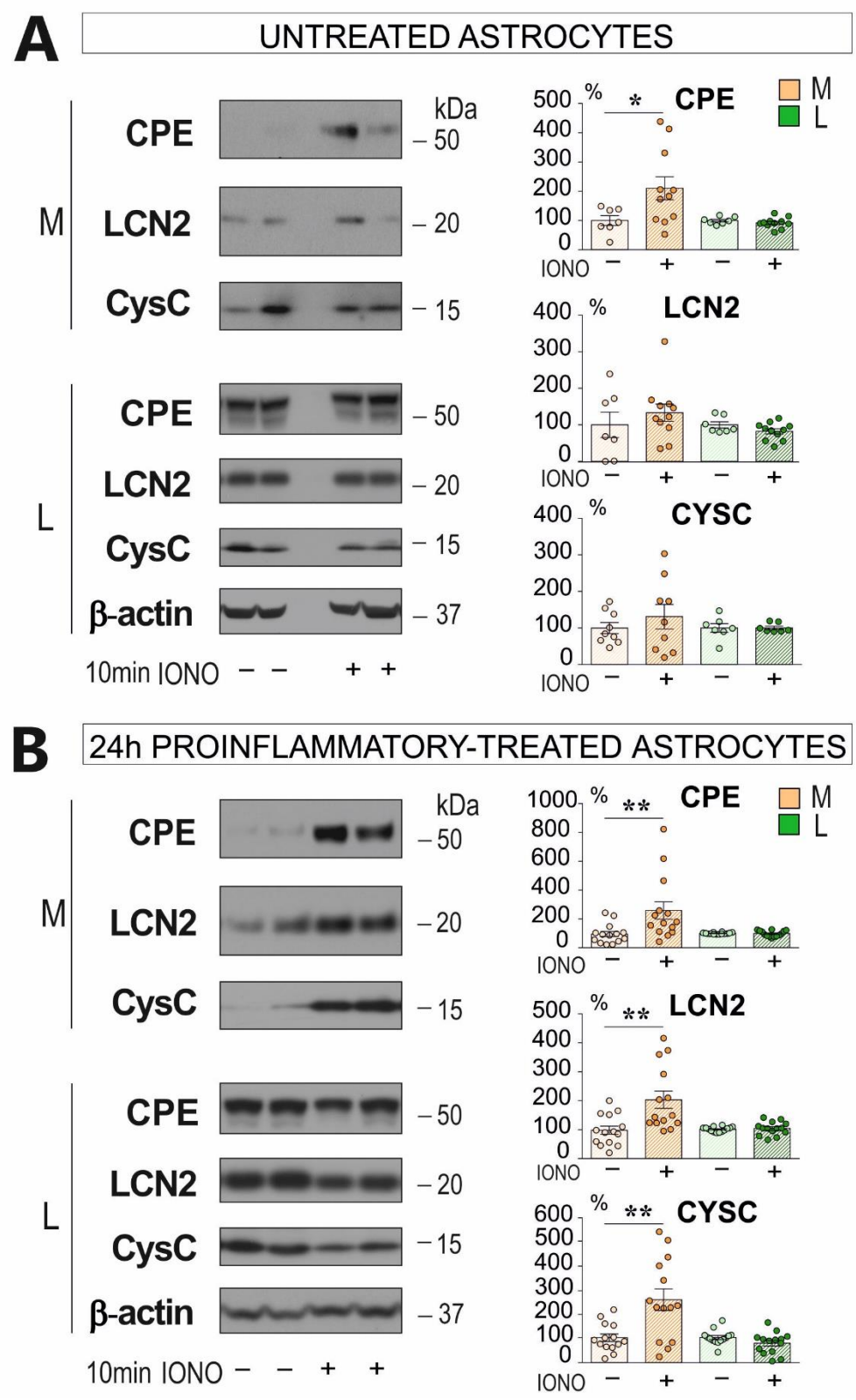

Figure 19. Ca^{2+}-mediated stimulation of peptidergic secretion is enhanced in proinflammatory-treated astrocytes. A. Representative immunoblots (left) and summarizing graphs (right) of media (M) and cellular lysates (L) from astrocytes *in vitro* treated with or without 1μM ionomycin (IONO) for 10min. Release of CPE increases in response to ionomycin stimulation, whereas evoked release for LCN2 and CysC is moderated and exhibits a substantially high basal release. Intracellular levels of all proteins are invariable. B. In cultured astrocytes treated for 24h with a proinflammatory cocktail of cytokines (TNFα, IFNγ and IL-1β) LCN2 is highly overexpressed compared to controls. (continues in next page)

Under proinflammatory conditions, release of all CPE, LCN2 and CysC proteins is significantly increased following Ca^{2+}-mediated stimulation. Additionally, secretion rates of lysosomal-related proteins LCN2 and CysC are lower than for DCV-contained CPE, specially LCN2 subpopulations, which display higher basal release levels. β-actin is used as a loading control. Results are normalized by total protein content data obtained from Ponceau staining scans (not shown). Data are presented as the mean ± SEM. Statistically significant difference is calculated using a two-tailed Mann-Whitney test. * indicates p-value < 0.05 and ** indicate p-value < 0.01.

Secretory proteins are barely retained and rapidly released in cultured astrocytes

As aforementioned, release dynamics of soluble DCV components differed between astrocytes and neurons *in vitro*. In contrast with neurons, astrocytes displayed high rates of basal release and low stimulus-triggered secretion of the DCV markers CPE and secretogranin SgIII (Plá et al., 2017). Results from the present work have evidenced moderate Ca^{2+} evoked release of CPE, LCN2 and CysC in proinflammatory-treated astrocytes *in vitro*. Besides, high rates of basal (unstimulated) secretion of all proteins have also been determined.

To better understand the mechanisms underlying unstimulated release in astrocytes *in vitro*, a cycloheximide (CHX) chase assay was performed. As a potent inhibitor of protein synthesis, CHX was used to study the retention and secretion kinetics of newly generated peptidergic transmitters. In untreated astrocytes (Figure 20A), an increase in extracellular and invariable intracellular levels of peptidergic transmitters over time (1.5, 3 and 6h) was evidenced. After the blockage of protein synthesis by CHX, intracellular levels of secretory peptides CPE and SgIII decreased gradually whilst its extracellular levels accumulated progressively (Plá et al., 2017).

Similar results were obtained for CPE, SgIII, CysC and LCN2 in proinflammatory-treated astrocytes (Figures $20B_1$ and $20B_2$). Additionally, SgIII expression and release levels over time were apparently higher in astrocytes under proinflammatory conditions, in consistence with previous work demonstrating SgIII overexpression in reactive glia (Paco et al., 2010). Of note, LCN2 basal release was likely greater than for the other proteins. No statistical analysis was applied as results were obtained from a single experiment performed in triplicates.

Overall, results indicated that secretory peptides were scarcely retained and immediately released in unstimulated astrocytes, both under control and proinflammatory conditions. Therefore, additional experiments were performed to further comprehend the mechanisms underlying astrocyte peptidergic unstimulated secretion.

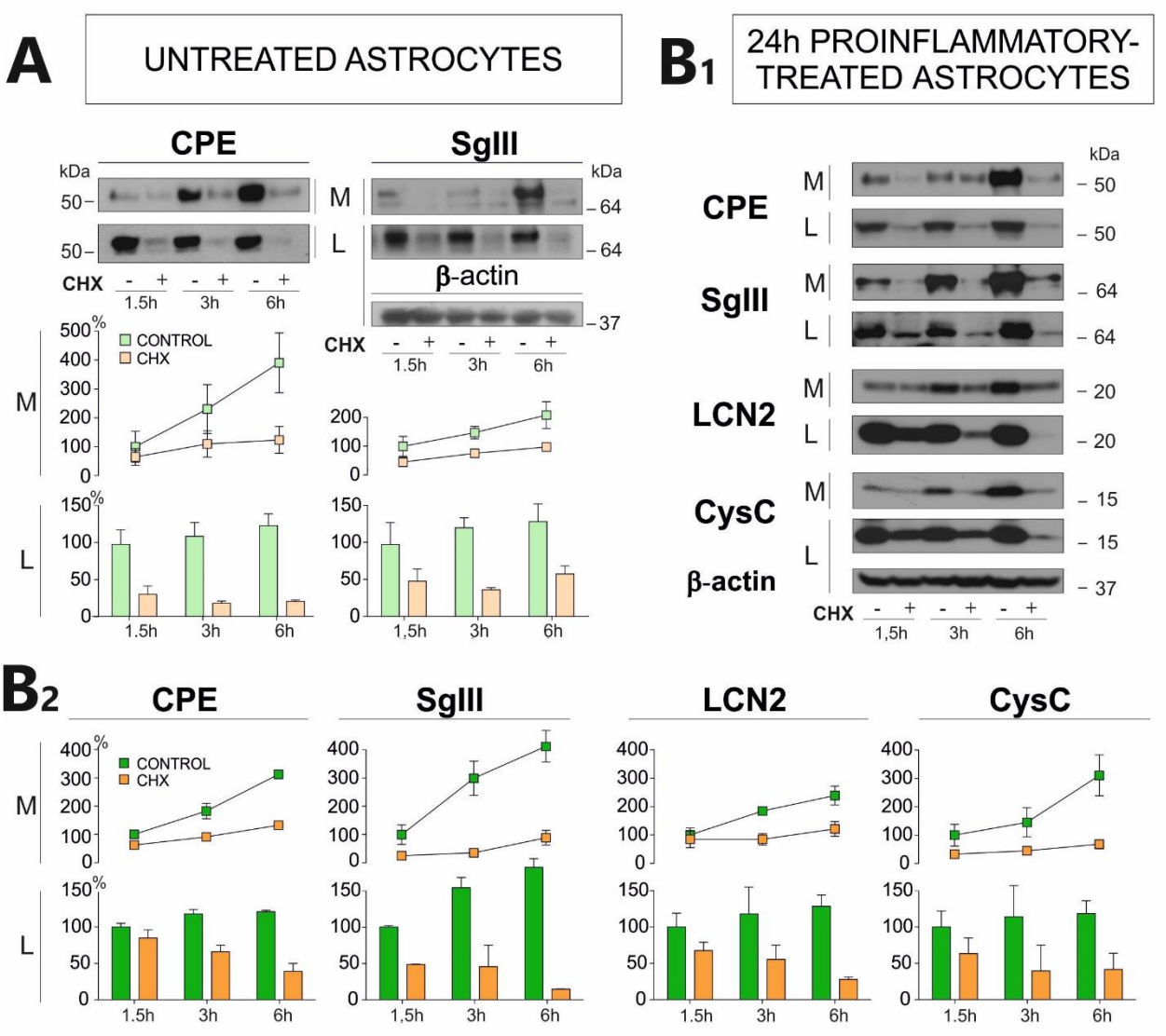

Figure 20. Secretory peptides are scarcely retained and rapidly released in unstimulated astrocytes. In untreated astrocytes (A) an increase in extracellular (media, M) and invariable intracellular levels (cell lysates, L) of peptidergic transmitters over time (1.5, 3 and 6h) is determined. After cycloheximide (CHX) treatment, intracellular levels of CPE and SgIII decrease gradually whilst their extracellular levels accumulate progressively, as observed in representative immunoblots and in graphs. In astrocytes treated for 24h with a combination of TNFα, IFNγ and IL-1β similar results were obtained for CPE, SgIII, CysC and LCN2 (B_1, representative western blots; B_2, summarizing graphs). SgIII expression and release levels over time is increased in proinflammatory-treated astrocytes compared to untreated conditions. Of note, LCN2 basal release is markedly higher than for the other proteins. β-actin is used as a loading control. Results are normalized by total protein content data obtained from Ponceau staining scans (not shown). Data are presented as the mean ± SEM. No statistical analysis is applied as results are obtained from a single experiment performed in triplicates.

Astrocyte unstimulated release of secretory proteins is independent of intrinsic Ca^{2+} oscillations

As it has already been described elsewhere, Ca^{2+} release from the ER is an important cellular mechanism for the initiation of spontaneous Ca^{2+} oscillations in astrocytes (Nett et al., 2002). Consistently, we next investigated whether astrocytes in our cultures exhibited spontaneous Ca^{2+} events that could correlate with the elevated rates of unstimulated release.

Thus, cultured cells were loaded with the membrane-permeant acetoxymethyl ester of fluo-3 AM and Ca^{2+} transients were visualized with confocal laser-scanning microscopy, as performed in similar studies (Wang et al., 2006). Spontaneous Ca^{2+} oscillations were observed in astrocyte cultures (82% oscillating cells/field; 7 oscillations/100s) (Figure 21A), which were virtually prevented with the addition of 1µM thapsigargin (TG), a strong inhibitor of the SERCA-ATPase (Figure 21B).

To study the possible relation between spontaneous Ca^{2+} oscillations and the secretion kinetics of newly synthesized secretory proteins, effects of TG in unstimulated release were analyzed after a pre-treatment with CHX, both in untreated (Figure 21C) and proinflammatory-treated (Figure 21D) astrocytes. Treatment with CHX was also necessary as TG has been determined to induce ER-stress by strong inhibition of protein synthesis (Gupta et al., 2010; Sen et al., 2019).

After controlled blockage of protein synthesis by CHX, the addition of TG maintained invariable both extracellular and intracellular levels of secretory proteins CPE, SgIII and CysC compared to untreated cells, in both control and activated astrocytes. Released and intracellular LCN2 levels were also preserved in TG treated astrocytes under proinflammatory conditions. No statistically significant differences were observed in any case. These results suggested that peptidergic secretion of unstimulated astrocytes was independent of intrinsic Ca^{2+} oscillations, both in proinflammatory-treated and untreated cells.

Astrocyte unstimulated release of secretory proteins depends on intracellular Ca^{2+}

To further investigate the mechanisms of unstimulated peptidergic secretion in astrocytes, additional release assays were carried out chelating the intracellular Ca^{2+} with the cell-permeable Ca^{2+} chelator BAPTA-AM in the absence and presence of CHX.

Release of peptidergic transmitters in the media of BAPTA-AM treated astrocytes decreased dramatically but their intracellular levels were also reduced (Figure 22B, left), probably as a consequence of BAPTA-AM interference in protein synthesis, which has been described to cause ER stress by a great blockage of protein translation (Flores-Morales et al., 2001).

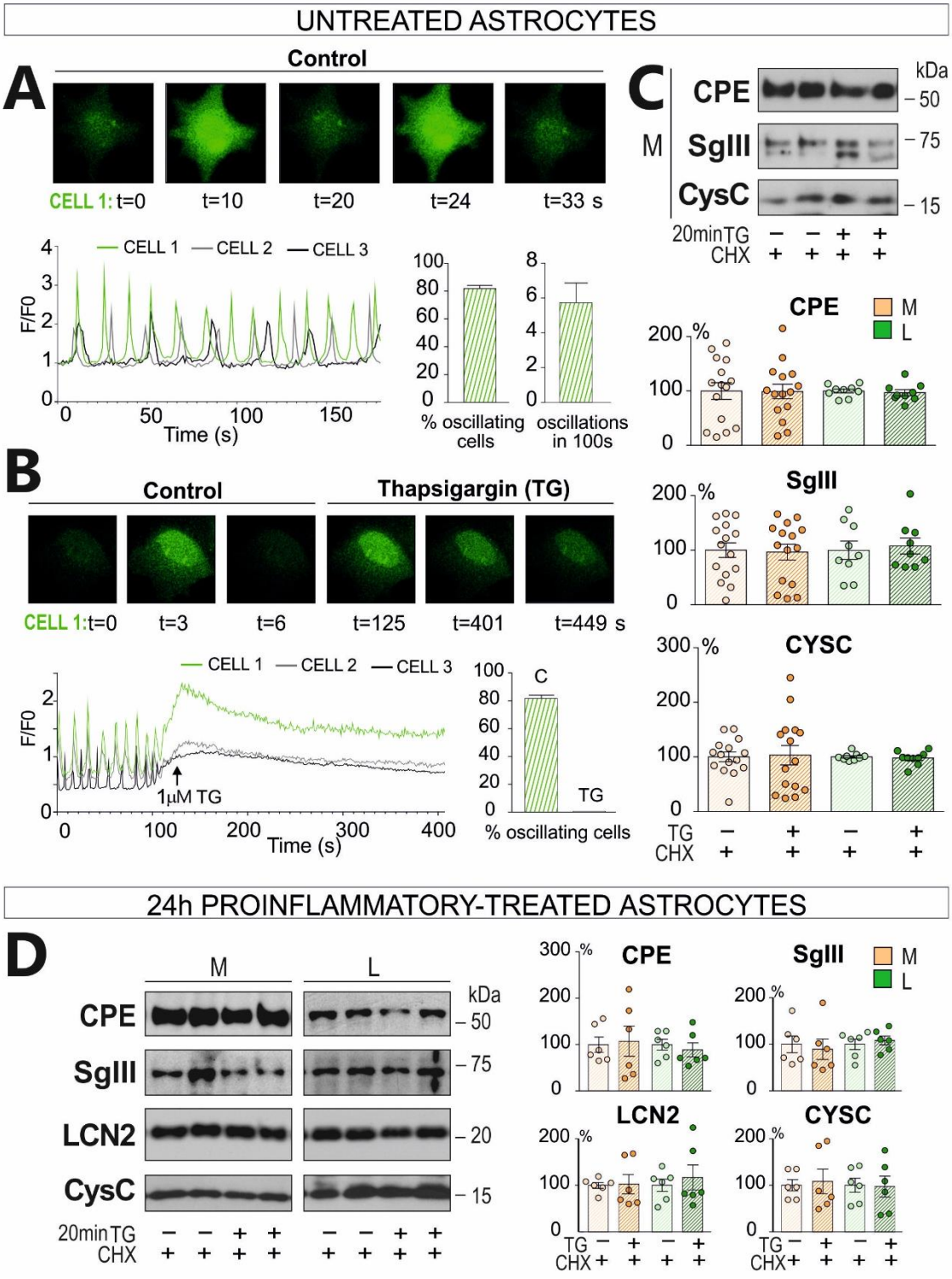

Figure 21. Peptidergic secretion of unstimulated astrocytes is independent of Ca^{2+} oscillations. A. Ca^{2+} events in cultured astrocytes loaded with fluo-3 AM are visualized. Spontaneous Ca^{2+} oscillations are observed in astrocyte cultures (82% oscillating cells/field; 7 oscillations/100s). B. Glial oscillations are virtually prevented with the addition of 1μM thapsigargin (TG). Unstimulated release is analyzed in untreated (C) and 24h proinflammatory-treated astrocytes (D) after addition of CHX and TG. In the presence of CHX, addition of TG maintains invariable both extracellular (media, M) and intracellular (cell lysates, L) levels of CPE, SgIII and CysC compared to untreated cells, in both control and activated astrocytes. Extracellular and intracellular LCN2 is also maintained in TG treated astrocytes under activation conditions. β-actin is used as a loading control (not shown). Results are normalized by total protein content data obtained from Ponceau staining scans (not shown). Data are presented as the mean ± SEM. Statistically significant difference is calculated using a two-tailed Mann-Whitney test. No statistically significant differences were observed.

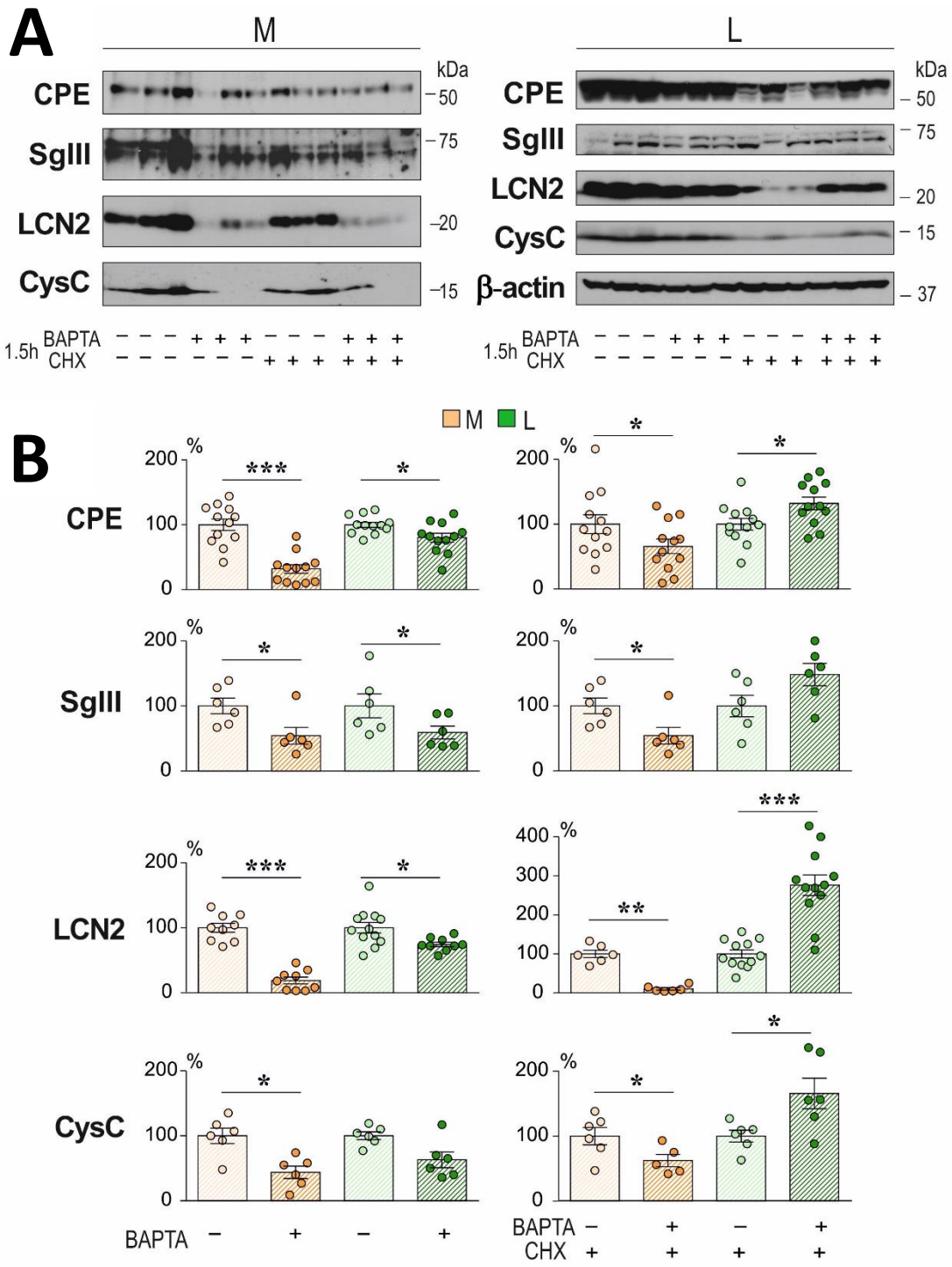

Figure 22. Peptidergic release of unstimulated astrocytes requires intracellular Ca^{2+}. A. Representative western blots of astrocyte unstimulated release carried out chelating the intracellular Ca^{2+} with BAPTA-AM in the absence or presence of CHX. B. Without CHX, release of peptidergic transmitters in the media (M) of BAPTA-AM treated astrocytes decreases dramatically but intracellular levels (cell lysates, L) are also reduced, probably as a consequence of BAPTA-AM interference in protein synthesis. When protein synthesis is blocked by CHX, unstimulated release of peptidergic transmitters in the presence of BAPTA-AM is similarly decreased, while their intracellular levels are elevated, suggesting that in the absence of intracellular Ca^{2+} secretory peptides are highly accumulated inside the cell. β-actin is used as a loading control. Results are normalized by total protein content data obtained from Ponceau staining scans (not shown). Data are presented as the mean ± SEM. Statistically significant difference is calculated using a two-tailed Mann-Whitney test. * indicates p-value < 0.05, ** indicate p-value < 0.01 and *** indicate p-value < 0.001.

To control protein synthesis inhibition, further assays were performed under the treatment of CHX. After CHX exposure, unstimulated release of peptidergic transmitters in the presence of BAPTA-AM was similarly decreased, while their intracellular levels were elevated (Figure 22B, right). Interestingly, the reduction in basal secretion of LCN2 (10%, p = 0.002) was apparently more notable than decreases in released CPE (65%, p = 0.03), SgIII (54%, p = 0.03) and CysC (62%, p = 0.05).

These results evidenced that in the absence of intracellular Ca^{2+} secretory peptides were highly accumulated inside the cell, indicating that intracellular Ca^{2+} was required for the rapid release of newly synthesized secretory proteins. Besides, unstimulated release of LCN2 was apparently more sensitive to intracellular Ca^{2+} concentrations than the other secretory proteins, which may explain LCN2 stimulated release being less influenced by extracellular Ca^{2+}.

In conclusion, a heterogeneity of peptidergic secretory vesicles was evidenced in astrocytes. CPE, SgIII, CysC and LCN2 were expressed and released in astrocytic cells in an unstimulated manner, independently of stimuli, which did not require intrinsic Ca^{2+} oscillations, but critically depended on intracellular Ca^{2+}. Besides, extracellular Ca^{2+}-mediated stimulated release of secretory proteins was enhanced in proinflammatory-treated astrocytes *in vitro* and in the LPS-induced neuroinflammation model *in situ*. Apparently, unstimulated release of lysosomal-related proteins as LCN2 and CysC displayed a higher Ca^{2+} sensitivity, which was in line with lesser responses to Ca^{2+}-mediated stimulation, compared to DCV-contained secretory proteins as CPE.

2. Dense-core vesicle markers decline in cerebrospinal fluid and accumulate in dystrophic neurites and granulovacuolar degeneration bodies in Alzheimer's disease

In previous studies performed by our research group, the DCV molecular components CPE and SgIII were analyzed in the cerebral cortex of AD patients. Great widespread accumulation of both proteins in dystrophic neurites surrounding Aβ plaques and SgIII overexpression in nearby reactive astrocytes were determined, thus evidencing an association between DCV cargos and Aβ-driven neuronal deterioration (Plá et al., 2013).

Consequently, the influence of soluble Aβ oligomers on DCV secretion in cortical neurons and astrocytes was further assessed in our laboratory. Aβ42 specifically impaired unstimulated and evoked release of CPE and SgIII in both primary cultures and adult brain slices (Plá et al., 2017). Importantly, these results demonstrated the existence of disturbances in peptide secretion triggered by Aβ, which raised the perspective of DCV cargos being altered in the CSF of AD patients.

In fact, certain DCV proteins as CgA, SgIII and CPE have already been investigated elsewhere in the CSF of AD patients by proteomic techniques (Fagan and Perrin, 2012). However, proteomic-derived results are usually variable and require further validation. Besides, other secreted DCV proteins as PC1/3 and PC2 have been poorly investigated in the context of AD. Thus, this second section of the present dissertation focuses in the study of these DCV-contained secretory proteins in the brain and CSF of AD patients.

Secretory proteins are abundantly detected in the human CSF and hippocampus

To initiate the study of DCV changes in the brain and CSF of AD patients, previous analyses to ensure the detection of DCV proteins in human tissues were required. Western blotting assays performed in control hippocampus and CSF (Figure 23) revealed high amounts of the DCV markers PC1, PC2, CPE and SgIII in hippocampal homogenates. Of note, SgIII and the two protein convertases displayed both precursor (unprocessed) and mature forms. Additional electrophoretic mobility bands likely corresponded to aggregated and cleaved protein species detected by polyclonal antibodies in accordance with existing literature (Bartolomucci et al., 2011; Hoshino and Lindberg, 2012).

A strong labeling for all DCV proteins (mature and precursor forms) was observed in the CSF, as well. Interestingly, and contrary to the hippocampal homogenates, precursors of DCV proteins were generally more abundant than their processed forms in the CSF. Even small CSF volumes as 1µL were enough to reveal the presence of some DCV markers (i.e. SgIII), which evidenced the relative abundance of these secreted components in the human CSF.

As formerly described, only the monomeric form of the secretory protein CysC (around 14 kDa) was distinguished in the CSF, whilst oligomeric CysC species (around 28 and 35 kDa, respectively) were also detected hippocampal tissues (Bjarnadottir et al., 2001; Mi et al., 2009). When analyzing similar CSF volumes, levels of vesicular membrane proteins as Syp, cytosolic components as β-actin and the candidate CSF biomarker neurofilament light chain (NFL), were below detection threshold.

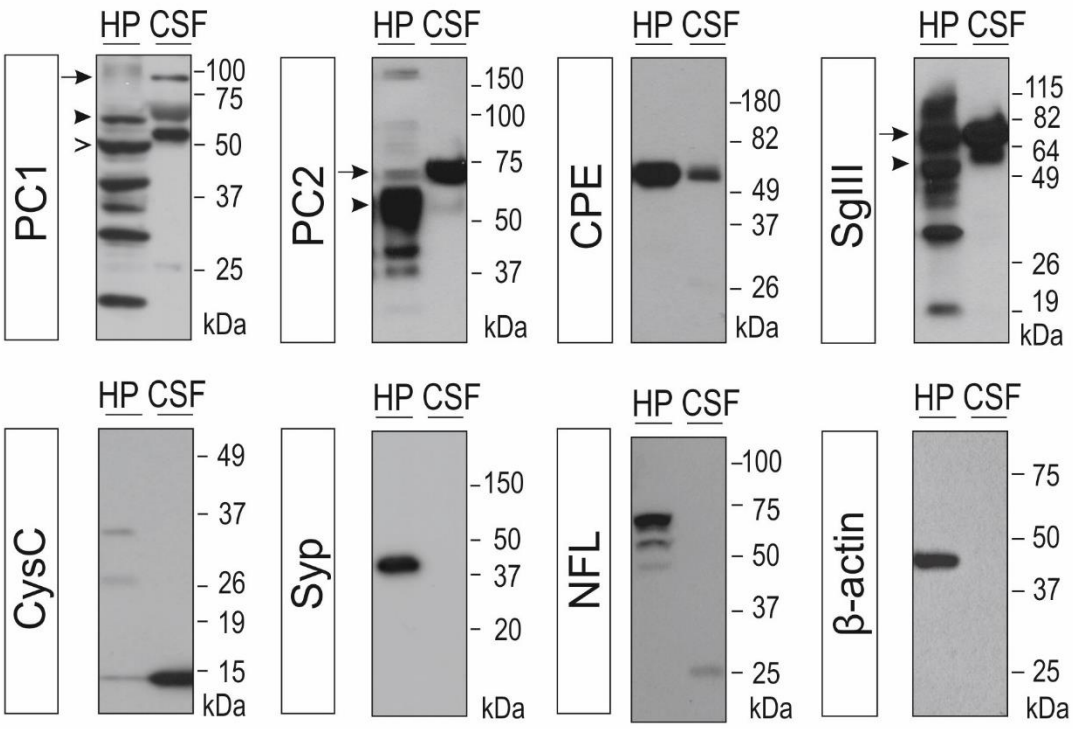

Figure 23. Brain secretory proteins are abundantly detected in the human CSF. Western blotting analysis of the secretory proteins PC1, PC2, CPE, SgIII and CysC in human hippocampus (HP, 20µg) and CSF (5-10µL). In CSF, precursor forms (arrows) of granins and convertases are more abundant than their mature forms (arrow-heads). For PC1, another specific processed band of around 50kDa present in both HP and CSF is indicated with an open arrow. Additional bands in HP samples likely correspond to aggregates and cleaved forms. Brain tissues display monomeric (around 14kDa) and oligomeric/aggregated (around 28 and 35kDa, respectively) forms of CysC, while only monomers are detected in CSF. Membrane and cytosolic proteins such as Syp, β-actin and NFL are not detected in the CSF when performing analyses of the same samples at similar volumes.

DCV markers are aberrantly accumulated in dystrophic neurites and GVD bodies in the human AD cerebral cortex

To evaluate changes in DCV proteins in the AD cerebral cortex, immunoblotting and immunohistochemical analyses were performed in AD brains (Braak stages V-VI) and age-matched controls (Braak stages I-II). Table 3 summarizes the number of control and AD tissues, the cerebral regions studied and other characteristics of the samples used for each type of investigation.

Case	Number of samples	Mean Age (years)	Gender	Mean post-mortem time (hours)	Cortical region	Type of investigation
Control	3	71.0	1M/2F	5.2	Parietal cortex	Immunohisto-chemistry
AD	5	78.4	5F	5.7		
Control	5	69.6	3M/2F	9.3	Hippocampus	
AD	4	75.8	2M/2F	5.9		
Control	7	73.7	4M/3F	6.0	Parietal cortex	Western blot
AD	7	80.1	2M/5F	6.3		
Control	7	73.3	7M	6.6	Hippocampus	
AD	7	81.9	4M/3F	6.4		

Table 3. Control and AD cortical tissues analyzed in the present study. Number of control and AD tissues, cerebral regions, age, gender (female – F, male – M) and mean post-mortem time of the samples used for each type of investigation.

First, the levels of the diverse molecular forms of secretory proteins were examined in AD and control parietal cortices and hippocampi (n = 7 for each condition and tissue) by western blot (Figure 24). Even though equal amounts of protein were charged into electrophoretic gels, results were normalized to membrane-transferred total protein. Levels of DCV proteins were preserved in both hippocampus and parietal cortex of AD cases, except for the precursor form of PC2 (pPC2) which increased in AD parietal cortex ($p = 0.038$) and hippocampus ($p = 0.0006$), compared to controls.

Regarding CysC, reductions of 35% and 30% were evidenced in the 28kDa form in the AD cortex ($p = 0.038$) and hippocampus ($p = 0.1$). For the SV membrane protein Syp, great reductions were determined in both AD tissues (30%, $p = 0.042$ and 50, $p = 0.017$, respectively) in comparison with controls. These results demonstrate that levels of DCV proteins are generally maintained in AD cortices, whilst levels of SV proteins are drastically diminished.

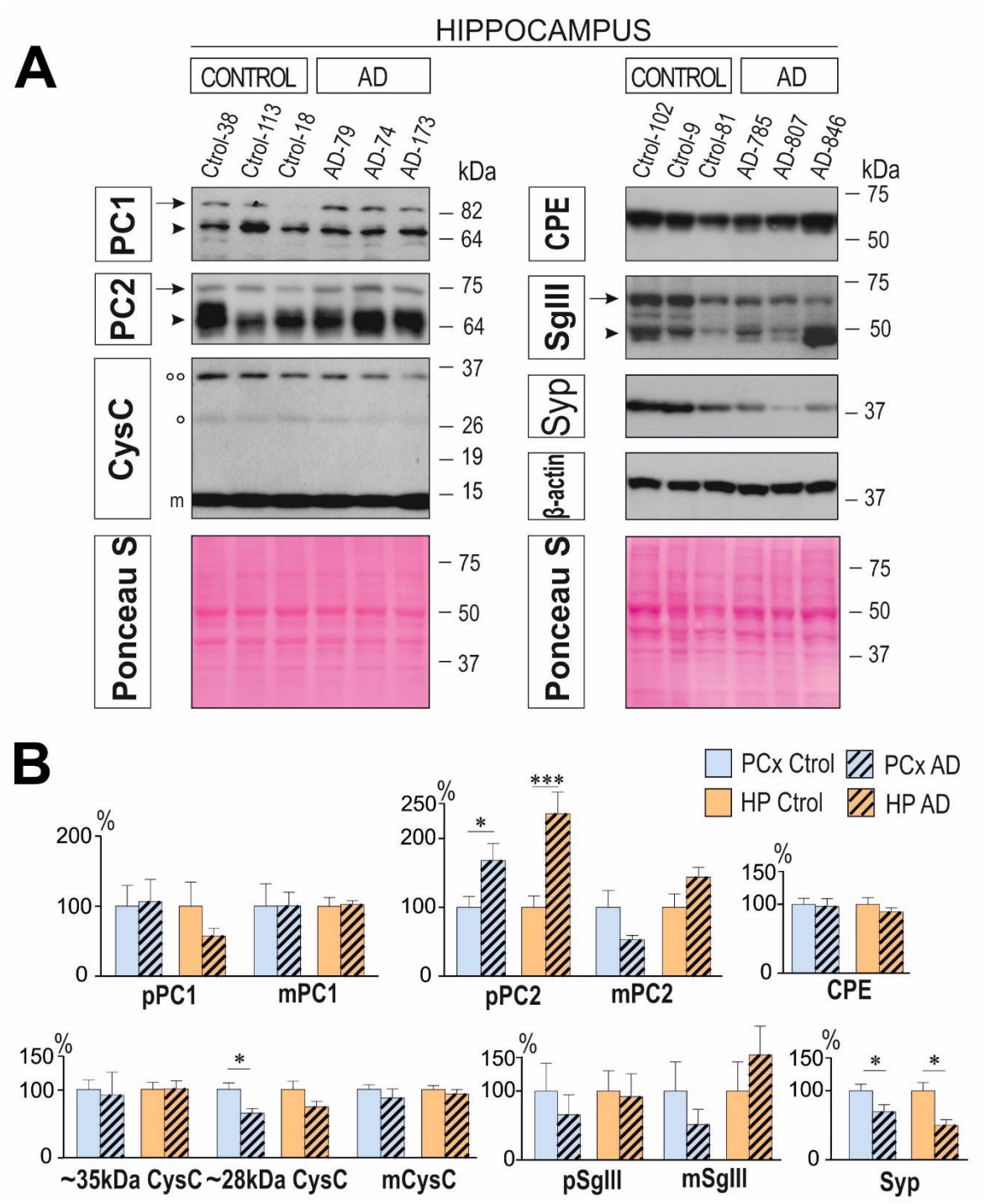

Figure 24. Levels of secretory proteins in the AD cerebral cortex. Hippocampal (HP) and parietal cortical (PCx) samples of controls and AD patients (Braak stages V-VI) analyzed by western blot (20µg). A. Representative immunoblots of HP tissues for some secretory proteins and Ponceau staining scans used to establish content of total proteins. Precursor and mature forms of DCV proteins are indicated with arrows and arrow-heads, respectively. For CysC, monomeric (m, 14kDa) and two oligomeric/aggregated (° and °°, 28kDa and 35kDa, respectively) forms are evidenced. B. Graphs summarize percent variation of secretory protein levels in the PCx and HP of AD patients compared to controls (n = 7 for each tissue). An increase of the precursor form of PC2 (pPC2) is observed in the PCx and in the HP of AD patients. Levels of the 28kDa form of CysC are reduced in the PCx of AD patients compared to controls. A reduction of Syp is detected in both HP and PCx tissues of AD patients. Data are presented as the mean ±SEM. Statistically significant difference is calculated using a two-tailed Mann-Whitney test. * indicates p-value < 0.05 and *** indicate p-value < 0.001.

To further investigate possible alterations of DCV markers *in situ*, peroxidase and fluorescence immunohistochemical analyses of parietal cortices and hippocampi of control (n = 8) and AD (n = 9) subjects were performed. Secretory proteins PC1, PC2, CPE, SgIII and CysC were broadly distributed throughout the control cerebral cortex (Figure 25A), as evidenced in previous investigations (Deng et al., 2001; Plá et al., 2013; Winsky-Sommerer et al., 2003).

Consistently with previous work from our laboratory, CPE was robustly detected filling dendrites, neuronal perikarya, some axons and slightly glial cells, whereas immunostaining for SgIII was mainly restricted to perinuclear secretory organelles, proximal dendrites and fibrous astroglial cells (Plá et al., 2013). Moreover, PC1 and PC2 immunoreactivity was found mainly in pyramidal neurons, whilst CysC immunolabeling was distinguished in both neurons and GFAP+ astrocytes. CysC was strongly associated with lysosomal structures immunoreactive for LAMP1, contrary to the other secretory proteins which, as classical DCV markers, were negative for LAMP1 immunostaining (data not shown).

In AD cortices, minor changes were observed for DCV proteins in non-plaque regions, including a slight increase of CysC immunoreactivity in pyramidal neurons of outer and inner layers (data not shown). Nevertheless, dystrophic neurites surrounding senile plaques displayed accumulations of secretory proteins (Figure 25B). Double immunofluorescence analyses revealed the colocalization of PC2 and SgIII with dystrophic neurites (AT8+ immunostaining), respectively. CPE and SgIII also displayed a high colocalization degree in dystrophic neurites and were found surrounding senile plaques. Double labeling with GFAP indicated alterations in plaque-surrounding activated glia, where levels of SgIII and CysC were occasionally increased in reactive astrocytes (data not shown).

Surprisingly, some DCV proteins were found to accumulate in large granules resembling granulovacuolar degenerating (GVD) bodies, a typical neuropathological hallmark of hippocampal CA1 pyramidal neurons in AD (Figure 26). In essence, PC2 and PC1 were strongly immunostained in GVD-shaped structures in each of the analyzed AD hippocampi (n = 4), whereas large granules positive for CPE were evidenced in only one of the four cases (Figure 26A). In average, 241 ± 4 pyramidal neurons per square millimeter of the CA1 region in AD hippocampi displayed PC2 anomalous granular accumulations, whilst only few neurons in only one of the five control cases exhibited similar alterations.

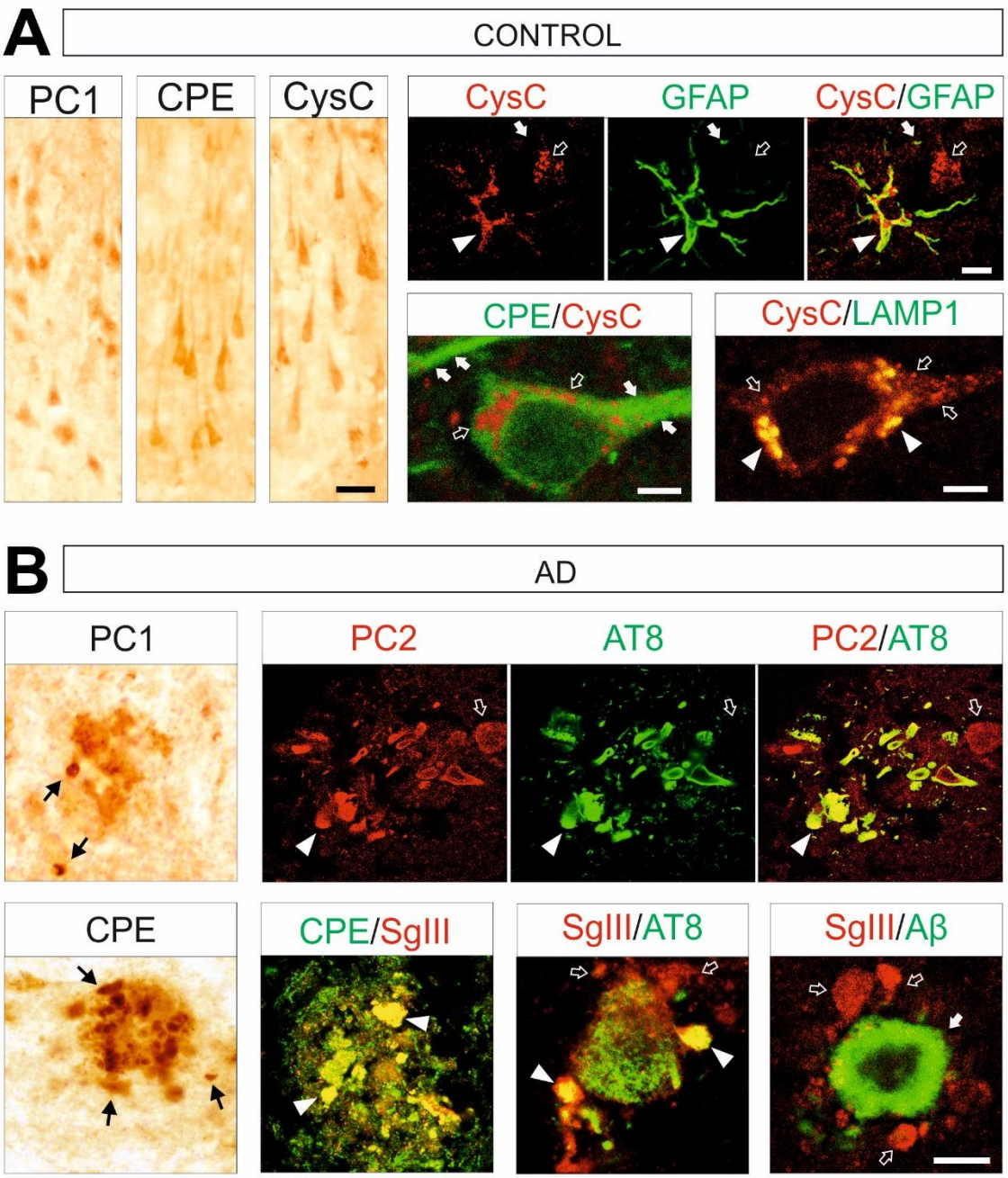

Figure 25. Distribution of secretory proteins in the control and AD cerebral cortex. A. Distribution of representative secretory proteins (PC1, SgIII and CysC) in the control hippocampus. Immunoreactivity is abundantly found in pyramidal neurons. Double immunolabeling for CysC (red; empty-arrows) and GFAP (green; arrows) confirms astroglial identity (yellow in the merged image; arrowheads). CPE (green; arrows) and CysC (red; empty-arrows) are located in different subcellular compartments in pyramidal neurons as shown by confocal fluorescent microscopy. CysC (red; empty-arrows) partially colocalizes (yellow; arrowheads) with lysosomal compartments expressing LAMP1 (green). Scale bars in µm: 20; 10; 5; 5. B. PC1, PC2, CPE and SgIII are accumulated in dystrophic neurites surrounding senile plaques of AD patients. In peroxidase immunohistochemistry images arrows indicate plaque-associated dystrophic neurites. Double immunofluorescence images indicate that PC2 and SgIII (red; empty-arrows) colocalize with AT8+ dystrophic neurites (green), respectively. CPE (green) and SgIII (red) also display a high colocalization degree in dystrophic neurites (yellow; arrowheads) and are found surrounding Aβ+ senile plaques (green; arrows). Scale bar: 20 µm.

As depicted in Figure 26B, GVD identity of the aberrant granules was confirmed with double immunolabeling of PC2 and PC1 with the established GVD markers CK1δ (Casein kinase 1 isoform delta), CHMP2B (Charged multivesicular body protein 2B, not shown) and LAMP1. Interestingly, PC2-positive GVD lesions were found in both p-tau (AT8 immunostaining) positive or negative pyramidal neurons, thus indicating an association between GVD bodies and neurofibrillary tangle pathology (Figure 26C). Approximately the 80% of pyramidal neurons containing PC1 and PC2 GVD inclusions also displayed AT8 immunolabeling, being GVD bodies more frequently found in neurons at early stages of the tauopathy (Figure 26D).

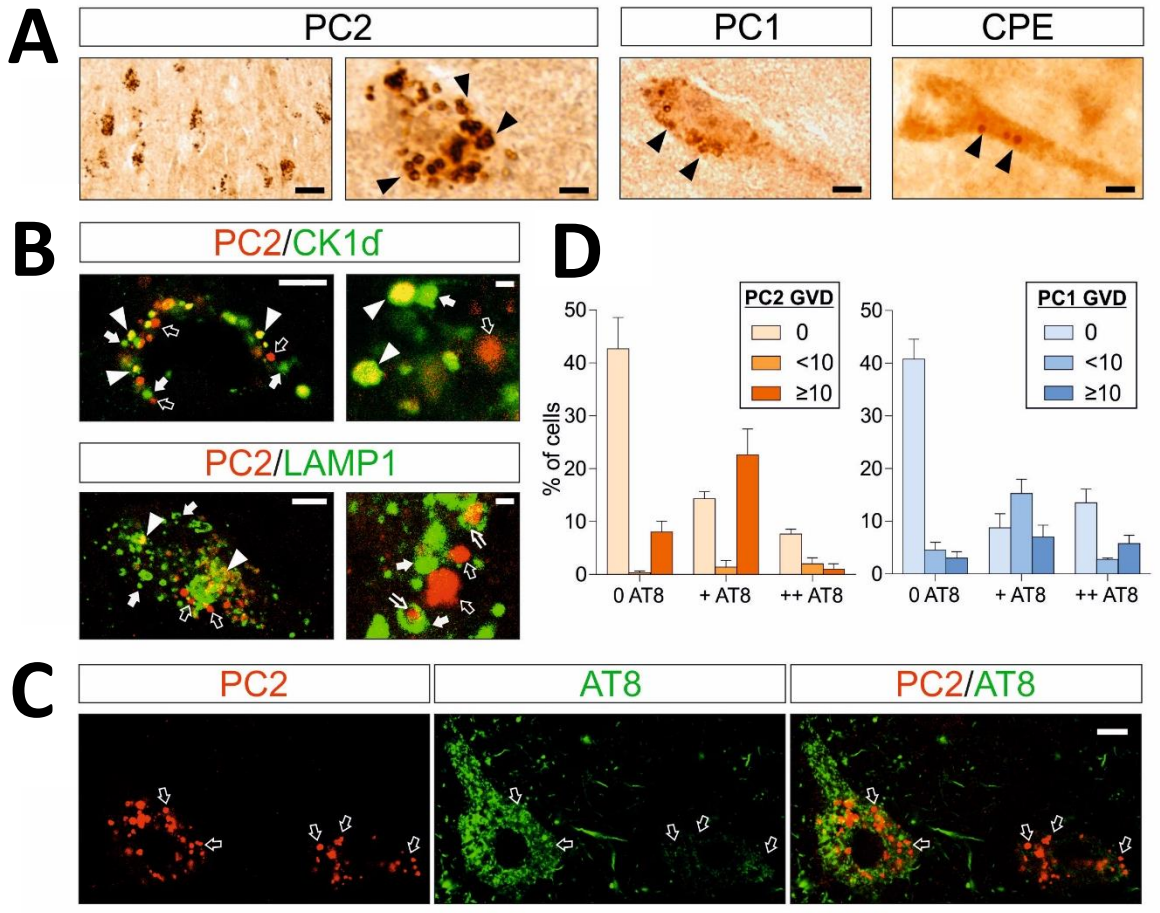

Figure 26. DCV proteins are accumulated in GVD bodies in CA1 pyramidal neurons of AD patients. A. Peroxidase immunohistochemical analyses reveal aberrant intraneuronal accumulations (arrows) of PC2, PC1 and CPE in pyramidal neurons of the hippocampal region CA1 of AD patients, which show the typical morphological pattern of GVD bodies. GVD identity of the inclusions is corroborated by the double immunolabeling of PC2 (red; empty-arrows) with CK1d (green; arrows) and LAMP1 (green; arrows), respectively. Arrow-heads indicate membrane colocalization whereas open-arrows show inside-granule colocalization (B). PC2-positive GVD lesions are found either in tangle (AT8; green) positive or negative pyramidal neurons. Arrows indicate the location of PC2+ GVD accumulations (C). In D, graphs show the percentage of cells displaying few (<10), many (≥10) or zero PC2 and PC1 positive GVD, depending on the presence of neurofibrillary tangles (+AT8, low labeling; ++AT8, strong labeling). Scale bars in µm: A, left, 20; right, 4; B, left, 5; right, 1; C, 7.

Altogether, these results evidenced that in AD cortices DCV markers aberrantly accumulated in association with two typical neuropathological features of AD: plaque-surrounding dystrophic neurites and aberrant hippocampal GVD inclusions.

DCV secretory cargos decline in the CSF of AD patients, which is likely associated with neurodegenerative stages of the disease

Subsequently, changes in the levels of DCV proteins were investigated in biopsied CSF samples from a very well characterized cohort of living AD patients (n = 33) and age-matched healthy controls (n = 33) by western blot (Table 4). For AD patients, the average score in the MMSE cognitive test was 21.58 ± 4.39 compared to scores ranging from 28 to 30 in control individuals. Additionally, according to selection criteria, CSF samples from subjects in the AD cohort displayed low levels of Aβ42 and high t-tau and p-tau in comparison with controls.

	Age (years)	Gender	MMSE	APOE allelic frequency	CSF Aβ42 (pg/mL)	CSF t-tau (pg/mL)	CSF p-tau (pg/mL)	CSF glucose (mmol/L)
Control (n=33)	63.75 (±7.18)	13M/20F	29.21 (±0.96)	ε2 = 0.05; ε3 = 0.83; ε4 = 0.12	836.09 (±154.7)	221.97 (±57.4)	43.38 (±10.4)	3.46 (±0.51)
AD (n=33)	66.94 (±6.13)	12M/21F	21.58 (±4.39) ***	ε2 = 0.03; ε3 = 0.44; ε4 = 0.53	353.27 (±101.2) ***	905.32 (±457.9) ***	99.33 (±31.3) ***	3.39 (±0.51)

Table 4. Demographics and CSF profiles of study individuals. According to selection criteria, AD patients display reduced levels of CSF Aβ42 and lower MMSE scores and levels of CSF t-tau and p-tau are significantly higher in AD patients in comparison with the control group. No significant differences are observed in age and CSF glucose levels between groups. Data are shown as means and standard deviations for age, MMSE, CSF Aβ42, tau, p-tau and total protein. Statistically significant difference is calculated using a two-tailed Mann-Whitney test. *** indicate p-value < 0.001.

Equal CSF total protein levels between control and AD groups was corroborated performing a Bradford assay with all samples, as well as with Coomassie staining of electrophoretic gels (Figure 27A). Figure 27B includes representative immunoblots for the different DCV markers, all analyzed in the same samples from AD and control cohorts. Importantly, the vast majority of DCV proteins displayed decreased levels in the CSF of AD patients in comparison with the control group. A global decrease of CPE, CysC and PC2 (both precursor – pPC2 and mature – mPC2 forms), and a reduction in the precursor forms of PC1 (pPC1) and SgIII (pSgIII) was detected in the CSF of AD patients compared to controls (Figure 27C).

In particular, both pPC2 and mPC2 were statistically diminished in AD samples (16% reduction, p = 0.024 and 12% reduction, p = 0.011, respectively) (Figure 27C), as well as in a pooled quantification of the two bands together (18% decrease, p = 0.0009) (data not shown). A statistically significant reduction of the 21% was also found for the DCV-contained carboxypeptidase CPE in the CSF of patient cohort (p = 0.016). An outstanding decrease of the 33% was observed for the secretory protein CysC in the CSF of AD patients (p = 0.0011) (Figure 27C).

Additionally, a reduction of around the 40% for pPC1 (p = 0.0003) was determined in AD, whereas mature PC1 (mPC1) decrease did not reach significance (p = 0.075) (Figure 27C). However, when quantifying together the levels of mature and precursor forms of PC1 a significant 24% decrease was evidenced in AD patients (p = 0.03) (data not shown). Another PC1 cleaved form with lower electrophoretic mobility (around 50kDa), consistently detected by three polyclonal antibodies, was also quantified. Its levels were analyzed separately and together in a whole quantitation with pPC1 and mPC1. Only in the case of the pooled analysis, a significant decrease in AD patients was observed in comparison with controls (21% reduction, p = 0.05, respectively) (data not shown).

A decline of the 12% for pSgIII (p = 0.047), the most abundant form of SgIII in the human CSF, was evidenced in the AD group, whereas no significantly differences were detected for the mature protein (15% decrease, p = 0.18) (Figure 27C). A pooled analysis of the two forms demonstrated no significant differences between groups (p = 0.612) (data not shown).

To further understand these obtained results, we questioned whether the observed differences could be influenced by the differential cognitive impairment degree among individuals from the AD cohort. In fact, even though the average MMSE score from the entire AD cohort was around 21, individual scores ranged between values as low as 7 and as high as 29 within this group, indicating a great variability in cognitive performance among subjects. Thus, CSF AD samples were re-classified into two different categories, according to individual cognitive ability assessed with the MMSE test. In consistence with similar studies (Lista et al., 2017), from the 33 AD patients of the initial cohort, subjects scoring between 28 and 24 were classified into the MMSE $\geq$ 24 group (n = 13) and individuals with scores of less than 24 were assigned to the MMSE < 24 cohort (n = 20).

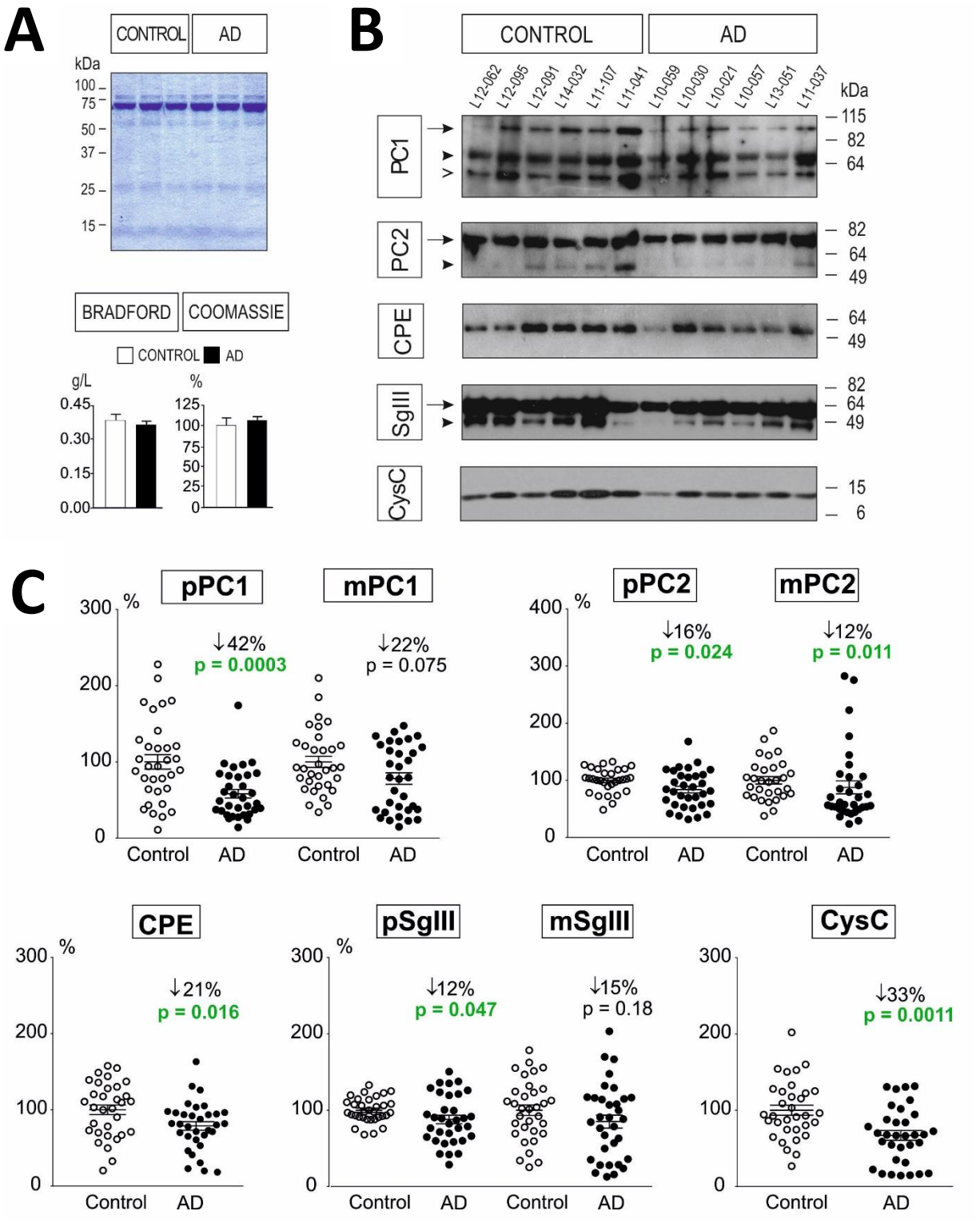

Figure 27. CSF samples of AD patients display decreased levels of secretory proteins. A. Total protein content in control and AD CSF samples determined by Coomassie staining and Bradford assay. B. Representative immunoblots show levels of CPE, PC1, PC2, SgIII and CysC forms in the same CSF control and AD samples (6µL). Precursor and mature forms of DCV proteins are indicated with arrows and arrow-heads, respectively. For PC1, another specific processed band of around 50kDa present in the CSF is indicated with an open arrow. C. Scatter dot-plots represent percent variation of secretory proteins levels in the CSF of AD patients (n = 33) compared to controls (n = 33). Arrows indicate percentage reduction and p-values the statistic significances. Data are presented as the mean ± SEM of analysis performed in duplicate. Statistically significant difference is calculated using a two-tailed Mann-Whitney test.

As seen in Figure 28, levels of pPC1 were significantly reduced in both MMSE ≥ 24 and MMSE < 24 groups compared to controls (p = 0.047 and p = 0.0001, respectively), which was also observed for CysC (p = 0.002 and p = 0.01). Interestingly, mPC1, pSgIII, pPC2 and mPC2 were maintained with a slight tendency to decline in the CSF of AD individuals with MMSE scores over 24, whilst were significantly decreased in the MMSE < 24 AD group (p-values for the latter group = 0.0023, 0.029, 0.033 and <0.0001, respectively). For mSgIII, similar results were observed being their levels almost significantly declined in the CSF of AD subjects with MMSE scores under 24 (reduction of 24.5%, p = 0.054). Otherwise, CPE CSF levels were exclusively reduced in the group with the better test performance, being its levels not significantly reduced in the MMSE < 24 AD group.

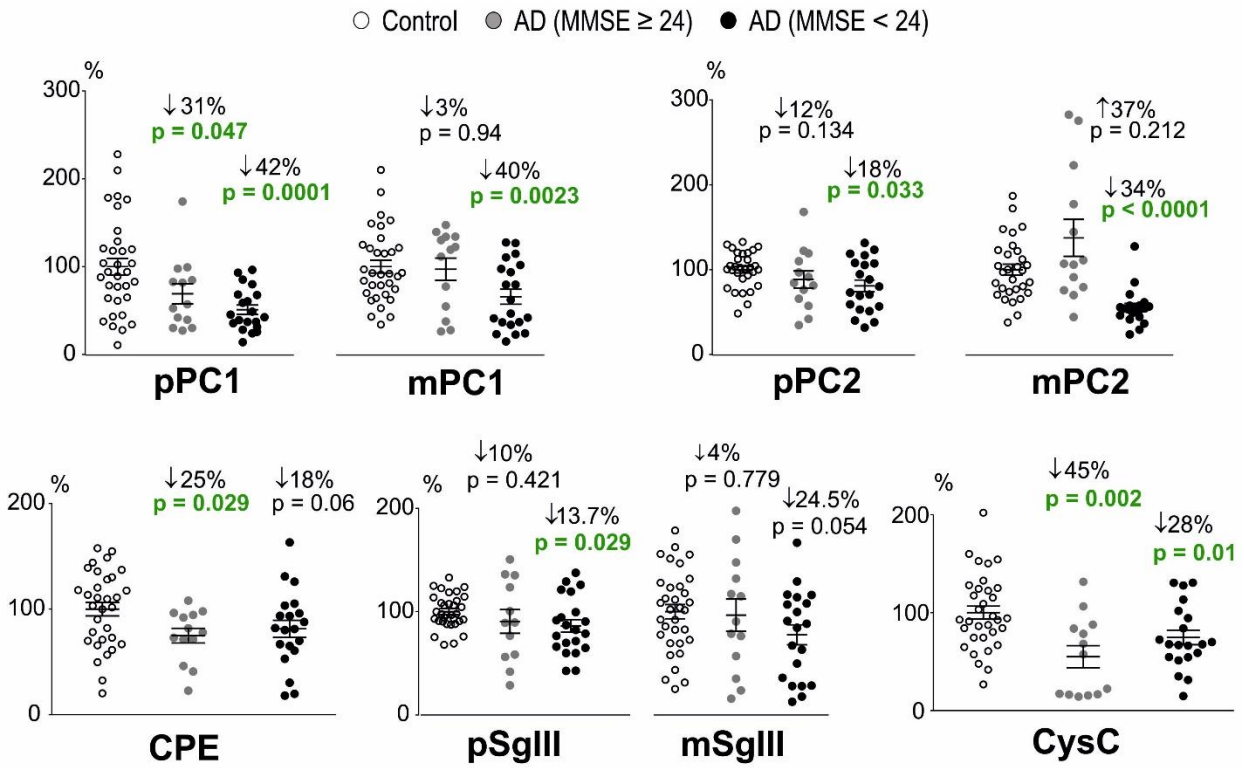

Figure 28. DCV proteins markedly decline in the CSF of AD patients with lower MMSE scores. Scatter dot-plots represent percent variation of secretory protein levels in the CSF of AD patients with MMSE scores over 24 (MMSE ≥ 24; n = 13) and AD patients with MMSE scores below 24 (MMSE < 24; n = 20) compared to controls (n = 33). Arrows indicate percentage reduction and p values the statistic significances. Data are presented as the mean ± SEM of analysis performed in duplicate. Statistically significant difference is calculated using a Kruskal-Wallis test followed by Dunn's multiple comparisons test.

To investigate associations between levels of CSF secretory proteins and age, cognitive status (MMSE) and the core CSF AD biomarkers (Aβ42, p-tau and t-tau), a Spearman correlation analysis was carried out in the AD cohort (33 individuals) (Figure 29).

After adjusting significance to a p-value ≤ 0.0019 based on Bonferroni correction of multiple comparisons, no correlations were found between CSF secretory proteins and age nor Aβ42. In contrast, strong inverse correlations between the mature PC2 form and MMSE score (p = 0.0001, r = 0.6449) and mPC2 and t-tau (p = 0.0004, r = 0.5837) were evidenced. Additionally, positive correlations between levels of p-tau and CPE (p = 0.0013, r = 0.5377) and the pSgIII (P = 0.0019, r = 0.5216) were determined, as well (Figure 29).

Taken together, DCV proteins were abnormally accumulated in dystrophic neurites and in GVD inclusions in AD cases and were strongly altered in the CSF. Decrease in levels of DCV markers in the CSF of AD patients occurred in parallel with disease progression. Moreover, the revealed correlation between mPC2 and MMSE scores, together with the described correlations between some DCV proteins and t-tau and p-tau but not with AB42, suggested a plausible association between these alterations and later stages of the disease, when neurodegeneration and cognitive impairment are advanced. Hence, DCV markers may be proposed as candidate CSF biomarkers for AD-associated neurodegeneration and consequent cognitive damage. Nevertheless, other studies would be required to further validate the obtained results.

vs CSF	pPC1		mPC1		pPC2		mPC2		CPE		pSgIII		mSgIII		CysC	
	r	p	r	p	r	p	r	p	r	p	r	p	r	p	r	p
Age	0.3137	0.0754	0.1852	0.3023	0.0635	0.7255	0.3436	0.0503	-0.2393	0.1798	-0.1280	0.4778	-0.0348	0.8477	-0.1156	0.5216
MMSE	0.3143	0.0749	0.4416	0.0101	-0.0517	0.7751	0.6449	0.0001	-0.1387	0.4413	0.0072	0.9681	0.1911	0.2867	-0.1197	0.5070
CSF Aβ42	-0.1945	0.2781	0.0239	0.8949	-0.1542	0.3914	0.2200	0.2186	0.0676	0.7086	0.1300	0.4709	0.2595	0.1448	0.1489	0.4083
CSF T-tau	-0.1896	0.2905	-0.4942	0.0035	0.0836	0.6438	-0.5837	0.0004	0.4717	0.0056	0.4326	0.0119	0.3010	0.0887	0.3714	0.0333
CSF P-tau	-0.0675	0.7089	-0.3660	0.0362	0.2094	0.2421	-0.4369	0.0110	0.5377	0.0013	0.5216	0.0019	0.4217	0.0145	0.2905	0.1010

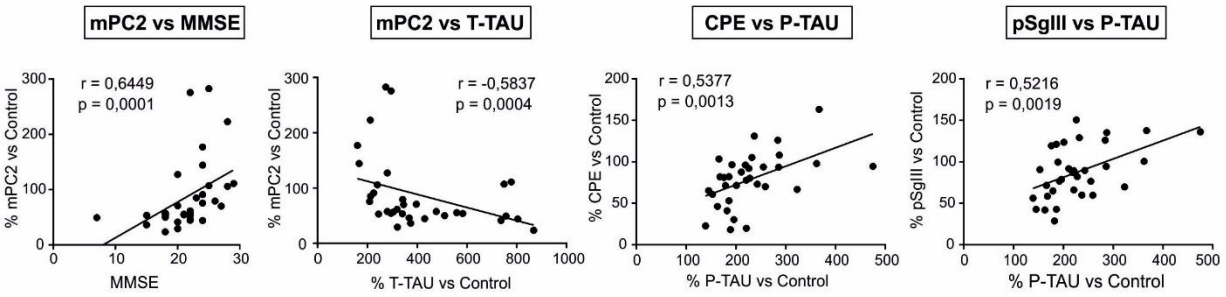

Figure 29. Correlation analysis of CSF secretory proteins with age, MMSE score and the CSF core-AD biomarkers in AD subjects. Top, table summarizing Bonferroni-corrected Spearman correlations between secretory proteins and age, MMSE score, Aβ42, tau and p-tau. Significant correlations are highlighted in green (Bonferroni-corrected; p < 0.0019) and in yellow (non-corrected; p < 0.05). Bottom, Bonferroni-corrected significant correlations are represented in correlation graphs.

3. Dense-core vesicle proteins decay in the brain and cerebrospinal fluid of the 5xFAD mouse model of familial Alzheimer's disease

To further understand the alterations of DCV markers evidenced in human AD cortices and CSF, DCV proteins have been analyzed in the brain and CSF of the 5xFAD mouse model of familial AD (FAD) from early (3 months) to more advanced stages (12 months). Even though tau pathology is missing in the 5xFAD model, these transgenic mice co-express five FAD mutations, which cause rapid Aβ42 accumulation in the brain as soon as at the age of 2 months (Oakley et al., 2006). Besides, early cognitive alterations and neuronal loss in 5xFAD mice have been evidenced at around 6 and 10 months, respectively (Esquerda-Canals et al., 2017; Spangenberg et al., 2016).

Previous work from our laboratory described CPE and SgIII accumulations in dystrophic neurites of APP/PS1 transgenic mice, thus recapitulating alterations observed in AD human brains (Plá et al., 2013). However, additional studies were needed to further decipher alterations of DCV secretory markers in the brain and CSF of other FAD-transgenic mice. Besides, and to our knowledge, no other studies have reported alterations of DCV-cargos in the CSF of transgenic mice, until the moment.

DCV secretory markers decay in the hippocampus of 12-month 5xFAD mice

Hippocampal homogenates from 3, 6 and 12-months male 5xFAD mice and their non-transgenic WT littermates (n = 6 for each genotype and age) were analyzed by western blot (Figure 30). Equal amounts of protein (20µg) were loaded into Criterion TGX Stain-Free™ gels and results were normalized by total protein content data obtained from GelDoc Blot scans. In graphs, levels of the different proteins were indicated as percent variation versus levels of WT mice at 3 months of age, which were presented as the 100% in all cases.

Synapse markers, as the SV membrane-associated protein Syp, revealed hippocampal synapse loss at 12 months in transgenic animals, being its levels significantly decreased (68%, $p = 0.004$) compared to WT. Additionally, in 5xFAD mice at 6- and 12-months statistically significant increases in proteins associated with glial reactivity, as GFAP (196%, $p = 0.002$ and 252%, $p = 0.02$, respectively) and Iba1 (172% and 211%, respectively; $p = 0.002$ for both ages), were determined compared to controls of the same age.

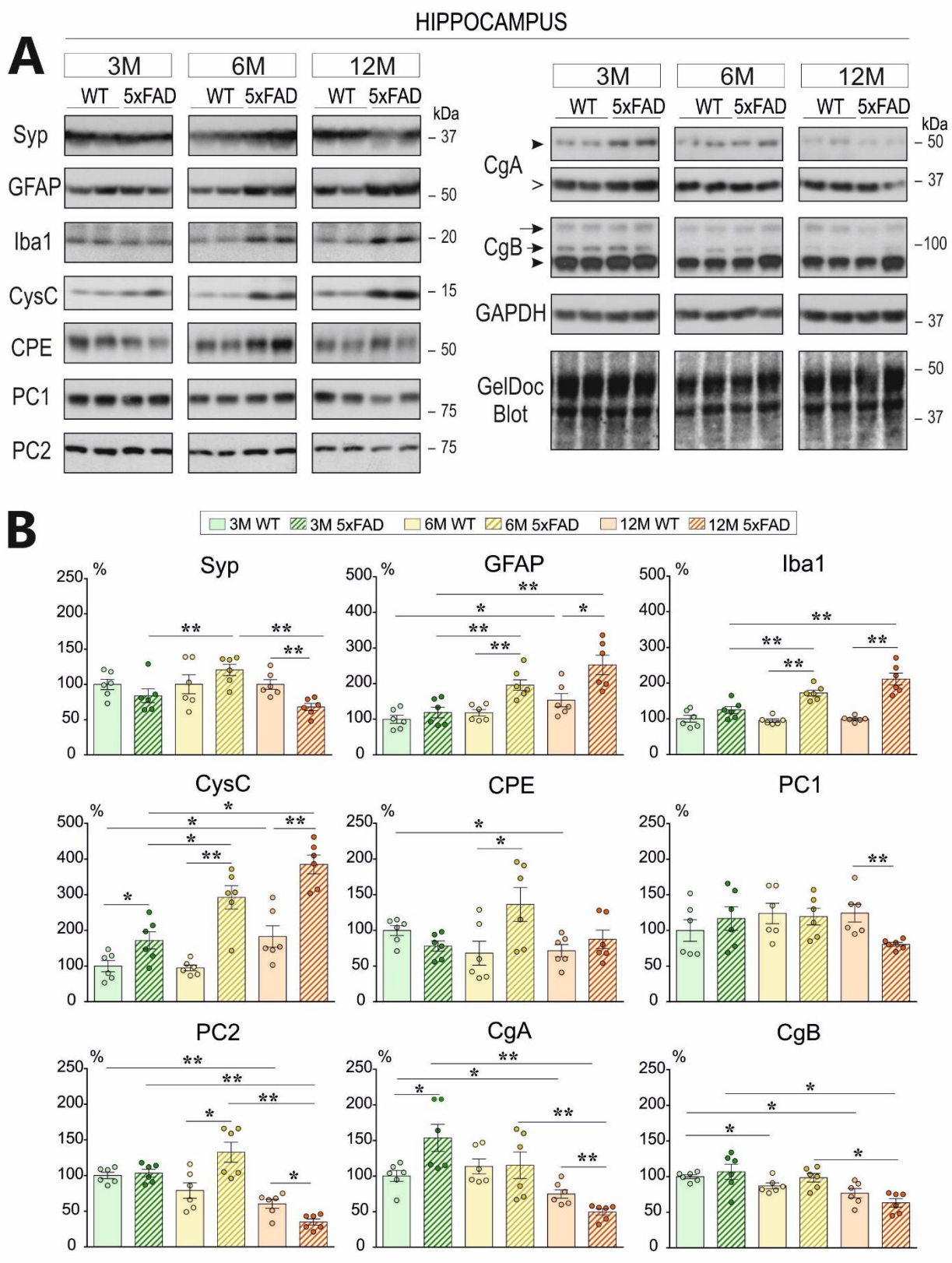

Figure 30. DCV secretory markers decline in the hippocampus of 12-month 5xFAD mice. A. Representative western blot analysis of hippocampal (HP) tissues (20µg) from WT and 5xFAD mice at 3, 6 and 12-month (M) of age (n = 6 for each genotype and age). PC1 and PC2 reveal only precursor (87 and 75kDa, respectively) forms. For CgA, two bands are detected, around 50kDa (arrow-head) and 37kDa (open-arrow). CgB displays a robust mature form around 80kDa (arrow-head) and two high-mobility additional bands around 100kDa (arrow and short-arrow, respectively). For both CgA and CgB all bands have been analyzed in a pooled quantification. B. Graphs summarize percent variation of

different protein levels in the HP of WT and 5xFAD mice versus levels of 3M WT (presented as 100%). Syp is significantly decreased in the HP of 12M 5xFAD mice compared to 12M WT. GFAP and Iba1 are meaningfully increased in 5xFAD mice at 6M and 12M compared to controls of the same age. GFAP is additionally augmented in an age-dependent manner (12M WT mice compared to 3M WT). Levels of CysC are found elevated in 5xFAD HP tissues compared to controls at all ages, including 3M. CysC is also age-dependently augmented in HP, comparing 3M with 12M WT mice. Except for CPE, levels of all DCV-contained proteins decline in the HP of 12M 5xFAD animals compared to 12M WT. Additionally, CPE, PC2 and CgA are increased in the HP of 6M (CPE and PC2) and 3M (CgA) 5xFAD mice in comparison with WT. Finally, levels of CPE, PC2 and CgB decline in an age-dependent fashion as indicate reductions in 12M versus 3M WT animals. GAPDH is used as a loading control. Results are normalized by total protein content data obtained from GelDoc Blot scans. Data are presented as the mean ± SEM. Statistically significant difference is calculated using a Kruskal-Wallis test followed by Dunn's multiple comparisons test. * indicates p-value < 0.05, ** indicate p-value < 0.01 and *** indicate p-value < 0.001.

Consistently, the 5xFAD mouse model efficiently recapitulated hippocampal synapse loss and glial reactivity, which are well-established features of AD pathology (Chun and Lee, 2018; Long and Holtzman, 2019). Of note, an age-dependent rise in GFAP expression was evidenced in WT mice as well, yet to a lesser extent than in transgenic mice (153%, $p = 0.04$), which may be consequence of adaptive plasticity mechanisms occurring in physiological aging (Rodríguez-Arellano et al., 2016).

In a similar manner, levels of the secretory protein CysC were found elevated in 5xFAD hippocampal tissues compared to controls at 3- (172%, $p = 0.04$), 6- (293%, $p = 0.022$) and 12-months (385%, $p = 0.022$). Moreover, CysC was also augmented in an age-dependent fashion in WT animals (183% in 12-months WT, $p = 0.026$). These results suggested that alterations in hippocampal CysC and glial reactivity may run in parallel. In fact, increased CysC in reactive astrocytes has been evidenced in transgenic mice expressing the human APP gene with the Swedish double mutation (Steinhoff et al., 2001).

DCV-contained secretory proteins were generally decreased in the hippocampi of 12-months 5xFAD mice. Regarding the protein convertases, immunoblots revealed for PC1 and PC2 only precursor (87 and 75kDa, respectively) but not mature forms, which declined significantly in 12-months transgenic hippocampal tissues ($p = 0.0022$ and $p = 0.013$, respectively). Moreover, a significant age-dependent reduction was observed for PC2 in both 5xFAD (69% and 98% decreases in 12-months compared to 3- and 6-months, respectively) and WT mice (40% decrease, $p = 0.002$). Lastly, levels of PC2 were significantly increased in the hippocampus of 6-months 5xFAD mice in comparison with their WT littermates (rise of 50%, $p = 0.026$).

Two bands of differential electrophoretic mobility were detected for CgA, likely corresponding to mature (around 50kDa) and sub-processed (around 37kDa) forms. To obtain global CgA levels, and due to great differences in band intensity, both bands were independently quantified and results were averaged. As for PC2, levels of CgA declined significantly in 12-months transgenic hippocampi ($p = 0.002$) and significant age-dependent reductions were observed in both 5xFAD (103% and 65% decreases in 12-months compared to 3- and 6-months, respectively) and WT animals (78% decrease, $p = 0.026$). Of note, a rise in CgA was evidenced in 3-months 5xFAD mice compared to WT of the same age (rise of 53%, $p = 0.03$).

CgB displayed a robust mature form of around 80kDa and two additional bands with higher mobility likely corresponding to differently-processed precursor forms (around 100kDa). In a pooled quantification, significant age-dependent decreases were evidenced for both WT (around 20% for both 6- and 12-months compared to 3-months) and 5xFAD mice (around 40% for 12-months compared to both 6- and 3-months).

Finally, levels of CPE similarly declined in an age-dependent manner in the hippocampi of WT animals (30% decrease, $p = 0.039$) and increased in 6-months 5xFAD mice compared to WT of the same age (36% increase, $p = 0.041$). However, their levels were preserved in 12-months 5xFAD hippocampal tissues compared to controls, which may be attributed to CPE being the only analyzed DCV-protein present in both neurons and astrocytes.

Overall, the 5xFAD mouse model apparently recapitulated hippocampal synapse loss and glial reactivity, which was also age-dependently increased in WT mice. Rises in CysC and CPE ran in parallel with alterations in markers of reactive gliosis. Other exclusively-neuronal DCV components as PC1, PC2, CgA and CgB decreased in transgenic hippocampal tissues at 12 months, which could be associated with the synapse loss evidenced at the same age. Nevertheless, alterations in synthesis, degradation or neuronal loss might not be discarded. Finally, many DCV-cargos increased in the hippocampi of 5xFAD mice at early ages. Altogether, these results suggest the existence of initial compensatory mechanisms and later failure of synaptic structures, in line with existing literature (Duits et al., 2018).

Secretory cargos of DCV are maintained in neuronal terminals of 5xFAD mice

As DCVs preferentially fuse at synapses, even though they are also well-represented in dendrites (Persoon et al., 2018), we next questioned whether levels of DCV proteins could be similarly altered in nerve terminals of 5xFAD mice. Therefore, synaptosome fractions were obtained from 3 and 12-months WT and 5xFAD mouse cerebral cortices following the protocol summarized in Figure 31A. Isolated synaptosomes were subsequently visualized in a transmission electron microscope, where electron micrographs evidenced that membrane and synaptic structures were properly maintained in both WT and 5xFAD synaptosomal fractions (Figure 31B).

As evidenced in the immunoblots of Figure 31C, SV and DCV proteins were detected in synaptosome preparations. Equal amount of protein (7.5µg) was loaded for cerebral cortex homogenate and cortical synaptosomes. Synapse markers, as the SV membrane-associated protein Syp and the post-synaptic density protein PSD95, were highly enriched in synaptosome fractions, compared to total cortex homogenate. Otherwise, DCV markers as CPE, PC2 and CysC were abundantly detected in the cerebral cortex and slightly less but still consistently well-detected in synaptosome preparations.

To further characterize synaptosomal fractions, release assays were performed in live synaptosomes maintained in an appropriate secretion medium. CPE and PC2 were slightly detected in the released media under basal conditions, whereas both were markedly increased in response to 55mM KCl stimulation (Figure 31D). Moreover, APP overexpression was corroborated in 12-months 5xFAD synaptosomes, as evidenced western blot analyses in Figure 31E. 5xFAD mice displayed increased intensities for a set of bands likely corresponding to APP (around 100kDa). Lower-mobility bands likely corresponding to the βAPP carboxyterminal fragment (β-CTF; around 17kDa) were strongly evidenced in 5xFAD but not in WT.

Subsequently, western blot analyses of synaptosomal preparations from hippocampal tissues of WT and 5xFAD mice at 3- (n = 6/ group) and 12- (n = 3/group) months were performed (Figure 32). 7.5µg of protein was loaded into gels, except for Syp and CPE analyses, which were detected in 3µg. Results were normalized by total protein content data obtained from Ponceau staining scans and represented as percent variation versus WT levels at each age, which were considered as the 100%.

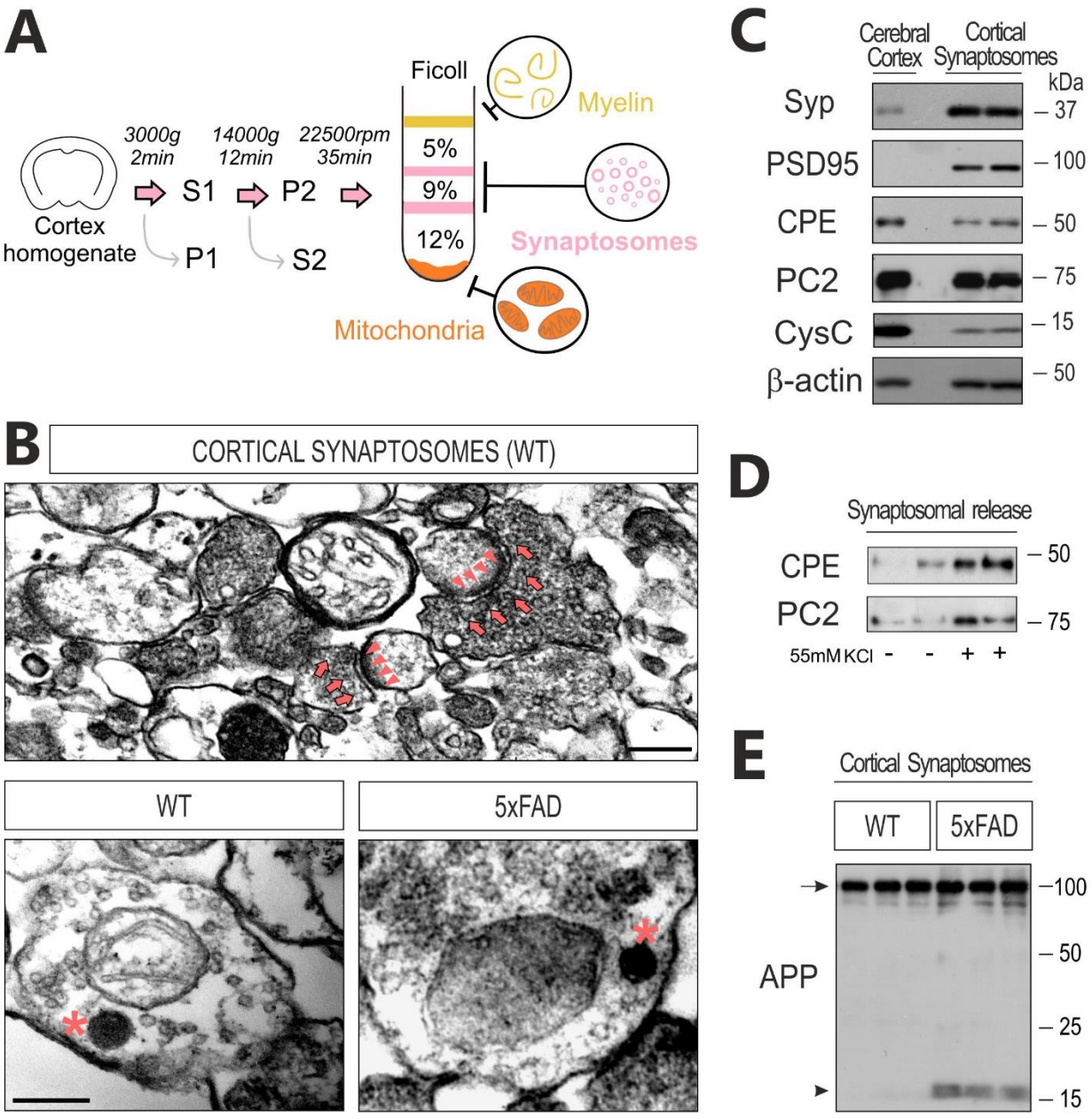

Figure 31. Characterization of synaptosomal preparations. A. Schematic representation of the synaptosome obtention protocol from mouse cerebral cortex homogenates. S and P indicate supernatant and pellet fractions, respectively. B. Transmission electron micrographs of cortical synaptosomes from 6-months WT and 5xFAD mice indicate that membrane and synaptic structures in synaptosomal preparations are properly maintained. Arrows point to SVs, arrow-heads delineate post-synaptic densities and asterisks indicate DCVs. Scale bars in nm: top, 250; bottom, 200. C. Western blot analyses of SV and DCV proteins in synaptosomal preparations (7.5µg) in comparison with total cortical levels (7.5µg). Syp and PSD95 are highly enriched in synaptosome fractions, whereas CPE, PC2 and CysC are abundantly detected in the cerebral cortex and slightly less but still consistently represented in synaptosome fractions. β-actin is used as loading control. D. Secretion assays performed in live synaptosomal preparations indicate that obtained synaptosomes are functional, as release of both CPE and PC2 markedly increases in response to 55mM KCl stimulation. E. Western blot analyses of cortical synaptosomes from 12-months WT and 5xFAD mice indicate that APP is present in both WT and 5xFAD mice, being overexpressed in 5xFAD (around 100kDa; arrow). Bands likely corresponding to the βAPP carboxyterminal fragment (β-CTF; around 17kDa; arrow-head) are strongly evidenced in 5xFAD but not in WT.

For PC1 and PC2 precursor forms were observed in synaptosome preparations (around 87 and 75kDa, respectively). For CgA, the mature form (around 50kDa) was evidenced. CgB revealed a robust mature form (around 80kDa) and two additional bands of higher mobility (both around 100kDa), which were all analyzed together in a pooled quantification. Results evidenced increased levels of GFAP (p = 0.0002), Iba1 (p = 0.028) and CysC (p = 0.032) at 12 months, but unexpectedly, invariable SV (Syp) and DCV proteins (CPE, PC1, PC2, CgA and CgB) in hippocampal synaptosomes of 5xFAD mice at both 3 and 12 months of age compared to controls (Figure 32).

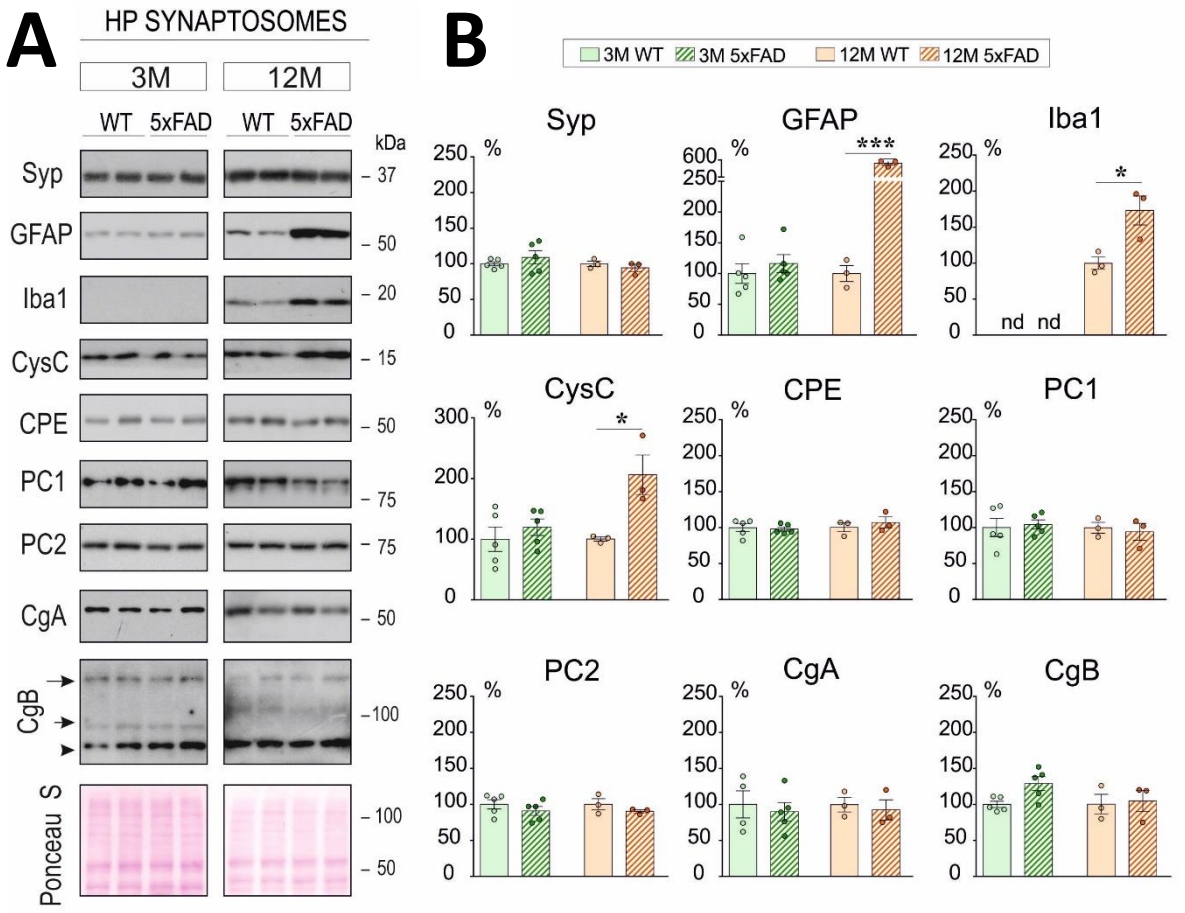

Figure 32. DCV secretory cargos are maintained in hippocampal synaptosomes of 3 and 12-month 5xFAD mice. A. Representative western blot analysis of synaptosome preparations from hippocampal (HP) tissues of WT and 5xFAD mice at 3 and 12-month (M) of age (n = 6 for each genotype at 3M; n = 3 for each genotype at 12M). 7.5µg of protein is loaded into gels, except for Syp and CPE analyses (detected in 3µg). PC1 and PC2 reveal only precursor (87 and 75kDa, respectively) forms. For CgA, only the mature form is revealed (50kDa). CgB displays a robust mature form (80kDa; arrow-head) and two additional bands (both around 100kDa, arrow and short-arrow, respectively). All bands of CgB have been quantified together. B. Graphs summarize percent variation of different protein levels in HP synaptosomes of 5xFAD mice versus WT levels at each age (represented as the 100%). Syp is maintained in 5xFAD HP synaptosomes at both 3 and 12M. GFAP and Iba1 are increased in HP neuronal terminals of 5xFAD mice at 12M compared to controls. Iba1 levels are below detection limit (n.d.) in 3M mice HP synaptosomes. CysC is also augmented in synaptosomes from 12M 5xFAD mice. Levels of DCV-markers (CPE, PC1, PC2, CgA and CgB) are maintained in synaptosomes from both 3 and 12M 5xFAD mice compared to controls. Results are normalized by total protein content data obtained from Ponceau staining scans. Data are presented as the mean ± SEM. Statistically significant difference is calculated using a two-tailed Mann-Whitney test. * indicates p-value < 0.05 and *** indicate p-value < 0.001.

To further corroborate and extend these results, secretory proteins were also analyzed in synaptosomal preparations from the entire cerebral cortex of 3 and 12-months WT and 5xFAD mice (n = 6 for each genotype and age). Representative immunoblots are shown in Figure 33A. Again, 7.5µg of protein was loaded into gels, except for Syp and CPE analyses, which were detected in 3µg. Results were normalized by total protein content data obtained from Ponceau staining scans and represented as percent variation versus WT levels at each age, which were considered as the 100%. The same electrophoretic bands were observed for all proteins in cortical synaptosomes, compared to hippocampal synaptosomes. Levels of DCV secretory proteins were similarly preserved in cortical synaptosomes of 3 and 12-month 5xFAD mice, except for CPE, which declined (70.5%, p = 0.026) in 3- and increased (195.2%, p = 0.0022) in 12-months 5xFAD cortical synaptosomes. Of note, Syp was reduced (57.5%, p = 0.0043) in 12-month 5xFAD cortical synaptosomes (Figure 33B).

Variations in the levels of secretory proteins in the CSF of 5xFAD mice

Consequently, we next investigated whether levels of secretory proteins could be altered in the CSF of 3, 6 and 12-month 5xFAD mice. Therefore, CSF extractions were performed from the cisterna magna with a borosilicate capillary, through which CSF flowed out as a result of pressure differences. In average, CSF volumes obtained from all extractions ranged between 3 and 12µL, which were rapidly transferred from capillaries into tubes. As DCV secretory proteins were present in mouse blood and plasma, even a minor blood residue originated from CSF extraction could reach the CSF and mask quantification results (Figure 34A).

Thus, all analyzed CSF samples were screened for blood contamination using two different exclusion criteria. First, and right after extraction, all samples were visually inspected for possible blood traces. Only visible clear CSF samples were considered for analysis. In addition, clear samples were immediately centrifuged to remove any other imperceptible blood or cellular residue. Since IgM is a large molecule usually present in very low concentrations in the CSF (Reiber, 2016), elevated IgM levels could evidence abnormal blood presence in CSF samples. Hence, a second exclusion criterium was used based on the amount of IgM detected in mice CSF by western blot. CSF samples with abnormally elevated levels of IgM were eliminated from analyses, as anomalous quantities of DCV proteins could be detected in such cases (Figure 34B). Finally, a total of 63 CSF samples were included in the present study for secretory protein analysis in 3, 6 and 12-month WT (n = 8, n = 8, n = 11) and 5xFAD (n = 11, n = 13, n = 12) mice, respectively.

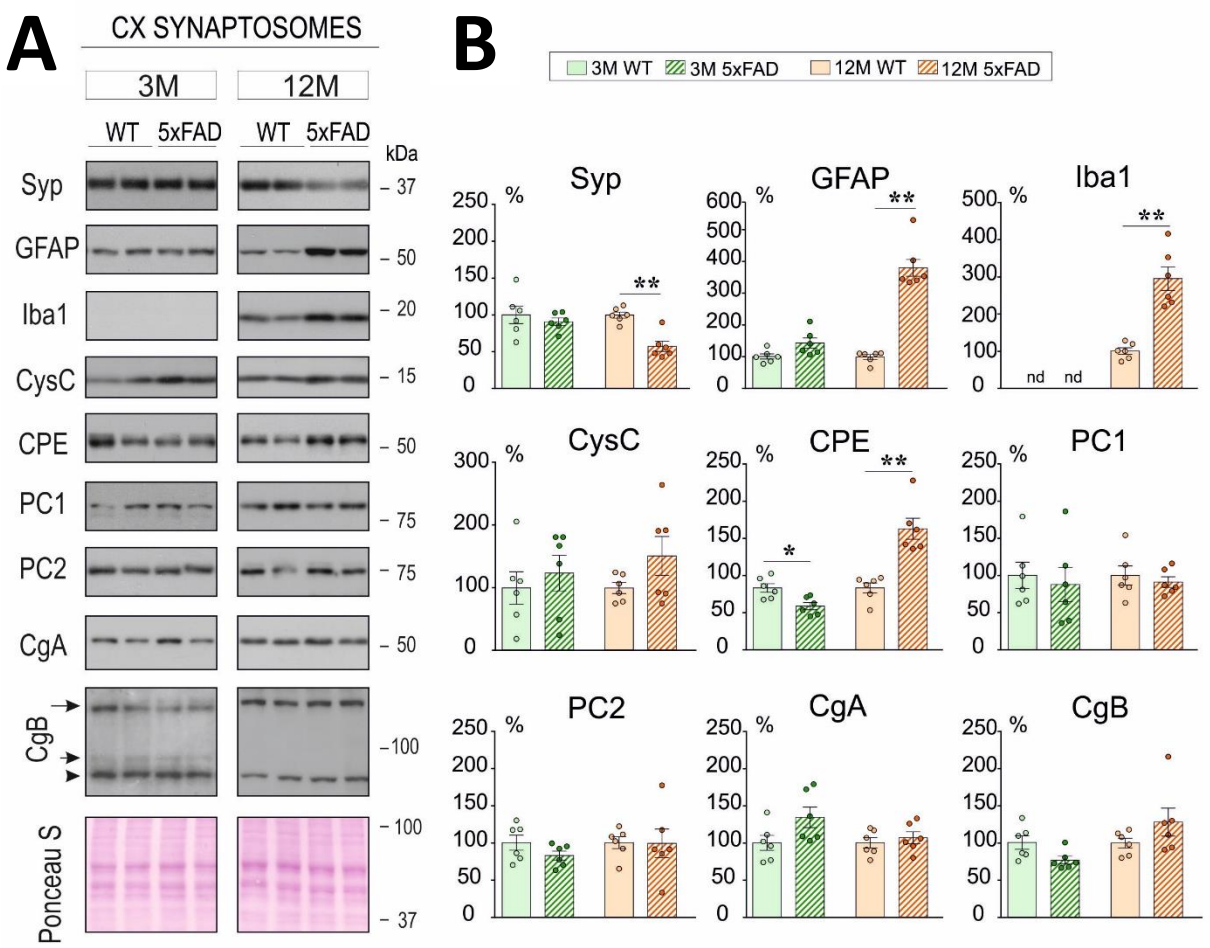

Figure 33. DCV secretory proteins are generally preserved in cortical synaptosomes of 3 and 12-month 5xFAD mice. A. Representative western blot analysis of synaptosomal preparations from cortical (CX) tissues of WT and 5xFAD mice at 3 and 12-month (M) of age (n = 6 for each genotype and age). 7.5µg of protein is loaded into gels, except for Syp and CPE analyses (detected in 3µg). PC1 and PC2 reveal only precursor (87 and 75kDa, respectively) forms. For CgA, only the mature form is revealed (50kDa). CgB displays a robust mature form (80kDa; arrow-head) and additional bands (around 100kDa, arrow and short-arrow, respectively). All bands of CgB have been quantified together. B. Graphs summarize percent variation of different protein levels in CX synaptosomes of 5xFAD mice versus WT levels at each age (represented as the 100%). Syp is reduced in 5xFAD CX synaptosomes at 12M. GFAP and Iba1 are increased in CX neuronal terminals of 5xFAD mice at 12M compared to controls. Iba1 levels are below detection limit (n.d.) in 3M mice CX synaptosomes. Levels of most DCV-markers (PC1, PC2, CgA and CgB) are maintained in CX synaptosomes from both 3 and 12M 5xFAD mice compared to controls. CPE, however, declines in 3M and increases in 12M 5xFAD CX synaptosomes. Results are normalized by total protein content data obtained from Ponceau staining scans. Data are presented as the mean ± SEM. Statistically significant difference is calculated using a two-tailed Mann-Whitney test. * indicates p-value < 0.05 and ** indicate p-value < 0.01.

Due to the limited CSF volumes, DCV proteins were analyzed by western blot in the same CSF samples (2µL) from WT and 5xFAD mice of 3, 6 and 12 months of age. Since our antibodies for several DCV markers originated in the same host, and many proteins had a similar molecular weight, only the levels of CPE, PC2 and CysC could be assessed. A single band was evidenced for all three proteins in mice CSF samples at these small volumes, likely corresponding to the mature forms of CPE (53 kDa) and PC2 (75kDa) and to the monomeric form of CysC (14kDa) (Figure 35A).

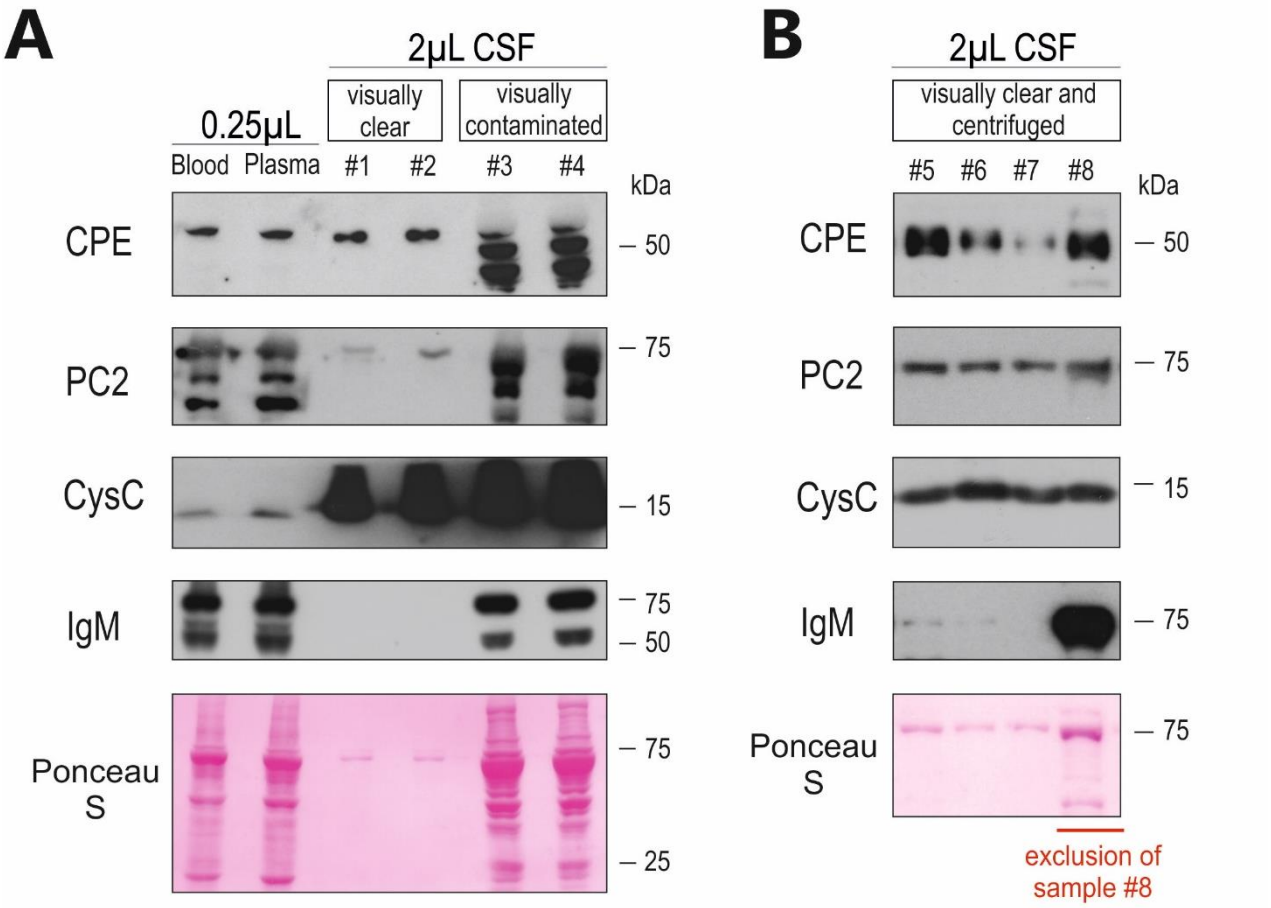

Figure 34. Mice CSF selection and exclusion criteria. A. Western blot analyses indicate that CPE, PC2 and CysC are abundantly represented in mouse blood and plasma (0.25µL) and in blood-contaminated CSF (2µL). Thus, after visual examination of extracted CSF, only completely clear samples, devoid of any visible blood residue, are selected for further analysis. Elevated IgM levels evidence abnormal blood presence in contaminated CSF. B. Besides visual inspection and centrifugation after extraction, a posterior western blot analysis of IgM levels is used to exclude samples with abnormal blood presence that could not be evidenced by visual inspection.

In Figure 35B, graphs summarized percent variation of secretory proteins levels in the CSF of 3, 6 and 12-months WT and 5xFAD versus levels of 3-months WT, which were represented as the 100%. CysC significantly increased to levels of around 150% in the CSF of 5xFAD mice at both 6 and 12 months compared to WT at each age ($p = 0.046$ and $p = 0.03$, respectively). Besides, a significant age-dependent increase in CysC was evidenced in 12-months compared to 3-months 5xFAD samples ($p = 0.03$). For CPE and PC2, no statistically significant differences were observed between 5xFAD and WT mice at any age. However, both proteins were significantly reduced in the CSF of 12-month compared to 3-month 5xFAD mice (46% decrease, $p = 0.03$ and 96% decrease, $p = 0.0001$, respectively). A similar age-dependent reduction was also evidenced, yet to a lesser extent, for PC2 in WT animals (58% reduction, $p = 0.0005$).

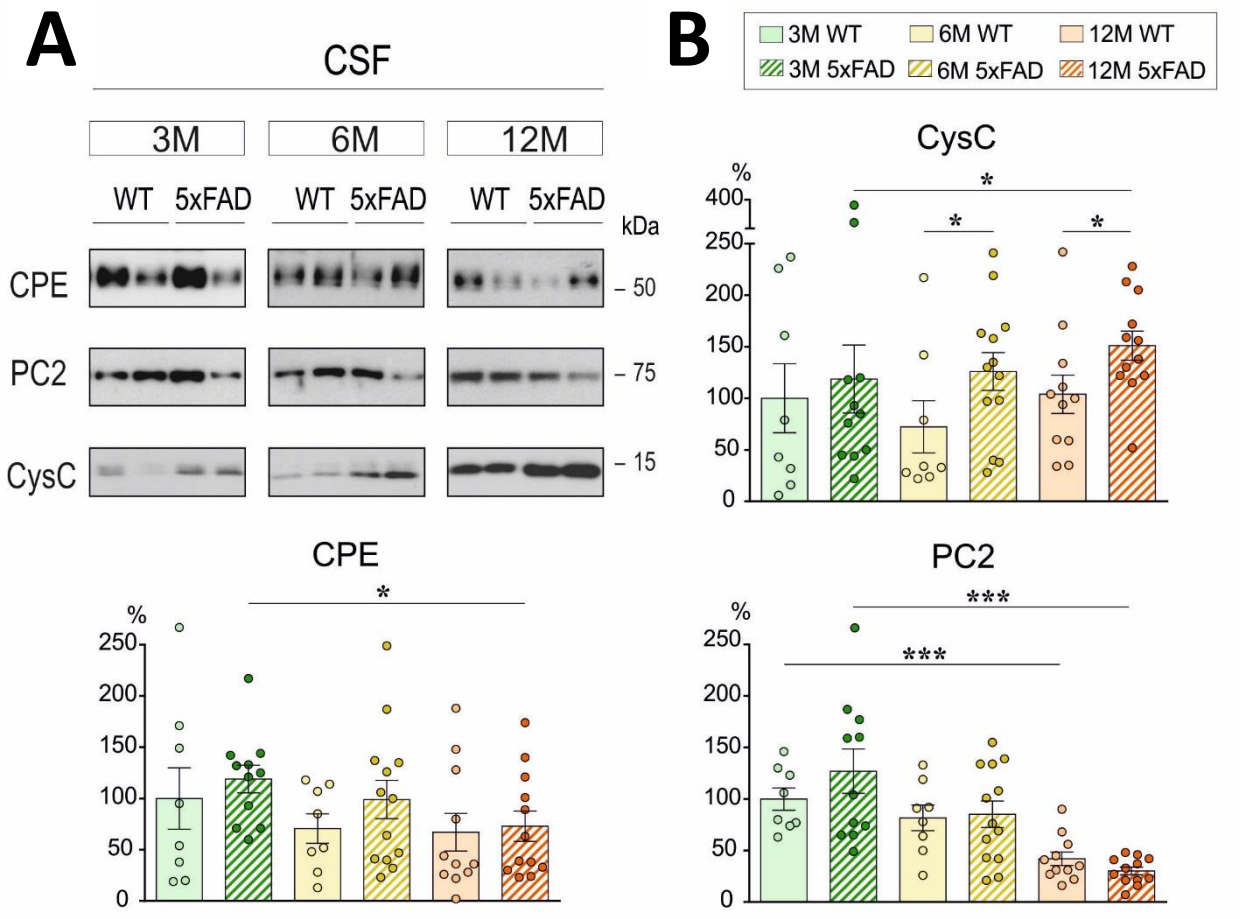

Figure 35. Secretory proteins are diversely altered in the CSF of 5xFAD mice. A. Representative immunoblots show levels of CPE, PC2 and CysC in the same CSF samples (2µL) from WT and 5xFAD mice of 3, 6 and 12 months (M) of age. Only a single band is detected for all three proteins in the CSF at these small volumes, corresponding to the mature forms of CPE (53 kDa) and PC2 (75kDa), respectively and to the monomeric form of CysC (14kDa). B. Graphs summarize percent variation of secretory proteins levels in the CSF of 3M (WT n = 8; 5xFAD n = 11), 6M (WT n = 8; 5xFAD n = 13) and 12M (WT n = 11; 5xFAD n = 12) versus levels of 3M WT (represented as the 100%). CysC significantly increases to levels of around 150% in the CSF of 5xFAD mice at 6 and 12M compared to controls of each age. Besides, 12M 5xFAD samples display elevated CysC compared to 3M 5xFAD. For CPE and PC2, no statistically significant differences are observed between 5xFAD and WT mice at any age. However, both proteins are significantly reduced in the CSF of 12M 5xFAD mice compared to 3M 5xFAD. A similar reduction is also observed, to a lesser extent, for PC2 between 12M and 3M WT mice. Data are presented as the mean ± SEM. Statistically significant difference is calculated using a Kruskal-Wallis test followed by Dunn's multiple comparisons test. * indicates p-value < 0.05 and *** indicate p-value < 0.001.

In conclusion, DCV proteins were generally increased in hippocampal tissues of 5xFAD mice at initial stages and finally decreased in 12-month-old transgenic mice. Moreover, their levels age-dependently decreased in the CSF. These results could be attributed to several causes, including changes in protein expression, synapse loss or neuronal loss. As their levels were invariable in hippocampal and cortical neuronal terminals, an impairment in secretion or an accumulation of DCV proteins at the terminal level, may also be suggested.

DISCUSSION

DISCUSSION

As an outstanding result of the present study, DCV secretory markers accumulate in dystrophic neurites and GVD bodies and decline in the CSF of AD patients. These markers include granins, carboxypeptidases and protein convertases, which are well-established molecular components of neuronal and endocrine DCVs (Bartolomucci et al., 2011; Vázquez-Martínez et al., 2012). In addition to their important intracellular roles in the sorting, trafficking and processing of significant peptidergic cargos as neurotrophins and hormones, key extracellular neurotrophic functions have been proposed for certain DCV markers (Bartolomucci et al., 2011; Cawley et al., 2012; Cheng et al., 2014). Hence, our reported variations in DCV proteins in the brain and CSF of AD patients and 5xFAD mice may reflect dysfunctions of the regulated secretory pathway, which could probably be taking part in aberrant cerebral functioning and neurodegeneration processes occurring in AD (Abolhassani et al., 2017; Artenstein and Opal, 2011; Bartolomucci et al., 2010; Lin and Salton, 2013; Nakabeppu and Ninomiya, 2019; Plá et al., 2017).

Certain DCV secretory markers are also abundantly synthesized and released by astrocytes *in vitro* and *in situ* (Paco et al., 2010; Plá et al., 2017). Here we have shown that astrocyte peptidergic secretory vesicles are heterogeneous and display variable release rates in response to extracellular Ca^{2+}-evoked stimulation, which are enhanced in proinflammatory-treated astrocytes *in vitro* and in an LPS-induced neuroinflammation model *in situ*. Furthermore, we have evidenced that unstimulated release of astrocyte secretory proteins *in vitro* does not require intrinsic Ca^{2+} oscillations but critically depends on intracellular Ca^{2+}. Understanding the mechanisms of fundamental astrocytic processes as peptidergic secretion under control and proinflammatory conditions is crucial, as reactive astrogliosis is a common feature of neurodegenerative diseases which has been associated to AD synaptic dysfunction (Brosseron et al., 2018; Van Eldik et al., 2016). In fact, besides neurotransmission impairments, aberrant astrocyte Ca^{2+} signalling and gliotransmission have been previously reported in AD (Mattson and Chan, 2003; Verkhratsky et al., 2017; Volk et al., 2015). All in all, since neuronal and glial communications are clearly affected in AD, our results suggest that alterations in the regulated secretory pathway may be mediators of underlying pathological mechanisms of AD and propose DCV secretory markers as candidate disease biomarkers.

Astrocyte peptidergic secretion dependence on intracellular Ca^{2+}

Ca^{2+}-evoked release of astrocyte secretory proteins *in situ* and *in vitro*

Astrocyte vesicular secretion of transmitters participates in fundamental cerebral processes as synaptic plasticity, neuronal development and neurovascular coupling, which are crucial for an appropriate brain functioning (Halassa et al., 2007; Malva et al., 2012; Otsu et al., 2015; De Pins et al., 2019). Additional research is needed to further comprehend the dynamics and the mechanisms underlying astroglial regulated secretion, especially *in vivo.* Previous investigations evidenced expression of DCV secretory markers as CPE, SgII and SgIII in astrocytes *in vivo* and variable release responses after Ca^{2+}-mediated evoked stimulation in astrocytes *in vitro* (Paco et al., 2009, 2010; Plá et al., 2013, 2017). Because CPE and secretogranins are expressed in both astrocytes and neurons (Plá et al., 2017), our analysis of astrocyte peptidergic release *in situ* required an endogenous astrocyte-specific secretory protein.

Consequently, in the present study, a model of LPS-induced neuroinflammation has been implemented to enhance astrocyte expression of the secretory protein LCN2 (Jin et al., 2014; Kang et al., 2017; Zamanian et al., 2012), as an approximation to investigate astrocyte endogenous regulated secretion *in situ*. Induction of glial reactivity and LCN2 overexpression has been confirmed 48h after LPS intraperitoneal injection, in line with existing literature (Jang et al., 2013; Jha et al., 2015; Jin et al., 2014; Lee et al., 2009; Naudé et al., 2012). LCN2 immunolabeling strongly colocalizes with GFAP, confirming its previously reported astrocytic localization (Jang et al., 2013; Jin et al., 2014; Mesquita et al., 2014; Naudé et al., 2012). In accordance with earlier research (Bi et al., 2013; Mesquita et al., 2014), our results have indicated virtually null LCN2 immunostaining in microglia, yet it is a controversial issue (Jang et al., 2013; Jin et al., 2014; Naudé et al., 2012).

Similarly, LCN2 neuronal expression has also been a highly debatable matter. In consistence with numerous investigations (Cvijetic et al., 2017; Kim et al., 2017; Mesquita et al., 2014), neurons are virtually devoid of LCN2 in our model. Interestingly, neuronal LCN2 protein, but not mRNA, has been reported in some studies, which could be explained by neuronal 24p3R receptor-mediated internalization of extracellular LCN2 (Devireddy et al., 2005; Ip et al., 2011). Moreover, since LCN2 is associated to innate immunity against infections, an expected LCN2 expression was observed in the choroid plexus (Flo et al., 2004; Ip et al., 2011; Marques et al., 2008).

Our assays in acute brain slices have revealed strong CPE and moderated CysC secretion in response to KCl stimulation. As CPE and CysC are localized in astrocytes and neurons here and by others (Mathews and Levy, 2016; Plá et al., 2013, 2017; Vázquez-Martínez et al., 2012), their presence in the media may have these two cellular origins. Differential responses to KCl-evoked stimulated release suggest the existence of heterogeneous subpopulations of peptidergic vesicles in neurons and astrocytes (Deng et al., 2001; Paco et al., 2009; Plá et al., 2017). Importantly, after carefully removing the choroid plexus from brain slices, KCl-stimulation also efficiently induces LCN2 release *in situ* in LPS-treated mice, yet to a lesser extent than for CPE. Lower rates of LCN2 stimulated secretion compared to CPE may substantiate the astrocytic origin of LCN2, since greater stimulated release is associated to specialized secretory cells as neurons (Bohmbach et al., 2016).

Astrocyte exocytosis of gliotransmitters and its physiological consequences *in vivo* has been a highly controversial issue for years (Hamilton and Attwell, 2010). With multiple evidences in favour and against, it is still under debate how astrocytes certainly contribute to the processing of neural information (Fiacco and McCarthy, 2018; Savtchouk and Volterra, 2018). Here, we have provided evidence for astrocyte regulated release of LCN2 *in situ* in a neuroinflammation-induced model, in a context close to *in vivo* conditions. Previous research in astrocyte regulated secretion have revealed astrocytic involvement in cholinergic plasticity and the release of diffusible vasodilators during activation of cortical neurons *in vivo* (Takata et al., 2011; Xu et al., 2008). In fact, astrocytes have been claimed as potential regulators of neurovascular coupling *in vivo* by means of neuronal-mediated increases of Ca^{2+} in astrocyte processes (Otsu et al., 2015).

It is mainly due to Ca^{2+}-mediated vesicular transmitter release that gliotransmission occurs (Savtchouk and Volterra, 2018). Neuronal signaling activates Ca^{2+} waves in astrocyte circuits (Dani et al., 1992) and astrocytes, in turn, release glutamate which ultimately regulates synaptic strength (Jourdain et al., 2007). In our model, KCl presumably triggers neuronal depolarization-induced Ca^{2+} increases that lead to neurotransmitter release (i.e. glutamate, ATP and cannabinoids) at synaptic terminals, which activate astrocyte receptors (Carmignoto et al., 1998; Filosa et al., 2012; Navarrete and Araque, 2010). Astrocytes then decode neuronal information generating local Ca^{2+} transients that propagate through the cell by Ca^{2+}-induced Ca^{2+} release from intracellular stores and reach astrocyte end-foot to favor vesicular release of gliotransmitters (Bazargani and Attwell, 2016; Filosa et al., 2006; Semyanov, 2019).

In our study, cultured astrocytes release CPE in response to rises in intracellular Ca^{2+} caused by ionomycin, whereas CysC and LCN2 display a high unstimulated release and a similar response after ionophore treatment. Importantly, stimulated release of astrocyte secretory proteins is enhanced under proinflammatory conditions, even though release of LCN2 is apparently less influenced by Ca^{2+} than CPE. Our results could be attributed to differential secretion mechanisms underlying astrocyte heterogeneous vesicle populations. In fact, we have found these secretory proteins localized in different vesicle types and a heterogeneity among vesicle subpopulations. CysC and LCN2 only partially colocalize with each other and, in accordance with existing literature, with lysosomal markers (Deng et al., 2001; Mathews and Levy, 2016; Yang et al., 2002), whereas CPE is contained in DCV-like in astrocytes (Paco et al., 2010; Plá et al., 2013, 2017).

Enhanced astrocyte stimulated secretion under proinflammatory treatment could be attributed to adjustments of the glial secretory pathway occurring in different cellular states (Paco et al., 2009). In fact, vesicle delivery is affected in reactive astrocytes (Verkhratsky et al., 2016) and variations in gliotransmission may be linked to the pathological mechanisms of several brain disorders characterized by reactive astrogliosis (Allan and Rothwell, 2001; Brosseron et al., 2018; Halassa et al., 2007). Importantly, hyperactivated astroglia display aberrant Ca^{2+} signalling, which could have an impact on the molecular mechanisms underlying astrocyte regulated secretion (Halassa et al., 2007; Shigetomi et al., 2019).

Previous investigations have also reported evidences of regulated exocytosis for the different astrocytic vesicles *in vitro.* For instance, stimulation by ATP causes Ca^{2+}-mediated release of glutamatergic SLMVs from cultured astrocytes (Jeremic et al., 2001). Secretory proteins of astrocyte DCVs as SgII, SgIII, CPE, ANP and NPY have also been described to undergo Ca^{2+}-dependent regulated secretion in response to different secretagogues, including ionomycin (Calegari et al., 1999; Krzan et al., 2003; Paco et al., 2009; Plá et al., 2017; Ramamoorthy and Whim, 2008; Verkhratsky et al., 2016). Regarding lysosomal secretion, ATP has been abundantly detected in astrocyte lysosomes and released in stimulus-dependent manner (Zhang et al., 2007). Of note, lysosomes are considered the main vesicular organelle undergoing Ca^{2+}-mediated exocytosis from cortical astrocytes (Li et al., 2008). *In vivo* studies have additionally corroborated that isolated astrocytes express the necessary genes for lysosome release and that ATP secreted by astrocytes modulates neurotransmission (Cahoy et al., 2008; Pascual et al., 2005).

In fact, astrocytes display the machinery for Ca^{2+}-dependent regulated secretion of vesicular gliotransmitters (Bohmbach et al., 2016), including neurotransmitter transporters, synaptotagmins and SNARE proteins, being syntaxin 4, SNAP23 and VAMP3 the most abundant isoforms (Bezzi et al., 2004; Blakely and Edwards, 2012; Guček et al., 2012; Montana et al., 2009; Paco et al., 2009). Regarding astrocytic DCV, secretogranins contribute to cargo concentration and vesicle biogenesis (Calegari et al., 1999; Paco et al., 2009, 2010). Additionally, both astrocyte DCVs and SLMVs display membrane VAMP2 or VAMP3 (Verkhratsky et al., 2016), whereas VAMP7 is associated to lysosomes (Verderio et al., 2012). While synaptotagmin 4 regulates glial SV-glutamate secretion (Zhang et al., 2004), synaptotagmin 7 facilitates Ca^{2+}-mediated lysosomal release (Arantes and Andrews, 2006; Chakrabarti et al., 2003; Jung et al., 2014), which has also been evidenced *in vivo* (Shin et al., 2012).

In conclusion, extracellular Ca^{2+}-mediated stimulated release of secretory proteins is enhanced in proinflammatory-treated astrocytes *in vitro* and in an LPS-induced neuroinflammation model *in situ*. DCV- and lysosomal-related proteins are released in response to intracellular Ca^{2+} increases caused by the ionophore ionomycin. However, release of LCN2 is apparently less influenced by extracellular Ca^{2+} entry than the secretion of CPE, which could be attributed to differential release mechanisms underlying astrocyte heterogeneous vesicle subpopulations. Our results are significant because they provide further evidence of astrocytic regulated secretion *in situ,* under induced-neuroinflammation conditions.

Astrocyte unstimulated release of secretory proteins depends on intracellular Ca^{2+}

In our secretion assays *in vitro,* astrocytes display high rates of unstimulated release and moderated evoked secretion of secretory peptides compared to neurons, which is in accordance with astrocyte unprofessional secretory nature (Calegari et al., 1999; Paco et al., 2009, 2010; Plá et al., 2017). Our results further indicate that secretory peptides are scarcely retained and immediately released after synthesis in an unstimulated manner, both in control and proinflammatory-treated astrocytes. Previous studies have reported spontaneous release of transmitters from astrocytes, which seem to have key functional implications as in the regulation of neurotransmitter release (Bonansco et al., 2011). Complete and transient (kiss-and-run and kiss-and-stay) fusion events occur in astrocytes (Bezzi et al., 2004; Prada et al., 2011) and both fusion modalities are responsible for astrocyte spontaneous vesicular release in a similar ratio (Bowser and Khakh, 2007; Malarkey and Parpura, 2011).

Furthermore, we have also determined that astrocyte unstimulated release of secretory proteins is independent of intrinsic Ca^{2+} oscillations, under both proinflammatory and control conditions. Even though astrocyte spontaneous Ca^{2+} fluctuations are virtually prevented after the strong blockage of SERCA with thapsigargin, intracellular Ca^{2+} levels are higher than in resting conditions (Innocenti et al., 2000; Wang et al., 2006), which could explain the observed invariable secretion rates. However, since astrocyte Ca^{2+} dynamics is highly compartmentalized and heterogeneous, the role of microdomain local Ca^{2+} activity in astrocyte peptidergic release should be additionally assessed (Araque et al., 2014; Bazargani and Attwell, 2016; Otsu et al., 2015; Savtchouk and Volterra, 2018).

The Ca^{2+} chelator BAPTA-AM has been used in gliotransmission studies to abolish induced and resting astrocyte Ca^{2+} levels (Agulhon et al., 2012). Here we have demonstrated that intracellular Ca^{2+} is required for the rapid release of newly synthesized secretory proteins in astrocytes. Similarly, previous studies reported intracellular Ca^{2+} dependence of astrocyte basal release of SgII (Paco et al., 2009) and glutamate (Malarkey and Parpura, 2011). As Ca^{2+} plays a fundamental role in astrocyte vesicle trafficking and fusion (Bohmbach et al., 2016; Potokar et al., 2013; Stenovec et al., 2007; Zhang et al., 2004), chelating intracellular Ca^{2+} may interfere these processes and finally lead to a lessened release, also in unstimulated conditions. Additionally, this Ca^{2+} dependence of unstimulated release is higher for lysosomal-related proteins (i.e. LCN2 and CysC), which could explain their greater unstimulated secretion rates and lower stimulated-responses in comparison with DCV proteins. In fact, it has been described that astrocyte small vesicles respond to Ca^{2+} elevations faster and more frequently than lysosomes (Liu et al., 2011). These observations could be attributed to the distinct molecular machineries implicated in the exocytosis of the different astrocyte vesicle types (Arantes and Andrews, 2006; Guček et al., 2012; Jung et al., 2014; Montana et al., 2009; Paco et al., 2009; Verderio et al., 2012).

Overall, our results indicate that secretory peptides are scarcely retained and immediately released in unstimulated astrocytes, under both control and proinflammatory conditions. Moreover, peptidergic secretion of unstimulated astrocytes does not require intrinsic Ca^{2+} oscillations, but critically depends on intracellular Ca^{2+}. Apparently, unstimulated release of lysosomal-related proteins displays a higher Ca^{2+} sensitivity, which nicely corresponds with their lesser secretion rates after Ca^{2+}-mediated stimulation, compared to DCV-contained secretory proteins.

Alterations of the regulated secretory pathway in Alzheimer's disease

Neuropathological alterations of DCV cargos in the AD cerebral cortex

As a main goal of the present dissertation, we have studied DCV secretory markers in the brain and CSF of AD patients. In advanced-AD brains, our immunoblotting assays of hippocampal and parietal tissues have revealed apparently invariable global levels of DCV proteins, except for the precursor form of PC2 (pPC2) which increases in both regions. Additionally, a significant reduction of the SV associated membrane protein Syp has been evidenced in AD cortices, in line with many studies focusing on synapse loss (Arendt, 2009). Specific alterations of other synaptic markers as SNAP25, Rab3A, PSD95 and neurogranin, which exert key roles in vesicle trafficking and exocytosis, have also been determined in AD (Bereczki et al., 2018; Ferrer et al., 1998).

Considering DCV peptides as putative markers of presynaptic structures may provide additional understanding of synapse impairment (Persoon et al., 2018; Willis et al., 2011). Alterations in total levels of some DCV proteins have been previously reported in AD brains. For instance, elevated CgA and lowered SgII were earlier evidenced in AD cortices (Lassmann et al., 1992). Consistently with prior research, we have found invariable levels of PC1 in AD brain homogenates (Winsky-Sommerer et al., 2003). Interestingly, increased pPC2 and unchanging mature PC2 (mPC2) are evidenced in our study, in accordance with existing literature likely associating greater PC2 amounts with decreased levels of its specific inhibitor, 7B2 (Winsky-Sommerer et al., 2003; Yakovleva et al., 2007).

A number of authors have also reported alterations of CysC in AD (Mathews and Levy, 2016). We have found decreased levels of the 28kDa form of CysC and invariable levels of the other forms in AD cortices. Otherwise, in our immunohistochemical analyses, CysC increases in pyramidal neurons and in reactive astrocytes close to Aβ plaques, as previously emphasized (Deng et al., 2001; Levy et al., 2001). Besides, intra- and extracellular binding of CysC and Aβ has been evidenced, suggesting an anti-amyloidogenic protective role for CysC in AD (Gauthier et al., 2011; Kaur and Levy, 2012). In human cortices, our data evidenced CysC immunolabeling in LAMP1+ structures, but not in DCV, which is in line with the described colocalization between CysC and the lysosomal cathepsin B (Deng et al., 2001). Interestingly, an association between CysC neuroprotective role in AD and cathepsin B inhibition has been defined (Gauthier et al., 2011). Above and beyond, a recent study has evidenced cathepsin D upregulation in AD cortices, in correlation with tauopathy (Chai et al., 2019).

Similarly, when analyzing DCV-markers distribution throughout the AD brain by immunohistochemical assays, most of them have been found aberrantly accumulated in dystrophic neurites surrounding Aβ plaques. In previous research from our laboratory, great accumulations of CPE and SgIII were described in dystrophic neurites (Plá et al., 2013). Here, we have additionally demonstrated accumulations for PC1 and PC2 in dystrophic neurites near amyloid plaques. Of note, most early studies focusing on chromogranins in AD have stated that around 20% and 25% of Aβ plaques contain CgA and CgB, respectively (Lechner et al., 2004; Marksteiner et al., 2002).

Granulovacuolar degeneration (GVD) is a key hallmark of AD which has been associated with tauopathy (Köhler, 2016). GVD bodies are aberrant lysosomal structures containing endocytic and autophagic cargo in core granules surrounded by outer membranes (Wiersma et al., 2019). Some proteins involved in vesicle trafficking and recycling (i.e. Golgin A4 and TMEM230) have been identified to accumulate in GVD bodies (Kork et al., 2018; Siedlak et al., 2017). However, as far as we know, no other research has investigated DCV proteins in GVD. Here, we provide new evidence of PC1 and PC2 being accumulated in GVD bodies in the CA1 region of AD hippocampi. In accordance with studies of GVD characterization (Köhler, 2016), PC1 and PC2 colocalized with the GVD core marker CK1δ and were surrounded by LAMP1+ membranes. Moreover, an association between PC1 and PC2+ GVD bodies and neurofibrillary tangle pathology has been also evidenced, in line with recent research (Köhler, 2016; Wiersma and Scheper, 2019).

All in all, we have described aberrant accumulations of DCV markers in AD cortices in relation with two typical neuropathological hallmarks of AD: dystrophic neurites and GVD bodies. As DCV are distributed throughout neurons but preferentially fuse at synapses (Persoon et al., 2018), an association between alterations in DCVs and SVs in AD would be expected. However, considering the reduction in Syp evidenced in the present study, the occurrence of distinct changes for both types of vesicles may be suggested, as formerly proposed (Willis et al., 2011). The currently reported accumulation of DCV cargos in AD may be attributed to other several causes. According to the amyloid cascade hypothesis of AD, an increase in the levels of Aβ is an initiating event in the pathology (Selkoe and Hardy, 2016). Thus, as Aβ species have been previously associated with dysregulations of the secretory pathway at different levels (Kimura and Yanagisawa, 2018; Plá et al., 2017; Seifert et al., 2016), alterations in vesicle trafficking and release may be suggested.

Given that Aβ production and secretion is controlled by several events along the membranous compartments of the secretory route (Tan and Gleeson, 2019), dysfunctional membrane trafficking in AD may have an impact on DCV biogenesis and release. Interactions between Aβ peptides and presynaptic proteins have been described to alter exocytosis (Fagiani et al., 2019; Yang et al., 2015). Additionally, aberrant endocytosis and endosome trafficking have also been reported in AD (Kimura and Yanagisawa, 2018). Importantly, endocytic dysfunction interrupts bidirectional axonal transport, thus leading to impairments in SV trafficking and docking (Kimura et al., 2012). Variations in microtubule-mediated transport occurring in AD may also influence DCV trafficking and secretion (Brandt and Bakota, 2017; Encalada and Goldstein, 2014).

Accordingly, changes in transport and secretion of BDNF-containing DCVs induced by extracellular Aβ species have been reported, yet together with invariable BDNF secretion rates (Seifert et al., 2016). Thus, even though activity-dependent mobilization of SVs and DCVs is similar (Levitan, 2008), the existence of differential pathological alterations for both types of vesicles may be suggested (Willis et al., 2011). Nevertheless, as Aβ oligomers have been determined to disrupt ER Ca^{2+} homeostasis and, consequently, induce ER stress, changes in protein expression may not be discarded (Alberdi et al., 2013). Likewise, dysfunction of protein degradation mechanisms should be considered, as hyperphosphorylated tau has been evidenced to constrain proteasome activity in AD (Keck et al., 2003; Komura et al., 2019).

Finally, dysfunction of auto- and endo-lysosomal pathways has also been evidenced in AD (Son et al., 2015; van Weering and Scheper, 2019). To eliminate misfolded proteins, unconventional secretory routes are activated (Li et al., 2017), which may have an impact on DCV release. In fact, the development of GVD inclusions could indicate a failure in lysosomal stress response (Wiersma and Scheper, 2019). As GVD is an early event of the tau-pathology progression (Köhler, 2016; Wiersma et al., 2019), accumulation of DCV markers in GVD bodies suggests that alterations in the peptidergic secretory pathway may be associated to tauopathy and neurodegeneration in AD.

DCV markers decay in CSF and correlate with cognitive decline and neurodegeneration in AD

In the present study, changes in DCV markers have been investigated in biopsied CSF from a very well characterized cohort of patients with early AD compared to age- and gender-matched healthy controls. Since the CSF directly interacts with the cerebral extracellular space, it may well reflect biochemical disturbances of the CNS (Johanson et al., 2008). As long-distance diffusion of peptide transmitters occurs via CSF (Alpár et al., 2019; Comeras et al., 2019), neurons may represent a core source of DCV markers reaching the CSF, yet astrocytic or ependymal origins might not be discarded (Alpár et al., 2018; Marques et al., 2007; Noble et al., 2018).

Certain chromogranins have been earlier studied in the CSF of AD patients. CgA, a major constituent of the DCVs, was one of the first candidate markers for AD-associated synaptic failure (Blennow et al., 1995). In more recent proteomic assays, changes in other DCV components as CgB, SgII and CPE have been identified in the AD CSF, yet results appear controversial (Brinkmalm et al., 2018; Chi et al., 2016; Duits et al., 2018; Fagan and Perrin, 2012). Here, we have substantiated a global decline of DCV markers in the CSF of early AD patients by immunoblotting, which enabled visualization of precursor and mature forms of DCV proteins. Additionally, we have found decreased amounts of CysC in the CSF of AD patients. Low levels of serum and CSF CysC were previously shown in AD individuals (Hansson et al., 2009; Kaur and Levy, 2012; Simonsen et al., 2007). Even though CysC positively correlated with changes in both tau and Aβ42 levels in the CSF in some studies (Mathews and Levy, 2016), our results evidenced only partial correlation with t-tau, but not with Aβ42.

As DCVs have been strongly associated with synaptic function (Levitan, 2008; Persoon et al., 2018), lower CSF concentrations of DCV markers may be related to synaptic dysfunction (Long and Holtzman, 2019). Given our reported accumulation of DCV proteins in AD cortices, alterations in vesicle transport or secretion are suggested. In fact, defective vesicle trafficking (Brandt and Bakota, 2017; Tan and Gleeson, 2019) and release (Fagiani et al., 2019; Plá et al., 2017) have been reported in AD. However, altered protein synthesis and degradation (Alberdi et al., 2013; Komura et al., 2019), neuronal loss (Arendt, 2009; Terry, 2000) or contributions of nonneuronal cells to CSF composition (Alpár et al., 2019; Marques et al., 2007) might not be discarded. In fact, as the choroid plexus is a significant source of CSF proteins and its function is disturbed in AD patients (Simon and Iliff, 2016), total protein levels of CSF samples from patients and controls have been assessed in our study and equal total protein amount between both cohorts is corroborated.

Interestingly, we have evidenced significant reductions in DCV proteins in the CSF of AD individuals with poorer MMSE scores, whereas their levels are maintained in AD patients with better test performance. Studies from 1990 already described an initial compensation of synapse loss in AD by increasing the size of remaining synapses (DeKosky and Scheff, 1990). Thus, and in further agreement with more recent investigations (Brinkmalm et al., 2014; Duits et al., 2018; Öhrfelt et al., 2016), our results could be attributed to compensatory mechanisms occurring in early-AD patients which would fail in later stages of the pathology, when synaptic failure is advanced.

Nowadays, there is still no established biomarker that accurately predicts cognitive impairment progression in AD (Molinuevo et al., 2018). In fact, there is a need for new biomarkers that could change during the course of the disease, as the three core established CSF biomarkers for AD (i.e. Aβ42, t-tau and p-tau) are already impaired in cognitively normal individuals with preclinical AD and are invariably maintained in prodromal and dementia stages (Dubois, 2018). Hence, CSF molecules correlating with test performance could be useful to track cognitive damage in AD (Brinkmalm et al., 2014). Actually, synaptic markers as SNAP25, Rab3A and neurogranin have been recently reported to be altered in the CSF of AD patients and correlate with cognitive impairment (Bereczki et al., 2018; Kirsebom et al., 2018; Lleó et al., 2019).

In this direction, as mPC2 positively correlates with the MMSE score of AD patients in our study, it may be a promising indicator of cognitive decline, as well. Proprotein convertases intracellularly cleave pro-BDNF into mature BDNF, which is well-established DCV cargo with key roles in neuronal development, differentiation and survival (Reichardt, 2006; Zhang et al., 2020). Interestingly, several studies have also reported reduced BDNF levels in both CSF and blood of AD patients in association with a higher risk of progression from MCI to dementia-AD (Du et al., 2018; Forlenza et al., 2015; Jung et al., 2009). Of note, increasing the levels of BDNF in the brain of FAD transgenic mice moderately recovered network alterations, prevented cognitive impairments and favored Aβ clearance (Nagahara et al., 2009; Saito et al., 2005; Zhang et al., 2015). Altogether, and since correlations between DCV proteins and tau but not Aβ42 have been described here, we propose that alterations in DCV transmission may be associated to the later stages of AD, when neurodegeneration and cognitive impairment are advanced.

DCV proteins decline in the brain and are maintained in neuronal terminals of 5xFAD mice

Even though AD has long been characterized by the occurrence of Aβ plaques and neurofibrillary tangles (Hardy and Selkoe, 2002), the precise mechanisms responsible for the initiation of the pathology are still unknown. Investigations in animal models of AD may facilitate the study of triggering factors, the comprehension of disease progression and the search of new disease biomarkers and therapeutic strategies (Sasaguri et al., 2017). Among the several existing transgenic models of AD, 5xFAD mice recapitulate many pathological hallmarks of the disease in a premature and consistent manner hardly found in other AD transgenic mice (Crouzin et al., 2013).

In fact, intracellular Aβ accumulations and neuroinflammation are observed from the first 2 months of age throughout the hippocampus and cortex in 5xFAD mice, and are followed by significant extracellular Aβ plaques from 3 months (Dietrich et al., 2018; Oakley et al., 2006). As assessed in several studies, 3-month-old 5xFAD mice are still not cognitively impaired (Liu et al., 2015; Xiao et al., 2015), whilst early cognitive alterations appear at 6-7 months of age (Lee et al., 2019). Greater cognitive impairment is determined in this mouse model at 9-10 months (Schneider et al., 2014), coinciding with synaptic degeneration and neuronal loss (Esquerda-Canals et al., 2017; Oakley et al., 2006; Spangenberg et al., 2016). Given the early neuropathological alterations and the subsequent functional and behavioral disorders, 5xFAD mice are considered a very suitable model to study AD (Gurel et al., 2018; Schneider et al., 2014).

Therefore, to further understand the mechanisms involved in the alterations of DCV secretory markers observed in human AD cortical tissues and CSF, experiments have been performed in WT and 5xFAD mice at 3, 6 and 12 months of age, as a screening from very early to more advanced stages of the amyloid pathology. Overall, we have found that 5xFAD mice apparently recapitulate hippocampal glial reactivity at 6 and 12 months in an age-dependent manner. These results are in line with previous investigations reporting increased expression of astrocyte and microglial reactivity markers (i.e. GFAP and Iba1) in the cerebral cortex of 5-, 6-, 10- and 12-month-old 5xFAD mice (Iram et al., 2016; Keaney et al., 2019; Kim et al., 2019; Mirzaei et al., 2016). Another recent study has also reported upregulation of microglial genes in transgenic mice from 8 to 15 months of age (Gatt et al., 2019). Additionally, we have also evidenced an age-dependent increase in hippocampal levels of GFAP and Iba1 in WT mice, in accordance with existing literature (Goodall et al., 2018), yet to a lesser extent than in their transgenic littermates.

Similarly, we have seen age-dependent rises in hippocampal CysC of 5xFAD and WT (at a smaller degree). Others have recognized increased CysC in cortical neurons of aging human brains, being generalized in AD patients (Deng et al., 2001; Levy et al., 2001). CysC and APP binding has also been confirmed for mouse tissue *in vivo* (Bai et al., 2008). CysC favors proteolytic elimination of autophagy products by lysosomes (Tizon et al., 2010), which is considered a protection mechanism against neurodegeneration (Nixon, 2013). In the light of our reported results, it is conceivable that early increases in CysC may be associated with its proposed neuroprotective role (Gauthier et al., 2011). Remarkably, CysC neuroprotective characteristics may rely on two different routes: inhibition of the lysosomal cathepsin B and induction of autophagy by inhibition of the mammalian target of rapamycin (mTOR) (Mathews and Levy, 2016). Accordingly, increases in proteins of the lysosomal pathway (Kim et al., 2019) and upregulation of autophagy genes (Gatt et al., 2019) have been evidenced in 5xFAD mice from 3 months of age.

Regarding DCV secretory proteins, our results have revealed decreased protein levels of neuronal DCV markers (i.e. PC1, PC2, CgA and CgB) in 12-month-old 5xFAD hippocampi. Similarly, decreased expression of PC1 has also been determined in the hippocampi of the triple transgenic mouse model for familial AD (3xTg-AD) at 14 months of age (Abolhassani et al., 2017; Hokama et al., 2014). In APP transgenic mice, however, no significant changes in total levels of CgA, CgB and SgII were observed at 12 months, despite positive co-immunolabeling for all three DCV markers and Aβ at 6 months (Willis et al., 2008). Differently, we found maintained levels of CPE, yet with a slight tendency to increase, in the hippocampi of 12-month-old 5xFAD mice, which is probably attributed to its presence in both neuronal and astrocyte DCVs. Comparable results regarding total amount of CPE were previously obtained in both APP/PS1 mice and AD brains (Plá et al., 2013).

Our results evidencing less DCV secretory markers in the hippocampi of aging 5xFAD mice could be associated with synapse loss, as we have also determined a reduction of Syp in 12-month-old transgenic mice. Loss of pre- and postsynaptic markers as Syp, syntaxin and PSD-95 were early described to age-dependently develop in the 5xFAD model from 9 months of age (Oakley et al., 2006). Decreased Syp immunolabeling has long been considered a hallmark of AD pathology greatly associated with cognitive impairment (Terry, 2000). Although some studies have stated invariable levels of Syp in APP23 mice, even when strong Aβ depositions were evidenced, Syp generally age-dependently decreases in PDAPP and PSEN1 single transgenic mice (Duyckaerts et al., 2008).

More recently, a decline in metabotropic glutamate receptors has also been reported in 9-month-old 5xFAD mice compared to transgenic mice at 3 months of age (Lee et al., 2019). Deficiencies in cortical plasticity have been described at 6 months of age in the 5xFAD mouse model, which suggest that synaptic alterations may be initial steps in neurodegeneration and neuronal death processes occurring in FAD (Buskila et al., 2013; Crouzin et al., 2013). Considering that neuronal loss has been observed in deep cortical layers of 5xFAD mice at 9 months (Ali et al., 2019), it might be another plausible explanation for our described decline in DCV markers. However, loss of neurons is mild or absent in single transgenic (e.g. PDAPP and Tg2576) and only moderately evidenced in double transgenic (e.g. APP/PS1 and 5xFAD) mice (Duyckaerts et al., 2008). Hence, as neuronal loss is in best of the cases discrete in transgenic mice, it is unlikely to be the most reasonable hypothesis.

Given that increases in ER stress have not been proven in 5xFAD mice (Sadleir et al., 2018), general decreases in protein synthesis are also improbable to explain the decline of DCV secretory proteins in 12-month-old 5xFAD mice. Nevertheless, downregulation of certain DCV-related genes (i.e. PC1 and SgII) has recently been reported in 5xFAD mouse brains at 8, 11 and 15 months (Gatt et al., 2019). As protein levels of PC1 are maintained at 6 months and only decrease at 12, the effect of downregulation would be initially not evidenced, which suggests the existence of AD specific alterations in the secretory pathway (e.g. vesicle transport or release) leading to DCV accumulation.

Additionally, we have found many DCV-cargos (i.e. PC2, CgA, CPE) increased in the hippocampi of 5xFAD mice at early stages (3-6 months) compared to WT of the same age. Consistently, PC2 upregulation was reported in 6-month-old tau transgenic mice (Maphis et al., 2017). As other DCV-associated genes were also upregulated in 3-month-old 5xFAD and later downregulated (Gatt et al., 2019), the existence of initial compensatory mechanisms induced by early synaptic failures before reaching a later stage of decompensated function may be suggested (Arendt, 2009; Brinkmalm et al., 2014; Crowe and Ellis-Davies, 2014; DeKosky and Scheff, 1990; Duits et al., 2018; Öhrfelt et al., 2016). Finally, our analyses of hippocampal DCV secretory markers have revealed several age-dependent decreases not only in 5xFAD but also in WT. Accordingly, alterations in the peptidergic secretory pathway (i.e. vesicle transport and fusion) have been linked to age-associated cognitive decline, suggesting that physiological aging may also interfere in different features of DCV release (Deák, 2014; Zanin et al., 2011).

As DCV proteins were globally decreased in the hippocampi of 12-month-old 5xFAD mice, and considering that DCVs preferentially fuse at synapses (Persoon et al., 2018), we next questioned whether similar alterations occurred in nerve terminals. A large body of knowledge on synapses has been acquired from studies on synaptosomes, which are functional preparations of synaptic contacts containing resealed presynaptic structures and post-synaptic fragments (Bai and Witzmann, 2007; Morciano et al., 2009; Whittaker, 1993). Moreover, synaptosomal fractions contain other synaptic and non-synaptic neuronal and glial compounds (Biesemann et al., 2014).

Consequently, synaptosomes from 3- and 12-month-old WT and transgenic mice display astrocyte markers as GFAP, in line with other research (Venturini et al., 2019). In fact, flow cytometry analyses of crude synaptosomal fractions proved that GFAP labeled 35% of the particles (Gylys et al., 2000). Other glial markers are also found in synaptosomes, such as astrocyte glutamate transporters, which are widely used to study astroglial contributions to neurotransmission (Biesemann et al., 2014; Perego et al., 2000; Petr et al., 2015). As the astrocytic phenotype is influenced by microglia in physiology and pathology (Jay et al., 2019; Liddelow et al., 2017), microglial presence was examined in our synaptosomal fractions. Unexpectedly, we only detected the microglial marker Iba1 in synaptosomes from 12-month-old animals, not at 3 months, suggesting that astroglial and microglial processes may differently associate with synapses over time (Gajera et al., 2019).

Synaptosomal preparations have also been extensively used in AD research (Cefaliello et al., 2019; Fein et al., 2008; Gylys et al., 2004; Sheng et al., 2019; Wang et al., 2016b). In 5xFAD synaptosomes GFAP and Iba1 immunodetection increased at 12 months, in line with the augmented levels in brain homogenates of both markers reported in our study and by others (Gatt et al., 2019; Kim et al., 2019). Rises in gliosis were similarly described in synaptosomes from AD patients (Gylys et al., 2004) and GFAP was found oxidized in synaptosomes treated with Aβ, thus contributing to synaptic disruption and energy metabolism impairment (Boyd-Kimball et al., 2005). Accordingly, synaptosomal mitochondrial dysfunction has been recently evidenced in 5xFAD mice and in transgenic rats (Adami et al., 2017; Wang et al., 2016b). Moreover, as microglia mediates synaptic pruning in development and synapse loss in AD (Hong et al., 2016), augmented Iba1 in transgenic synaptosomes further strengthens their participation in synaptic degeneration. Of note, the microglial receptor TREM2 induces early synaptic impairment in APP/PS1 mice and has been identified as a risk factor for AD in humans (Sheng et al., 2019; Sims et al., 2017).

When examining CysC, we evidenced its presence in mouse synaptosomal preparations even though it was more abundant in cortical homogenates, in line with its expected localization (Deng et al., 2001). Cysteine protease inhibitors were earlier detected in synaptosomal fractions from rat brains (Marks et al., 1988). More recently, cystatin B (CysB) has been reported to be locally synthesized at synaptosomes, altogether suggesting an involvement of cysteine protease inhibitors in synaptic plasticity (Penna et al., 2019). Furthermore, we have reported elevated CysC in synaptosomes from 12-month-old 5xFAD mice, in accordance with increased hippocampal levels described in our study and by others in AD (Gauthier et al., 2011; Kaur and Levy, 2012).

As SVs are the main presynaptic organelles, vesicle-membrane proteins as Syp are useful to determine synaptic enrichment in synaptosomal preparations (Bai and Witzmann, 2007). The presynaptic proteome further includes cellular adhesion proteins, mitochondria, endosomal organelles and proteins controlling the arrangement of presynaptic terminals (Biesemann et al., 2014; Morciano et al., 2009; Witzmann et al., 2005). Moreover, DCV-cargos as BDNF and its receptor TrkB are also detected in murine synaptosomal preparations (Fawcett et al., 1997; Jovanovic et al., 2000; Schrimpf et al., 2005). We have found generally reduced levels of Syp in synaptosomes from 12-month-old 5xFAD mice, consistently with the previously reported synapse loss in these mice here and in other studies (Buskila et al., 2013; Crouzin et al., 2013; Crowe and Ellis-Davies, 2014; Schneider et al., 2014). However, invariable levels of neuronal DCV secretory markers (convertases and chromogranins) in both hippocampal and cortical neuronal terminals of 5xFAD mice at 12 months have been determined in the present study.

Because DCV secretory markers are reduced in hippocampal homogenates and maintained in neuronal terminals, whereas Syp is reduced in both tissue homogenates and synaptosomes, synapse loss is unlikely to be responsible for the reported DCV alterations in 12-month-old 5xFAD mice. In contrast, we hypothesize that DCVs may be accumulating at the terminal level possibly as a result of a secretion impairment occurring in transgenic mice. As BDNF-TrkB signaling is necessary for an appropriate glutamatergic and GABAergic neurotransmission (Canas et al., 2004; Carmona et al., 2003), retention of DCVs and subsequent decreased BDNF release could have a negative impact on synaptic transmission. Accordingly, TrkB has been reported to be reduced in synaptosomes of APP/PS1 transgenic mice at 10 months, probably contributing to synaptic dysfunction (Ahmad et al., 2018).

Previous research described impaired axonal BDNF retrograde trafficking in Tg2576 transgenic mice (Poon et al., 2011). Our results suggest that similar rates of DCV transport seem to be maintained in transgenic mice compared to WT. Nonetheless, as dysregulations in local protein synthesis have been described in brain synaptosomes of APP transgenic mice (Cefaliello et al., 2019), and presynaptic synthesis of certain proteins has been reported to control neurotransmitter release (Younts et al., 2016), alterations in local protein synthesis might also indirectly affect DCV release. All in all, dysregulations in DCV secretion may contribute to AD neuropathology, as similarly proposed in recent investigations (Ginsberg et al., 2019).

DCV secretory markers in the CSF of the 5xFAD mouse model of familial AD

To further investigate whether alterations of DCV secretory markers observed in the brain and neuronal terminals of 5xFAD mice could be associated to secretion impairments, analyses have been performed in the CSF of WT and 5xFAD mice at 3, 6 and 12 months of age. Since DCV proteins are abundantly expressed throughout the CNS (Vázquez-Martínez et al., 2012), variations in peptidergic secretion may be well reflected in the CSF, as it directly interacts with the extracellular milieu of the brain (Johanson et al., 2008). Thus, we have optimized a very consistent protocol to collect relatively great volumes of mouse CSF devoid of blood contamination, following previously reported methods with slight adjustments (DeMattos et al., 2002; Lim et al., 2018; Liu and Duff, 2008). After visual inspection and centrifugation, CSF samples have been screened for elevated IgM levels as an evidence of blood presence, since IgM is a large molecule usually found in very low concentrations in the CSF (Reiber, 2016). Similar approaches were previously implemented using apoB100, a protein enriched in the plasma and virtually absent in the CNS (DeMattos et al., 2002).

For CPE and PC2, no statistically significant differences have been observed in the CSF of 5xFAD mice compared to WT at any age. However, both proteins are significantly reduced in the CSF of 12-month- compared to 3-month-old 5xFAD mice. A similar age-dependent reduction is also evidenced, yet to a lesser extent, for PC2 in WT. Differently, CysC significantly increases in the CSF of 5xFAD mice at both 6 and 12 months compared to WT at each age. A significant age-dependent rise in CysC levels is also demonstrated in 12-months compared to 3-months 5xFAD samples. These results are in line with the recently reported age-dependent reduced expression of neuronal-specific genes in both WT and 5xFAD mice and the enhanced expression of inflammatory-related genes occurring in an age-dependent manner in the transgenic group only (Gatt et al., 2019).

Because of our reported decline of DCV secretory markers in the brain and maintenance in neuronal terminals of 12-month-old 5xFAD mice, we expected levels of DCV proteins would be also reduced in the CSF of 12-month transgenic mice in comparison to their WT littermates. However, and contrary to our results in AD patients, DCV proteins are maintained with only a slight tendency to decrease in the case of the neuronal-specific PC2. We hypothesize that DCVs may be accumulating at the terminal level as a result of a probable secretion impairment, which might not be fully evidenced in the CSF due to several plausible reasons.

For instance, dysfunctions of the blood-CSF barrier have been reported in several transgenic mouse models of AD, causing an impaired clearance of diverse molecules from the CSF (González-Marrero et al., 2015). CSF outflow from the brain is mediated by the arachnoid villi which, together with the meningeal and olfactory lymphatics, drain into the peripheral lymphatics (Johanson et al., 2008). 5xFAD mice display significant alterations in CSF outflow that have been attributed to lessened peripheral lymphatic function and contribute to AD pathogenesis (Kwon et al., 2019). Hence, it may be reasonable that the expected reductions in DCV secretory proteins in the CSF of 5xFAD mice at 12 months are not becoming apparent as a result of such impaired CSF outflow.

In addition to the reduced CSF drainage, dysfunction of the BBB has also been claimed responsible for rises in CSF protein concentration (Asgari et al., 2017). However, BBB disruption is unlikely to be the most plausible explanation for our results, as passage of molecules has been evidenced to be equally low in AD transgenic mice compared to WT, suggesting that BBB stability is maintained even with Aβ pathology (Gustafsson et al., 2018). In fact, another recent study has reported that the BBB of aging 5xFAD mice is intact compared to controls of the same age (Matsubara et al., 2018). Nevertheless, similar research performed only in control ageing mice has demonstrated age-dependent BBB dysfunctions (Goodall et al., 2018).

As DCV are broadly localized in neurons throughout the brain (Vázquez-Martínez et al., 2012), DCV secretory proteins reaching the CSF may primarily originate in neurons, even though other possible cellular origins may be considered. In fact, as evidenced here and in previous studies, some DCV markers are also expressed and released in astrocytes (Paco et al., 2010; Plá et al., 2017). Moreover, ependymal cells, modified ependymal cells of the choroid plexus and tanycytes contributing to CSF protein composition might not be discarded (Johanson et al., 2008; Marques et al., 2007).

There is a large number of investigations currently seeking for synaptic alterations in the CSF of AD patients that can be used as disease biomarkers (Brinkmalm et al., 2014; Falgàs et al., 2019; Lewczuk et al., 2017; Molinuevo et al., 2018; Sutphen et al., 2018). Recent research has described increased levels of neurogranin in the CSF of an early inducible mouse model of neurodegeneration as an evidence for synaptic degeneration (Höglund et al., 2020). However, there is a lack of other studies analyzing similar alterations in the CSF of mouse models of AD, which may be attributed to several causes, including the complexity of the surgical procedure, the limited collected volume of mouse CSF and the neuropathological differences existing between mouse models and human AD (Duyckaerts et al., 2008; Lim et al., 2018).

In this direction, and as a main limitation of the present study, neurofibrillary tangle pathology is missing in the 5xFAD model, since mutations in tau are absent in these transgenic mice (Oakley et al., 2006; Stancu et al., 2014). Therefore, the relationship between tauopathy and DCV alterations evidenced here in AD patients could not be assessed in 5xFAD mice. Moreover, given that the 5xFAD strain is a quickly progressing transgenic model of FAD, the pathogenic alterations occurring in these mice might differ at some degree with the more gradually evolving lesions observed in SAD (Tible et al., 2019). Altogether, even though 5xFAD mice are considered a very suitable model to study AD (Gurel et al., 2018; Schneider et al., 2014), our results should be further corroborated and extended in another AD model. For instance, bigenic mouse models combining mutations in APP and tau would probably better recapitulate our observed alterations in AD patients (Chen et al., 2016). Alternatively, the use of rat models of FAD would also be extremely advantageous, as their larger bodies simplify CSF extraction, enable the obtention of greater CSF volumes and display a more complex behavioural profile (Do Carmo and Cuello, 2013; Cohen et al., 2013).

In summary, we have revealed alterations in the brain and CSF of the 5xFAD mouse model of AD during pathology progression. DCV proteins globally decreased in the hippocampi of 12-months transgenic mice and age-dependently decreased in the CSF. These results could be attributed to several causes, including changes in protein expression, synapse or neuronal losses. However, as their levels were invariable in hippocampal and cortical neuronal terminals, an impairment in secretion or an accumulation of DCV proteins at the terminal level, may be proposed as the more reasonable hypotheses.

Closing remarks

The findings of the present dissertation have shed some light on the molecular mechanisms of AD pathogenesis, which could help in the development of new therapeutic and preventive strategies. Variations in CSF composition regarding DCV markers seem to reflect synaptic dysfunction and neurodegeneration and suggest the occurrence of disease-associated secretion impairments. As DCV-cargos are important for appropriate neuronal activity functioning and brain metabolism, alterations in DCV release may contribute to energy failure in neurons, probably resulting in synaptic dysfunction and impaired cognition (Abolhassani et al., 2017; Cawley et al., 2012; Cheng et al., 2014; Lin and Salton, 2013; Nakabeppu and Ninomiya, 2019). Moreover, astrocyte release of DCV-cargos has been reported as essential for neuronal morphology and synaptic plasticity (De Pins et al., 2019). Hence, yet validation in further research is needed, we suggest the participation of neuronal and astroglial DCV secretory proteins in the pathological progression of AD and propose their potential use as complementary biomarkers for tracking AD neurodegeneration and cognitive impairment.

CONCLUSIONS

CONCLUSIONS

From the results presented in this dissertation it can be concluded that:

1. Astrocyte peptidergic vesicles are heterogeneous and display variable release after Ca^{2+}-mediated stimulation, which is modulated in proinflammatory conditions *in vitro* and *in situ*.

2. Unstimulated astrocytes slightly retain and rapidly release secretory proteins *in vitro*, which is independent of spontaneous Ca^{2+} oscillations but critically relies on intracellular Ca^{2+}.

3. In advanced AD brains, DCV secretory markers accumulate in dystrophic neurites and GVD bodies. Since GVD is an early event in tau-pathology progression, alterations of DCV proteins may be associated to tauopathy and neurodegeneration in AD.

4. Secretory proteins of DCVs globally decay in the CSF of early AD patients. As a correlation exists between PC2 and the core AD biomarker t-tau and the MMSE score, an association with neurodegeneration and cognitive decline may be anticipated.

5. In the 5xFAD mouse model of familial AD, secretory markers of DCVs are initially increased and later decreased in cortical areas, maintained in neuronal terminals, and age-dependently declined in the CSF.

6. Since alterations in DCV secretory proteins are evidenced in AD patients and transgenic mice, their participation in the pathological progression of AD and their potential use as disease biomarkers is proposed.

REFERENCES

REFERENCES

Abbott, NJ, Rönnbäck, L and Hansson, E. (2006). Astrocyte-Endothelial Interactions at the Blood-Brain Barrier. Nature Reviews Neuroscience, 7(1), 41–53.

Abolhassani, N, Leon, J, Sheng, Z, Oka, S, Hamasaki, H, Iwaki, T and Nakabeppu, Y. (2017). Molecular Pathophysiology of Impaired Glucose Metabolism, Mitochondrial Dysfunction, and Oxidative DNA Damage in Alzheimer's Disease Brain. Mechanisms of Ageing and Development, 161, 95–104.

Acosta, C, Anderson, HD and Anderson, CM. (2017). Astrocyte Dysfunction in Alzheimer Disease. Journal of Neuroscience Research, 95(12), 2430–47.

Adami, PVM, Quijano, C, Magnani, N, Galeano, P, Evelson, P, Cassina, A, Do Carmo, S, Leal, MC, Castaño, EM, Cuello, AC and Morelli, L. (2017). Synaptosomal Bioenergetic Defects Are Associated with Cognitive Impairment in a Transgenic Rat Model of Early Alzheimer's Disease. Journal of Cerebral Blood Flow and Metabolism, 37(1), 69–84.

Agarwal, A, Wu, PH, Hughes, EG, Fukaya, M, Tischfield, MA, Langseth, AJ, Wirtz, D and Bergles, DE. (2017). Transient Opening of the Mitochondrial Permeability Transition Pore Induces Microdomain Calcium Transients in Astrocyte Processes. Neuron, 93(3), 587-605.e7.

Agosta, F, Vossel, KA, Miller, BL, Migliaccio, R, Bonasera, SJ, Filippi, M, Boxer, AL, Karydas, A, Possin, KL and Gorno-Tempini, ML. (2009). Apolipoprotein E E4 Is Associated with Disease-Specific Effects on Brain Atrophy in Alzheimer's Disease and Frontotemporal Dementia. Proceedings of the National Academy of Sciences of the United States of America, 106(6), 2018–22.

Aguado, F, Espinosa-Parrilla, JF, Carmona, MA and Soriano, E. (2002). Neuronal Activity Regulates Correlated Network Properties of Spontaneous Calcium Transients in Astrocytes in Situ. Journal of Neuroscience, 22(1529–2401), 9430–44.

Agulhon, C, Sun, MY, Murphy, T, Myers, T, Lauderdale, K and Fiacco, TA. (2012). Calcium Signaling and Gliotransmission in Normal vs. Reactive Astrocytes. Frontiers in Pharmacology, 3 JUL.

Ahmad, F, Das, D, Kommaddi, RP, Diwakar, L, Gowaikar, R, Rupanagudi, KV, Bennett, DA and Ravindranath, V. (2018). Isoform-Specific Hyperactivation of Calpain-2 Occurs Presymptomatically at the Synapse in Alzheimer's Disease Mice and Correlates with Memory Deficits in Human Subjects. Scientific Reports, 8(1).

Ahmad, MH, Fatima, M and Mondal, AC. (2019). Influence of Microglia and Astrocyte Activation in the Neuroinflammatory Pathogenesis of Alzheimer's Disease: Rational Insights for the Therapeutic Approaches. Journal of Clinical Neuroscience, 59, 6–11.

Alabi, AA and Tsien, RW. (2013). Perspectives on Kiss-and-Run: Role in Exocytosis, Endocytosis, and Neurotransmission. Annual Review of Physiology, 75(1), 393–422.

Alberdi, E, Wyssenbach, A, Alberdi, M, Sánchez-Gómez, M V., Cavaliere, F, Rodríguez, JJ, Verkhratsky, A and Matute, C. (2013). Ca2+-Dependent Endoplasmic Reticulum Stress Correlates with Astrogliosis in Oligomeric Amyloid β-Treated Astrocytes and in a Model of Alzheimer's Disease. Aging Cell, 12(2), 292–302.

Ali, F, Baringer, SL, Neal, A, Choi, EY and Kwan, AC. (2019). Parvalbumin-Positive Neuron Loss and Amyloid-β Deposits in the Frontal Cortex of Alzheimer's Disease-Related Mice. Journal of Alzheimer's disease: JAD.

Allan, SM and Rothwell, NJ. (2001). Cytokines and Acute Neurodegeneration. Nature Reviews Neuroscience, 2(10), 734–44.

Allen, NJ and Barres, BA. (2009). Glia — More than Just Brain Glue. Nature, 457(7230), 675–77.

Alpár, A, Zahola, P, Hanics, J, Hevesi, Z, Korchynska, S, Benevento, M, Pifl, C, Zachar, G, Perugini, J, Severi, I, Leitgeb, P, Bakker, J, Miklosi, AG, Tretiakov, E, Keimpema, E, Arque, G, Tasan, RO, Sperk, G, Malenczyk, K et al. (2018). Hypothalamic CNTF Volume Transmission Shapes Cortical Noradrenergic Excitability upon Acute Stress. The EMBO Journal, 37(21).

Alpár, AN, Benevento, M, Romanov, RA, Kfelt, TH and Harkany, T. (2019). Hypothalamic Cell Diversity: Non-Neuronal Codes for Long-Distance Volume Transmission by Neuropeptides. Current Opinion in Neurobiology, 56, 16–23.

Alvarez de Toledo, G, Fernández-Chacón, R and Fernández, JM. (1993). Release of Secretory Products during Transient Vesicle Fusion. Nature, 363(6429), 554–58.

Alzheimer's Association. (2018). 2018 Alzheimer's Disease Facts and Figures. Alzheimer's & Dementia, 14(3), 367–429.

Alzheimer's Disease International. (2018). Alzheimer's Disease International World Alzheimer Report 2018: The State of the Art of Dementia Research: New Frontiers.

An, S and Zenisek, D. (2004). Regulation of Exocytosis in Neurons and Neuroendocrine Cells. Current Opinion in Neurobiology, 14(5), 522–30.

Anderson, CM and Swanson, RA. (2000). Astrocyte Glutamate Transport: Review of Properties, Regulation, and Physiological Functions. GLIA, 32, 1–14.

Ang, AL, Taguchi, T, Francis, S, Fölsch, H, Murrells, LJ, Pypaert, M, Warren, G and Mellman, I. (2004). Recycling Endosomes Can Serve as Intermediates during Transport from the Golgi to the Plasma Membrane of MDCK Cells. Journal of Cell Biology, 167(3), 531–43.

Arantes, RME and Andrews, NW. (2006). A Role for Synaptotagmin VII-Regulated Exocytosis of Lysosomes in Neurite Outgrowth from Primary Sympathetic Neurons. Journal of Neuroscience, 26(17), 4630–37.

Araque, A, Carmignoto, G, Haydon, PG, Oliet, SHR, Robitaille, R and Volterra, A. (2014). Gliotransmitters Travel in Time and Space. Neuron, 81(4), 728–39.

Arendt, T. (2009). Synaptic Degeneration in Alzheimer's Disease. Acta Neuropathologica, 118(1), 167–79.

Arnaoutova, I, Smith, AM, Coates, LC, Sharpe, JC, Dhanvantari, S, Snell, CR, Birch, NP and Loh, YP. (2003). The Prohormone Processing Enzyme PC3 Is a Lipid Raft-Associated Transmembrane Protein. Biochemistry, 42(35), 10445–55.

Artenstein, AW and Opal, SM. (2011). Proprotein Convertases in Health and Disease. The New England journal of medicine, 365(26), 2507–18.

Asgari, M, de Zélicourt, DA and Kurtcuoglu, V. (2017). Barrier Dysfunction or Drainage Reduction: Differentiating Causes of CSF Protein Increase. Fluids and Barriers of the CNS, 14(1), 14.

Ashton, NJ, Schöll, M, Heurling, K, Gkanatsiou, E, Portelius, E, Höglund, K, Brinkmalm, G, Hye, A, Blennow, K and Zetterberg, H. (2018). Update on Biomarkers for Amyloid Pathology in Alzheimer's Disease. Biomarkers in Medicine, 12(7), 799–812.

Aslankoc, R, Savran, M, Ozmen, O and Asci, S. (2018). Hippocampus and Cerebellum Damage in Sepsis Induced by Lipopolysaccharide in Aged Rats - Pregabalin Can Prevent Damage. Biomedicine and Pharmacotherapy, 108, 1384–92.

Avila-Muñoz, E and Arias, C. (2014). When Astrocytes Become Harmful: Functional and Inflammatory Responses That Contribute to Alzheimer's Disease. Ageing Research Reviews, 18, 29–40.

Bai, F and Witzmann, FA. (2007). Synaptosome Proteomics. In Subcellular Biochemistry, eds. Bertrand, E and Faupel, M. Springer, 77–98.

Bai, Y, Markham, K, Chen, F, Weerasekera, R, Watts, J, Horne, P, Wakutani, Y, Bagshaw, R, Mathews, PM, Fraser, PE, Westaway, D, St. George-Hyslop, P and Schmitt-Ulms, G. (2008). The in Vivo Brain Interactome of the Amyloid Precursor Protein. Molecular and Cellular Proteomics, 7(1), 15–34.

Bak, LK, Schousboe, A and Waagepetersen, HS. (2006). The Glutamate/GABA-Glutamine Cycle: Aspects of Transport, Neurotransmitter Homeostasis and Ammonia Transfer. Journal of Neurochemistry, 98(3), 641–53.

Balkowiec, A and Katz, DM. (2002). Cellular Mechanisms Regulating Activity-Dependent Release of Native Brain-Derived Neurotrophic Factor from Hippocampal Neurons. Journal of Neuroscience, 22(23), 10399–407.

Bartkowska, K, Turlejski, K and Djavadian, RL. (2010). Neurotrophins and Their Receptors in Early Development of the Mammalian Nervous System. Acta Neurobiologiae Experimentalis, 70(4), 454–67.

Bartolomucci, A, Pasinetti, GM and Salton, SRJ. (2010). Granins as Disease-Biomarkers: Translational Potential for Psychiatric and Neurological Disorders. Neuroscience, 170(1), 289–97.

Bartolomucci, A, Possenti, R, Mahata, SK, Fischer-Colbrie, R, Loh, YP and Salton, SRJ. (2011). The Extended Granin Family: Structure, Function, and Biomedical Implications. Endocrine reviews, 32(6), 755–97.

Bass, NH, Hess, HH, Pope, A and Thalheimer, C. (1971). Quantitative Cytoarchitectonic Distribution of Neurons, Glia, and DNA in Rat Cerebral Cortex. Journal of Comparative Neurology, 143(4), 481–90.

Bauer, RA, Overlease, RL, Lieber, JL and Angleson, JK. (2004). Retention and Stimulus-Dependent Recycling of Dense Core Vesicle Content in Neuroendocrine Cells. Journal of Cell Science, 117(11), 2193–2202.

Bazargani, N and Attwell, D. (2016). Astrocyte Calcium Signaling: The Third Wave. Nature Neuroscience, 19(2), 182–89.

Bennett, MVL and Zukin, RS. (2004). Electrical Coupling and Neuronal Synchronization in the Mammalian Brain. Neuron, 41(4), 495–511.

Bereczki, E, Branca, RM, Francis, PT, Pereira, JB, Baek, JH, Hortobágyi, T, Winblad, B, Ballard, C, Lehtiö, J and Aarsland, D. (2018). Synaptic Markers of Cognitive Decline in Neurodegenerative Diseases: A Proteomic Approach. Brain, 141(2), 582–95.

Bergersen, LH and Gundersen, V. (2009). Morphological Evidence for Vesicular Glutamate Release from Astrocytes. Neuroscience, 158(1), 260–65.

Berridge, MJ, Bootman, MD and Roderick, HL. (2003). Calcium Signalling: Dynamics, Homeostasis and Remodelling. Nature Reviews Molecular Cell Biology, 4(7), 517–29.

Beuret, N, Stettler, H, Renold, A, Rutishauser, J and Spiess, M. (2004). Expression of Regulated Secretory Proteins Is Sufficient to Generate Granule-like Structures in Constitutively Secreting Cells. The Journal of biological chemistry, 279(19), 20242–49.

Bezzi, P, Gundersen, V, Galbete, JL, Seifert, G, Steinhäuser, C, Pilati, E and Volterra, A. (2004). Astrocytes Contain a Vesicular Compartment That Is Competent for Regulated Exocytosis of Glutamate. Nature Neuroscience, 7(6), 613–20.

Bi, F, Huang, C, Tong, J, Qiu, G, Huang, B, Wu, Q, Li, F, Xu, Z, Bowser, R, Xia, XG and Zhou, H. (2013). Reactive Astrocytes Secrete Lcn2 to Promote Neuron Death. Proceedings of the National Academy of Sciences of the United States of America, 110(10), 4069–74.

Biesemann, C, Grønborg, M, Luquet, E, Wichert, SP, Bernard, V, Bungers, SR, Cooper, B, Varoqueaux, F, Li, L, Byrne, JA, Urlaub, H, Jahn, O, Brose, N and Herzog, E. (2014). Proteomic Screening of Glutamatergic Mouse Brain Synaptosomes Isolated by Fluorescence Activated Sorting. EMBO Journal, 33(2), 157–70.

Bjarnadottir, M, Nilsson, C, Lindström, V, Westman, A, Davidsson, P, Thormodsson, F, Blöndal, H, Gudmundsson, G and Grubb, A. (2001). The Cerebral Hemorrhage-Producing Cystatin C Variant (L68Q) in Extracellular Fluids. Amyloid, 8(1), 1–10.

Blakely, RD and Edwards, RH. (2012). Vesicular and Plasma Membrane Transporters for Neurotransmitters. Cold Spring Harbor Perspectives in Biology, 4(2).

Blennow, K, Davidsson, P, Wallin, A and Ekman, R. (1995). Chromogranin A in Cerebrospinal Fluid: A Biochemical Marker for Synaptic Degeneration in Alzheimer's Disease? Dementia and Geriatric Cognitive Disorders, 6(6), 306–11.

Blennow, K, Hampel, H, Weiner, M and Zetterberg, H. (2010). Cerebrospinal Fluid and Plasma Biomarkers in Alzheimer Disease. Nature reviews. Neurology, 6(3), 131–44.

Blennow, K and Zetterberg, H. (2018). Biomarkers for Alzheimer's Disease: Current Status and Prospects for the Future. Journal of Internal Medicine, 284(6), 643–63.

Bohmbach, K, Schwarz, MK, Schoch, S and Henneberger, C. (2016). The Structural and Functional Evidence for Vesicular Release from Astrocytes in Situ. Brain Research Bulletin, 1–11.

Bolós, M, Llorens-Martín, M, Jurado-Arjona, J, Hernández, F, Rábano, A and Avila, J. (2016). Direct Evidence of Internalization of Tau by Microglia in Vitro and in Vivo. Journal of Alzheimer's Disease, 50(1), 77–87.

Bonansco, C, Couve, A, Perea, G, Ferradas, CAÁ, Roncagliolo, M and Fuenzalida, M. (2011). Glutamate Released Spontaneously from Astrocytes Sets the Threshold for Synaptic Plasticity. European Journal of Neuroscience, 33(8), 1483–92.

Bonnemaison, ML, Eipper, BA and Mains, RE. (2013). Role of Adaptor Proteins in Secretory Granule Biogenesis and Maturation. Frontiers in endocrinology, 4, 101.

van de Bospoort, R, Farina, M, Schmitz, SK, de Jong, A, de Wit, H, Verhage, M and Toonen, RF. (2012). Munc13 Controls the Location and Efficiency of Dense-Core Vesicle Release in Neurons. Journal of Cell Biology, 199(6), 883–91.

Bowser, DN and Khakh, BS. (2007). Two Forms of Single-Vesicle Astrocyte Exocytosis Imaged with Total Internal Reflection Fluorescence Microscopy. Proceedings of the National Academy of Sciences of the United States of America, 104(10), 4212–17.

Boyd-Kimball, D, Castegna, A, Sultana, R, Poon, HF, Petroze, R, Lynn, BC, Klein, JB and Butterfield, DA. (2005). Proteomic Identification of Proteins Oxidized by Aβ (1-42) in Synaptosomes: Implications for Alzheimer's Disease. Brain Research, 1044(2), 206–15.

Von Boyen, GBT, Steinkamp, M, Reinshagen, M, Schäfer, KH, Adler, G and Kirsch, J. (2004). Proinflammatory Cytokines Increase Glial Fibrillary Acidic Protein Expression in Enteric Glia. Gut, 53(2), 222–28.

Brandt, R and Bakota, L. (2017). Microtubule Dynamics and the Neurodegenerative Triad of Alzheimer's Disease: The Hidden Connection. Journal of Neurochemistry, 143(4), 409–17.

Brinkmalm, A, Brinkmalm, G, Honer, WG, Frölich, L, Hausner, L, Minthon, L, Hansson, O, Wallin, A, Zetterberg, H, Blennow, K and Öhrfelt, A. (2014). SNAP-25 Is a Promising Novel Cerebrospinal Fluid Biomarker for Synapse Degeneration in Alzheimer's Disease. Molecular neurodegeneration, 9, 53.

Brinkmalm, G, Sjödin, S, Simonsen, AH, Hasselbalch, SG, Zetterberg, H, Brinkmalm, A and Blennow, K. (2018). A Parallel Reaction Monitoring Mass Spectrometric Method for Analysis of Potential CSF Biomarkers for Alzheimer's Disease. Proteomics. Clinical applications, 12(1), 1700131.

Brosseron, F, Traschütz, A, Widmann, CN, Kummer, MP, Tacik, P, Santarelli, F, Jessen, F and Heneka, MT. (2018). Characterization and Clinical Use of Inflammatory Cerebrospinal Fluid Protein Markers in Alzheimer's Disease. Alzheimer's Research and Therapy, 10(1).

Bulgari, D, Deitcher, DL, Schmidt, BF, Carpenter, MA, Szent-Gyorgyi, C, Bruchez, MP and Levitan, ES. (2019). Activity-Evoked and Spontaneous Opening of Synaptic Fusion Pores. Proceedings of the National Academy of Sciences, 201905322.

Burda, JE and Sofroniew, M V. (2014). Reactive Gliosis and the Multicellular Response to CNS Damage and Disease. Neuron, 81(2), 229–48.

Buskila, Y, Crowe, SE and Ellis-Davies, GCR. (2013). Synaptic Deficits in Layer 5 Neurons Precede Overt Structural Decay in 5xFAD Mice. Neuroscience, 254, 152–59.

Cachope, R and Pereda, AE. (2012). Two Independent Forms of Activity-Dependent Potentiation Regulate Electrical Transmission at Mixed Synapses on the Mauthner Cell. Brain Research, 1487, 173–82.

Cahoy, JD, Emery, B, Kaushal, A, Foo, LC, Zamanian, JL, Christopherson, KS, Xing, Y, Lubischer, JL, Krieg, PA, Krupenko, SA, Thompson, WJ and Barres, BA. (2008). A Transcriptome Database for Astrocytes, Neurons, and Oligodendrocytes: A New Resource for Understanding Brain Development and Function. Journal of Neuroscience, 28(1), 264–78.

Caldwell, CC, Yao, J and Brinton, RD. (2015). Targeting the Prodromal Stage of Alzheimer's Disease: Bioenergetic and Mitochondrial Opportunities. Neurotherapeutics, 12(1), 66–80.

Calegari, F, Coco, S, Taverna, E, Bassetti, M, Verderio, C, Corradi, N, Matteoli, M and Rosa, P. (1999). A Regulated Secretory Pathway in Cultured Hippocampal Astrocytes. Journal of Biological Chemistry, 274(32), 22539–47.

Campion, D, Pottier, C, Nicolas, G, Le Guennec, K and Rovelet-Lecrux, A. (2016). Alzheimer Disease: Modeling an Aβ-Centered Biological Network. Molecular Psychiatry, 21(7), 861–71.

Canas, N, Pereira, IT, Ribeiro, JA and Sebastião, AM. (2004). Brain-Derived Neurotrophic Factor Facilitates Glutamate and Inhibits GABA Release from Hippocampal Synaptosomes through Different Mechanisms. Brain Research, 1016(1), 72–78.

Carmignoto, G, Pasti, L and Pozzan, T. (1998). On the Role of Voltage-Dependent Calcium Channels in Calcium Signaling of Astrocytes in Situ. Journal of Neuroscience, 18(12), 4637–45.

Do Carmo, S and Cuello, AC. (2013). Modeling Alzheimer's Disease in Transgenic Rats. Molecular Neurodegeneration, 8(1), 37.

Carmona, MA, Martínez, A, Soler, A, Blasi, J, Soriano, E and Aguado, F. (2003). Ca2+-Evoked Synaptic Transmission and Neurotransmitter Receptor Levels Are Impaired in the Forebrain of Trkb (-/-) Mice. Molecular and Cellular Neuroscience, 22(2), 210–26.

Cattin-Ortolá, J, Topalidou, I, Dosey, A, Merz, AJ and Ailion, M. (2017). The Dense-Core Vesicle Maturation Protein CCCP-1 Binds RAB-2 and Membranes through Its C-Terminal Domain. Traffic, 18(11), 720–32.

Cawley, NX, Wetsel, WC, Murthy, SRK, Park, JJ, Pacak, K and Loh, YP. (2012). New Roles of Carboxypeptidase E in Endocrine and Neural Function and Cancer. Endocrine reviews, 33(2), 216–53.

Cefaliello, C, Penna, E, Barbato, C, Di Ruberto, G, Mollica, MP, Trinchese, G, Cigliano, L, Borsello, T, Chun, JT, Giuditta, A, Perrone-Capano, C, Miniaci, MC and Crispino, M. (2019). Deregulated Local Protein Synthesis in the Brain Synaptosomes of a Mouse Model for Alzheimer's Disease. Molecular Neurobiology.

Chai, YL, Chong, JR, Weng, J, Howlett, D, Halsey, A, Lee, JH, Attems, J, Aarsland, D, Francis, PT, Chen, CP and Lai, MKP. (2019). Lysosomal Cathepsin D Is Upregulated in Alzheimer's Disease Neocortex and May Be a Marker for Neurofibrillary Degeneration. Brain Pathology, 29(1), 63–74.

Chakrabarti, S, Kobayashi, KS, Flavell, RA, Marks, CB, Miyake, K, Liston, DR, Fowler, KT, Gorelick, FS and Andrews, NW. (2003). Impaired Membrane Resealing and Autoimmune Myositis in Synaptotagmin VII-Deficient Mice. Journal of Cell Biology, 162(4), 543–49.

Chakravarty, S and Herkenham, M. (2005). Toll-like Receptor 4 on Nonhematopoietic Cells Sustains CNS Inflammation during Endotoxemia, Independent of Systemic Cytokines. Journal of Neuroscience, 25(7), 1788–96.

Chen, W, Abud, EA, Yeung, ST, Lakatos, A, Nassi, T, Wang, J, Blum, D, Buée, L, Poon, WW and Blurton-Jones, M. (2016). Increased Tauopathy Drives Microglia-Mediated Clearance of Beta-Amyloid. Acta neuropathologica communications, 4(1), 63.

Chen, Y, Liang, Z, Blanchard, J, Dai, CL, Sun, S, Lee, MH, Grundke-Iqbal, I, Iqbal, K, Liu, F and Gong, CX. (2013). A Non-Transgenic Mouse Model (Icv-STZ Mouse) of Alzheimer's Disease: Similarities to and Differences from the Transgenic Model (3xTg-AD Mouse). Molecular neurobiology, 47(2), 711–25.

Cheng, Y, Cawley, NX and Loh, YP. (2014). Carboxypeptidase E (NF-A1): A New Trophic Factor in Neuroprotection. Neuroscience Bulletin, 30(4), 692–96.

Chi, LM, Wang, X and Nan, GX. (2016). In Silico Analyses for Molecular Genetic Mechanism and Candidate Genes in Patients with Alzheimer's Disease. Acta Neurologica Belgica, 116(4), 543–47.

Chun, H and Lee, CJ. (2018). Reactive Astrocytes in Alzheimer's Disease: A Double-Edged Sword. Neuroscience Research, 126, 44–52.

Citri, A and Malenka, RC. (2008). Synaptic Plasticity: Multiple Forms, Functions, and Mechanisms. Neuropsychopharmacology, 33(1), 18–41.

Coelho, DS and Moreno, E. (2019). Emerging Links between Cell Competition and Alzheimer's Disease. Journal of Cell Science, 132(13), jcs231258.

Coelho, DS, Schwartz, S, Merino, MM, Hauert, B, Topfel, B, Tieche, C, Rhiner, C and Moreno, E. (2018). Culling Less Fit Neurons Protects against Amyloid-β-Induced Brain Damage and Cognitive and Motor Decline. Cell Reports, 25(13), 3661-3673.e3.

Cohen, RM, Rezai-Zadeh, K, Weitz, TM, Rentsendorj, A, Gate, D, Spivak, I, Bholat, Y, Vasilevko, V, Glabe, CG, Breunig, JJ, Rakic, P, Davtyan, H, Agadjanyan, MG, Kepe, V, Barrio, JR, Bannykh, S, Szekely, CA, Pechnick, RN and Town, T. (2013). A Transgenic Alzheimer Rat with Plaques, Tau Pathology, Behavioral Impairment, Oligomeric Aβ, and Frank Neuronal Loss. Journal of Neuroscience, 33(15), 6245–56.

Colmers, WF, Lukowiak, K and Pittman, QJ. (1988). Neuropeptide Y Action in the Rat Hippocampal Slice: Site and Mechanism of Presynaptic Inhibition. Journal of Neuroscience, 8(10), 3827–37.

Comeras, LB, Herzog, H and Tasan, RO. (2019). Neuropeptides at the Crossroad of Fear and Hunger: A Special Focus on Neuropeptide Y. Annals of the New York Academy of Sciences.

Condello, C, Yuan, P, Schain, A and Grutzendler, J. (2015). Microglia Constitute a Barrier That Prevents Neurotoxic Protofibrillar Aβ42 Hotspots around Plaques. Nature Communications, 6.

Connors, BW and Long, MA. (2004). Electrical Synapses in the Mammalian Brain. Annual Review of Neuroscience, 27(1), 393–418.

Counts, SE, Ikonomovic, MD, Mercado, N, Vega, IE and Mufson, EJ. (2017). Biomarkers for the Early Detection and Progression of Alzheimer's Disease. Neurotherapeutics, 14(1), 35–53.

Courel, M, Soler-Jover, A, Rodriguez-Flores, JL, Mahata, SK, Elias, S, Montero-Hadjadje, M, Anouar, Y, Giuly, RJ, O'Connor, DT and Taupenot, L. (2010). Pro-Hormone Secretogranin II Regulates Dense Core Secretory Granule Biogenesis in Catecholaminergic Cells. The Journal of biological chemistry, 285(13), 10030–43.

Crouzin, N, Baranger, K, Cavalier, M, Marchalant, Y, Cohen-Solal, C, Roman, FS, Khrestchatisky, M, Rivera, S, Féron, F and Vignes, M. (2013). Area-Specific Alterations of Synaptic Plasticity in the 5XFAD Mouse Model of Alzheimer's Disease: Dissociation between Somatosensory Cortex and Hippocampus ed. Lakshmana, MK. PLoS ONE, 8(9), e74667.

Crowe, SE and Ellis-Davies, GCR. (2014). Spine Pruning in 5xFAD Mice Starts on Basal Dendrites of Layer 5 Pyramidal Neurons. Brain Structure and Function, 219(2), 571–80.

Curti, S and O'Brien, J. (2016). Characteristics and Plasticity of Electrical Synaptic Transmission. BMC Cell Biology, 17(1).

Cvijetic, S, Bortolotto, V, Manfredi, M, Ranzato, E, Marengo, E, Salem, R, Canonico, PL and Grilli, M. (2017). Cell Autonomous and Noncell-Autonomous Role of NF-KB P50 in Astrocyte-Mediated Fate Specification of Adult Neural Progenitor Cells. GLIA, 65(1), 169–81.

Danbolt, NC. (2001). Glutamate Uptake. Progress in Neurobiology, 65(1), 1–105.

Dani, JW, Chernjavsky, A and Smith, SJ. (1992). Neuronal Activity Triggers Calcium Waves in Hippocampal Astrocyte Networks. Neuron, 8(3), 429–40.

Deák, F. (2014). Neuronal Vesicular Trafficking and Release in Age-Related Cognitive Impairment. Journals of Gerontology - Series A Biological Sciences and Medical Sciences, 69(11), 1325–30.

Deb, A, Thornton, JD, Sambamoorthi, U and Innes, K. (2017). Direct and Indirect Cost of Managing Alzheimer's Disease and Related Dementias in the United States. Expert Review of Pharmacoeconomics & Outcomes Research, 17(2), 189–202.

DeKosky, ST and Scheff, SW. (1990). Synapse Loss in Frontal Cortex Biopsies in Alzheimer's Disease: Correlation with Cognitive Severity. Annals of Neurology, 27(5), 457–64.

DeMattos, RB, Bales, KR, Parsadanian, M, O'Dell, M a, Foss, EM, Paul, SM and Holtzman, DM. (2002). Plaque-Associated Disruption of CSF and Plasma Amyloid-Beta (Abeta) Equilibrium in a Mouse Model of Alzheimer's Disease. Journal of neurochemistry, 81, 229–36.

Deng, A, Irizarry, MC, Nitsch, RM, Growdon, JH and Rebeck, GW. (2001). Elevation of Cystatin C in Susceptible Neurons in Alzheimer's Disease. The American journal of pathology, 159(3), 1061–68.

Devireddy, LR, Gazin, C, Zhu, X and Green, MR. (2005). A Cell-Surface Receptor for Lipocalin 24p3 Selectively Mediates Apoptosis and Iron Uptake. Cell, 123(7), 1293–1305.

Dhiman, K, Blennow, K, Zetterberg, H, Martins, RN and Gupta, VB. (2019). Cerebrospinal Fluid Biomarkers for Understanding Multiple Aspects of Alzheimer's Disease Pathogenesis. Cellular and Molecular Life Sciences, 76(10), 1833–63.

Díaz-Vera, J, Camacho, M, Machado, JD, Domínguez, N, Montesinos, MS, Hernández-Fernaud, JR, Luján, R and Borges, R. (2012). Chromogranins A and B Are Key Proteins in Amine Accumulation, but the Catecholamine Secretory Pathway Is Conserved without Them. FASEB Journal, 26(1), 430–38.

Dietrich, K, Bouter, Y, M ller, M and Bayer, TA. (2018). Synaptic Alterations in Mouse Models for Alzheimer Disease—A Special Focus on N-Truncated Abeta 4-42. Molecules, 23(4), 718.

Dikeakos, JD, Di Lello, P, Lacombe, MJ, Ghirlando, R, Legault, P, Reudelhuber, TL and Omichinski, JG. (2009). Functional and Structural Characterization of a Dense Core Secretory Granule Sorting Domain from the PC1/3 Protease. Proceedings of the National Academy of Sciences of the United States of America, 106(18), 7408–13.

Doehner, J, Genoud, C, Imhof, C, Krstic, D and Knuesel, I. (2012). Extrusion of Misfolded and Aggregated Proteins - a Protective Strategy of Aging Neurons? European Journal of Neuroscience, 35(12), 1938–50.

Dorszewska, J, Prendecki, M, Oczkowska, A, Dezor, M and Kozubski, W. (2016). Molecular Basis of Familial and Sporadic Alzheimer's Disease. Current Alzheimer Research, 13(9), 952–63.

Dringen, R and Hirrlinger, J. (2003). Glutathione Pathways in the Brain. Biological Chemistry, 384(4), 505–16.

Du, Y, Wu, HT, Qin, XY, Cao, C, Liu, Y, Cao, ZZ and Cheng, Y. (2018). Postmortem Brain, Cerebrospinal Fluid, and Blood Neurotrophic Factor Levels in Alzheimer's Disease: A Systematic Review and Meta-Analysis. J Mol Neurosci, 65(3), 289–300.

Dubois, B. (2018). The Emergence of a New Conceptual Framework for Alzheimer's Disease. Journal of Alzheimer's Disease, 62, 1059–66.

Duits, FH, Brinkmalm, G, Teunissen, CE, Brinkmalm, A, Scheltens, P, Van Der Flier, WM, Zetterberg, H and Blennow, K. (2018). Synaptic Proteins in CSF as Potential Novel Biomarkers for Prognosis in Prodromal Alzheimer's Disease. Alzheimer's Research and Therapy, 10(1).

Duyckaerts, C, Potier, MC and Delatour, B. (2008). Alzheimer Disease Models and Human Neuropathology: Similarities and Differences. Acta Neuropathologica, 115(1), 5–38.

Van Eldik, LJ, Carrillo, MC, Cole, PE, Feuerbach, D, Greenberg, BD, Hendrix, JA, Kennedy, M, Kozauer, N, Margolin, RA, Molinuevo, JL, Mueller, R, Ransohoff, RM, Wilcock, DM, Bain, L and Bales, K. (2016). The Roles of Inflammation and Immune Mechanisms in Alzheimer's Disease. Alzheimer's and Dementia: Translational Research and Clinical Interventions, 2(2), 99–109.

Eliasson, L, Proks, P, Ämmälä, C, Ashcroft, FM, Bokvist, K, Renström, E, Rorsman, P and Smith, PA. (1996). Endocytosis of Secretory Granules in Mouse Pancreatic β-Cells Evoked by Transient Elevation of Cytosolic Calcium. Journal of Physiology, 493(3), 755–67.

Emes, RD and Grant, SGN. (2012). Evolution of Synapse Complexity and Diversity. Annual Review of Neuroscience, 35(1), 111–31.

Emperador Melero, J, Nadadhur, AG, Schut, D, Weering, J V., Heine, VM, Toonen, RF and Verhage, M. (2017). Differential Maturation of the Two Regulated Secretory Pathways in Human IPSC-Derived Neurons. Stem Cell Reports, 8(3), 659–72.

Encalada, SE and Goldstein, LSB. (2014). Biophysical Challenges to Axonal Transport: Motor-Cargo Deficiencies and Neurodegeneration. Annual Review of Biophysics, 43(1), 141–69.

Erickson, MA and Banks, WA. (2011). Cytokine and Chemokine Responses in Serum and Brain after Single and Repeated Injections of Lipopolysaccharide: Multiplex Quantification with Path Analysis. Brain, Behavior, and Immunity, 25(8), 1637–48.

Esquerda-Canals, G, Montoliu-Gaya, L, Güell-Bosch, J and Villegas, S. (2017). Mouse Models of Alzheimer's Disease. Journal of Alzheimer's Disease, 57(4), 1171–83.

Fagan, AM and Perrin, RJ. (2012). Upcoming Candidate Cerebrospinal Fluid Biomarkers of Alzheimer's Disease. Biomarkers in Medicine, 6(4), 455–76.

Fagiani, F, Lanni, C, Racchi, M, Pascale, A and Govoni, S. (2019). Amyloid-β and Synaptic Vesicle Dynamics: A Cacophonic Orchestra. Journal of Alzheimer's Disease, 72(1), 1–14.

Falgàs, N, Tort-Merino, A, Balasa, M, Borrego-Écija, S, Castellví, M, Olives, J, Bosch, B, Férnandez-Villullas, G, Antonell, A, Augé, JM, Lomeña, F, Perissinotti, A, Bargalló, N, Sánchez-Valle, R and Lladó, A. (2019). Clinical Applicability of Diagnostic Biomarkers in Early-Onset Cognitive Impairment. European Journal of Neurology, 26(8), 1098–1104.

Farina, M, van de Bospoort, R, He, E, Persoon, CM, van Weering, JRT, Broeke, JH, Verhage, M and Toonen, RF. (2015). CAPS-1 Promotes Fusion Competence of Stationary Dense-Core Vesicles in Presynaptic Terminals of Mammalian Neurons. eLife, 2015(4).

Fawcett, JP, Aloyz, R, McLean, JH, Pareek, S, Miller, FD, McPherson, PS and Murphy, RA. (1997). Detection of Brain-Derived Neurotrophic Factor in a Vesicular Fraction of Brain Synaptosomes. Journal of Biological Chemistry, 272(14), 8837–40.

Fein, JA, Sokolow, S, Miller, CA, Vinters, H V., Yang, F, Cole, GM and Gylys, KH. (2008). Co-Localization of Amyloid Beta and Tau Pathology in Alzheimer's Disease Synaptosomes. American Journal of Pathology, 172(6), 1683–92.

Ferrer, I, Martí, E, Tortosa, A and Blasi, J. (1998). Dystrophic Neurites of Senile Plaques Are Defective in Proteins Involved in Exocytosis and Neurotransmission. Journal of Neuropathology and Experimental Neurology, 57(3), 218–25.

Fesce, R, Grohovaz, F, Valtorta, F and Meldolesi, J. (1994). Neurotransmitter Release: Fusion or "Kiss-and-Run"? Trends in Cell Biology, 4(1), 1–4.

Fiacco, TA and McCarthy, KD. (2018). Multiple Lines of Evidence Indicate That Gliotransmission Does Not Occur under Physiological Conditions. Journal of Neuroscience, 38(1), 3–13.

Fiandaca, MS, Kapogiannis, D, Mapstone, M, Boxer, A, Eitan, E, Schwartz, JB, Abner, EL, Petersen, RC, Federoff, HJ, Miller, BL and Goetzl, EJ. (2015). Identification of Preclinical Alzheimer's Disease by a Profile of Pathogenic Proteins in Neurally Derived Blood Exosomes: A Case-Control Study. Alzheimer's and Dementia, 11(6), 600-607.e1.

Filosa, JA, Bonev, AD, Straub, S V., Meredith, AL, Wilkerson, MK, Aldrich, RW and Nelson, MT. (2006). Local Potassium Signaling Couples Neuronal Activity to Vasodilation in the Brain. Nature Neuroscience, 9(11), 1397–1403.

Filosa, JA, Naskar, K, Perfume, G, Iddings, JA, Biancardi, VC, Vatta, MS and Stern, JE. (2012). Endothelin-Mediated Calcium Responses in Supraoptic Nucleus Astrocytes Influence Magnocellular Neurosecretory Firing Activity. Journal of Neuroendocrinology, 24(2), 378–92.

Flo, TH, Smith, KD, Sato, S, Rodriguez, DJ, Holmes, MA, Strong, RK, Akira, S and Aderem, A. (2004). Lipocalin 2 Mediates an Innate Immune Response to Bacterial Infection by Sequestrating Iron. Nature, 432(7019), 917–21.

Flood, DG, Lin, YG, Lang, DM, Trusko, SP, Hirsch, JD, Savage, MJ, Scott, RW and Howland, DS. (2009). A Transgenic Rat Model of Alzheimer's Disease with Extracellular Aβ Deposition. Neurobiology of Aging, 30(7), 1078–90.

Flores-Morales, A, Fernandez, L, Rico-Bautista, E, Umana, A, Negrín, C, Zhang, JG and Norstedt, G. (2001). Endoplasmic Reticulum Stress Prolongs GH-Induced Janus Kinase (JAK2)/Signal Transducer and Activator of Transcription (STAT5) Signaling Pathway. Molecular Endocrinology, 15(9), 1471–83.

Forlenza, OV, Diniz, BS, Teixeira, AL, Radanovic, M, Talib, LL, Rocha, NP and Gattaz, WF. (2015). Lower Cerebrospinal Fluid Concentration of Brain-Derived Neurotrophic Factor Predicts Progression from Mild Cognitive Impairment to Alzheimer's Disease. NeuroMolecular Medicine, 17(3), 326–32.

Frank, RA and Grant, SG. (2017). Supramolecular Organization of NMDA Receptors and the Postsynaptic Density. Current Opinion in Neurobiology, 45, 139–47.

Frischknecht, R, Fejtova, A, Viesti, M, Stephan, A and Sonderegger, P. (2008). Activity-Induced Synaptic Capture and Exocytosis of the Neuronal Serine Protease Neurotrypsin. Journal of Neuroscience, 28(7), 1568–79.

Frisoni, GB, Fox, NC, Jack, CR, Scheltens, P and Thompson, PM. (2010). The Clinical Use of Structural MRI in Alzheimer Disease. Nature Reviews Neurology, 6(2), 67–77.

Fu, LY, Acuna-Goycolea, C and Van Den Pol, AN. (2004). Neuropeptide Y Inhibits Hypocretin/Orexin Neurons by Multiple Presynaptic and Postsynaptic Mechanisms: Tonic Depression of the Hypothalamic Arousal System. Journal of Neuroscience, 24(40), 8741–51.

Gajera, CR, Fernandez, R, Postupna, N, Montine, KS, Fox, EJ, Tebaykin, D, Angelo, M, Bendall, SC, Keene, CD and Montine, TJ. (2019). Mass Synaptometry: High-Dimensional Multi Parametric Assay for Single Synapses. Journal of Neuroscience Methods, 312, 73–83.

Games, D, Adams, D, Wolozin, B and Zhao, J. (1995). Alzheimer-Type Neuropathology in Transgenic Mice Overexpressing V717F APP. Letters to Nature, 373(9), 523–27.

Gan, Q and Watanabe, S. (2018). Synaptic Vesicle Endocytosis in Different Model Systems. Frontiers in Cellular Neuroscience, 12, 171.

Gasparotto, J, Ribeiro, CT, Bortolin, RC, Somensi, N, Fernandes, HS, Teixeira, AA, Guasselli, MOR, Agani, CAJO, Souza, NC, Grings, M, Leipnitz, G, Gomes, HM, de Bittencourt Pasquali, MA, Dunkley, PR, Dickson, PW, Moreira, JCF and Gelain, DP. (2017). Anti-RAGE Antibody Selectively Blocks Acute Systemic Inflammatory Responses to LPS in Serum, Liver, CSF and Striatum. Brain, Behavior, and Immunity, 62, 124–36.

Gatt, A, Whitfield, DR, Ballard, C, Doherty, P and & Williams, G. (2019). Alzheimer's Disease Progression in the 5×FAD Mouse Captured with a Multiplex Gene Expression Array. Journal of Alzheimer's Disease, 72(4), 1–12.

Gauthier, S, Kaur, G, Mi, W, Tizon, B and Levy, E. (2011). Protective Mechanisms by Cystatin C in Neurodegenerative Diseases. Frontiers in Bioscience - Scholar, 3 S (2), 541–54.

Geloso, MC, Corvino, V, Di Maria, V, Marchese, E and Michetti, F. (2015). Cellular Targets for Neuropeptide Y-Mediated Control of Adult Neurogenesis. Frontiers in Cellular Neuroscience, 9(MAR), 1–11.

Ghidoni, R, Paterlini, A, Albertini, V, Glionna, M, Monti, E, Schiaffonati, L, Benussi, L, Levy, E and Binetti, G. (2011). Cystatin C Is Released in Association with Exosomes: A New Tool of Neuronal Communication Which Is Unbalanced in Alzheimer's Disease. Neurobiology of Aging, 32(8), 1435–42.

Giaume, C and Liu, X. (2012). From a Glial Syncytium to a More Restricted and Specific Glial Networking. Journal of Physiology Paris, 106(1–2), 34–39.

Ginsberg, SD, Malek-Ahmadi, MH, Alldred, MJ, Chen, Y, Chen, K, Chao, M V, Counts, SE and Mufson, EJ. (2019). Brain-Derived Neurotrophic Factor (BDNF) and TrkB Hippocampal Gene Expression Are Putative Predictors of Neuritic Plaque and Neurofibrillary Tangle Pathology. Neurobiology of Disease, 104540.

Goda, Y and Südhof, TC. (1997). Calcium Regulation of Neurotransmitter Release: Reliably Unreliable? Current Opinion in Cell Biology, 9(4), 513–18.

González-Marrero, I, Giménez-Llort, L, Johanson, CE, Carmona-Calero, EM, Castañeyra-Ruiz, L, Brito-Armas, JM, Castañeyra-Perdomo, A and Castro-Fuentes, R. (2015). Choroid Plexus Dysfunction Impairs Beta-Amyloid Clearance in a Triple Transgenic Mouse Model of Alzheimer's Disease. Frontiers in Cellular Neuroscience, 9(FEB).

Goodall, EF, Wang, C, Simpson, JE, Baker, DJ, Drew, DR, Heath, PR, Saffrey, MJ, Romero, IA and Wharton, SB. (2018). Age-Associated Changes in the Blood-Brain Barrier: Comparative Studies in Human and Mouse. Neuropathology and Applied Neurobiology, 44(3), 328–40.

Gordon, SL, Harper, CB, Smillie, KJ and Cousin, MA. (2016). A Fine Balance of Synaptophysin Levels Underlies Efficient Retrieval of Synaptobrevin II to Synaptic Vesicles ed. Gasman, S. PLOS ONE, 11(2), e0149457.

Gramlich, MW and Klyachko, VA. (2019). Nanoscale Organization of Vesicle Release at Central Synapses. Trends in Neurosciences, 42(6), 425–37.

Guček, A, Vardjan, N and Zorec, R. (2012). Exocytosis in Astrocytes: Transmitter Release and Membrane Signal Regulation. Neurochemical Research, 37(11), 2351–63.

Guo, NY, Jeon, H, Lee, S, Ho, WL, Cho, JY and Suk, K. (2009). Role of Soluble CD14 in Cerebrospinal Fluid as a Regulator of Glial Functions. Journal of Neuroscience Research, 87(11), 2578–90.

Gupta, S, Samali, A, Fitzgerald, U and Deegan, S. (2010). Methods for Monitoring Endoplasmic Reticulum Stress and the Unfolded Protein Response. International Journal of Cell Biology.

Gurel, B, Cansev, M, Sevinc, C, Kelestemur, S, Ocalan, B, Cakir, A, Aydin, S, Kahveci, N, Ozansoy, M, Taskapilioglu, O, Ulus, IH, Başar, MK, Sahin, B, Tuzuner, MB and Baykal, AT. (2018). Early Stage Alterations in CA1 Extracellular Region Proteins Indicate Dysregulation of IL6 and Iron Homeostasis in the 5XFAD Alzheimer's Disease Mouse Model. Journal of Alzheimer's Disease, 61(4), 1399–1410.

Gustafsson, S, Gustavsson, T, Roshanbin, S, Hultqvist, G, Hammarlund-Udenaes, M, Sehlin, D and Syvänen, S. (2018). Blood-Brain Barrier Integrity in a Mouse Model of Alzheimer's Disease with or without Acute 3D6 Immunotherapy. Neuropharmacology, 143, 1–9.

Gylys, KH, Fein, JA and Cole, GM. (2000). Quantitative Characterization of Crude Synaptosomal Fraction (P-2) Components by Flow Cytometry. Journal of Neuroscience Research, 61(2), 186–92.

Gylys, KH, Fein, JA, Yang, F, Wiley, DJ, Miller, CA and Cole, GM. (2004). Synaptic Changes in Alzheimer's Disease. The American Journal of Pathology, 165(5), 1809–17.

Haass, C. (2004). Take Five - BACE and the γ-Secretase Quartet Conduct Alzheimer's Amyloid β-Peptide Generation. EMBO Journal, 23(3), 483–88.

Haass, C, Kaether, C, Thinakaran, G and Sisodia, S. (2012). Trafficking and Proteolytic Processing of APP. Cold Spring Harbor Perspectives in Medicine, 2(5).

Haass, C and Selkoe, DJ. (2007). Soluble Protein Oligomers in Neurodegeneration: Lessons from the Alzheimer's Amyloid β-Peptide. Nature Reviews Molecular Cell Biology, 8(2), 101–12.

Habeck, C, Risacher, S, Lee, GJ, Glymour, MM, Mormino, E, Mukherjee, S, Kim, S, Nho, K, DeCarli, C, Saykin, AJ and Crane, PK. (2012). Relationship between Baseline Brain Metabolism Measured Using [18 F] FDG PET and Memory and Executive Function in Prodromal and Early Alzheimer's Disease. Brain Imaging and Behavior, 6(4), 568–83.

Hackett, JT and Ueda, T. (2015). Glutamate Release. Neurochemical Research, 40(12), 2443–60.

Haim, L Ben, Carrillo-de Sauvage, MA, Ceyzériat, K and Escartin, C. (2015). Elusive Roles for Reactive Astrocytes in Neurodegenerative Diseases. Frontiers in Cellular Neuroscience, 9(august).

Halassa, MM, Fellin, T and Haydon, PG. (2007). The Tripartite Synapse: Roles for Gliotransmission in Health and Disease. Trends in Molecular Medicine, 13(2), 54–63.

Hamilton, NB and Attwell, D. (2010). Do Astrocytes Really Exocytose Neurotransmitters? Nature Reviews Neuroscience, 11(4), 227–38.

Hane, FT, Robinson, M, Lee, BY, Bai, O, Leonenko, Z and Albert, MS. (2017). Recent Progress in Alzheimer's Disease Research, Part 3: Diagnosis and Treatment. Journal of Alzheimer's Disease, 57(3), 645–65.

Hanseeuw, BJ, Betensky, RA, Jacobs, HIL, Schultz, AP, Sepulcre, J, Becker, JA, Cosio, DMO, Farrell, M, Quiroz, YT, Mormino, EC, Buckley, RF, Papp, K V., Amariglio, RA, Dewachter, I, Ivanoiu, A, Huijbers, W, Hedden, T, Marshall, GA, Chhatwal, JP et al. (2019). Association of Amyloid and Tau with Cognition in Preclinical Alzheimer Disease: A Longitudinal Study. JAMA Neurology, 76(8), 915.

Hansson, SF, Andréasson, U, Wall, M, Skoog, I, Andreasen, N, Wallin, A, Zetterberg, H and Blennow, K. (2009). Reduced Levels of Amyloid-Beta-Binding Proteins in Cerebrospinal Fluid from Alzheimer's Disease Patients. Journal of Alzheimer's disease: JAD, 16(2), 389–97.

Hardy, J and Allsop, D. (1991). Amyloid Deposition as the Central Event in the Aetiology of Alzheimer's Disease. Trends in Pharmacological Sciences, 12(C), 383–88.

Hardy, J and Selkoe, DJ. (2002). The Amyloid Hypothesis of Alzheimer's Disease: Progress and Problems on the Road to Therapeutics. Science (New York, N.Y.), 297(5580), 353–56.

Hellwig, K, Kvartsberg, H, Portelius, E, Andreasson, U, Oberstein, TJ, Lewczuk, P, Blennow, K, Kornhuber, J, Maler, JM, Zetterberg, H and Spitzer, P. (2015). Neurogranin and YKL-40: Independent Markers of Synaptic Degeneration and Neuroinflammation in Alzheimer's Disease. Alzheimer's Research & Therapy, 7(1), 74.

Heslegrave, A, Heywood, W, Paterson, R, Magdalinou, N, Svensson, J, Johansson, P, Öhrfelt, A, Blennow, K, Hardy, J, Schott, J, Mills, K and Zetterberg, H. (2016). Increased Cerebrospinal Fluid Soluble TREM2 Concentration in Alzheimer's Disease. Molecular Neurodegeneration, 11(1), 3.

Höglund, K, Schussler, N, Kvartsberg, H, Smailovic, U, Brinkmalm, G, Liman, V, Becker, B, Zetterberg, H, Cedazo-Minguez, A, Janelidze, S, Lefevre, IA, Eyquem, S, Hansson, O and Blennow, K. (2020). Cerebrospinal Fluid Neurogranin in an Inducible Mouse Model of Neurodegeneration: A Translatable Marker of Synaptic Degeneration. Neurobiology of Disease, 134.

Hokama, M, Oka, S, Leon, J, Ninomiya, T, Honda, H, Sasaki, K, Iwaki, T, Ohara, T, Sasaki, T, LaFerla, FM, Kiyohara, Y and Nakabeppu, Y. (2014). Altered Expression of Diabetes-Related Genes in Alzheimer's Disease Brains: The Hisayama Study. Cerebral Cortex, 24(9), 2476–88.

Hökfelt, T, Broberger, C, Xu, ZQD, Sergeyev, V, Ubink, R and Diez, M. (2000). Neuropeptides - An Overview. Neuropharmacology, 39(8), 1337–56.

Holtzman, DM, Morris, JC and Goate, AM. (2011). Alzheimer's Disease: The Challenge of the Second Century. Science Translational Medicine, 3(77).

Hong, S, Beja-Glasser, VF, Nfonoyim, BM, Frouin, A, Li, S, Ramakrishnan, S, Merry, KM, Shi, Q, Rosenthal, A, Barres, BA, Lemere, CA, Selkoe, DJ and Stevens, B. (2016). Complement and Microglia Mediate Early Synapse Loss in Alzheimer Mouse Models. Science, 352(6286), 712–16.

Hook, V, Brennand, KJ, Kim, Y, Toneff, T, Funkelstein, L, Lee, KC, Ziegler, M and Gage, FH. (2014). Human IPSC Neurons Display Activity-Dependent Neurotransmitter Secretion: Aberrant Catecholamine Levels in Schizophrenia Neurons. Stem Cell Reports, 3(4), 531–38.

Hosaka, M and Watanabe, T. (2010). Secretogranin III: A Bridge between Core Hormone Aggregates and the Secretory Granule Membrane. Endocrine journal, 57(4), 275–86.

Hoshino, A and Lindberg, I. (2012). Peptide Biosynthesis: Prohormone Convertases 1/3 and 2. Colloquium Series on Neuropeptides, 1(1), 1–112.

Hua, X, Malarkey, EB, Sunjara, V, Rosenwald, SE, Li, WH and Parpura, V. (2004). Ca2+-Dependent Glutamate Release Involves Two Classes of Endoplasmic Reticulum Ca2+ Stores in Astrocytes. Journal of Neuroscience Research, 76(1), 86–97.

Hummer, BH, De Leeuw, NF, Burns, C, Chen, L, Joens, MS, Hosford, B, Fitzpatrick, JAJ and Asensio, CS. (2017). HID-1 Controls Formation of Large Dense Core Vesicles by Influencing Cargo Sorting and Trans-Golgi Network Acidification. Molecular Biology of the Cell, 28(26), 3870–80.

Hyman, BT, Phelps, CH, Beach, TG, Bigio, EH, Cairns, NJ, Carrillo, MC, Dickson, DW, Duyckaerts, C, Frosch, MP, Masliah, E, Mirra, SS, Nelson, PT, Schneider, JA, Thal, DR, Thies, B, Trojanowski, JQ, Vinters, H V. and Montine, TJ. (2012). National Institute on Aging-Alzheimer's Association Guidelines for the Neuropathologic Assessment of Alzheimer's Disease. Alzheimer's and Dementia, 8(1), 1–13.

Hynd, MR, Scott, HL and Dodd, PR. (2004). Glutamate-Mediated Excitotoxicity and Neurodegeneration in Alzheimer's Disease. Neurochemistry International, 45(5), 583–95.

Iijima-Ando, K, Sekiya, M, Maruko-Otake, A, Ohtake, Y, Suzuki, E, Lu, B and Iijima, KM. (2012). Loss of Axonal Mitochondria Promotes Tau-Mediated Neurodegeneration and Alzheimer's Disease-Related Tau Phosphorylation Via PAR-1. PLoS Genetics, 8(8).

Imai, Y and Kohsaka, S. (2002). Intracellular Signaling in M-CSF-Induced Microglia Activation: Role of Iba1. GLIA, 40(2), 164–74.

Innocenti, B, Parpura, V and Haydon, PG. (2000). Imaging Extracellular Waves of Glutamate during Calcium Signaling in Cultured Astrocytes. Journal of Neuroscience, 20(5), 1800–1808.

Ip, Noçon, Hofer, Lim, Müller and Campbell. (2011). Lipocalin 2 in the Central Nervous System Host Response to Systemic Lipopolysaccharide Administration. Journal of neuroinflammation, 8(September), 124.

Iram, T, Trudler, D, Kain, D, Kanner, S, Galron, R, Vassar, R, Barzilai, A, Blinder, P, Fishelson, Z and Frenkel, D. (2016). Astrocytes from Old Alzheimer's Disease Mice Are Impaired in Aβ Uptake and in Neuroprotection. Neurobiology of Disease, 96, 84–94.

Isaac, RE, Bland, ND and Shirras, AD. (2009). Neuropeptidases and the Metabolic Inactivation of Insect Neuropeptides. General and Comparative Endocrinology, 162(1), 8–17.

Israel, MA, Yuan, SH, Bardy, C, Reyna, SM, Mu, Y, Herrera, C, Hefferan, MP, Van Gorp, S, Nazor, KL, Boscolo, FS, Carson, CT, Laurent, LC, Marsala, M, Gage, FH, Remes, AM, Koo, EH and Goldstein, LSB. (2012). Probing Sporadic and Familial Alzheimer's Disease Using Induced Pluripotent Stem Cells. Nature, 482(7384), 216–20.

Jahn, R and Südhof, TC. (1994). Synaptic Vesicles and Exocytosis. Annual review of neuroscience, 17, 219–46.

Jang, E, Kim, JH, Lee, S, Kim, JH, Seo, JW, Jin, M, Lee, MG, Jang, IS, Lee, WH and Suk, K. (2013). Phenotypic Polarization of Activated Astrocytes: The Critical Role of Lipocalin-2 in the Classical Inflammatory Activation of Astrocytes. The Journal of Immunology, 191(10), 5204–19.

Jarvela, TS, Womack, T, Georgiou, P, Gould, TD, Eriksen, JL and Lindberg, I. (2018). 7B2 Chaperone Knockout in APP Model Mice Results in Reduced Plaque Burden. Scientific Reports, 8(1).

Jay, TR, von Saucken, VE, Muñoz, B, Codocedo, JF, Atwood, BK, Lamb, BT and Landreth, GE. (2019). TREM2 Is Required for Microglial Instruction of Astrocytic Synaptic Engulfment in Neurodevelopment. GLIA, 67(10), 1873–92.

Jembrek, M and Vlainic, J. (2015). GABA Receptors: Pharmacological Potential and Pitfalls. Current Pharmaceutical Design, 21(34), 4943–59.

Jeremic, A, Jeftinija, K, Stevanovic, J, Glavaski, A and Jeftinija, S. (2001). ATP Stimulates Calcium-Dependent Glutamate Release from Cultured Astrocytes. Journal of Neurochemistry, 77(2), 664–75.

Jha, MK, Lee, S, Park, DH, Kook, H, Park, KG, Lee, IK and Suk, K. (2015). Diverse Functional Roles of Lipocalin-2 in the Central Nervous System. Neuroscience and Biobehavioral Reviews, 49, 135–56.

Ji, L, Wu, HT, Qin, XY and Lan, R. (2017). Dissecting Carboxypeptidase E: Properties, Functions and Pathophysiological Roles in Disease. Endocrine Connections, 6(4), R18–38.

Jin, M, Kim, JH, Jang, E, Lee, YM, Soo Han, H, Woo, DK, Park, DH, Kook, H and Suk, K. (2014). Lipocalin-2 Deficiency Attenuates Neuroinflammation and Brain Injury after Transient Middle Cerebral Artery Occlusion in Mice. Journal of Cerebral Blood Flow and Metabolism, 34(8), 1306–14.

Johanson, CE, Duncan, JA, Klinge, PM, Brinker, T, Stopa, EG and Silverberg, GD. (2008). Multiplicity of Cerebrospinal Fluid Functions: New Challenges in Health and Disease. Cerebrospinal fluid research, 5(1), 10.

de Jong, AP and Verhage, M. (2009). Presynaptic Signal Transduction Pathways That Modulate Synaptic Transmission. Current Opinion in Neurobiology, 19(3), 245–53.

Jourdain, P, Bergersen, LH, Bhaukaurally, K, Bezzi, P, Santello, M, Domercq, M, Matute, C, Tonello, F, Gundersen, V and Volterra, A. (2007). Glutamate Exocytosis from Astrocytes Controls Synaptic Strength. Nature Neuroscience, 10(3), 331–39.

Jovanovic, JN, Czernik, AJ, Fienberg, AA, Greengard, P and Sihra, TS. (2000). Synapsins as Mediators of BDNF-Enhanced Neurotransmitter Release. Nature Neuroscience, 3(4), 323–29.

Jung, GL, Bae, SS, Young, SY, Ji, EK, Sung, WY, Dong, WJ, Jun, HB, Sung, WP and Young, HK. (2009). Decreased Serum Brain-Derived Neurotrophic Factor Levels in Elderly Korean with Dementia. Psychiatry Investigation, 6(4), 299–305.

Jung, J, Jo, HW, Kwon, H and Jeong, NY. (2014). ATP Release through Lysosomal Exocytosis from Peripheral Nerves: The Effect of Lysosomal Exocytosis on Peripheral Nerve Degeneration and Regeneration after Nerve Injury. BioMed Research International, 2014.

Kamat, PK, Kalani, A, Rai, S, Swarnkar, S, Tota, S, Nath, C and Tyagi, N. (2016). Mechanism of Oxidative Stress and Synapse Dysfunction in the Pathogenesis of Alzheimer's Disease: Understanding the Therapeutics Strategies. Molecular Neurobiology, 53(1), 648–61.

Kanaan, NM, Morfini, GA, LaPointe, NE, Pigino, GF, Patterson, KR, Song, Y, Andreadis, A, Fu, Y, Brady, ST and Binder, LI. (2011). Pathogenic Forms of Tau Inhibit Kinesin-Dependent Axonal Transport through a Mechanism Involving Activation of Axonal Phosphotransferases. Journal of Neuroscience, 31(27), 9858–68.

Kang, SS, Ren, Y, Liu, CC, Kurti, A, Baker, KE, Bu, G, Asmann, Y and Fryer, JD. (2017). Lipocalin-2 Protects the Brain during Inflammatory Conditions. Molecular Psychiatry, (October 2016), 1–7.

Katsnelson, A, De Strooper, B and Zoghbi, HY. (2016). Neurodegeneration: From Cellular Concepts to Clinical Applications. Science Translational Medicine, 8(364).

Katz, B and Miledi, R. (1969). Tetrodotoxin-resistant Electric Activity in Presynaptic Terminals. The Journal of Physiology, 203(2), 459–87.

Kaur, G and Levy, E. (2012). Cystatin C in Alzheimer's Disease. Frontiers in molecular neuroscience, 5(July 2012), 79.

Kawasaki, F, Iyer, J, Posey, LL, Sun, CE, Mammen, SE, Yan, H and Ordway, RW. (2011). The DISABLED Protein Functions in CLATHRIN-Mediated Synaptic Vesicle Endocytosis and Exoendocytic Coupling at the Active Zone. Proceedings of the National Academy of Sciences of the United States of America, 108(25).

Keaney, J, Gasser, J, Gillet, G, Scholz, D and Kadiu, I. (2019). Inhibition of Bruton's Tyrosine Kinase Modulates Microglial Phagocytosis: Therapeutic Implications for Alzheimer's Disease. Journal of Neuroimmune Pharmacology, 14(3), 448–61.

Keck, S, Nitsch, R, Grune, T and Ullrich, O. (2003). Proteasome Inhibition by Paired Helical Filament-Tau in Brains of Patients with Alzheimer's Disease. Journal of Neurochemistry, 85(1), 115–22.

Van Kempen, GTH, Vanderleest, HT, Van Den Berg, RJ, Eilers, P and Westerink, RHS. (2011). Three Distinct Modes of Exocytosis Revealed by Amperometry in Neuroendocrine Cells. Biophysical Journal, 100(4), 968–77.

Kester, MI, Teunissen, CE, Sutphen, C, Herries, EM, Ladenson, JH, Xiong, C, Scheltens, P, van der Flier, WM, Morris, JC, Holtzman, DM and Fagan, AM. (2015). Cerebrospinal Fluid VILIP-1 and YKL-40, Candidate Biomarkers to Diagnose, Predict and Monitor Alzheimer's Disease in a Memory Clinic Cohort. Alzheimer's Research & Therapy, 7(1), 59.

Kim, DK, Han, D, Park, J, Choi, H, Park, JC, Cha, MY, Woo, J, Byun, MS, Lee, DY, Kim, Y and Mook-Jung, I. (2019). Deep Proteome Profiling of the Hippocampus in the 5XFAD Mouse Model Reveals Biological Process Alterations and a Novel Biomarker of Alzheimer's Disease. Experimental and Molecular Medicine, 51(11).

Kim, E and Sheng, M. (2004). PDZ Domain Proteins of Synapses. Nature Reviews Neuroscience, 5(10), 771–81.

Kim, JH, Ko, PW, Lee, HW, Jeong, JY, Lee, MG, Kim, JH, Lee, WH, Yu, R, Oh, WJ and Suk, K. (2017). Astrocyte-Derived Lipocalin-2 Mediates Hippocampal Damage and Cognitive Deficits in Experimental Models of Vascular Dementia. GLIA, 65(9), 1471–90.

Kim, T, Gondré-Lewis, MC, Arnaoutova, I and Loh, YP. (2006). Dense-Core Secretory Granule Biogenesis. Physiology, 21(2), 124–33.

Kim, W and Kim, SK. (2016). Neural Circuit Remodeling and Structural Plasticity in the Cortex during Chronic Pain. Korean Journal of Physiology and Pharmacology, 20(1), 1–8.

Kimelberg, HK and Nedergaard, M. (2010). Functions of Astrocytes and Their Potential As Therapeutic Targets. Neurotherapeutics, 7(4), 338–53.

Kimura, N and Yanagisawa, K. (2018). Traffic Jam Hypothesis: Relationship between Endocytic Dysfunction and Alzheimer's Disease. Neurochemistry International, 119, 35–41.

Kirischuk, S. (1996). Calcium Signalling in Mouse Bergmann Glial Cells Mediated by A1-Adrenoreceptors and H1 Histamine Receptors. European Journal of Neuroscience, 8(6), 1198–1208.

Kirischuk, S, Héja, L, Kardos, J and Billups, B. (2016). Astrocyte Sodium Signaling and the Regulation of Neurotransmission. GLIA, 64(10), 1655–66.

Kirischuk, S, Scherer, J, Kettenmann, H and Verkhratsky, A. (1995). Activation of P2-purinoreceptors Triggered Ca2+ Release from InsP3-sensitive Internal Stores in Mammalian Oligodendrocytes. The Journal of Physiology, 483(1), 41–57.

Kirsebom, BE, Nordengen, K, Selnes, P, Waterloo, K, Torsetnes, SB, Gísladóttir, B, Brix, B, Vanmechelen, E, Bråthen, G, Hessen, E, Aarsland, D and Fladby, T. (2018). Cerebrospinal Fluid Neurogranin/β-Site APP-Cleaving Enzyme 1 Predicts Cognitive Decline in Preclinical Alzheimer's Disease. Alzheimer's and Dementia: Translational Research and Clinical Interventions, 4, 617–27.

Klein-Szanto, AJ and Bassi, DE. (2017). Proprotein Convertase Inhibition: Paralyzing the Cell's Master Switches. Biochemical Pharmacology, 140, 8–15.

Kocherhans, S, Madhusudan, A, Doehner, J, Breu, KS, Nitsch, RM, Fritschy, JM and Knuesel, I. (2010). Reduced Reelin Expression Accelerates Amyloid-β Plaque Formation and Tau Pathology in Transgenic Alzheimer's Disease Mice. Journal of Neuroscience, 30(27), 9228–40.

Kögel, T and Gerdes, HH. (2010). Maturation of Secretory Granules. Results and Problems in Cell Differentiation, 50, 1–20.

Köhler, C. (2016). Granulovacuolar Degeneration: A Neurodegenerative Change That Accompanies Tau Pathology. Acta Neuropathologica, 132(3), 339–59.

Komura, H, Kakio, S, Sasahara, T, Arai, Y, Takino, N, Sato, M, Satomura, K, Ohnishi, T, Nabeshima, Y ichi, Muramatsu, S ichi, Kii, I and Hoshi, M. (2019). Alzheimer Aβ Assemblies Accumulate in Excitatory Neurons upon Proteasome Inhibition and Kill Nearby NAKα3 Neurons by Secretion. iScience, 13, 452–77.

Kork, F, Jankowski, J, Goswami, A, Weis, J, Brook, G, Yamoah, A, Anink, J, Aronica, E, Fritz, S, Huck, C, Schipke, C, Peters, O, Tepel, M, Noels, H and Jankowski, V. (2018). Golgin A4 in CSF and Granulovacuolar Degenerations of Patients with Alzheimer Disease. Neurology, 91(19), e1799–1808.

Kreutzberger, AJB, Kiessling, V, Stroupe, C, Liang, B, Preobraschenski, J, Ganzella, M, Kreutzberger, MAB, Nakamoto, R, Jahn, R, Castle, JD and Tamm, LK. (2019). In Vitro Fusion of Single Synaptic and Dense Core Vesicles Reproduces Key Physiological Properties. Nature Communications, 10(1).

Krstic, D and Knuesel, I. (2013). Deciphering the Mechanism Underlying Late-Onset Alzheimer Disease. Nature Reviews Neurology, 9(1), 25–34.

Krstic, D, Madhusudan, A, Doehner, J, Vogel, P, Notter, T, Imhof, C, Manalastas, A, Hilfiker, M, Pfister, S, Schwerdel, C, Riether, C, Meyer, U and Knuesel, I. (2012). Systemic Immune Challenges Trigger and Drive Alzheimer-like Neuropathology in Mice. Journal of Neuroinflammation, 9, 151.

Krzan, M, Stenovec, M, Kreft, M, Pangrsic, T, Grilc, S, Haydon, PG and Zorec, R. (2003). Calcium-Dependent Exocytosis of Atrial Natriuretic Peptide from Astrocytes. The Journal of neuroscience: the official journal of the Society for Neuroscience, 23(5), 1580–83.

Kurokawa, K and Nakano, A. (2019). The ER Exit Sites Are Specialized ER Zones for the Transport of Cargo Proteins from the ER to the Golgi Apparatus. Journal of Biochemistry, 165(2), 109–14.

Kwinter, DM, Lo, K, Mafi, P and Silverman, MA. (2009). Dynactin Regulates Bidirectional Transport of Dense-Core Vesicles in the Axon and Dendrites of Cultured Hippocampal Neurons. Neuroscience, 162(4), 1001–10.

Kwon, S, Moreno-Gonzalez, I, Taylor-Presse, K, Edwards, G, Gamez, N, Calderon, O, Zhu, B, Velasquez, FC, Soto, C and Sevick-Muraca, EM. (2019). Impaired Peripheral Lymphatic Function and Cerebrospinal Fluid Outflow in a Mouse Model of Alzheimer's Disease. Journal of Alzheimer's Disease, 69(2), 585–93.

Lahmy, V, Meunier, J, Malmström, S, Naert, G, Givalois, L, Kim, SH, Villard, V, Vamvakides, A and Maurice, T. (2013). Blockade of Tau Hyperphosphorylation and Aβ 1-42 Generation by the Aminotetrahydrofuran Derivative ANAVEX2-73, a Mixed Muscarinic and σ 1 Receptor Agonist, in a Nontransgenic Mouse Model of Alzheimer's Disease. Neuropsychopharmacology, 38(9), 1706–23.

Lanjakornsiripan, D, Pior, BJ, Kawaguchi, D, Furutachi, S, Tahara, T, Katsuyama, Y, Suzuki, Y, Fukazawa, Y and Gotoh, Y. (2018). Layer-Specific Morphological and Molecular Differences in Neocortical Astrocytes and Their Dependence on Neuronal Layers. Nature Communications, 9(1).

Lanoiselée, HM, Nicolas, G, Wallon, D, Rovelet-Lecrux, A, Lacour, M, Rousseau, S, Richard, AC, Pasquier, F, Rollin-Sillaire, A, Martinaud, O, Quillard-Muraine, M, de la Sayette, V, Boutoleau-Bretonniere, C, Etcharry-Bouyx, F, Chauviré, V, Sarazin, M, le Ber, I, Epelbaum, S, Jonveaux, T et al. (2017). APP, PSEN1, and PSEN2 Mutations in Early-Onset Alzheimer Disease: A Genetic Screening Study of Familial and Sporadic Cases. PLoS Medicine, 14(3).

Lashley, T, Schott, JM, Weston, P, Murray, CE, Wellington, H, Keshavan, A, Foti, SC, Foiani, M, Toombs, J, Rohrer, JD, Heslegrave, A and Zetterberg, H. (2018). Molecular Biomarkers of Alzheimer's Disease: Progress and Prospects. Disease Models & Mechanisms, 11(5), dmm031781.

Lassmann, H, Weiler, R, Fischer, P, Bancher, C, Jellinger, K, Floor, E, Danielczyk, W, Seitelberger, F and Winkler, H. (1992). Synaptic Pathology in Alzheimer's Disease: Immunological Data for Markers of Synaptic and Large Dense-Core Vesicles. Neuroscience, 46(1), 1–8.

Lechner, T, Adlassnig, C, Humpel, C, Kaufmann, WA, Maier, H, Reinstadler-Kramer, K, Hinterhölzl, J, Mahata, SK, Jellinger, KA and Marksteiner, J. (2004). Chromogranin Peptides in Alzheimer's Disease. Experimental Gerontology, 39(1), 101–13.

Lee, DC, Close, FT, Goodman, CB, Jackson, IM, Wight-Mason, C, Wells, LM, Womble, TA and Palm, DE. (2006). Enhanced Cystatin C and Lysosomal Protease Expression Following 6-Hydroxydopamine Exposure. NeuroToxicology, 27(2), 260–76.

Lee, M, Lee, HJ, Jeong, YJ, Oh, SJ, Kang, KJ, Han, SJ, Nam, KR, Lee, YJ, Lee, KC, Ryu, YH, Hyun, IY and Choi, JY. (2019). Age Dependency of MGluR5 Availability in 5xFAD Mice Measured by PET. Neurobiology of Aging.

Lee, S, Park, JY, Lee, WH, Kim, H, Park, HC, Mori, K and Suk, K. (2009). Lipocalin-2 Is an Autocrine Mediator of Reactive Astrocytosis. Journal of Neuroscience, 29(1), 234–49.

Lee, SN, Prodhomme, E and Lindberg, I. (2004). Prohormone Convertase 1 (PC1) Processing and Sorting: Effect of PC1 Propeptide and ProSAAS PCSK1 Mutations and Human Obesity View Project Synthesis and Biological Evaluation of Linear and Cyclic Peptides Containing Cysteine and Arginine as a Drug Delivery. Journal of Endocrinology, 182, 353–364.

Lehnardt, S, Massillon, L, Follett, P, Jensen, FE, Ratan, R, Rosenberg, PA, Volpe, JJ and Vartanian, T. (2003). Activation of Innate Immunity in the CNS Triggers Neurodegeneration through a Toll-like Receptor 4-Dependent Pathway. Proceedings of the National Academy of Sciences of the United States of America, 100(14), 8514–19.

Leon, WC, Canneva, F, Partridge, V, Allard, S, Ferretti, MT, Dewilde, A, Vercauteren, F, Atifeh, R, Ducatenzeiler, A, Klein, W, Szyf, M, Alhonen, L and Cuello, AC. (2010). A Novel Transgenic Rat Model with a Full Alzheimer's - Like Amyloid Pathology Displays Pre - Plaque Intracellular Amyloid -β- Associated Cognitive Impairment. Journal of Alzheimer's Disease, 20(1), 113–26.

Levitan, ES. (2008). Signaling for Vesicle Mobilization and Synaptic Plasticity. Molecular Neurobiology, 37(1), 39–43.

Levy, E, Sastre, M, Kumar, A, Gallo, G, Piccardo, P, Ghetti, B and Tagliavini, F. (2001). Codeposition of Cystatin C with Amyloid-β Protein in the Brain of Alzheimer Disease Patients. Journal of Neuropathology and Experimental Neurology, 60(1), 94–104.

Lewczuk, P, Riederer, P, O'bryant, SE, Verbeek, MM, Dubois, B, Visser, PJ, Jellinger, KA, Engelborghs, S, Ramirez, A, Parnetti, L, Jack, CR, Teunissen, CE, Hampel, H, Lleó, A, Jessen, F, Glodzik, L, De Leon, MJ, Fagan, AM, Molinuevo, L et al. (2017). Cerebrospinal Fluid and Blood Biomarkers for Neurodegenerative Dementias: An Update of the Consensus of the Task Force on Biological Markers in Psychiatry of the World Federation of Societies of Biological Psychiatry. The World Journal of Biological Psychiatry, 19(4), 244–328.

Li, D, Ropert, N, Koulakoff, A, Giaume, C and Oheim, M. (2008). Lysosomes Are the Major Vesicular Compartment Undergoing Ca 2-Regulated Exocytosis from Cortical Astrocytes. Journal of Neuroscience, 28(30), 7648–58.

Li, Q, Liu, Y and Sun, M. (2017). Autophagy and Alzheimer's Disease. Cellular and Molecular Neurobiology, 37(3), 377–88.

Liang, C, Carrel, D, Omelchenko, A, Kim, H, Patel, A, Fanget, I and Firestein, BL. (2018). Cortical Neuron Migration and Dendrite Morphology Are Regulated by Carboxypeptidase E. Work, Aging and Retirement, 1–14.

Liang, K, Wei, L and Chen, L. (2017). Exocytosis, Endocytosis, and Their Coupling in Excitable Cells. Frontiers in Molecular Neuroscience, 10, 109.

Liddelow, SA, Guttenplan, KA, Clarke, LE, Bennett, FC, Bohlen, CJ, Schirmer, L, Bennett, ML, Münch, AE, Chung, WS, Peterson, TC, Wilton, DK, Frouin, A, Napier, BA, Panicker, N, Kumar, M, Buckwalter, MS, Rowitch, DH, Dawson, VL, Dawson, TM et al. (2017). Neurotoxic Reactive Astrocytes Are Induced by Activated Microglia. Nature, 541(7638), 481–87.

Lim, A, Rechtsteiner, A and Saxton, WM. (2017). Two Kinesins Drive Anterograde Neuropeptide Transport. Molecular Biology of the Cell, 28(24), 3542–53.

Lim, NKH, Moestrup, V, Zhang, X, Wang, WA, Møller, A and Huang, F De. (2018). An Improved Method for Collection of Cerebrospinal Fluid from Anesthetized Mice. Journal of Visualized Experiments, 2018(133), e56774.

Limanaqi, F, Biagioni, F, Busceti, CL, Ryskalin, L, Soldani, P, Frati, A and Fornai, F. (2019). Cell Clearing Systems Bridging Neuro-Immunity and Synaptic Plasticity. International Journal of Molecular Sciences, 20(9).

Lin, RC and Scheller, RH. (2000). Mechanisms of Synaptic Vesicle Exocytosis. Annual Review of Cell and Developmental Biology, 16(1), 19–49.

Lin, WJJ and Salton, SR. (2013). The Regulated Secretory Pathway and Human Disease: Insights from Gene Variants and Single Nucleotide Polymorphisms. Frontiers in endocrinology, 4(August), 96.

Lipska, BK, Khaing, ZZ, Weickert, CS and Weinberger, DR. (2001). BDNF MRNA Expression in Rat Hippocampus and Prefrontal Cortex: Effects of Neonatal Ventral Hippocampal Damage and Antipsychotic Drugs. European Journal of Neuroscience, 14(1), 135–44.

Lista, S, Faltraco, F, Prvulovic, D and Hampel, H. (2013). Blood and Plasma-Based Proteomic Biomarker Research in Alzheimer's Disease. Progress in Neurobiology, 101–102(1), 1–17.

Lista, S, Toschi, N, Baldacci, F, Zetterberg, H, Blennow, K, Kilimann, I, Teipel, SJ, Cavedo, E, Dos Santos, AM, Epelbaum, S, Lamari, F, Dubois, B, Nisticò, R, Floris, R, Garaci, F, Hampel, H and Alzheimer Precision Medicine Initiative (APMI). (2017). Cerebrospinal Fluid Neurogranin as a Biomarker of Neurodegenerative Diseases: A Cross-Sectional Study. Journal of Alzheimer's disease: JAD, 59, 1–8.

Liu, DS, Pan, XD, Zhang, J, Shen, H, Collins, NC, Cole, AM, Koster, KP, Ben Aissa, M, Dai, XM, Zhou, M, Tai, LM, Zhu, YG, Ladu, MJ and Chen, XC. (2015). APOE4 Enhances Age-Dependent Decline in Cognitive Function by down-Regulating an NMDA Receptor Pathway in EFAD-Tg Mice. Molecular Neurodegeneration, 10(1).

Liu, HT, Tashmukhamedov, BA, Inoue, H, Okada, Y and Sabirov, RZ. (2006). Roles of Two Types of Anion Channels in Glutamate Release from Mouse Astrocytes under Ischemic or Osmotic Stress. GLIA, 54(5), 343–57.

Liu, L and Duff, K. (2008). A Technique for Serial Collection of Cerebrospinal Fluid from the Cisterna Magna in Mouse. Journal of Visualized Experiments, (21), e960.

Liu, T, Sun, L, Xiong, Y, Shang, S, Guo, N, Teng, S, Wang, Y, Liu, B, Wang, C, Wang, L, Zheng, L, Zhang, CX, Han, W and Zhou, Z. (2011). Calcium Triggers Exocytosis from Two Types of Organelles in a Single Astrocyte. Journal of Neuroscience, 31(29), 10593–601.

Lleó, A, Núñez-Llaves, R, Alcolea, D, Chiva, C, Balateu-Paños, D, Colom-Cadena, M, Gomez-Giro, G, Muñoz, L, Querol-Vilaseca, M, Pegueroles, J, Rami, L, Lladó, A, Molinuevo, JL, Tainta, M, Clarimón, J, Spires-Jones, T, Blesa, R, Fortea, J, Martínez-Lage, P et al. (2019). Changes in Synaptic Proteins Precede Neurodegeneration Markers in Preclinical Alzheimer's Disease Cerebrospinal Fluid. Mol Cell Proteomics.

Long, JM and Holtzman, DM. (2019). Alzheimer Disease: An Update on Pathobiology and Treatment Strategies. Cell, 179(2), 312–39.

López-Huerta, VG, Blanco-Hernández, E, Bargas, J and Galarraga, E. (2012). Presynaptic Modulation by Somatostatin in the Rat Neostriatum Is Altered in a Model of Parkinsonism. Journal of Neurophysiology, 108(4), 1032–43.

Love, S, Siew, LK, Dawbarn, D, Wilcock, GK, Ben-Shlomo, Y and Allen, SJ. (2006). Premorbid Effects of APOE on Synaptic Proteins in Human Temporal Neocortex. Neurobiology of Aging, 27(6), 797–803.

Ma, B, Buckalew, R, Du, Y, Kiyoshi, CM, Alford, CC, Wang, W, Mctigue, DM, Enyeart, JJ, Terman, D and Zhou, M. (2016). Gap Junction Coupling Confers Isopotentiality on Astrocyte Syncytium. GLIA, 64(2), 214–26.

MacDonald, AJ, Robb, JL, Morrissey, NA, Beall, C and Ellacott, KLJ. (2019). Astrocytes in Neuroendocrine Systems: An Overview. Journal of Neuroendocrinology, 31(5), e12726.

Maetzler, W, Schmid, B, Synofzik, M, Schulte, C, Riester, K, Huber, H, Brockmann, K, Gasser, T, Berg, D and Melms, A. (2010). The CST3 BB Genotype and Low Cystatin C Cerebrospinal Fluid Levels Are Associated with Dementia in Lewy Body Disease. Journal of Alzheimer's Disease, 19(3), 937–42.

Malarkey, EB and Parpura, V. (2011). Temporal Characteristics of Vesicular Fusion in Astrocytes: Examination of Synaptobrevin 2-Laden Vesicles at Single Vesicle Resolution. Journal of Physiology, 589(17), 4271–4300.

Malva, JO, Xapelli, S, Baptista, S, Valero, J, Agasse, F, Ferreira, R and Silva, AP. (2012). Multifaces of Neuropeptide Y in the Brain - Neuroprotection, Neurogenesis and Neuroinflammation. Neuropeptides, 46(6), 299–308.

Maphis, NM, Jiang, S, Binder, J, Wright, C, Gopalan, B, Lamb, BT and Bhaskar, K. (2017). Whole Genome Expression Analysis in a Mouse Model of Tauopathy Identifies MECP2 as a Possible Regulator of Tau Pathology. Frontiers in Molecular Neuroscience, 10.

Marks, N, Stern, F, Chi, LM and Berg, MJ. (1988). Diversity of Rat Brain Cysteine Proteinase Inhibitors: Isolation of Low-Molecular-Weight Cystatins and a Higher-Molecular Weight T-Kininogen-like Glycoprotein. Archives of Biochemistry and Biophysics, 267(2), 448–58.

Marksteiner, J, Kaufmann, WA, Gurka, P and Humpel, C. (2002). Synaptic Proteins in Alzheimer's Disease. Journal of Molecular Neuroscience, 53.

Marques, F, Rodrigues, AJ, Sousa, JC, Coppola, G, Geschwind, DH, Sousa, N, Correia-Neves, M and Palha, JA. (2008). Lipocalin 2 Is a Choroid Plexus Acute-Phase Protein. Journal of Cerebral Blood Flow & Metabolism, 28, 450–55.

Marques, F, Sousa, JC, Correia-Neves, M, Oliveira, P, Sousa, N and Palha, JA. (2007). The Choroid Plexus Response to Peripheral Inflammatory Stimulus. Neuroscience, 144(2), 424–30.

Martineau, M, Shi, T, Puyal, J, Knolhoff, AM, Dulong, J, Gasnier, B, Klingauf, J, Sweedler, J V, Jahn, R and Mothet, JP. (2013). Storage and Uptake of D-Serine into Astrocytic Synaptic-Like Vesicles Specify Gliotransmission. Journal of Neuroscience, 33(8), 3413–23.

Mathews, PM and Levy, E. (2016). Cystatin C in Aging and in Alzheimer's Disease. Ageing Research Reviews, 32, 38–50.

Mathiisen, TM, Lehre, KP, Danbolt, NC and Ottersen, OP. (2010). The Perivascular Astroglial Sheath Provides a Complete Covering of the Brain Microvessels: An Electron Microscopic 3D Reconstruction. GLIA, 58(9), 1094–1103.

Matos, M, Bosson, A, Riebe, I, Reynell, C, Vallée, J, Laplante, I, Panatier, A, Robitaille, R and Lacaille, JC. (2018). Astrocytes Detect and Upregulate Transmission at Inhibitory Synapses of Somatostatin Interneurons onto Pyramidal Cells. Nature Communications, 9(1).

Matsubara, JA, Barton, SM, Pham, W, Gore, JC, Janve, VA, McClure, R and Anderson, A. (2018). Lipopolysaccharide Induced Opening of the Blood Brain Barrier on Aging 5XFAD Mouse Model. Journal of Alzheimer's Disease, 67(2), 503–13.

Matsuda, N, Lu, H, Fukata, Y, Noritake, J, Gao, H, Mukherjee, S, Nemoto, T, Fukata, M and Poo, MM. (2009). Differential Activity-Dependent Secretion of Brain-Derived Neurotrophic Factor from Axon and Dendrite. Journal of Neuroscience, 29(45), 14185–98.

Mattson, MP and Chan, SL. (2003). Neuronal and Glial Calcium Signaling in Alzheimer's Disease. Cell Calcium, 34(4–5), 385–97.

McKhann, GM, Knopman, DS, Chertkow, H, Hyman, BT, Jack, CR, Kawas, CH, Klunk, WE, Koroshetz, WJ, Manly, JJ, Mayeux, R, Mohs, RC, Morris, JC, Rossor, MN, Scheltens, P, Carrillo, MC, Thies, B, Weintraub, S and Phelps, CH. (2011). The Diagnosis of Dementia Due to Alzheimer's Disease: Recommendations from the National Institute on Aging-Alzheimer's Association Workgroups on Diagnostic Guidelines for Alzheimer's Disease. Alzheimer's and Dementia, 7(3), 263–69.

Merighi, A. (2009). Neuropeptides and Coexistence. In Encyclopedia of Neuroscience, 843–49.

Merighi, A. (2018). Costorage of High Molecular Weight Neurotransmitters in Large Dense Core Vesicles of Mammalian Neurons. Frontiers in Cellular Neuroscience, 12.

Merkle, FT, Maroof, A, Wataya, T, Sasai, Y, Studer, L, Eggan, K and Schier, AF. (2015). Generation of Neuropeptidergic Hypothalamic Neurons from Human Pluripotent Stem Cells. Development (Cambridge), 142(4), 633–43.

Mesquita, SD, Ferreira, AC, Falcao, AM, Sousa, JC, Oliveira, TG, Correia-Neves, M, Sousa, N, Marques, F and Palha, JA. (2014). Lipocalin 2 Modulates the Cellular Response to Amyloid Beta. Cell death and differentiation, 21(10), 1588–99.

Meyer-Lindenberg, A, Domes, G, Kirsch, P and Heinrichs, M. (2011). Oxytocin and Vasopressin in the Human Brain: Social Neuropeptides for Translational Medicine. Nature Reviews Neuroscience, 12(9), 524–38.

Mi, W, Jung, SS, Yu, H, Schmidt, SD, Nixon, RA, Mathews, PM, Tagliavini, F and Levy, E. (2009). Complexes of Amyloid-β and Cystatin C in the Human Central Nervous System. Journal of Alzheimer's Disease, 18(2), 273–80.

Mirzaei, N, Tang, SP, Ashworth, S, Coello, C, Plisson, C, Passchier, J, Selvaraj, V, Tyacke, RJ, Nutt, DJ and Sastre, M. (2016). In Vivo Imaging of Microglial Activation by Positron Emission Tomography with [11C] PBR28 in the 5XFAD Model of Alzheimer's Disease. GLIA, 64(6), 993–1006.

Mittelsteadt, T, Seifert, G, Alvárez-Barón, E, Steinhäuser, C, Becker, AJ and Schoch, S. (2009). Differential MRNA Expression Patterns of the Synaptotagmin Gene Family in the Rodent Brain. Journal of Comparative Neurology, 512(4), 514–28.

Molinuevo, JL, Ayton, S, Batrla, R, Bednar, MM, Bittner, T, Cummings, J, Fagan, AM, Hampel, H, Mielke, MM, Mikulskis, A, O'Bryant, S, Scheltens, P, Sevigny, J, Shaw, LM, Soares, HD, Tong, G, Trojanowski, JQ, Zetterberg, H and Blennow, K. (2018). Current State of Alzheimer's Fluid Biomarkers. Acta Neuropathologica, 136(6), 821–53.

Montana, V, Liu, W, Mohideen, U and Parpura, V. (2009). Single Molecule Measurements of Mechanical Interactions within Ternary SNARE Complexes and Dynamics of Their Disassembly: SNAP25 vs. SNAP23. Journal of Physiology, 587(9), 1943–60.

Montero-Hadjadje, M, Vaingankar, S, Elias, S, Tostivint, H, Mahata, SK and Anouar, Y. (2008). Chromogranins A and B and Secretogranin II: Evolutionary and Functional Aspects. In Acta Physiologica, 309–24.

Morciano, M, Beckhaus, T, Karas, M, Zimmermann, H and Volknandt, W. (2009). The Proteome of the Presynaptic Active Zone: From Docked Synaptic Vesicles to Adhesion Molecules and Maxi-Channels. Journal of Neurochemistry, 108(3), 662–75.

Moreno-Jiménez, EP, Flor-García, M, Terreros-Roncal, J, Rábano, A, Cafini, F, Pallas-Bazarra, N, Ávila, J and Llorens-Martín, M. (2019). Adult Hippocampal Neurogenesis Is Abundant in Neurologically Healthy Subjects and Drops Sharply in Patients with Alzheimer's Disease. Nature Medicine, 25(4), 554–60.

Moreth, J, Kroker, KS, Schwanzar, D, Schnack, C, Arnim, C a F Von, Hengerer, B, Rosenbrock, H and Kussmaul, L. (2013). Globular and ProtofIbrillar Aβ Aggregates Impair Neurotransmission by Different Mechanisms.

Morris, JC. (1997). Clinical Dementia Rating: A Reliable and Valid Diagnostic and Staging Measure for Dementia of the Alzheimer Type. In International Psychogeriatrics, 173–76.

Morris, JC. (2005). Early-Stage and Preclinical Alzheimer Disease. Alzheimer Disease and Associated Disorders, 19(3), 163–65.

Nagahara, AH, Merrill, DA, Coppola, G, Tsukada, S, Schroeder, BE, Shaked, GM, Wang, L, Blesch, A, Kim, A, Conner, JM, Rockenstein, E, Chao, M V., Koo, EH, Geschwind, D, Masliah, E, Chiba, AA and Tuszynski, MH. (2009). Neuroprotective Effects of Brain-Derived Neurotrophic Factor in Rodent and Primate Models of Alzheimer's Disease. Nature Medicine, 15(3), 331–37.

Nakabeppu, Y and Ninomiya, T. (2019). Advances in Experimental Medicine and Biology Diabetes Mellitus A Risk Factor for Alzheimer's Disease.

Nakamura, A, Kaneko, N, Villemagne, VL, Kato, T, Doecke, J, Doré, V, Fowler, C, Li, QX, Martins, R, Rowe, C, Tomita, T, Matsuzaki, K, Ishii, K, Ishii, K, Arahata, Y, Iwamoto, S, Ito, K, Tanaka, K, Masters, CL et al. (2018). High Performance Plasma Amyloid-β Biomarkers for Alzheimer's Disease. Nature, 554(7691), 249–54.

Nässel, DR. (2009). Neuropeptide Signaling near and Far: How Localized and Timed Is the Action of Neuropeptides in Brain Circuits? Invertebrate Neuroscience, 9(2), 57–75.

Naudé, PJW, Nyakas, C, Eiden, LE, Ait-Ali, D, van der Heide, R, Engelborghs, S, Luiten, PGM, De Deyn, PP, den Boer, JA and Eisel, ULM. (2012). Lipocalin 2: Novel Component of Proinflammatory Signaling in Alzheimer's Disease. The FASEB Journal, 26(7), 2811–23.

Navarrete, M and Araque, A. (2010). Endocannabinoids Potentiate Synaptic Transmission through Stimulation of Astrocytes. Neuron, 68(1), 113–26.

Nett, WJ, Oloff, SH and Mccarthy, KD. (2002). Hippocampal Astrocytes in Situ Exhibit Calcium Oscillations That Occur Independent of Neuronal Activity. Journal of Neurophysiology, 87(1), 528–37.

Ng, F and Tang, BL. (2016). Unconventional Protein Secretion in Animal Cells. In Methods in Molecular Biology, Humana Press, New York, NY, 31–46.

Nilsen, LH, Melø, TM, Sæther, O, Witter, MP and Sonnewald, U. (2012). Altered Neurochemical Profile in the McGill-R-Thy1-APP Rat Model of Alzheimer's Disease: A Longitudinal in Vivo1H MRS Study. Journal of Neurochemistry, 123(4), 532–41.

Niswender, CM and Conn, PJ. (2010). Metabotropic Glutamate Receptors: Physiology, Pharmacology, and Disease. Annual Review of Pharmacology and Toxicology, 50(1), 295–322.

Nixon, RA. (2013). The Role of Autophagy in Neurodegenerative Disease. Nature Medicine, 19(8), 983–97.

Noble, EE, Hahn, JD, Konanur, VR, Hsu, TM, Page, SJ, Cortella, AM, Liu, CM, Song, MY, Suarez, AN, Szujewski, CC, Rider, D, Clarke, JE, Darvas, M, Appleyard, SM and Kanoski, SE. (2018). Control of Feeding Behavior by Cerebral Ventricular Volume Transmission of Melanin-Concentrating Hormone. Cell Metabolism, 28(1), 55-68. e7.

Nobuta, H, Ghiani, CA, Paez, PM, Spreuer, V, Dong, H, Korsak, RA, Manukyan, A, Li, J, Vinters, H V, Huang, EJ, Rowitch, DH, Sofroniew, M V, Campagnoni, AT, de Vellis, J and Waschek, JA. (2012). STAT3-Mediated Astrogliosis Protects Myelin Development in Neonatal Brain Injury. Annals of neurology, 72(5), 750–65.

Nusbaum, MP and Blitz, DM. (2012). Neuropeptide Modulation of Microcircuits. Current Opinion in Neurobiology, 22(4), 592–601.

Nusbaum, MP, Blitz, DM and Marder, E. (2017). Functional Consequences of Neuropeptide and Small-Molecule Co-Transmission. Nature Reviews Neuroscience, 18(7), 389–403.

Oakley, H, Cole, SL, Logan, S, Maus, E, Shao, P, Craft, J, Guillozet-Bongaarts, A, Ohno, M, Disterhoft, J, Van Eldik, L, Berry, R and Vassar, R. (2006). Intraneuronal Beta-Amyloid Aggregates, Neurodegeneration, and Neuron Loss in Transgenic Mice with Five Familial Alzheimer's Disease Mutations: Potential Factors in Amyloid Plaque Formation. Journal of Neuroscience, 26(40), 10129–40.

Oddo, S, Caccamo, A, Shepherd, JD, Murphy, MP, Golde, TE, Kayed, R, Metherate, R, Mattson, MP, Akbari, Y and LaFerla, FM. (2003). Triple-Transgenic Model of Alzheimer's Disease with Plaques and Tangles: Intracellular Aβ and Synaptic Dysfunction. Neuron, 39(3), 409–21.

Oheim, M, Schmidt, E and Hirrlinger, J. (2018). Local Energy on Demand: Are "Spontaneous" Astrocytic Ca2+-Microdomains the Regulatory Unit for Astrocyte-Neuron Metabolic Cooperation? Brain Research Bulletin, 136, 54–64.

Öhrfelt, A, Brinkmalm, A, Dumurgier, J, Brinkmalm, G, Hansson, O, Zetterberg, H, Bouaziz-Amar, E, Hugon, J, Paquet, C and Blennow, K. (2016). The Pre-Synaptic Vesicle Protein Synaptotagmin Is a Novel Biomarker for Alzheimer's Disease. Alzheimer's Research and Therapy, 8(1), 1–10.

Okada, S, Nakamura, M, Katoh, H, Miyao, T, Shimazaki, T, Ishii, K, Yamane, J, Yoshimura, A, Iwamoto, Y, Toyama, Y and Okano, H. (2006). Conditional Ablation of Stat3 or Socs3 Discloses a Dual Role for Reactive Astrocytes after Spinal Cord Injury. Nature Medicine, 12(7), 829–34.

Olabarria, M, Noristani, HN, Verkhratsky, A and Rodríguez, JJ. (2010). Concomitant Astroglial Atrophy and Astrogliosis in a Triple Transgenic Animal Model of Alzheimer's Disease. GLIA, 58(7), 831–38.

Otsu, Y, Couchman, K, Lyons, DG, Collot, M, Agarwal, A, Mallet, JM, Pfrieger, FW, Bergles, DE and Charpak, S. (2015). Calcium Dynamics in Astrocyte Processes during Neurovascular Coupling. Nature Neuroscience, 18(2), 210–18.

Ovsepian, S V. (2017). The Birth of the Synapse. Brain Structure and Function, 222(8), 3369–74.

Paco, S, Margelí, MA, Olkkonen, VM, Imai, A, Blasi, J, Fischer-Colbrie, R and Aguado, F. (2009). Regulation of Exocytotic Protein Expression and Ca2+-Dependent Peptide Secretion in Astrocytes. Journal of Neurochemistry, 110(1), 143–56.

Paco, S, Pozas, E and Aguado, F. (2010). Secretogranin III Is an Astrocyte Granin That Is Overexpressed in Reactive Glia. Cerebral cortex, 20(6), 1386–97.

Palygin, O, Lalo, U, Verkhratsky, A and Pankratov, Y. (2010). Ionotropic NMDA and P2X1/5 Receptors Mediate Synaptically Induced Ca2+ Signalling in Cortical Astrocytes. Cell Calcium, 48(4), 225–31.

Pankratov, Y and Lalo, U. (2014). Calcium Permeability of Ligand-Gated Ca2+ Channels. European Journal of Pharmacology, 739(C), 60–73.

Park, H, Li, Y and Tsien, RW. (2012). Influence of Synaptic Vesicle Position on Release Probability and Exocytotic Fusion Mode. Science, 335, 1362–66.

Park, H and Poo, M ming. (2013). Neurotrophin Regulation of Neural Circuit Development and Function. Nature Reviews Neuroscience, 14(1), 7–23.

Parpura, V, Grubišic, V and Verkhratsky, A. (2011). Ca2+ Sources for the Exocytotic Release of Glutamate from Astrocytes. Biochimica et Biophysica Acta - Molecular Cell Research, 1813(5), 984–91.

Parpura, V and Zorec, R. (2010). Gliotransmission: Exocytotic Release from Astrocytes. Brain Research Reviews, 63(1–2), 83–92.

Pascual, O, Casper, K, Kubera, C, … JZ and 2005, U. (2005). Astrocytic Purinergic Signaling Coordinates Synaptic Networks. Science.

Pekny, M, Wilhelmsson, U and Pekna, M. (2014). The Dual Role of Astrocyte Activation and Reactive Gliosis. Neuroscience Letters, 565, 30–38.

Penna, E, Cerciello, A, Chambery, A, Russo, R, Cernilogar, FM, Pedone, EM, Perrone-Capano, C, Cappello, S, Di Giaimo, R and Crispino, M. (2019). Cystatin B Involvement in Synapse Physiology of Rodent Brains and Human Cerebral Organoids. Frontiers in Molecular Neuroscience, 12.

Perea, G, Navarrete, M and Araque, A. (2009). Tripartite Synapses: Astrocytes Process and Control Synaptic Information. Trends in Neurosciences, 32(8), 421–31.

Perea, G, Sur, M and Araque, A. (2014). Neuron-Glia Networks: Integral Gear of Brain Function. Frontiers in Cellular Neuroscience, 8(November), 1–8.

Pereda, AE. (2014). Electrical Synapses and Their Functional Interactions with Chemical Synapses. Nature Reviews Neuroscience, 15(4), 250–63.

Perego, C, Vanoni, C, Bossi, M, Massari, S, Basudev, H, Longhi, R and Pietrini, G. (2000). The GLT-1 and GLAST Glutamate Transporters Are Expressed on Morphologically Distinct Astrocytes and Regulated by Neuronal Activity in Primary Hippocampal Cocultures. Journal of Neurochemistry, 75(3), 1076–84.

Perneczky, R, Wagenpfeil, S, Komossa, K, Grimmer, T, Diehl, J and Kurz, A. (2006). Mapping Scores onto Stages: Mini-Mental State Examination and Clinical Dementia Rating. American Journal of Geriatric Psychiatry, 14(2), 139–44.

Persoon, CM, Moro, A, Nassal, JP, Farina, M, Broeke, JH, Arora, S, Dominguez, N, van Weering, JR, Toonen, RF and Verhage, M. (2018). Pool Size Estimations for Dense-core Vesicles in Mammalian CNS Neurons. The EMBO Journal, 37(20), e99672.

Petr, GT, Sun, Y, Frederick, NM, Zhou, Y, Dhamne, SC, Hameed, MQ, Miranda, C, Bedoya, EA, Fischer, KD, Armsen, W, Wang, J, Danbolt, NC, Rotenberg, A, Aoki, CJ and Rosenberg, PA. (2015). Conditional Deletion of the Glutamate Transporter GLT-1 Reveals That Astrocytic GLT-1 Protects against Fatal Epilepsy While Neuronal GLT-1 Contributes Significantly to Glutamate Uptake into Synaptosomes. Journal of Neuroscience, 35(13), 5187–5201.

Pickett, LA, Yourshaw, M, Albornoz, V, Chen, Z, Solorzano-Vargas, RS, Nelson, SF, Martín, MG and Lindberg, I. (2013). Functional Consequences of a Novel Variant of PCSK1. PloS one, 8(1), e55065.

De Pins, B, Cifuentes-Díaz, C, Thamila Farah, A, López-Molina, L, Montalban, E, Sancho-Balsells, A, López, A, Ginés, S, Delgado-García, JM, Alberch, J, Gruart, A, Girault, JA and Giralt, A. (2019). Conditional BDNF Delivery from Astrocytes Rescues Memory Deficits, Spine Density, and Synaptic Properties in the 5xFAD Mouse Model of Alzheimer Disease. Journal of Neuroscience, 39(13), 2441–58.

Plá, V, Barranco, N, Pozas, E and Aguado, F. (2017). Amyloid-β Impairs Vesicular Secretion in Neuronal and Astrocyte Peptidergic Transmission. Frontiers in Molecular Neuroscience, 10(June), 1–15.

Plá, V, Paco, S, Ghezali, G, Ciria, V, Pozas, E, Ferrer, I and Aguado, F. (2013). Secretory Sorting Receptors Carboxypeptidase E and Secretogranin III in Amyloid β-Associated Neural Degeneration in Alzheimer's Disease. Brain pathology (Zurich, Switzerland), 23(3), 274–84.

van den Pol, AN. (2012). Neuropeptide Transmission in Brain Circuits. Neuron, 76(1), 98–115.

Pontecorvo, MJ, Devous, MD, Kennedy, I, Navitsky, M, Lu, M, Galante, N, Salloway, S, Doraiswamy, PM, Southekal, S, Arora, AK, McGeehan, A, Lim, NC, Xiong, H, Truocchio, SP, Joshi, AD, Shcherbinin, S, Teske, B, Fleisher, AS and Mintun, MA. (2019). A Multicentre Longitudinal Study of Flortaucipir (18F) in Normal Ageing, Mild Cognitive Impairment and Alzheimer's Disease Dementia. Brain: a journal of neurology, 142(6), 1723–35.

Poo, M ming. (2001). Neurotrophins as Synaptic Modulators. Nature Reviews Neuroscience, 2(1), 24–32.

Poon, WW, Blurton-Jones, M, Tu, CH, Feinberg, LM, Chabrier, MA, Harris, JW, Jeon, NL and Cotman, CW. (2011). β-Amyloid Impairs Axonal BDNF Retrograde Trafficking. Neurobiology of Aging, 32(5), 821–33.

Porter, JT and McCarthy, KD. (1995). Adenosine Receptors Modulate [Ca2+] i in Hippocampal Astrocytes in Situ. Journal of Neurochemistry, 65(4), 1515–23.

Potokar, M, Stenovec, M, Gabrijel, M, Li, L, Kreft, M, Grilc, S, Pekny, M and Zorec, R. (2010). Intermediate Filaments Attenuate Stimulation-Dependent Mobility of Endosomes/Lysosomes in Astrocytes. GLIA, 58(10), 1208–19.

Potokar, M, Vardjan, N, Stenovec, M, Gabrijel, M, Trkov, S, Jorgačevski, J, Kreft, M and Zorec, R. (2013). Astrocytic Vesicle Mobility in Health and Disease. International Journal of Molecular Sciences, 14(6), 11238–58.

Potter, LR, Yoder, AR, Flora, DR, Antos, LK and Dickey, DM. (2009). Natriuretic Peptides: Their Structures, Receptors, Physiologic Functions and Therapeutic Applications. In Handbook of Experimental Pharmacology, Springer, Berlin, Heidelberg, 341–66.

Prada, I, Marchaland, J, Podini, P, Magrassi, L, D'Alessandro, R, Bezzi, P and Meldolesi, J. (2011). REST/NRSF Governs the Expression of Dense-Core Vesicle Gliosecretion in Astrocytes. The Journal of cell biology, 193(3), 537–49.

Prescott, JW. (2013). Quantitative Imaging Biomarkers: The Application of Advanced Image Processing and Analysis to Clinical and Preclinical Decision Making. Journal of Digital Imaging, 26(1), 97–108.

Pugazhenthi, S. (2017). Metabolic Syndrome and the Cellular Phase of Alzheimer's Disease. In Progress in Molecular Biology and Translational Science, Elsevier B.V., 243–58.

Qu, L, Akbergenova, Y, Hu, Y and Schikorski, T. (2009). Synapse-to-Synapse Variation in Mean Synaptic Vesicle Size and Its Relationship with Synaptic Morphology and Function. Journal of Comparative Neurology, 514(4), 343–52.

Rajkowska, G, Miguel-Hidalgo, JJ, Makkos, Z, Meltzer, H, Overholser, J and Stockmeier, C. (2002). Layer-Specific Reductions in GFAP-Reactive Astroglia in the Dorsolateral Prefrontal Cortex in Schizophrenia. Schizophrenia Research, 57(2–3), 127–38.

Ramamoorthy, P and Whim, MD. (2008). Trafficking and Fusion of Neuropeptide Y-Containing Dense-Core Granules in Astrocytes. Journal of Neuroscience, 28(51), 13815–27.

Regehr, WG, Carey, MR and Best, AR. (2009). Activity-Dependent Regulation of Synapses by Retrograde Messengers. Neuron, 63(2), 154–70.

Reiber, H. (2016). Knowledge-Base for Interpretation of Cerebrospinal Fluid Data Patterns. Essentials in Neurology and Psychiatry. Arquivos de Neuro-Psiquiatria, 74(6), 501–12.

Reichardt, LF. (2006). Neurotrophin-Regulated Signalling Pathways. Philosophical Transactions of the Royal Society B: Biological Sciences, 361(1473), 1545–64.

Ren, J, Qin, C, Hu, F, Tan, J, Qiu, L, Zhao, S, Feng, G and Luo, M. (2011). Habenula "Cholinergic" Neurons Corelease Glutamate and Acetylcholine and Activate Postsynaptic Neurons via Distinct Transmission Modes. Neuron, 69(3), 445–52.

Ribe, EM, Serrano-Saiz, E, Akpan, N and Troy, CM. (2008). Mechanisms of Neuronal Death in Disease: Defining the Models and the Players. Biochemical Journal, 415(2), 165–82.

Riedel, BC, Thompson, PM and Brinton, RD. (2016). Age, APOE and Sex: Triad of Risk of Alzheimer's Disease. Journal of Steroid Biochemistry and Molecular Biology, 160, 134–47.

Rizo, J and Xu, J. (2015). The Synaptic Vesicle Release Machinery. Annual Review of Biophysics, 44(1), 339–67.

Rizzoli, SO. (2014). Synaptic Vesicle Recycling: Steps and Principles. The EMBO Journal, 33(8), 788–822.

Rizzoli, SO and Jahn, R. (2007). Kiss-and-Run, Collapse and "readily Retrievable" Vesicles. Traffic, 8(9), 1137–44.

Rizzuto, R, De Stefani, D, Raffaello, A and Mammucari, C. (2012). Mitochondria as Sensors and Regulators of Calcium Signalling. Nature Reviews Molecular Cell Biology, 13(9), 566–78.

Rodríguez-Arellano, JJ, Parpura, V, Zorec, R and Verkhratsky, A. (2016). Astrocytes in Physiological Aging and Alzheimer's Disease. Neuroscience, 323, 170–82.

Rungta, RL, Bernier, LP, Dissing-Olesen, L, Groten, CJ, LeDue, JM, Ko, R, Drissler, S and MacVicar, BA. (2016). Ca2+ Transients in Astrocyte Fine Processes Occur via Ca2+ Influx in the Adult Mouse Hippocampus. GLIA, 64(12), 2093–2103.

Sadleir, KR, Popovic, J and Vassar, R. (2018). ER Stress Is Not Elevated in the 5XFAD Mouse Model of Alzheimer's Disease. Journal of Biological Chemistry, 293(48), 18434–43.

Sah, R and Geracioti, TD. (2013). Neuropeptide y and Posttraumatic Stress Disorder. Molecular Psychiatry, 18(6), 646–55.

Saito, T, Iwata, N, Tsubuki, S, Takaki, Y, Takano, J, Huang, SM, Suemoto, T, Higuchi, M and Saido, TC. (2005). Somatostatin Regulates Brain Amyloid β Peptide Aβ42 through Modulation of Proteolytic Degradation. Nature Medicine, 11(4), 434–39.

Sakuragi, S, Niwa, F, Oda, Y, Mikoshiba, K and Bannai, H. (2017). Astroglial Ca2+ Signaling Is Generated by the Coordination of IP3R and Store-Operated Ca2+ Channels. Biochemical and Biophysical Research Communications, 486(4), 879–85.

Salio, C, Averill, S, Priestley, J V. and Merighi, A. (2007). Costorage of BDNF and Neuropeptides within Individual Dense-Core Vesicles in Central and Peripheral Neurons. Developmental Neurobiology, 67(3), 326–38.

Salta, E and De Strooper, B. (2017). MicroRNA-132: A Key Noncoding RNA Operating in the Cellular Phase of Alzheimer's Disease. FASEB Journal, 31(2), 424–33.

Santello, M, Calì, C and Bezzi, P. (2012). Gliotransmission and the Tripartite Synapse. Advances in Experimental Medicine and Biology, 970, 307–31.

Santo-Domingo, J and Demaurex, N. (2010). Calcium Uptake Mechanisms of Mitochondria. Biochimica et Biophysica Acta - Bioenergetics, 1797(6–7), 907–12.

Sasaguri, H, Nilsson, P, Hashimoto, S, Nagata, K, Saito, T, De Strooper, B, Hardy, J, Vassar, R, Winblad, B and Saido, TC. (2017). APP Mouse Models for Alzheimer's Disease Preclinical Studies. The EMBO Journal,, e201797397.

Sato, C, Barthélemy, NR, Mawuenyega, KG, Patterson, BW, Gordon, BA, Jockel-Balsarotti, J, Sullivan, M, Crisp, MJ, Kasten, T, Kirmess, KM, Kanaan, NM, Yarasheski, KE, Baker-Nigh, A, Benzinger, TLS, Miller, TM, Karch, CM and Bateman, RJ. (2018). Tau Kinetics in Neurons and the Human Central Nervous System. Neuron, 97(6), 1284-1298.e7.

Savtchouk, I and Volterra, A. (2018). Gliotransmission: Beyond Black-and-White. Journal of Neuroscience, 38(1), 14–25.

Scemes, E, Suadicani, SO, Dahl, G and Spray, DC. (2007). Connexin and Pannexin Mediated Cell-Cell Communication. Neuron Glia Biology, 3(3), 199–208.

Scheff, SW, Price, DA, Schmitt, FA, Dekosky, ST and Mufson, EJ. (2007). Synaptic Alterations in CA1 in Mild Alzheimer Disease and Mild Cognitive Impairment. Neurology, 68(18), 1501–8.

Scheff, SW, Price, DA, Schmitt, FA and Mufson, EJ. (2006). Hippocampal Synaptic Loss in Early Alzheimer's Disease and Mild Cognitive Impairment. Neurobiology of aging, 27(10), 1372–84.

Schneider, F, Baldauf, K, Wetzel, W and Reymann, KG. (2014). Behavioral and EEG Changes in Male 5xFAD Mice. Physiology and Behavior, 135, 25–33.

Schrimpf, SP, Meskenaite, V, Brunner, E, Rutishauser, D, Walther, P, Eng, J, Aebersold, R and Sonderegger, P. (2005). Proteomic Analysis of Synaptosomes Using Isotope-Coded Affinity Tags and Mass Spectrometry. Proteomics, 5(10), 2531–41.

Schwarz, Y, Zhao, N, Kirchhoff, F and Bruns, D. (2017). Astrocytes Control Synaptic Strength by Two Distinct V-SNARE-Dependent Release Pathways. Nature Neuroscience, 20(11), 1529–39.

Scuderi, C, Stecca, C, Iacomino, A and Steardo, L. (2013). Role of Astrocytes in Major Neurological Disorders: The Evidence and Implications. IUBMB Life, 65(12), 957–61.

Seidah, NG, Mayer, G, Zaid, A, Rousselet, E, Nassoury, N, Poirier, S, Essalmani, R and Prat, A. (2008). The Activation and Physiological Functions of the Proprotein Convertases. International Journal of Biochemistry and Cell Biology, 40(6–7), 1111–25.

Seifert, B, Eckenstaler, R, Ronicke, R, Leschik, J, Lutz, B, Reymann, K, Lessmann, V and Brigadski, T. (2016). Amyloid-Beta Induced Changes in Vesicular Transport of BDNF in Hippocampal Neurons. Neural Plasticity, 2016.

Selkoe, DJ. (2002). Alzheimer's Disease Is a Synaptic Failure. Science (New York, N.Y.), 298(5594), 789–91.

Selkoe, DJ and Hardy, J. (2016). The Amyloid Hypothesis of Alzheimer's Disease at 25 Years. EMBO Molecular Medicine, 8(6), 595–608.

Semyanov, A. (2019). Spatiotemporal Pattern of Calcium Activity in Astrocytic Network. Cell Calcium, 78, 15–25.

Sen, T, Saha, P, Gupta, R, Foley, LM, Jiang, T, Abakumova, OS, Hitchens, KT and Sen, N. (2019). Aberrant ER-Stress Induced Neuronal-IFNβ Elicits White Matter Injury Due to Microglial Activation and T-Cell Infiltration after TBI. The Journal of Neuroscience, 0718–19.

Shahpasand, K, Uemura, I, Saito, T, Asano, T, Hata, K, Shibata, K, Toyoshima, Y, Hasegawa, M and Hisanaga, SI. (2012). Regulation of Mitochondrial Transport and Inter-Microtubule Spacing by Tau Phosphorylation at the Sites Hyperphosphorylated in Alzheimer's Disease. Journal of Neuroscience, 32(7), 2430–41.

Sheng, L, Chen, M, Cai, K, Song, Y, Yu, D, Zhang, H and Xu, G. (2019). Microglial Trem2 Induces Synaptic Impairment at Early Stage and Prevents Amyloidosis at Late Stage in APP/PS1 Mice. FASEB journal: official publication of the Federation of American Societies for Experimental Biology, 33(9), 10425–42.

Sheridan, GK and Murphy, KJ. (2013). Neuron-Glia Crosstalk in Health and Disease: Fractalkine and CX3CR1 Take Centre Stage. Open Biology, 3(1 DEC).

Sherwood, MW, Arizono, M, Hisatsune, C, Bannai, H, Ebisui, E, Sherwood, JL, Panatier, A, Oliet, SHR and Mikoshiba, K. (2017). Astrocytic IP3Rs: Contribution to Ca2+ Signalling and Hippocampal LTP. GLIA, 65(3), 502–13.

Shigetomi, E, Saito, K, Sano, F and Koizumi, SC. (2019). Aberrant Calcium Signals in Reactive Astrocytes: A Key Process in Neurological Disorders. International Journal of Molecular Sciences, 20(4).

Shin, W, Ge, L, Arpino, G, Villarreal, SA, Hamid, E, Liu, H, Zhao, WD, Wen, PJ, Chiang, HC and Wu, LG. (2018). Visualization of Membrane Pore in Live Cells Reveals a Dynamic-Pore Theory Governing Fusion and Endocytosis. Cell, 173(4), 934-945.e12.

Shin, YH, Lee, SJ and Jung, J. (2012). Secretion of ATP from Schwann Cells through Lysosomal Exocytosis during Wallerian Degeneration. Biochemical and Biophysical Research Communications, 429(3–4), 163–67.

Siedlak, SL, Jiang, Y, Huntley, ML, Wang, L, Gao, J, Xie, F, Liu, J, Su, B, Perry, G and Wang, X. (2017). TMEM230 Accumulation in Granulovacuolar Degeneration Bodies and Dystrophic Neurites of Alzheimer's Disease. Journal of Alzheimer's Disease, 58(4), 1027–33.

Simard, M and Nedergaard, M. (2004). The Neurobiology of Glia in the Context of Water and Ion Homeostasis. Neuroscience, 129(4), 877–96.

Simon, E, Obst, J and Gomez-Nicola, D. (2019). The Evolving Dialogue of Microglia and Neurons in Alzheimer's Disease: Microglia as Necessary Transducers of Pathology. Neuroscience, 405, 24–34.

Simon, MJ and Iliff, JJ. (2016). Regulation of Cerebrospinal Fluid (CSF) Flow in Neurodegenerative, Neurovascular and Neuroinflammatory Disease. Biochimica et Biophysica Acta - Molecular Basis of Disease, 1862(3), 442–51.

Simonsen, AH, McGuire, J, Podust, VN, Hagnelius, NO, Nilsson, TK, Kapaki, E, Vassilopoulos, D and Waldemar, G. (2007). A Novel Panel of Cerebrospinal Fluid Biomarkers for the Differential Diagnosis of Alzheimer's Disease versus Normal Aging and Frontotemporal Dementia. Dementia and geriatric cognitive disorders, 24(6), 434–40.

Sims, R, Van Der Lee, SJ, Naj, AC, Bellenguez, C, Badarinarayan, N, Jakobsdottir, J, Kunkle, BW, Boland, A, Raybould, R, Bis, JC, Martin, ER, Grenier-Boley, B, Heilmann-Heimbach, S, Chouraki, V, Kuzma, AB, Sleegers, K, Vronskaya, M, Ruiz, A, Graham, RR et al. (2017). Rare Coding Variants in PLCG2, ABI3, and TREM2 Implicate Microglial-Mediated Innate Immunity in Alzheimer's Disease. Nature Genetics, 49(9), 1373–84.

Sochocka, M, Zwolińska, K and Leszek, J. (2017). The Infectious Etiology of Alzheimer's Disease. Current Neuropharmacology, 15(7), 996–1009. Son, SM, Nam, DW, Cha, MY, Kim, KH, Byun, J, Ryu, H and Mook-Jung, I. (2015). Thrombospondin-1 Prevents Amyloid Beta-Mediated Synaptic Pathology in Alzheimer's Disease. Neurobiology of Aging, 36(12), 3214–27.

Sosa, MAG, De Gasperi, R and Elder, GA. (2012). Modeling Human Neurodegenerative Diseases in Transgenic Systems. Hum Genet, 131, 535–63.

Souza, DG, Almeida, RF, Souza, DO and Zimmer, ER. (2019). The Astrocyte Biochemistry. Seminars in Cell and Developmental Biology.

Spangenberg, EE, Lee, RJ, Najafi, AR, Rice, RA, Elmore, MRP, Blurton-Jones, M, West, BL and Green, KN. (2016). Eliminating Microglia in Alzheimer's Mice Prevents Neuronal Loss without Modulating Amyloid-β Pathology. Brain, 139(4), 1265–81.

Sperling, RA, Aisen, PS, Beckett, LA, Bennett, DA, Craft, S, Fagan, AM, Iwatsubo, T, Jack, CR, Kaye, J, Montine, TJ, Park, DC, Reiman, EM, Rowe, CC, Siemers, E, Stern, Y, Yaffe, K, Carrillo, MC, Thies, B, Morrison-Bogorad, M et al. (2011). Toward Defining the Preclinical Stages of Alzheimer's Disease: Recommendations from the National Institute on Aging-Alzheimer's Association Workgroups on Diagnostic Guidelines for Alzheimer's Disease. Alzheimer's and Dementia, 7(3), 280–92.

Stancu, IC, Ris, L, Vasconcelos, B, Marinangeli, C, Goeminne, L, Laporte, V, Haylani, LE, Couturier, J, Schakman, O, Gailly, P, Pierrot, N, Kienlen-Campard, P, Octave, JN and Dewachter, I. (2014). Tauopathy Contributes to Synaptic and Cognitive Deficits in a Murine Model for Alzheimer's Disease. FASEB Journal, 28(6), 2620–31.

Steinhoff, T, Moritz, E, Wollmer, MA, Mohajeri, MH, Kins, S and Nitsch, RM. (2001). Increased Cystatin C in Astrocytes of Transgenic Mice Expressing the K670N-M671L Mutation of the Amyloid Precursor Protein and Deposition in Brain Amyloid Plaques. Neurobiology of Disease, 8(4), 647–54.

Stenovec, M, Kreft, M, Grilc, S, Potokar, M, Kreft, ME, Pangršič, T and Zorec, R. (2007). Ca2+-Dependent Mobility of Vesicles Capturing Anti-VGLUT1 Antibodies. Experimental Cell Research, 313(18), 3809–18.

Sternson, SM. (2013). Hypothalamic Survival Circuits: Blueprints for Purposive Behaviors. Neuron, 77(5), 810–24.

Stevens, CF. (2003). Neurotransmitter Release at Central Synapses. Neuron, 40(2), 381–88.

De Strooper, B and Karran, E. (2016). The Cellular Phase of Alzheimer's Disease. Cell, 164(4), 603–15.

Suadicani, SO, Brosnan, CF and Scemes, E. (2006). P2X7 Receptors Mediate ATP Release and Amplification of Astrocytic Intercellular Ca2+ Signaling. Journal of Neuroscience, 26(5), 1378–85.

Südhof, TC. (2004). The Synaptic Vesicle Cycle. Annual Review of Neuroscience, 27(1), 509–47.

Südhof, TC. (2012). The Presynaptic Active Zone. Neuron, 75(1), 11–25.

Sun, BL, Li, WW, Zhu, C, Jin, WS, Zeng, F, Liu, YH, Bu, X Le, Zhu, J, Yao, XQ and Wang, YJ. (2018). Clinical Research on Alzheimer's Disease: Progress and Perspectives. Neuroscience Bulletin, 34(6), 1111–18.

Sun, MY, Devaraju, P, Xie, AX, Holman, I, Samones, E, Murphy, TR and Fiacco, TA. (2014). Astrocyte Calcium Microdomains Are Inhibited by Bafilomycin A1 and Cannot Be Replicated by Low-Level Schaffer Collateral Stimulation in Situ. Cell Calcium, 55(1), 1–16.

Suter, MR, Wen, YR, Decosterd, I and Ji, RR. (2007). Do Glial Cells Control Pain? Neuron Glia Biology, 3(3), 255–68.

Sutphen, CL, McCue, L, Herries, EM, Xiong, C, Ladenson, JH, Holtzman, DM and Fagan, AM. (2018). Longitudinal Decreases in Multiple Cerebrospinal Fluid Biomarkers of Neuronal Injury in Symptomatic Late Onset Alzheimer's Disease. Alzheimer's and Dementia, 14(7), 869–79.

Szaruga, M, Veugelen, S, Benurwar, M, Lismont, S, Sepulveda-Falla, D, Lleo, A, Ryan, NS, Lashley, T, Fox, NC, Murayama, S, Gijsen, H, De Strooper, B and Chávez-Gutiérrez, L. (2015). Qualitative Changes in Human γ-Secretase Underlie Familial Alzheimer's Disease. Journal of Experimental Medicine, 212(12), 2003–13.

Tabata, H. (2015). Diverse Subtypes of Astrocytes and Their Development during Corticogenesis. Frontiers in Neuroscience, 9(APR).

Takata, N, Mishima, T, Hisatsune, C, Nagai, T, Ebisui, E, Mikoshiba, K and Hirase, H. (2011). Astrocyte Calcium Signaling Transforms Cholinergic Modulation to Cortical Plasticity in Vivo. Journal of Neuroscience, 31(49), 18155–65.

Takeda, K and Akira, S. (2004). TLR Signaling Pathways. Seminars in Immunology, 16(1), 3–9.

Tan, JZA and Gleeson, PA. (2019). The Role of Membrane Trafficking in the Processing of Amyloid Precursor Protein and Production of Amyloid Peptides in Alzheimer's Disease. Biochimica et Biophysica Acta - Biomembranes, 1861(4), 697–712.

Tani, H, Dulla, CG, Farzampour, Z, Taylor-Weiner, A, Huguenard, JR and Reimer, RJ. (2014). A Local Glutamate-Glutamine Cycle Sustains Synaptic Excitatory Transmitter Release. Neuron, 81(4), 888–900.

Taraska, JW, Perrais, D, Ohara-Imaizumi, M, Nagamatsu, S and Almers, W. (2003). Secretory Granules Are Recaptured Largely Intact after Stimulated Exocytosis in Cultured Endocrine Cells. Proceedings of the National Academy of Sciences of the United States of America, 100(4), 2070–75.

Taupenot, L, Harper, KL and O'Connor, DT. (2003). The Chromogranin-Secretogranin Family. New England Journal of Medicine, 348(12), 1134–49.

Terry, RD. (2000). Cell Death or Synaptic Loss in Alzheimer Disease. Journal of Neuropathology and Experimental Neurology, 59(12), 1118–19.

Thrane, AS, Rangroo Thrane, V and Nedergaard, M. (2014). Drowning Stars: Reassessing the Role of Astrocytes in Brain Edema. Trends in Neurosciences, 37(11), 620–28.

Tian, GF, Azmi, H, Takano, T, Xu, Q, Peng, W, Lin, J, Oberheim, NA, Lou, N, Wang, X, Zielke, HR, Kang, J and Nedergaard, M. (2005). An Astrocytic Basis of Epilepsy. Nature Medicine, 11(9), 973–81.

Tible, M, Mouton Liger, F, Schmitt, J, Giralt, A, Farid, K, Thomasseau, S, Gourmaud, S, Paquet, C, Rondi Reig, L, Meurs, E, Girault, JA and Hugon, J. (2019). PKR Knockout in the 5xFAD Model of Alzheimer's Disease Reveals Beneficial Effects on Spatial Memory and Brain Lesions. Aging Cell, 18(3).

Tizon, B, Sahoo, S, Yu, H, Gauthier, S, Kumar, AR, Mohan, P, Figliola, M, Pawlik, M, Grubb, A, Uchiyama, Y, Bandyopadhyay, U, Cuervo, AM, Nixon, RA and Levy, E. (2010). Induction of Autophagy by Cystatin C: A Mechanism That Protects Murine Primary Cortical Neurons and Neuronal Cell Lines. PLoS ONE, 5(3).

Tönnies, E and Trushina, E. (2017). Oxidative Stress, Synaptic Dysfunction, and Alzheimer's Disease. Journal of Alzheimer's Disease, 57(4), 1105–21.

Tooze, J and Tooze, SA. (1986). Clathrin-Coated Vesicular Transport of Secretory Proteins during the Formation of ACTH-Containing Secretory Granules in AtT20 Cells. The Journal of cell biology, 103(3), 839–50.

Topalidou, I, Cattin-Ortolá, J, Pappas, AL, Cooper, K, Merrihew, GE, MacCoss, MJ and Ailion, M. (2016). The EARP Complex and Its Interactor EIPR-1 Are Required for Cargo Sorting to Dense-Core Vesicles. PLoS Genetics, 12(5).

Traynelis, SF, Wollmuth, LP, McBain, CJ, Menniti, FS, Vance, KM, Ogden, KK, Hansen, KB, Yuan, H, Myers, SJ and Dingledine, R. (2010). Glutamate Receptor Ion Channels: Structure, Regulation, and Function. Pharmacological Reviews, 62(3), 405–96.

Triantafilou, M and Triantafilou, K. (2002). Lipopolysaccharide Recognition: CD14, TLRs and the LPS-Activation Cluster. Trends in Immunology, 23(6), 301–4.

Tsuboi, T, McMahon, HT and Rutter, GA. (2004). Mechanisms of Dense Core Vesicle Recapture Following "Kiss and Run" ("cavicapture") Exocytosis in Insulin-Secreting Cells. Journal of Biological Chemistry, 279(45), 47115–24.

Unichenko, P, Myakhar, O and Kirischuk, S. (2012). Intracellular Na + Concentration Influences Short-Term Plasticity of Glutamate Transporter-Mediated Currents in Neocortical Astrocytes. GLIA, 60(4), 605–14.

Vaaga, CE, Borisovska, M and Westbrook, GL. (2014). Dual-Transmitter Neurons: Functional Implications of Co-Release and Co-Transmission. Current Opinion in Neurobiology, 29, 25–32.

Vaden, JH, Banumurthy, G, Gusarevich, ES, Overstreet-Wadiche, L and Wadiche, JI. (2019). The Readily-Releasable Pool Dynamically Regulates Multivesicular Release. eLife, 8.

Vardjan, N, Kreft, M and Zorec, R. (2014). Regulated Exocytosis in Astrocytes Is as Slow as the Metabolic Availability of Gliotransmitters: Focus on Glutamate and ATP. In Advances in Neurobiology, 81–101.

Vardjan, N, Parpura, V and Zorec, R. (2016). Loose Excitation-Secretion Coupling in Astrocytes. GLIA, 64(5), 655–67.

Vázquez-Martínez, R, Díaz-Ruiz, A, Almabouada, F, Rabanal-Ruiz, Y, Gracia-Navarro, F and Malagón, MM. (2012). Revisiting the Regulated Secretory Pathway: From Frogs to Human. General and Comparative Endocrinology, 175(1), 1–9.

Venturini, A, Passalacqua, M, Pelassa, S, Pastorino, F, Tedesco, M, Cortese, K, Gagliani, MC, Leo, G, Maura, G, Guidolin, D, Agnati, LF, Marcoli, M and Cervetto, C. (2019). Exosomes from Astrocyte Processes: Signaling to Neurons. Frontiers in pharmacology, 10, 1452.

Verderio, C, Cagnoli, C, Bergami, M, Francolini, M, Schenk, U, Colombo, A, Riganti, L, Frassoni, C, Zuccaro, E, Danglot, L, Wilhelm, C, Galli, T, Canossa, M and Matteoli, M. (2012). TI-VAMP/VAMP7 Is the SNARE of Secretory Lysosomes Contributing to ATP Secretion from Astrocytes. Biology of the Cell, 104(4), 213–28.

Verkhratsky, A. (2019). Astroglial Calcium Signaling in Aging and Alzheimer's Disease. Cold Spring Harbor Perspectives in Biology, 11(7), a035188.

Verkhratsky, A, Matteoli, M, Parpura, V, Mothet, JP and Zorec, R. (2016). Astrocytes as Secretory Cells of the Central Nervous System: Idiosyncrasies of Vesicular Secretion. The EMBO Journal, 35(3), 239–57.

Verkhratsky, A, Zorec, R and Parpura, V. (2017). Stratification of Astrocytes in Healthy and Diseased Brain. Brain Pathology, 27(5), 629–44.

Vinters, H V. (2015). Emerging Concepts in Alzheimer's Disease. Annual review of pathology, 10, 291–319.

Volk, L, Chiu, SL, Sharma, K and Huganir, RL. (2015). Glutamate Synapses in Human Cognitive Disorders. Annual Review of Neuroscience, 38(1), 127–49.

Volterra, A and Bezzi, P. (2002). Release of Transmitters from Glial Cells. In The Tripartite Synapse: Glia in Synaptic Transmission, eds. Volterra, A, Magistretti, PJ and Haydon, PG. Oxford: Oxford University Press, 164–184.

Wang, L, Benzinger, TL, Su, Y, Christensen, J, Friedrichsen, K, Aldea, P, McConathy, J, Cairns, NJ, Fagan, AM, Morris, JC and Ances, BM. (2016a). Evaluation of Tau Imaging in Staging Alzheimer Disease and Revealing Interactions between β-Amyloid and Tauopathy. JAMA Neurology, 73(9), 1070–77.

Wang, L, Guo, L, Lu, L, Sun, H, Shao, M, Beck, SJ, Li, L, Ramachandran, J, Du, Y and Du, H. (2016b). Synaptosomal Mitochondrial Dysfunction in 5xFAD Mouse Model of Alzheimer's Disease. PLoS ONE, 11(3).

Wang, TF, Zhou, C, Tang, AH, Wang, SQ and Chai, Z. (2006). Cellular Mechanism for Spontaneous Calcium Oscillations in Astrocytes. Acta Pharmacologica Sinica, 27(7), 861–68.

Waschek, JA. (2013). VIP and PACAP: Neuropeptide Modulators of CNS Inflammation, Injury, and Repair. British Journal of Pharmacology, 169(3), 512–23.

Wasmeier, C, Burgos, P V., Trudeau, T, Davidson, HW and Hutton, JC. (2005). An Extended Tyrosine-Targeting Motif for Endocytosis and Recycling of the Dense-Core Vesicle Membrane Protein Phogrin. Traffic, 6(6), 474–87.

Watanabe, S. (2015). Slow or Fast? A Tale of Synaptic Vesicle Recycling: A New Model Accounts for Synaptic Transmission Speed. Science, 350(6256), 46–47.

Watanabe, S and Boucrot, E. (2017). Fast and Ultrafast Endocytosis. Current Opinion in Cell Biology, 47, 64–71.

Watanabe, S, Rost, BR, Camacho-Pérez, M, Davis, MW, Söhl-Kielczynski, B, Rosenmund, C and Jorgensen, EM. (2013). Ultrafast Endocytosis at Mouse Hippocampal Synapses. Nature, 504(7479), 242–47.

van Weering, JRT and Scheper, W. (2019). Endolysosome and Autolysosome Dysfunction in Alzheimer's Disease: Where Intracellular and Extracellular Meet. CNS Drugs, 33(7), 639–48.

Wen, D, Xue, Y, Liang, K, Yuan, T, Lu, J, Zhao, W, Xu, T and Chen, L. (2012). Bulk-like Endocytosis Plays an Important Role in the Recycling of Insulin Granules in Pancreatic Beta Cells. Protein and Cell, 3(8), 618–26.

Whittaker, VP. (1993). Thirty Years of Synaptosome Research. Journal of Neurocytology, 22(9), 735–42.

Wiersma, VI and Scheper, W. (2019). Granulovacuolar Degeneration Bodies: Red Alert for Neurons with MAPT/Tau Pathology. Autophagy.

Wiersma, VI, van Ziel, AM, Vazquez-Sanchez, S, Nölle, A, Berenjeno-Correa, E, Bonaterra-Pastra, A, Clavaguera, F, Tolnay, M, Musters, RJP, van Weering, JRT, Verhage, M, Hoozemans, JJM and Scheper, W. (2019). Granulovacuolar Degeneration Bodies Are Neuron-Selective Lysosomal Structures Induced by Intracellular Tau Pathology. Acta Neuropathologica,, 1–28.

Wilhelm, A, Volknandt, W, Langer, D, Nolte, C, Kettenmann, H and Zimmermann, H. (2004). Localization of SNARE Proteins and Secretory Organelle Proteins in Astrocytes in Vitro and in Situ. Neuroscience Research, 48(3), 249–57.

Williams, GSB, Boyman, L, Chikando, AC, Khairallah, RJ and Lederer, WJ. (2013). Mitochondrial Calcium Uptake. PNAS, 110(26), 10479–86.

Willis, M, Leitner, I, Jellinger, KA and Marksteiner, J. (2011). Chromogranin Peptides in Brain Diseases. Journal of neural transmission (Vienna, Austria: 1996), 118(5), 727–35.

Willis, M, Prokesch, M, Hutter-Paier, B, Windisch, M, Stridsberg, M, Mahata, SK, Kirchmair, R, Wietzorrek, G, Knaus, HG, Jellinger, K, Humpel, C and Marksteiner, J. (2008). Chromogranin B and Secretogranin II in Transgenic Mice Overexpressing Human APP751 with the London (V717I) and Swedish (K670M/N671L) Mutations and in Alzheimer Patients. Journal of Alzheimer's Disease, 13(2), 123–35.

Willis, WD. (2006). John Eccles' Studies of Spinal Cord Presynaptic Inhibition. Progress in Neurobiology, 78(3–5), 189–214.

Winsky-Sommerer, R, Grouselle, D, Rougeot, C, Laurent, V, David, JP, Delacourte, A, Dournaud, P, Seidah, N., Lindberg, I, Trottier, S and Epelbaum, J. (2003). The Proprotein Convertase PC2 Is Involved in the Maturation of Prosomatostatin to Somatostatin-14 but Not in the Somatostatin Deficit in Alzheimer's Disease. Neuroscience, 122(2), 437–47.

De Wit, J, Toonen, RF and Verhage, M. (2009). Matrix-Dependent Local Retention of Secretory Vesicle Cargo in Cortical Neurons. Journal of Neuroscience, 29(1), 23–37.

Witzmann, FA, Arnold, RJ, Bai, F, Hrncirova, P, Kimpel, MW, Mechref, YS, McBride, WJ, Novotny, M V., Pedrick, NM, Ringham, HN and Simon, JR. (2005). A Proteomic Survey of Rat Cerebral Cortical Synaptosomes. Proteomics, 5(8), 2177–2201.

Wolfe, CM, Fitz, NF, Nam, KN, Lefterov, I and Koldamova, R. (2019). The Role of APOE and TREM2 in Alzheimer ' s Disease—Current Understanding and Perspectives. International Journal of Molecular Sciences, 20(1).

Wolters, FJ and Ikram, MA. (2018). Epidemiology of Dementia: The Burden on Society, the Challenges for Research. In Biomarkers for Alzheimer's Disease Drug Development. Methods in Molecular Biology, ed. Perneczky R. Humana Press, New York, NY, 3–14.

Wong, MY, Cavolo, SL and Levitan, ES. (2015). Synaptic Neuropeptide Release by Dynamin-Dependent Partial Release from Circulating Vesicles. Molecular Biology of the Cell, 26(13), 2466–74.

Wood, DE and Nusbaum, MP. (2002). Extracellular Peptidase Activity Tunes Motor Pattern Modulation. Journal of Neuroscience, 22(10), 4185–95.

Wu, W and Wu, LG. (2007). Rapid Bulk Endocytosis and Its Kinetics of Fission Pore Closure at a Central Synapse. Proceedings of the National Academy of Sciences of the United States of America, 104(24), 10234–39.

Xiao, AW, He, J, Wang, Q, Luo, Y, Sun, Y, Zhou, YP, Guan, Y, Lucassen, PJ and Dai, JP. (2011). The Origin and Development of Plaques and Phosphorylated Tau Are Associated with Axonopathy in Alzheimer's Disease. Neuroscience Bulletin, 27(5), 287–99.

Xiao, L, Chang, SY, Xiong, ZG, Selveraj, P and Peng Loh, Y. (2017). Absence of Carboxypeptidase E/Neurotrophic Factor-A1 in Knock-Out Mice Leads to Dysfunction of BDNF-TRKB Signaling in Hippocampus. Journal of Molecular Neuroscience, 62(1), 79–87.

Xiao, NA, Zhang, J, Zhou, M, Wei, Z, Wu, XL, Dai, XM, Zhu, YG and Chen, XC. (2015). Reduction of Glucose Metabolism in Olfactory Bulb Is an Earlier Alzheimer's Disease-Related Biomarker in 5XFAD Mice. Chinese Medical Journal, 128(16), 2220–27.

Xu, HL, Mao, L, Ye, S, Paisansathan, C, Vetri, F and Pelligrino, DA. (2008). Astrocytes Are a Key Conduit for Upstream Signaling of Vasodilation during Cerebral Cortical Neuronal Activation in Vivo. Am J Physiol Heart Circ Physiol, 294, 622–32.

Xu, Q, Bernardo, A, Walker, D, Kanegawa, T, Mahley, RW and Huang, Y. (2006). Profile and Regulation of Apolipoprotein E (ApoE) Expression in the CNS in Mice with Targeting of Green Fluorescent Protein Gene to the ApoE Locus. Journal of Neuroscience, 26(19), 4985–94.

Yaguchi, T and Nishizaki, T. (2010). Extracellular High K+ Stimulates Vesicular Glutamate Release from Astrocytes by Activating Voltage-Dependent Calcium Channels. Journal of Cellular Physiology, 225(2), 512–18.

Yakovleva, T, Marinova, Z, Kuzmin, A, Seidah, NG, Haroutunian, V, Terenius, L and Bakalkin, G. (2007). Dysregulation of Dynorphins in Alzheimer Disease. Neurobiology of Aging, 28(11), 1700–1708.

Yang, J, Goetz, D, Li, JY, Wang, W, Mori, K, Setlik, D and Du, T. (2002). An Iron Delivery Pathway Mediated by a Lipocalin. Molecular Cell, 10, 1045–56.

Yang, Y, Kim, J, Kim, HY, Ryoo, N, Lee, S, Kim, YS, Rhim, H and Shin, YK. (2015). Amyloid-β Oligomers May Impair SNARE-Mediated Exocytosis by Direct Binding to Syntaxin 1a. Cell Reports, 12(8), 1244–51.

Yaron, A and Schuldiner, O. (2016). Common and Divergent Mechanisms in Developmental Neuronal Remodeling and Dying Back Neurodegeneration. Current Biology, 26(13), R628–39.

Yeh, CY, Vadhwana, B, Verkhratsky, A and Rodríguez, JJ. (2011). Early Astrocytic Atrophy in the Entorhinal Cortex of a Triple Transgenic Animal Model of Alzheimer's Disease. ASN Neuro, 3(5), 271–79.

Younts, TJ, Monday, HR, Dudok, B, Klein, ME, Jordan, BA, Katona, I and Castillo, PE. (2016). Presynaptic Protein Synthesis Is Required for Long-Term Plasticity of GABA Release. Neuron, 92(2), 479–92.

Yuan, T, Liu, L, Zhang, Y, Wei, L, Zhao, S, Zheng, X, Huang, X, Boulanger, J, Gueudry, C, Lu, J, Xie, L, Du, W, Zong, W, Yang, L, Salamero, J, Liu, Y and Chen, L. (2015). Diacylglycerol Guides the Hopping of Clathrin-Coated Pits along Microtubules for Exo-Endocytosis Coupling. Developmental Cell, 35(1), 120–30.

Zaben, MJ and Gray, WP. (2013). Neuropeptides and Hippocampal Neurogenesis. Neuropeptides, 47(6), 431–38.

Zamanian, JJL, Xu, L, Foo, LCL, Nouri, N, Zhou, L, Giffard, RG and Barres, BA. (2012). Genomic Analysis of Reactive Astrogliosis. The Journal of Neuroscience, 32(18), 6391–6410.

Zanin, MP, Phillips, L, Mackenzie, KD and Keating, DJ. (2011). Aging Differentially Affects Multiple Aspects of Vesicle Fusion Kinetics. PLoS ONE, 6(11).

Zeng, Z, Miao, N and Sun, T. (2018). Revealing Cellular and Molecular Complexity of the Central Nervous System Using Single Cell Sequencing. Stem Cell Research and Therapy, 9(1).

Zhan, S, Zhao, H, J White, A, Minami, M, Pignataro, G, Yang, T, Zhu, X, Lan, J, Xiong, Z, Steiner, DF, Simon, RP and Zhou, A. (2009). Defective Neuropeptide Processing and Ischemic Brain Injury: A Study on Proprotein Convertase 2 and Its Substrate Neuropeptide in Ischemic Brains. Journal of Cerebral Blood Flow and Metabolism, 29(4), 698–706.

Zhang, L, Fang, Y, Xu, Y, Lian, Y, Xie, N, Wu, T, Zhang, H, Sun, L, Zhang, R and Wang, Z. (2015). Curcumin Improves Amyloid β-Peptide (1-42) Induced Spatial Memory Deficits through BDNF-ERK Signaling Pathway. PLoS ONE, 10(6).

Zhang, Q, Fukuda, M, Van Bockstaele, E, Pascual, O and Haydon, PG. (2004). Synaptotagmin IV Regulates Glial Glutamate Release. Proceedings of the National Academy of Sciences of the United States of America, 101(25), 9441–46.

Zhang, Q, Li, Y and Tsien, RW. (2009). The Dynamic Control of Kiss-And-Run and Vesicular Reuse Probed with Single Nanoparticles. Science, 323, 1448–52.

Zhang, X, Jiang, S, Mitok, KA, Li, L, Attie, AD and Martin, TFJ. (2017). BAI AP3, a C2 Domain-Containing Munc 13 Protein, Controls the Fate of Dense-Core Vesicles in Neuroendocrine Cells. Journal of Cell Biology, 216(7), 2151–66.

Zhang, XY, Liu, F, Chen, Y, Guo, WC and Zhang, ZH. (2020). Proprotein Convertase 1/3-Mediated Down-Regulation of Brain-Derived Neurotrophic Factor in Cortical Neurons Induced by Oxygen-Glucose Deprivation. Neural Regeneration Research, 15(6), 1066.

Zhang, Z, Chen, G, Zhou, W, Song, A, Xu, T, Luo, Q, Wang, W, Gu, XS and Duan, S. (2007). Regulated ATP Release from Astrocytes through Lysosome Exocytosis. Nature Cell Biology, 9(8), 945–53.

Zhou, Y and Lindberg, I. (1994). Enzymatic Properties of Carboxyl-Terminally Truncated Prohormone Convertase 1 (PC1/SPC3) and Evidence for Autocatalytic Conversion. Journal of Biological Chemistry, 269(28), 18408–13.

Zhu, Y, Xu, J and Heinemann, SF. (2009). Two Pathways of Synaptic Vesicle Retrieval Revealed by Single-Vesicle Imaging. Neuron, 61(3), 397–411.

Zorec, R, Verkhratsky, A, Rodríguez, JJ and Parpura, V. (2016). Astrocytic Vesicles and Gliotransmitters: Slowness of Vesicular Release and Synaptobrevin2-Laden Vesicle Nanoarchitecture. Neuroscience, 323, 67–75.

APPENDIX

APPENDIX

Part of the data presented in the first section of results in the present dissertation were included in the following scientific article, in which the author also contributed with additional experimental procedures and figure preparation.

Plá, V., **Barranco, N**., Pozas, E. and Aguado, F. (2017). Amyloid-β Impairs Vesicular Secretion in Neuronal and Astrocyte Peptidergic Transmission. *Frontiers in Molecular Neuroscience 10*(June), 1–15.

Published: 28 June 2017
DOI: 10.3389/fnmol.2017.00202.

frontiers in Molecular Neuroscience

ORIGINAL RESEARCH
published: 28 June 2017
doi: 10.3389/fnmol.2017.00202

Amyloid-β Impairs Vesicular Secretion in Neuronal and Astrocyte Peptidergic Transmission

Virginia Plá[1,2], *Neus Barranco*[1,2], *Esther Pozas*[1] *and Fernando Aguado*[1,2]*

[1] *Department of Cell Biology, Physiology and Immunology, University of Barcelona, Barcelona, Spain,*
[2] *Institute of Neurosciences, University of Barcelona, Barcelona, Spain*

Regulated secretion of neuropeptides and neurotrophic factors critically modulates function and plasticity of synapses and circuitries. It is believed that rising amyloid-β (Aβ) concentrations, synaptic dysfunction and network disorganization underlie early phases of Alzheimer's disease (AD). Here, we analyze the impact of soluble $A\beta_{1-42}$ assemblies on peptidergic secretion in cortical neurons and astrocytes. We show that neurons and astrocytes differentially produce and release carboxypeptidase E (CPE) and secretogranin III (SgIII), two dense-core vesicle (DCV) markers belonging to the regulated secretory pathway. Importantly, $A\beta_{1-42}$, but not scrambled $A\beta_{1-42}$, dramatically impairs basal and Ca^{2+}-regulated secretions of endogenously produced CPE and SgIII in cultured neurons and astrocytes. Additionally, KCl-evoked secretion of the DCV cargo brain-derived neurotrophic factor (BDNF) is lowered by $A\beta_{1-42}$ administration, whereas glutamate release from synaptic vesicle (SVs) remains unchanged. In agreement with cell culture results, $A\beta_{1-42}$ effects on CPE and SgIII secretion are faithfully recapitulated in acute adult brain slices. These results demonstrate that neuronal and astrocyte secretion of DCV cargos is impaired by Aβ *in vitro* and *in situ*. Furthermore, Aβ-induced dysregulated peptidergic transmission could have an important role in the pathogenesis of AD and DCV cargos are possible candidates as cerebrospinal fluid (CSF) biomarkers.

Keywords: Alzheimer's disease, BDNF, cerebral cortex, dense-core vesicles, exocytosis

OPEN ACCESS

Edited by:
Detlev Boison,
Legacy Health, United States

Reviewed by:
Ursula Susan Sandau,
Oregon Health & Science University, United States
Samaneh Maysami,
University of Manchester, United Kingdom

***Correspondence:**
Fernando Aguado
faguado@ub.edu

Received: *25 April 2017*
Accepted: *08 June 2017*
Published: *28 June 2017*

Citation:
Plá V, Barranco N, Pozas E and Aguado F (2017) Amyloid-β Impairs Vesicular Secretion in Neuronal and Astrocyte Peptidergic Transmission. Front. Mol. Neurosci. 10:202. doi: 10.3389/fnmol.2017.00202

INTRODUCTION

Alzheimer's disease (AD) is by far the most common cause of dementia in the elderly. The characteristic clinical phenotype of AD is a gradual and progressive loss of memory and cognition (Scheltens et al., 2016). Accumulation of abnormally folded amyloid-β (Aβ) peptides in extracellular plaques and hyperphosphorylated tau proteins in intracellular tangles are two major pathological hallmarks of AD. However, neuritic plaques and neurofibrillary tangles are only weakly correlated with the degree of dementia in AD patients (Selkoe and Hardy, 2016). In contrast, decreased synapse number is the major quantitative correlate of loss of memory and cognition in AD brain (DeKosky and Scheff, 1990). Accordingly, a growing body of electrophysiological, biochemical and behavioral evidence suggests that synaptic dysfunction and network disorganization centrally underlie the progressive cognitive manifestations of the clinical AD occurring before the onset of symptoms (Mucke and Selkoe, 2012; Palop and Mucke, 2016).

It has been shown that the concentration of soluble Aβ, but not insoluble Aβ deposits, is a predictor of synaptic changes in AD and tracks the disease progression and cognitive decline

(Lue et al., 1999; Koss et al., 2016). In fact, soluble Aβ species, mainly $A\beta_{1-42}$ oligomers, exert a pivotal role in the pathogenesis of the synaptic damage at early stages of AD (Ferreira et al., 2015; Viola and Klein, 2015; De Strooper and Karran, 2016). Binding of Aβ to neuronal and glial plasma membranes causes multiple aberrant effects that could trigger synaptic failure, such as dysfunction of Ca^{2+} homeostasis, axonal transport, neurotransmitter receptors and transporters and mitochondria. Moreover, several studies have proposed that Aβ peptides can affect synaptic function by altering vesicular release of classical transmitters (i.e., glutamate) from neurons and astrocytes (Arias et al., 1995; Abramov et al., 2009; Parodi et al., 2010; Brito-Moreira et al., 2011; Talantova et al., 2013; Hascup and Hascup, 2016). In this regard, two recent studies showing that Aβ oligomers directly impair SNARE complex formation and synaptic vesicle (SV) exocytosis further support a deleterious function of aberrant Aβ on transmitter secretion (Russell et al., 2012; Yang et al., 2015).

Besides SVs, the so-called dense-core vesicle (DCVs, secretory granules in endocrine cells) store a wide array of neuropeptides, hormones and growth factors that enable peptidegic transmission. In neurons, and as recently proposed astrocytes, DCVs-containing transmitters budding from trans-Golgi network mature during transport along microtubules toward the cell surface and secrete their cargos by Ca^{2+}-triggered exocytosis (Gondré-Lewis et al., 2012; Araque et al., 2014). Although structure and function of synapses and networks critically depend on the adjusted peptidergic transmission (van den Pol, 2012), secretory features of DCVs in the normal and pathological central nervous system have been little studied. Here, we determined the impact of Aβ on secretion of DCV cargos in cortical neurons and astrocytes. Therefore, we analyzed *in vitro* and *in situ* release of carboxypeptidase E (CPE) and secretogranin III (SgIII), two established DCVs markers which are aberrantly accumulated in neurons and astrocytes in the cerebral cortex of AD patients and amyloid-forming transgenic mice (Plá et al., 2013). First, we show that neurons and astrocytes produce distinctive forms of CPE and SgIII, which undergo release via differential mechanisms. Importantly, basal and regulated secretions of endogenously produced CPE and SgIII, as well as brain-derived neurotrophic factor (BDNF), are dramatically impaired by Aβ both in cultured dispersed cells and acute brain slices. The present results indicate that DCVs secretion is a significant target of amyloidogenic Aβ forms. Moreover, a participation of Aβ-induced peptidergic secretion alterations in the pathogenesis of AD and its potential use as a cerebrospinal fluid (CSF) biomarker are suggested.

MATERIALS AND METHODS

Antibodies and Reagents

Monoclonal and polyclonal antibodies against CPE were obtained from BD Transduction Laboratories (San Jose, CA, USA) and GeneTex (Irvine, CA, USA). Polyclonal antibodies against SgIII were purchased from Sigma-Aldrich (Madrid, Spain). Aβ monoclonal antibodies, clones 4G8 and 6E10, were from Covance (Emeryville, CA, USA). Polyclonal PC1/3 and PC2 were from Thermo Fisher Scientific (Madrid, Spain) and kindly provided by Dr I. Lindberg (University of Maryland), respectively. Antibodies against GFAP, MAP-2, CD11b, Tuj1, β-actin and Iba1 were from Millipore Iberica (Madrid, Spain), Serotec (Oxford, UK), Sigma-Aldrich and Wako GmbH (Neuss, Germany). DL-*threo*-β-benzyloxyaspartic acid (TBOA) was from Tocris Bioscience (Bristol, UK). Most chemicals and cell culture reagents were obtained from Sigma-Aldrich and Gibco (Thermo Fisher Scientific), respectively.

Animals and Ethics Statement

CD1 mice were provided by Envigo Rms (Sant Feliu de Codines, Spain), kept under controlled temperature (22 ± 2°C), humidity (40%–60%), and light (12-h cycles). All animals were handled in accordance with the guidelines for animal research set out in the European Community Directive 2010/63/EU, and all procedures were approved by the Ethics Committee for Animal Experimentation (CEEA), University of Barcelona (Barcelona, Spain). All efforts were made to minimize the number used and animal suffering.

Primary Cell Cultures and Acute Brain Slices

Astroglial and neuronal cultures were obtained from CD1 mice and prepared as described previously (Paco et al., 2009). Astrocyte cultures were prepared from the whole cerebral cortex of P0-P1-day-old mice. Cortical tissues were isolated, meninges were carefully dissected away, minced and incubated in 0.5% trypsin and 0.01% DNase. Dissociated cells were seeded in flasks and grown in high-glucose Dulbecco's Modified Eagle's Medium and F-12 (1:1) containing 10% fetal bovine serum, 10 mM HEPES and penicillin/streptomycin at 37°C in a 5% CO_2 incubator. At confluence (10–12 days), flasks were shaken overnight and the cells were rinsed, detached and subcultured at 1×10^5 cells/cm^2 onto poly-D-lysine-coated plastic culture dishes and glass coverslips. Under these conditions, cell cultures were essentially formed by astrocytes (>95% GFAP+), a small percentage of microglia (<5% CD11b+) and virtually devoid of neurons (<0.5% Tuj-1+). Neuronal cultures were grown from either whole cerebral cortex (including hippocampus) or isolated hippocampus of E16-E17 mouse embryos. After trypsin and DNase treatment, dissociated cells were seeded at 1.5×10^5 cells/cm^2 onto poly-D-lysine-coated culture plates and glass coverslips. Neurons were grown in Neurobasal A medium containing B27 and 1% FBS (Thermo Fisher Scientific), glutamine and penicillin/streptomycin at 37°C in a 5% CO_2 atmosphere for 10 days. During the first 4 days, cultures were also supplemented with 20 μg/mL 5-Fluoro-2′-deoxyuridine and 50 μg/mL Uridine (Sigma-Aldrich) to inhibit mitotic activity of glial cells. Tuj-1 and MAP2 immunostaining showed that more than 95% of the cells were neurons, whereas a <5% were GFAP+ astrocytes.

Brain slices were obtained from anesthetized adult mice (ketamine 120 μg/g and xylazine 6 μg/g i.p.), as described previously (Aguado et al., 2002). Their brains were removed and placed in cold artificial CSF (ACSF) containing (in mM): NaCl

120, KCl 3, D-glucose 10, $NaHCO_3$ 26, NaH_2PO_4 2.25, $CaCl_2$ 2, $MgSO_4$ 1, pH 7.4, bubbled with 95% O_2 and 5% CO_2. Horizontal tissue slices (300 μm thick) were cut with a vibratome, stabilized and transferred to a release chamber. All the experiments were conducted in ACSF bubbled continuously with 95% O_2 and 5% CO_2 at room temperature (22–25°C).

Aβ Aggregation and Cell Viability

Synthetic human Amyloid-β_{1-42} (Aβ) peptide (H-1368), and peptide comprised of the same amino acid composition of but in a randomized sequence, Scrambled Amyloid-β_{1-42} (H-7406; ScAβ), used as a control, were purchased from Bachem (Bubendorf, Switzerland) and prepared as described previously (Dahlgren et al., 2002). Lyophilized Aβ or ScAβ peptides were initially dissolved to 1 mM in 1,1,1,3,3,3-Hexafluoro-2-propanol (Sigma-Aldrich) and separated into aliquots in sterile microcentrifuge tubes. Then, hexafluoroisopropanol was evaporated under low temperature vacuum in a Speed Vac, and the peptide film was stored desiccated at −80°C until use. For the assembly, the peptide was first resuspended in anhydrous sterile dimethylsulfoxide (Sigma-Aldrich) to a concentration of 5 mM, diluted to a final concentration of 100 μM in 10 mM HCl and incubated for 24 h at 37°C. Aggregated species in Aβ stocks were identified by western blotting. Cultured cells and brain slices were treated with either 5 μM Aβ/ScAβ preparation or an equal volume of vehicle solution (controls). Cell viability was determined by WST-1 (Roche, Basel, Switzerland), lactate dehydrogenase (Roche) and propidium iodide/Hoechst (Sigma-Aldrich) assays. Levels of reduced WST-1 and released lactate dehydrogenase were measured with an ELISA plate reader (Tecan, Männedorf, Switzerland) at 450 nm and 492 nm, respectively. Propidium iodide/Hoechst uptake was analyzed by fluorescence microscopy and analyzed with ImageJ software.

Release Assays

Secretion in cultured cells was assayed in 12-well culture plates except for BDNF, for which it was done in 100 mm dishes and for glutamate, for which 48-well plates were used. Poly-D-lysine-attached cells were serum and supplement starved prior to release experiments. Release assays in brain slices were performed in superfused or static chambers (displaying the same results). Secretion from cultured cells was performed in commercial media and, when K^+ and Ca^{2+} concentrations were modified, in ACSF, whereas the release from brain slices was always carried out in ACSF. The composition of the 55 mM K^+ ACSF was adjusted to maintain the osmolarity with a corresponding NaCl decrease. In cultured cells, conditioned media were collected and cells were washed in phosphate buffer saline (PBS) and homogenized in lysis buffer (see below). Cell media and superfusate and static ACSF from brain slices were centrifuged at 600 *g* for 5 min to remove dislodged cells and all samples were stored at −20°C. Proteins in all release samples were precipitated with 5% trichloroacetic acid, using sodium deoxycholate as a carrier, or concentrated by Amicon® Ultra-15 and −0.5 Centrifugal filter devices (Merck Millipore, Madrid, Spain).

CPE and SgIII were detected by western blotting (see below) and Prep Cell Protein Standard was used as a control for the precipitation protocol for conditioned media (Bio-Rad Laboratories, Hercules, CA, USA). In cell culture media, β-actin was used to normalize the secretion in order to minimize variations in cell quantity. Levels of BDNF were quantified using the BDNF EMAX® ImmunoAssay System according to the manufacturer's instructions (Promega Corporation, Madison, WI, USA). Glutamate levels were measured using Amplex Red Glutamic Acid/Glutamate Oxidase Assay kit (Molecular Probes, Eugene, OR, USA) following the manufacturer's protocol. BDNF and glutamate levels were normalized by total protein levels.

Western Blotting

Cultured cells and tissues were homogenized in ice-cold lysis buffer containing 50 mM Tris-HCl pH 7.4, 150 mM NaCl, 5 mM $MgCl_2$, 1 mM ethyleneglycol-bis(2-aminoethylether)-N,N,N′,N′-tetra acetic acid (EGTA), 1% Triton X-100, and protease inhibitor cocktail (Roche Diagnostics). Samples of conditioned media and postnuclear lysates were electrophoresed in 8%–12% sodium dodecyl sulfate-polyacrylamide gel electrophoresis (SDS-PAGE; Bio-Rad Laboratories) and then transferred to PVDF membranes (Bio-Rad Laboratories). The membranes were activated and blocked in a solution containing 5% nonfat milk powder in tris-buffered saline tween-20 (140 mM NaCl, 10 mM Tris-HCl, pH 7.4, and 0.1% Tween 20; TBS-Tween) for 1 h at room temperature and then incubated with primary antibodies in blocking buffer for 2 h at room temperature or overnight at 4°C. After several washes in TBS-Tween solution, the membranes were incubated for 1 h with horseradish peroxidase-conjugated secondary antibodies (Bio-Rad Laboratories). Bound antibodies were visualized with enhanced chemiluminescence reagents (Bio-Rad Laboratories). Blot images were scanned and densitometric analyses were performed using ImageJ software.

Immunocytochemistry

Cells grown on glass coverslips were washed in ice-cold PBS and fixed with 4% paraformaldehyde in PB for 15 min. Animals were perfused transcardially under deep ketamine/xylacine anesthesia with 4% paraformaldehyde in 0.1 M PB, pH 7.4. The brains were removed from skulls, postfixed for 4 h in the same fixative solution, and cryoprotected overnight at 4°C by immersion in a 30% sucrose solution in 0.1 M PB. Forty-micrometer thick frozen sections were obtained with a cryostat and collected in PBS. Sections processed for the peroxidase method were soaked for 30 min in PBS containing 10% methanol and 3% H_2O_2 and subsequently washed in PBS. To suppress nonspecific binding, cell cultures and brain sections were incubated in 10% serum-PBS containing 0.1% Triton X-100, 0.2% glycine and 0.2% gelatin for 1 h at room temperature. Incubations with primary antibodies were carried out overnight at 4°C in PBS containing 5% fetal bovine serum, 0.1% Triton X-100 and 0.2% gelatin. Some histological sections were processed using the avidin-biotin-peroxidase method (Vectastain ABC kit, VECTOR, Burlingame, CA, USA). The peroxidase complex was visualized by incubating the sections with 0.05% diaminobenzidine and

0.01% H_2O_2 in PBS. Sections were mounted, dehydrated and coverslipped in Eukitt. Cell cultures and some brain sections were processed for immunofluorescence using secondary fluorochrome-conjugated antibodies (Alexa Fluor 488 and Alexa Fluor 568, Molecular Probes, Eugene, OR), and cell nuclei were stained with 4′,6-diamidino-2-phenylindole (DAPI, Molecular Probes, Eugene, OR, USA). Cell-containing coverslips and histological sections were mounted with Mowiol. The specificity of the immunostaining was tested by omitting the primary antibodies or by replacing them with an equivalent concentration of nonspecific IgG. No immunostaining was observed in these conditions. Bright field and fluorescent images were obtained with the Olympus fluorescent BX-61 and Leica TCS SPE scanning confocal microscopes.

Quantitative Real-Time PCR

RNA from cells was isolated by treatment with Trizol® reagent (Invitrogen) following the manufacturer's instructions and the quantity and quality were determined with a NanoDrop ND-1000 (NanoDrop Technologies, Wilmington, DE, USA) and Bioanalyzer 2100 (Agilent, Waldbronn, Germany). cDNA was synthesized using the Superscript III Reverse Transcriptase kit (Invitrogen) from 1 μg of total RNA. Reactions were incubated at 25°C for 10 min, 50°C for 30 min, 85°C for 5 min, chilled on ice and finally *E. coli* RNAse H was added and incubated at 37°C for 20 min. Quantitative real-time PCR (qPCR) was performed using the StepOneTM Real-Time PCR System (Applied Biosystems) using TaqMan Probes Mm00516341_m1 (CPE), Mm00485961_m1 (SgIII) and Mm01277042_m1 (TBP, as housekeeping gene). The 20 μl PCR included 0.01 μl RT product, 1× PerfeCTa® qPCR FastMix® II with ROX (Quanta BioSciences, Inc.) and 1 μL TaqMan probe. The reactions were incubated in a 48-well plate at 95°C for 5 min, followed by 42 cycles of 95°C for 15 s, 58°C for 15 s and 72°C for 30 s. All reactions were run in triplicate. The threshold cycle (C_T) is defined as the fractional cycle number at which the fluorescence passes the fixed threshold.

Statistical Analysis

Data are shown as the mean ± Standard Error of the Mean (SEM) summarizing three or more independent experiments, performed at least in triplicates. Non-parametric one-way ANOVA were calculated to determine significant effects of treatments, using Kruskal-Wallis or Friedman test when appropriate. Changes were calculated in relation to the average of controls using Mann–Whitney or Wilcoxon tests as *post hoc* analysis. Significance was set at $^{*}p < 0.05$, $^{**}p < 0.01$ and $^{***}p < 0.001$.

RESULTS

Differential Mechanisms Underlie CPE and SgIII Secretion from Neurons and Astrocytes

First, we determined the *in situ* cellular location of the DCV markers CPE and SgIII in the mouse cerebral cortex by immunohistological methods. High levels of both proteins were found in processes and cell bodies of pyramidal and non-pyramidal neurons and astrocyte-like glial cells (**Figure 1**). For neuronal CPE and SgIII, we detected differential location patterns at the regional and subcellular levels. In general, CPE immunostaining was more intense and more extended than for SgIII (**Figure 1**). Both proteins were present in perikarya, but only CPE was associated with dendritic shafts. Characteristically, SgIII was found abundantly as immunoreactive puncta throughout the neuropil, resembling axon terminals (**Figure 1**). Differential location of these two DCV proteins in neurons was apparent for the CA3 region of the hippocampus, where CPE- and SgIII-labeled projections corresponded with dendrites and mossy fibers, respectively (**Figure 1**). Regarding glial cells, most cortical astrocyte-like somata through the gray and white matters copiously displayed both CPE and SgIII (**Figure 1**). Double immunofluorescence showed that non-neuronal CPE and SgIII were associated with virtually all GFAP+ astrocytes and absent in Iba1+ microglial cells (data not shown), in agreement with our previous report (Paco et al., 2010).

To study peptidergic secretion from astrocytes and neurons, we prepared cortical primary cultures highly enriched in each cell type. Astrocyte cultures were virtually devoid of neurons, while a small number of astrocytes (<5%) was present in neuronal cultures which improved survival. In cultured astrocytes, CPE and SgIII were associated with secretory organelles showing a non-overlapping location, mainly for distal vesicles (**Figure 2A**). CPE- and SgIII-immunolabeled vesicular compartments were also evident in astrocytes grown within neuronal cultures (**Figure 2B**). GFAP co-labeling was used to validate astroglial identity. Careful analysis of media and cell lysates of glial cultures by western blotting revealed that astrocyte CPE and SgIII proteins corresponded to the nonprocessed forms (∼55 kDa for CPE and ∼80–75 kDa for precursor SgIII, pSgIII; **Figure 2C**). Because glial-produced proteins likely corresponded to the uncleaved precursor forms, we determined whether astrocytes lacked the corresponding PC1/3 and PC2 processing prohormone convertases. Double immunocytochemical labeling and Western blotting showed that *in vitro* astrocytes did not express either PC1/3 or PC2 proteins (data not shown).

As previously reported for SgIII (Paco et al., 2010), we show here that cultured astrocytes displayed high rates of basal release of both CPE and SgIII (**Figure 2C**). To analyze secretory kinetics of *de novo* synthesized CPE and SgIII in astrocytes, extracellular and intracellular protein pools were analyzed during cycloheximide (CHX) chase. As expected for secretory proteins, untreated cells showed rising extracellular levels and steady intracellular pools of CPE and SgIII over time. When protein synthesis was blocked by CHX, decreasing levels of intracellular CPE and SgIII were coupled with an almost invariable secreted pool (**Figure 2C**). These observations show that newly generated DCVs-like in astrocytes are poorly retained and rapidly undergo exocytosis, independently of stimuli. Next, we evaluated the regulated secretion of glial CPE and SgIII triggering $[Ca^{2+}]_i$ elevation by ionophores. Noteworthy, exposure to 1 μM ionomycin over 15 min gave variable responses from one culture set to another. Compared to unstimulated cultures, released

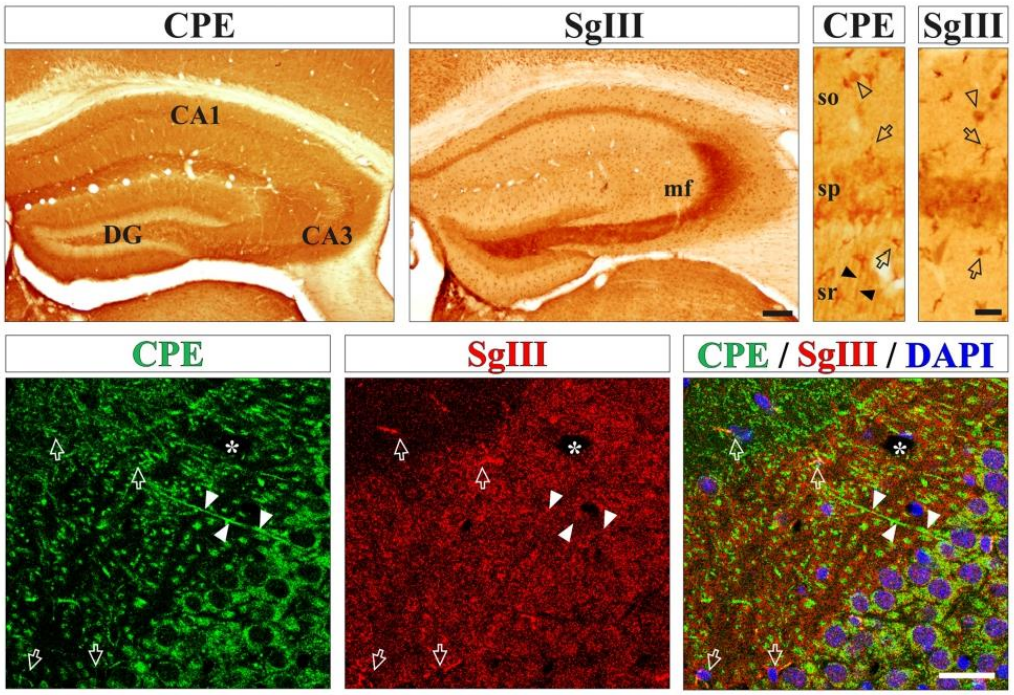

FIGURE 1 | Neurons and astrocytes abundantly express carboxypeptidase E (CPE) and SgIII proteins in the cerebral cortex *in vivo*. Upper boxes illustrate immunoperoxidase staining for CPE and SgIII in panoramic (left) and CA1 region (right) views of the hippocampal formation. Both proteins display a remarkable area specific and laminar distribution. Neuronal CPE is primarily found in dendritic shafts (filled arrowheads) and perikarya, where mossy fibers robustly exhibit SgIII. Intense immunolabeling for SgIII and CPE is detected in astroglial cell bodies and processes (arrows). Bottom boxes show confocal images of CPE (green) and SgIII (red) double immunofluorescences in the hippocampal CA3 region. Both proteins are mainly associated with different neuronal domains. CPE is largely located in somatodendritic compartments and SgIII is mainly distributed in terminal-like buttons of mossy fibers. Intense SgIII and CPE immunofluorescences colocalize in the same astrocyte processes (arrows). Nuclei are stained in blue. Arrows and arrow-heads point to astroglial cells and interneurons, respectively. Filled arrow-heads outline dendrites and asterisk indicates blood vessels. Scale bars in μm: upper-left, 250; upper-right and bottom, 50. Abbreviations: CA, regions of the hippocampus; DG, dentate gyrus; mf, mossy fibers; so, stratum oriens; sp, stratum pyramidale; sr, stratum radiatum.

CPE was higher after ionophore administration (181.4 ± 29.8% over basal; $p = 0.03$), while no statistically significant changes were observed for SgIII during stimulation (146.1 ± 25.4% over basal; $p = 0.3$). Moreover, CPE and SgIII intracellular levels were decreased after treatment (**Figure 2D**). Finally, the addition of 55 mM KCl to the media did not substantially change the levels of CPE nor SgIII secreted from astrocytes (**Figure 2D**). We conclude that cultured astrocytes robustly produce unprocessed forms of CPE and SgIII and largely release them in a stimulus-independent fashion.

In neuronal cultures, CPE and SgIII were associated with secretory organelles of pyramidal- and stellate-shaped neurons (**Figure 3A**). In agreement with the above *in vivo* data, a preferential location in dendrites was observed for CPE, whereas SgIII was mainly associated with axon-like projections and terminals. Neuronal and dendritic identities were confirmed by double immunolabeling with MAP2. In contrast to glial cells, cultured neurons produce and release both the precursor and mature forms of CPE (~55 and 53 kDa) and SgIII (~75 and 55 kDa; pSgIII and mSgIII respectively; **Figure 3B**). Moreover, as anticipated by the mature form occurrence of CPE and SgIII, cultured neurons abundantly displayed the DCV-associated convertases PC1/3 and PC2 (**Figure 3A**).

Opposite to astrocytes, cultured neurons showed a very low basal and high stimulus-triggered secretion of CPE and SgIII (**Figures 3B–D**). Therefore, forcing Ca^{2+} entry during 15 min by 1 μM ionomycin addition increased up to fivefold secretion from neuronal cells (**Figure 3D**). Depolarization by KCl for 15 min resulted in a dramatic enhancement of CPE and SgIII release (**Figure 3C**). Although shorter stimulation times, such as 5 min, offered similar results, 15 min of depolarization was maintained to ensure detection of released proteins by Western blotting. K^+-evoked secretion of CPE

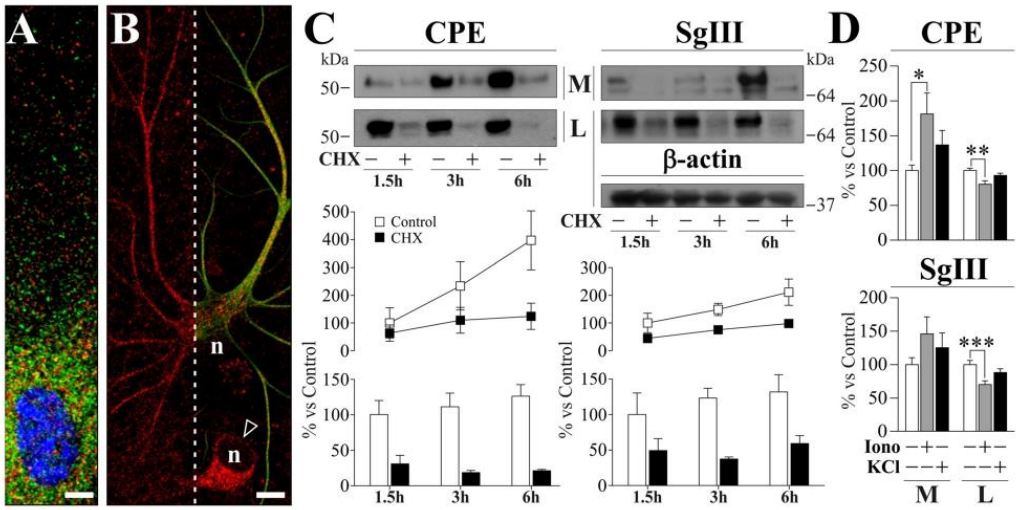

FIGURE 2 | Localization and release of CPE and SgIII in cultured cortical astrocytes. **(A,B)**. Confocal immunofluorecence images in astrocytes grown in glial **(A)** and neuronal **(B)** enriched cultures. High magnification in **(A)** shows a poor co-localization (yellow signal) of CPE (green) and SgIII (red) around the nucleus (blue). The astrocyte identity of a process-bearing cell positive for SgIII (red) is revealed by GFAP (green) co-staining (right in **B**). In **(B)**, arrow-head points to a neuronal soma displaying SgIII (red) and *n* indicates nucleus location. Scale bars in μm: **(A)** 5; **(B)** 15. **(C)** Immunoblots illustrate cellular content (lysates, L) and basal secretion into the medium (M) of CPE and SgIII in astrocyte cultures treated or not with 7.5 μM CHX during 1.5 h, 3 h and 6 h. β-actin was used as loading control. The graphs below summarize percent variation of the extracellular (lines) and intracellular (bars) levels of CPE and SgIII after CHX administration compared to controls. Data are presented as the mean ± standard error of the mean (SEM) of a representative experiment performed in quadruplicates. **(D)** Histograms summarizing the effect of 1 μM ionomycin (Iono) and 55 mM KCl incubations over 15 min on release (M) and cell content (L) of CPE and SgIII. Values represent percent variation compared with controls and are presented as the mean ± SEM. All the data (M and L) was normalized by intracellular levels of β-actin. $^{*}p < 0.05$; $^{**}p < 0.01$; $^{***}p < 0.001$, Mann-Whitney test.

was enhanced by a 279% over basal, whereas a 289% was observed for SgIII forms. Because nominally Ca^{2+}-free medium virtually abolished DCVs release, K^{+}-induced release of CPE and SgIII in cultured neurons entirely depended on the influx of this cation (**Figure 3C**). Interestingly, Ca^{2+}-evoked SgIII secretion was stronger for mature forms than for precursors in both ionomycin (1.7 m/p ratio) and KCl (2.0 m/p ratio) stimulations. These data indicate that neuronal and astroglial DCVs undergo differential proteolytic processing and exocytotic profiles.

Aβ Alters Production and Release of CPE and SgIII in Cultured Astrocytes

To determine whether Aβ alters glial and neuronal DCVs secretion, we prepared Aβ assemblies incubating $Aβ_{1–42}$ peptides for 24 h at 37°C. Immunoblotting with 6E10 and 4G8 Aβ antibodies revealed that Aβ preparations contained a broad mixture of low- (20–50 kDa) and high-molecular-weight (>50 kDa) aggregates, as well as the Aβ monomers, trimers and tetramers (**Figure 4**). Consistent with previous reports (Moreth et al., 2013), mono-tetrameric species were instantaneously formed, whereas larger oligomeric aggregates appeared over time of aging. No immunoreactive bands were detected from ~200 kDa to the top/entrance of the gels (**Figure 4**).

Cell viability of cultured cells incubated with 5 μM Aβ was evaluated at 24 h for astrocytes and 16 h for neurons. Cellular membrane integrity was analyzed by a propidium iodide/Hoechst uptake test. No changes were observed between Aβ-treated and untreated cell cultures (Aβ vs. control: 99.6 ± 0.7%, $p = 0.8$ for neurons and 100.2 ± 0.8%, $p = 0.9$ for astrocytes). Due to the vulnerability of neurons, 2 additional tests were performed. WST-1 reduction was evaluated to detect variations in the mitochondrial metabolic rate, finding no significant changes (111.7 ± 4.7% of the control, $p = 0.14$). Additionally, the release of the cytoplasmic enzyme lactate dehydrogenase was analyzed in neuronal supernatant, showing no increase in response to Aβ (97.7 ± 3.6% of the control, $p = 0.6$). Because no differences were found between Aβ- and vehicle-treated cultures in any of the tests performed, no toxicity was found at the incubation times used.

Next, we analyzed the effect of Aβ on astrocyte CPE and SgIII secretion. Because the weak regulated release of these proteins in glia, we focused on their basal secretion at 8 and 24 h. Incubation of astrocytes with 5 μM Aβ caused a significant reduction in the extracellular levels of SgIII and CPE, mainly at 8 h (65% for SgIII and 41% for CPE) compared with controls (vehicle-treated cells; **Figures 5A,B**). The unchanged

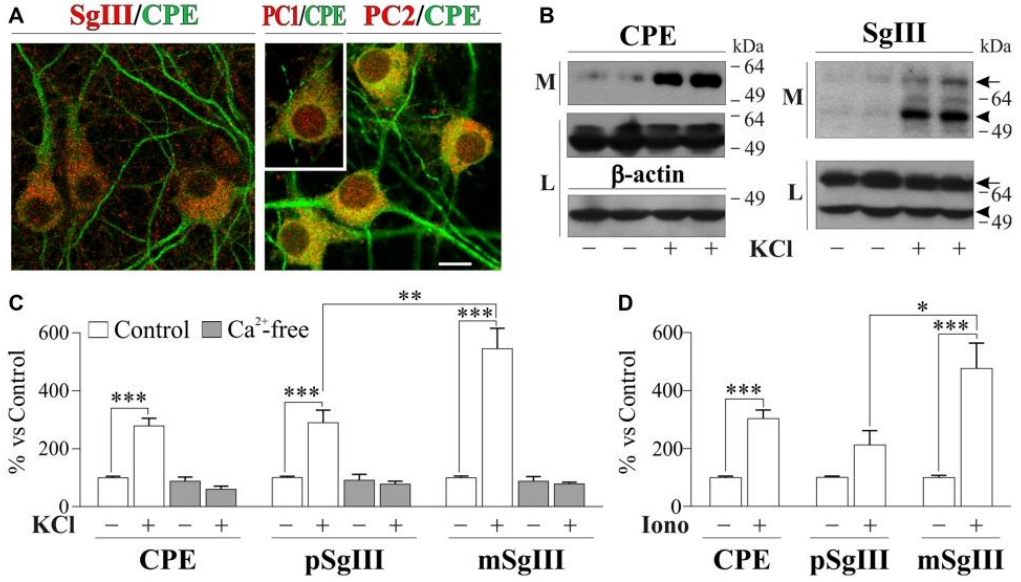

FIGURE 3 | Cellular distribution and release of CPE and SgIII in cultured neurons of the cerebral cortex. **(A)** Confocal immunofluorescence shows a prominent dendritic location for CPE (green) in pyramidal- and stellate-shaped neurons, while SgIII (red, left) is found in cell bodies and axon-like processes. No apparent colocalization was observed for the 2 proteins. Abundant signal shows the presence of the PC1/3 (red, inset) and PC2 (red, right) in the cultured neurons, with a broad somatic distribution. Scale bar in μm: 10. **(B)** Western blots show a very low basal secretion for CPE and SgIII, which were abundantly released in response to depolarization by KCl 55 mM for 15 min. Both forms of SgIII (arrow: proform, p and arrowhead: mature, m) were found in the extracellular media (M). No changes were found at intracellular levels in the lysate fraction (L). β-actin was used as loading control. **(C)** Release in response to KCl-depolarization was significant for CPE and both *p*- and mSgIII, the latter being especially high. In all cases, evoked secretion was abolished in absence of Ca^{2+}, showing a Ca^{2+} dependance. **(D)** 1 μM Ionomycin was used to trigger the CPE and SgIII release. Graphs show the percent variation compared with controls and are presented as the mean ± SEM normalized by intracellular levels of β-actin. $^{*}p < 0.05$; $^{**}p < 0.01$; $^{***}p < 0.001$, Mann-Whitney test.

CPE and SgIII levels in culture media of astrocytes incubated with a scrambled amino acid sequence of $A\beta_{1-42}$ (5 μM ScAβ) substantiated the specific effect of the aberrant amyloid on released glial proteins. To assess whether decreased levels into the media correlated with a diminished production or an impaired release, intracellular SgIII and CPE levels were assayed in Aβ- and ScAβ-treated cells. Concomitantly with a reduction in secreted CPE and SgIII, Aβ markedly increased their cellular content, mainly for SgIII (320% at 8 h and 257% at 24 h, $p < 0.0001$). No differences were detected after incubation with ScAβ peptides (**Figures 5A,B**). In addition to an impaired secretion, an Aβ-induced transcriptional dysregulation could contribute to change extra- and intracellular levels of secretory proteins. Therefore, we performed qPCR analysis for CPE and SgIII mRNA in Aβ-treated and control astrocytes. We found that levels of CPE transcripts were upregulated by amyloid species (158.1 ± 18.7% of control, $p = 0.03$), whereas SgIII mRNA expression was declined (70.2 ± 7.8% of control, $p = 0.004$; **Figure 5C**). Taking together, these results indicate that Aβ differentially regulates CPE and SgIII transcription and consistently impairs their protein secretion in astrocytes.

Regulated Secretion of DCV Cargos from Cultured Neurons is Impaired by Aβ

To evaluate the impact of Aβ on neuronal DCV release, primary cultures were exposed to vehicle (control) and 5 μM Aβ and ScAβ preparations for 16 h, then basal and K^+-evoked release were analyzed by immunoblotting. A representative experiment in **Figure 6A** illustrates no differences in the intracellular levels of CPE, SgIII forms and β-actin after Aβ-treatments (data quantification not shown). However, a significant decrease of basal secretion was detected for CPE (73% of control, $p < 0.0001$) and precursor (75% of control, $p = 0.007$) and mature (66% of control, $p = 0.0005$) SgIII forms in Aβ-exposed neurons, but not in cells incubated with ScAβ (**Figures 6A,B**). Importantly, Aβ specifically impaired K^+-depolarized release of CPE (Aβ 203.3% vs. control 363.2%, $p < 0.0001$), pSgIII (Aβ 190.0% vs. control 302.1%, $p = 0.006$) and mSgIII (Aβ 245.3% vs. control 426.0%, $p < 0.0001$) but not ScAβ (**Figures 5A,B**). Furthermore, an immunocytochemical analysis was performed on MAP2-identified neurons to examine subcellular distribution. Comparing neurons exposed to amyloid with vehicle (control), aberrant immunoreactive accumulations around the nuclei were detected in Aβ-treated cultures. This

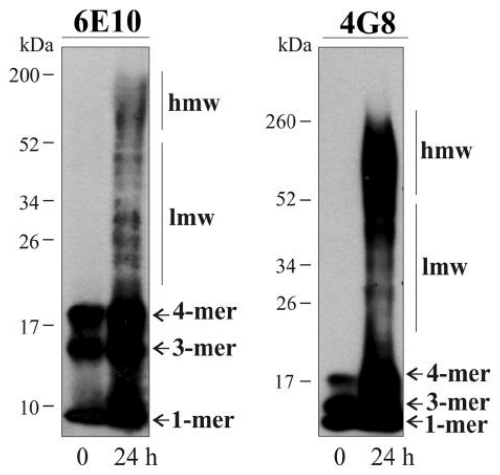

FIGURE 4 | Characterization of aggregates present in the Aβ preparations. Immunoblots illustrate 6E10- and 4G8-immunoreactive soluble $A\beta_{1-42}$ peptide before and after 24 h incubation at 37°C. Monomeric (1-mer), trimeric (3-mer) and tetrameric (4-mer) forms of Aβ are detected in both preparations, whilst low molecular weight (lmw) and high molecular weight (hmw) aggregates are only detected after the 24 h-incubation.

abnormal distribution was mainly associated with pyramidal-shaped cells and principally occurred for SgIII (**Figure 6C**). The present observations evidence that Aβ strongly alters the regulated secretory pathway in neurons, impairing the evoked release of CPE and SgIII.

Probably, the most studied DCV protein in brain-related diseases is the pleiotrophic growth factor BDNF (Adachi et al., 2014). With the aim to analyze whether release of physiologically relevant DCV cargos is affected by Aβ, we investigated secretion of endogenously produced BDNF by a sensitive sandwich immunoassay. First, we assessed BDNF levels in the same cortical-derived neuronal cultures used for CPE and SgIII analysis. However, cellular content of BDNF in cultured whole cortices was very low (8.6 ± 2.7 pg per 5×10^6 cells). Therefore, although K^+-evoked secretion could be determined, basal secretion was under detectable levels. In order to achieve detectable basal levels, we prepared BDNF-enriched cultures by isolating hippocampal neurons (Chen et al., 2006). Intracellular BDNF in hippocampal neurons was around four-fold higher than in whole cortical cultures (38.8 ± 4.9 pg per 5×10^6 cells). No significant differences were found in intracellular BDNF levels in untreated and 5 μM Aβ treated cells for 16 h (control 0.61 vs. Aβ 0.53 pg BDNF/μg protein, $p = 0.6$). As shown in **Figure 7**, depolarization-stimulated secretion of BDNF in hippocampal neurons was greatly impaired by Aβ exposure (Aβ 439.6% vs. control 1055.0%, $p = 0.003$), whereas basal release levels were unchanged (94.8% of control, $p = 0.5$). Furthermore, immunoblot examination of CPE and SgIII secretion patterns in Aβ-treated hippocampal neurons offered similar results to those obtained in whole cortical cultures. Decrease in basal secretion was 44% for CPE ($p = 0.0002$), 23% for pSgIII ($p = 0.003$) and 53% for mSgIII ($p = 0.01$) in Aβ-treated hippocampal cultures, whereas K^+-depolarized release was impaired by a 64.7% ($p = 0.007$),

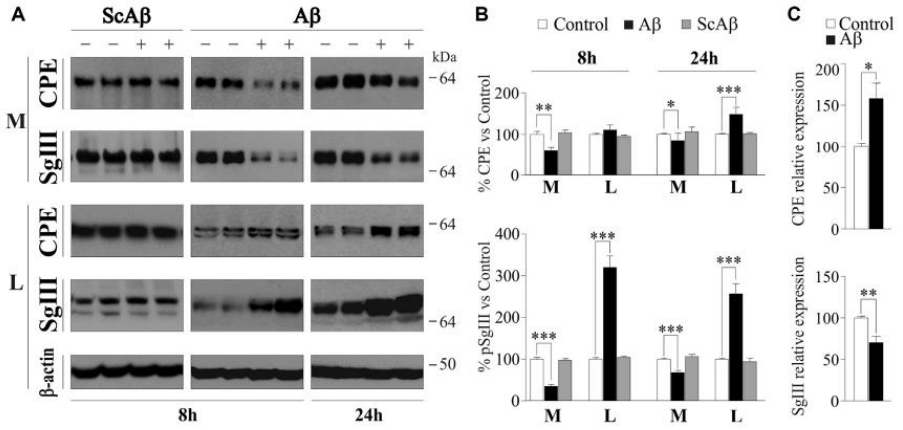

FIGURE 5 | Basal release and production of CPE and SgIII is altered in Aβ-treated cultured astrocytes. **(A)** Western blots showed basal release from cortical astrocytes treated with 5 μM Aβ during 8 or 24 h. A marked reduction in the extracellular levels (media, M) of SgIII and CPE compared with controls and an intracellular (lysates, L) accumulation is found in response to treatment with Aβ. No changes were found in response to ScAβ, either in the extracellular medium or the content. β-actin was used as loading control. **(B)** Graphical representation of the levels of CPE and SgIII compared with the vehicle-treated levels. Data are presented as the β-actin-normalized mean ± SEM. **(C)** mRNA quantification by Quantitative Real-Time PCR (qPCR) of CPE and SgIII of Aβ-treated cells (16 h) compared with the vehicle-treated levels. Values represent percent variation compared with controls and are presented as the mean ± SEM. $^*p < 0.05$; $^{**}p < 0.01$; $^{***}p < 0.001$, Mann-Whitney test.

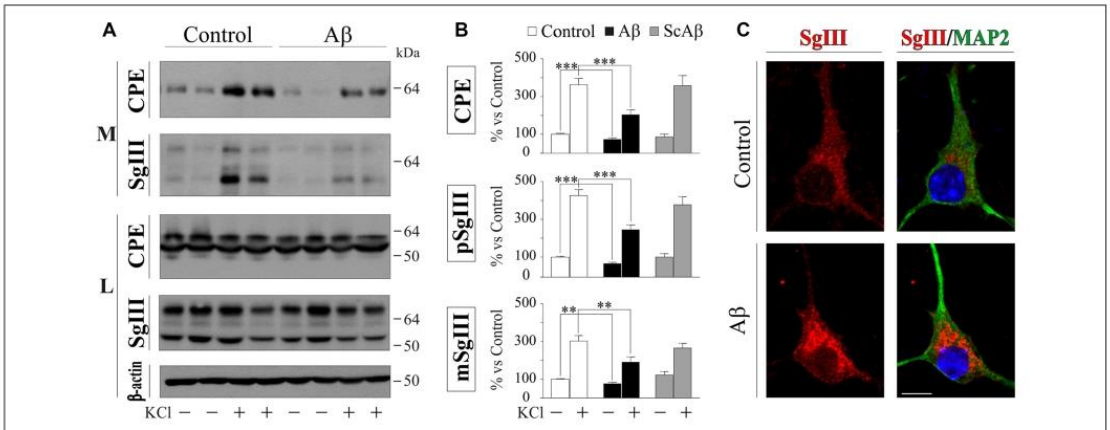

FIGURE 6 | Aβ impairs regulated secretion of CPE and SgIII in cultured cortical neurons. **(A)** Western Blot analysis shows a decrease in the release of CPE and SgIII both in basal and stimulated conditions in response to β-amyloid compared with vehicle-treated controls. Intracellular levels were unaffected by the treatment. β-actin was used as loading control. **(B)** Summary of Aβ and ScAβ effects on basal and evoked secretion of CPE, pSgIII and mSgIII. Data are presented as the β-actin-normalized mean ± SEM. $^{**}p < 0.01$; $^{***}p < 0.001$, Mann-Whitney test. **(C)** Confocal immunofluorescent images show an aberrant intracellular accumulation of SgIII in Aβ-treated neurons, mainly localized around the nucleus. Scale bar in μm: 10.

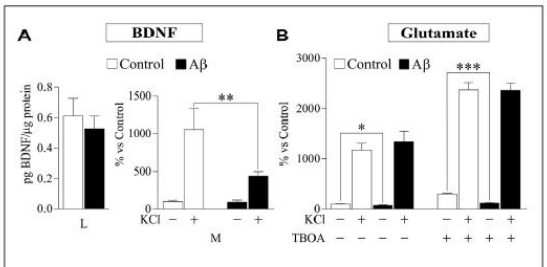

FIGURE 7 | Aβ effects on brain-derived neurotrophic factor (BDNF) and glutamate release in hippocampal cultured neurons. **(A)** Intracellular BDNF content (lysates, L) in neuronal cultures was no affected by 5 μM Aβ during 16 h, whereas K^+-stimulated release was decreased (media, M). **(B)** Extracellular glutamate levels were decreased in basal media of neurons treated with 5 μM Aβ during 16 h, whereas no changes were observed after KCl stimulation. Inhibiting glutamate re-uptake by TBOA shows that released neurotransmitter was unchanged during depolarization but decreased at basal conditions. Values were normalized by total proteins levels and represent percent variation compared with controls and are presented as the mean ± SEM. $^{*}p < 0.05$; $^{**}p < 0.01$; $^{***}p < 0.001$, Wilcoxon test.

50.9% ($p = 0.01$) and 43.4% ($p = 0.03$) for CPE, pSgIII and mSgIII, respectively.

Finally, to compare Aβ effects on neuronal DCV secretion with those on SV exocytosis, we determined glutamate release in hippocampal neurons exposed to 5 μM Aβ for 16 h by a fluorometric assay. Compared to unstimulated conditions, glutamate levels in the media were robustly increased during K^+-evoked depolarization (1176% over basal). Incubation of Aβ caused a significant decrease in extracellular glutamate levels at basal conditions (78.1% of control), whereas no changes were observed during stimulation (**Figure 7**). To ascertain the reliable contribution of secretion in extracellular glutamate levels, its re-uptake was blocked by addition of the excitatory amino acid transporter inhibitor TBOA (75 μM). In all TBOA-treated samples, extracellular glutamate concentrations were higher than in non-blocked conditions. Similar to the results obtained without the transporter inhibitor, in absence of glutamate re-uptake, Aβ reduces levels of glutamate released in unstimulated cells (41.4% of control) but does not influence secretion in KCl-depolarized neurons (**Figure 7**). Taken together, these results show that Aβ specifically impairs Ca^{2+}-regulated secretion of DCVs in neuronal populations.

Aβ Impairs DCV Secretion in Adult Neural Cells *In Situ*

To gain further insight into the impact of Aβ on regulated secretory pathway in neural cells, we next performed experiments on acute brain slices from adult mice. A major advantage of slice preparations is that cells *in situ* largely retain the states of differentiation, cytoarchitecture, extracellular matrix and synaptic circuits of the intact adult brain. First, we characterized CPE and SgIII secretion in horizontal adult brain slices under different conditions by western blot analysis (**Figure 8**). Low levels of both proteins were detected in unstimulated slices. However, CPE and SgIII release markedly increased after 10 min of a depolarizing stimulus (55 mM $[K^+]_0$). Cell integrity in the slice was confirmed by the lack of vesicular integral and cytosolic proteins, such as synaptophysin and actin, in the extracellular media. As occurred in cultured neurons (**Figure 3C**), KCl-evoked secretion of mSgIII form was stronger than for precursors (**Figure 8B**). To determine the involvement of Ca^{2+} in the evoked secretion of CPE and SgIII, we performed similar experiments in

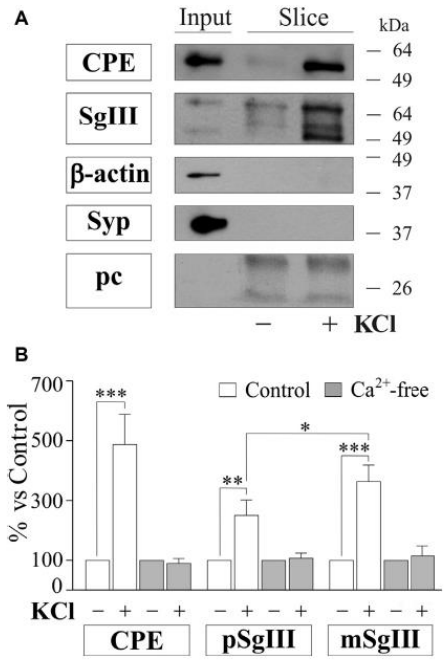

FIGURE 8 | Basal and depolarization-evoked release of CPE and SgIII from adult acute brain slices. **(A)** Representative immunoblots detecting different proteins in the perfused artificial CSF (ACSF) of the same slice after 15 min of basal (–) and 55 mM KCl (+) conditions. β-actin and synaptophysin (Syp) were used to confirm slice integrity and prestained proteins were added to ensure correct sample concentration (precipitation control, pc). Forebrain homogenates were used as input. **(B)** Histograms summarize variations of released CPE, pSgIII and mSgIII after KCl stimulation in normal (2mM $[Ca^{2+}]_o$) and nominally Ca^{2+}-free (0 mM $[Ca^{2+}]_o$, 2 mM EGTA) ACSF compared with basal conditions, showing mean ± SEM. $^*p < 0.05$; $^{**}p < 0.01$; $^{***}p < 0.001$, Mann-Whitney test.

a nominally Ca^{2+}-free ACSF. Lack of extracellular Ca^{2+} totally prevented the K^+-induced CPE and SgIII secretion (**Figure 8B**). These results show that *in situ* adult neural cells of the brain release CPE and SgIII in a depolarization- and Ca^{2+}-dependent manner.

To compare DCV secretion in the same cell populations between control and Aβ-treated brain slices, we split horizontal brain slices into left and right hemispheres (**Figure 9A**), minimizing the variability associated with cellular composition and responsiveness inherent to each slice. Each pair of hemispheres was incubated with vehicle (control) and 5 μM Aβ or 5 μM ScAβ for 8 h and basal and K^+-evoked secretion of CPE and SgIII were analyzed by immunoblotting and statistical analysis was performed using a Wilcoxon test (**Figures 9B,C**). Aβ notably reduced depolarization-evoked release of CPE (Aβ 334% vs. control 475.9%, $p = 0.0005$), pSgIII (Aβ 232.9% vs. control 348.3%, $p = 0.0068$) and mSgIII (Aβ 299.1% vs. control 456.2%, $p = 0.0015$). Moreover, basal secretion of CPE and mSgIII was also impaired by Aβ (88.0% and 89.1% of controls, respectively). No changes were observed in hemispheric slices incubated with ScAβ (**Figures 9B,C**).

In summary, these results evidence that Aβ impairs DCV secretion in cultured cortical cells and adult neural networks *in situ*.

DISCUSSION

The major finding of this study is that aberrant Aβ markedly impairs neuronal and astrocyte secretion of endogenously-produced DCV cargos *in vitro* and *in situ*. CPE and SgIII are two established DCV markers that belong to the regulated secretory pathway of neurons and endocrine cells with recognized roles in sorting, trafficking and processing of peptidic cargos and proposed new functions as intercellular transmitters (Bartolomucci et al., 2011; Cawley et al., 2012; Cheng et al., 2014). Here we show that neurons and astrocytes produce specific CPE and SgIII forms which are released in a cell type specific manner. CPE, SgIII and BDNF secretion, but not glutamate release, is dramatically impaired by Aβ in dispersed neurons and astrocytes in culture. Furthermore, similar detrimental effects of Aβ assemblies on basal and evoked release of DCV cargos are observed on treated acute brain slices.

Secretion of DCV Cargos in Neurons and Astrocytes

As well as their known expression by neurons, CPE and SgIII are also abundantly produced by astrocytes *in vitro* and *in vivo* (Paco et al., 2010). In agreement with a previous study performed in human brains (Plá et al., 2013), we found a segregate location of CPE and SgIII in DCV subsets in mouse neurons and astrocytes. Irrespective whether neurons were analyzed in cultures o *in situ*, a preferential somatodendritic location was observed for CPE, whereas SgIII was mainly associated with axons and terminal-like buttons. A non-overlapping vesicular location of these proteins was also found in cultured astrocytes. These observations lend support to the idea of differential routing and release of DCV cargos in the same secretory cell (Fisher et al., 1988; Zhang et al., 2011). Furthermore, the separate vesicular distribution of CPE and SgIII noticed here may imply differences in sorting mechanisms of neural cells compared with those described in endocrine cells (Hosaka et al., 2005; Cawley et al., 2016).

Although both CPE and SgIII are indeed expressed by neurons and astrocytes, we found important differences in the forms produced and their release dynamics comparing cultures of each cell type. First, probably due to the lack of the prototypical prohormone convertases of the regulated secretory pathway (PC1/3 and PC2; Winsky-Sommerer et al., 2000), astrocyte CPE and SgIII forms correspond to nonprocessed precursors. Additionally, a differential secretory profile was observed between neurons and astrocytes. Stimuli that evoked robust CPE and SgIII release in neurons barely provoked a response in astrocytes. In good agreement with a seminal work analyzing secreted CPE enzymatic activity from Fricker's lab

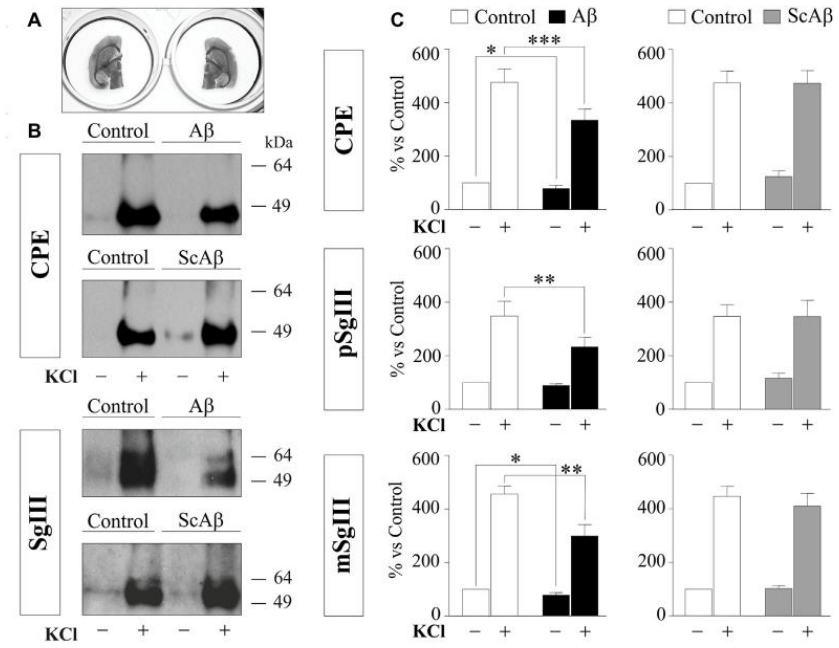

FIGURE 9 | Aβ impairs CPE and SgIII secretion in acute adult brain slices. **(A)** Left and right hemispheres of the same slice were incubated in parallel with vehicle and Aβ or vehicle and ScAβ for 8 h. **(B)** Immunoblots showing released CPE and SgIII from representative paired hemispheres after 15 min of basal (–) and 55 mM KCl (+) conditions. **(C)** Summary of Aβ and ScAβ effects on basal and evoked secretion of CPE, pSgIII and mSgIII. Values represent percent variation compared with basal release of controls (mean ± SEM). Statistical significance: $*p < 0.05$; $**p < 0.01$; $***p < 0.001$, Wilcoxon test.

(Vilijn et al., 1989), we observed no response of released CPE and SgIII to elevated $[KCl]_o$ from astrocytes. In addition, increasing $[Ca^{2+}]_i$ by ionophores caused variable and weak release responses in glial cells. Furthermore, we show that newly synthesized CPE and SgIII in non-stimulated astrocytes are poorly retained and rapidly released. Taken together, these observations would suggest that although bonafide CPE and SgIII are produced in astrocytes, they are not sorted and stored in typical DCVs. Based essentially on cell cultures, recent studies have proposed the occurrence of DCVs in astrocytes (Verkhratsky et al., 2016). However, several typical hallmarks of neuronal and endocrine DCVs (e.g., size, core density, long residence in cytoplasm, presence of synaptobrevin2, robust stimulus-dependent exocytosis) have hardly been demonstrated in cultured astrocytes (Crippa et al., 2006; Potokar et al., 2008; Paco et al., 2009). Because astrocytes *in vitro* display a partially immature phenotype and they do not accurately reproduce their *in vivo* attributes, DCV features in astroglial cells may be higher *in situ* than in culture. In fact, regulated gliosecretion of DCV components in cultured cells is enhanced under differentiating conditions, such as activation of the cAMP pathway and tone attenuation of the REST/NRSF transcription factor (Paco et al., 2009, 2016; Prada et al., 2011). On this basis, the typical size and dense core characteristics of neuroendocrine DCVs have been evidenced in granin-containing vesicles of human astrocytes *in vivo* (Hur et al., 2010).

Peptidergic Secretion as a New Target for Aβ

Aβ dramatically impairs neuronal and astrocyte secretion of DCV cargos *in vitro* and *in situ*. In unstimulated astrocyte cultures Aβ exposure dramatically reduced levels of CPE and SgIII released over 8–24 h. Conversely, intracellular amounts were increased without an apparent correlation with transcriptional mechanisms. Due to the poor cytoplasm retention observed for exocytic vesicles, CPE and SgIII secretion decrease and intracellular accumulation induced by Aβ in astrocytes probably reflects an impairment of the secretory pathway. In neuronal cultures, overnight incubation with Aβ did not provoke apparent changes in intracellular levels of the DCV cargos CPE, SgIII and BDNF, but did affect their basal and KCl-stimulated secretion. Interestingly, basal release of the SV transmitter glutamate was also impaired by Aβ, while its evoked discharge was largely preserved. Because Aβ incubations reduce spontaneous neuronal activity of recurrent networks

in primary cultures (Rönicke et al., 2011; Lee et al., 2013; Zurita et al., 2013), it is possible that the intrinsic activity-driven exocytosis of both SVs and DCVs decreases as Aβ lowers activation rates. In contrast to basal secretion, when release was forced by K^+-induced depolarization, Aβ selectively impairs secretion of cargos from DCVs but not from SVs. Although the cell type source of secreted cargos cannot be addressed in intact neuro-glial circuitries, alterations in CPE and SgIII release in treated acute slices from adult brains further substantiate the notion that Aβ impairs peptidergic secretion in cortical cells. The present conclusion is supported by previous studies showing secretion failures in exogenous (ANP.emd) and endogenous (cystatin C and thrombospondin 1) vesicular cargos in cultured astrocytes and neurons expressing presenilins carrying mutations linked to familial Alzheimer disease and incubated with Aβ (Ghidoni et al., 2007; Rama Rao et al., 2013; Stenovec et al., 2016).

Because Aβ can induce dysfunctions in different factors and stages involved in the secretory pathway, how amyloidogenic peptides affect neural vesicular secretion is uncertain. Aβ could alter peptidergic secretion influencing vesicular biogenesis, trafficking and exocytosis. It has been shown that soluble Aβ forms induce key changes which could compromise the integrity of the secretory pathway at early stages, such as endoplasmic reticulum stress, Golgi fragmentation and autophagy (Alberdi et al., 2013; Joshi et al., 2014; Son et al., 2015). Moreover, Aβ can also impair transport, docking and discharge of secretory vesicles. Recent evidence has shown that Aβ disrupts regulated exocytosis through its direct interaction with SNARE proteins (Russell et al., 2012; Yang et al., 2015). However, given that DCVs and SVs share the basic SNARE machinery for Ca^{2+}-evoked secretion (Gondré-Lewis et al., 2012), the Aβ-induced impairment in DCV cargo release from KCl-depolarized neurons and not for glutamate makes a major contribution of SNAREs unlikely. On the contrary, a failure of vesicular trafficking could underlie the secretion changes reported here. A large body of evidence indicates that defects in microtubule-mediated transport contribute to the initiation or progression of neurodegenerative diseases, including AD (Encalada and Goldstein, 2014; Llorens-Martín et al., 2014). Specifically, soluble Aβ species impair dendritic and axonal BDNF transport in cultured neurons (Decker et al., 2010; Gan and Silverman, 2015). Moreover, spontaneous and Ca^{2+}-dependent mobility of ANP.emd-containing vesicles was diminished in astrocytes expressing mutated presenilin 1 (Stenovec et al., 2016). Although a dysregulation of Ca^{2+} homeostasis and mitochondrial function could also participate in secretion failure (Ferreira et al., 2015; Viola and Klein, 2015; De Strooper and Karran, 2016), we propose that impaired trafficking exerts a central role in the Aβ-mediated secretion alterations showed in this study. Furthermore, the aberrant accumulation of granin family members and CPE detected in dystrophic neurites and neuronal and astrocyte somata in the cerebral cortex of AD patients and amyloid-forming transgenic mice strongly supports an Aβ-induced impairment of vesicular transport and secretion in the peptidergic transmission (Willis et al., 2011; Plá et al., 2013). Lastly, which Aβ species are affecting neural peptidergic secretion is an intricate issue. In our Aβ preparation we virtually detected aggregates under 200 kDa. However, the array of different forms and the complex equilibrium among them at physiological conditions over time make difficult to ascertain the specific identity of the Aβ assemblies involved in peptidergic secretion failure (Jan et al., 2011; Moreth et al., 2013; Yang et al., 2017).

Pathophysiologic Implication of Impaired Peptidergic Transmission in AD

Due to critical functions of CPE, SgIII and BDNF together with their wide distribution in the cerebral cortex, it is expected that the Aβ-induced release impairment showed here is involved in the AD pathophysiology. It has been shown that CPE and SgIII sort granins, proneuropeptides, prohormones and pro-BDNF to DCVs (Cool et al., 1997; Hosaka et al., 2005; Lou et al., 2005). Therefore, it is likely that proteins belonging to the regulated secretory pathway, at least those interacting with CPE and SgIII, are aberrantly co-secreted in the presence of Aβ. In addition, a dysregulated secretion could disturb the new extracellular functions attributed to CPE (alternatively named neurotrophic factor-alpha 1, NF-α1; Cheng et al., 2014). Moreover, the association of an uncovered CPE/NF-α1 gene mutation with AD comorbidity further connects CPE with this neurodegenerative disease (Cheng et al., 2016). Because BDNF has powerful and recognized effects on synaptic transmission, plasticity and neuronal survival and is strongly linked with AD, independently of transcriptional defects, the impact of an impaired release on neural network functions is anticipated (Adachi et al., 2014).

Beyond secretion failures for CPE, SgIII and BDNF and based on a common vesicular trafficking impairment, we suggest a more general effect of Aβ on both neuronal and astroglial peptidergic secretion. Because a rise in of soluble Aβ concentrations in early phases of AD is linked with synaptic dysfunction and network disorganization, it is conceivable that alteration of peptidergic transmission, which controls circuitry function and homeostasis, is involved in AD progression. It is worth noting that improving levels of DCV cargos (i.e., BDNF and somatostatin) partially recover AD-altered networks, preventing cognitive deficits and favoring Aβ clearance (Saito et al., 2005; Nagahara et al., 2009; Zhang et al., 2015). Moreover, the aberrant secretion and intracellular accumulation of CPE and SgIII observed in Aβ-treated and AD mouse and human brains (Plá et al., 2013) are in line with the low levels found in the CSF of AD patients by quantitative proteomics (Fagan and Perrin, 2012). Taking into account the importance of CSF biomarkers for clinical practice and trial design (Lleó et al., 2015), CSF changes based on peptidergic secretion failures could reflect synaptic dysfunction and serve as complementary diagnostic biomarkers of AD at early stages.

In summary, this study demonstrates that neuronal and astrocyte secretion of endogenous DCV proteins is impaired by Aβ *in vitro* and *in situ*. Additionally, Aβ-induced dysregulated peptidergic transmission could play an important role in the pathogenesis of AD and DCV cargos are possible candidates as CSF biomarkers.

AUTHOR CONTRIBUTIONS

VP planned and conducted all the experiments, data analysis and interpretation. NB contributed to performing some experiments and figure preparation. EP provided materials and contributed to data analysis. FA conceived, planned, interpreted and supervised the study and wrote the manuscript. All authors read and approved its final manuscript.

FUNDING

This work was supported (FA) by grants from Spanish Ministry of Economy and Competitiveness (BFU2013-48822-R and BFU2016-80868-R; MINECO/FEDER) and from Catalonian Government (2014SGR-01178). VP and NB are grateful to the Universitat de Barcelona (APIF) and Generalitat de Catalunya (FI) for their financial support, respectively.

ACKNOWLEDGMENTS

We are grateful to Dr I. Lindberg (University of Maryland) for PC2 antibody, Drs I. Ferrer, J.A. del Rio and J. Pérez-Clausell (Universitat de Barcelona), T. Fernández (Universidad Rey Juan Carlos) and A. Lleó and D Alcolea (Hospital de la Santa Creu i Sant Pau) for helpful discussions, V. Fagetti for technical assistance and H. Evans for editorial assistance.

REFERENCES

Abramov, E., Dolev, I., Fogel, H., Ciccotosto, G. D., Ruff, E., and Slutsky, I. (2009). Amyloid-β as a positive endogenous regulator of release probability at hippocampal synapses. *Nat. Neurosci.* 12, 1567–1576. doi: 10.1038/nn.2433

Adachi, N., Numakawa, T., Richards, M., Nakajima, S., and Kunugi, H. (2014). New insight in expression, transport and secretion of brain-derived neurotrophic factor: implications in brain-related diseases. *World J. Biol. Chem.* 5, 409–428. doi: 10.4331/wjbc.v5.i4.409

Aguado, F., Espinosa-Parrilla, J. F., Carmona, M. A., and Soriano, E. (2002). Neuronal activity regulates correlated network properties of spontaneous calcium transients in astrocytes in situ. *J. Neurosci.* 22, 9430–9444.

Alberdi, E., Wyssenbach, A., Alberdi, M., Sánchez-Gómez, M. V., Cavaliere, F., Rodríguez, J. J., et al. (2013). Ca^{2+}-dependent endoplasmic reticulum stress correlates with astrogliosis in oligomeric amyloid β-treated astrocytes and in a model of Alzheimer's disease. *Aging Cell* 12, 292–302. doi: 10.1111/acel.12054

Araque, A., Carmignoto, G., Haydon, P. G., Oliet, S. H. R., Robitaille, R., and Volterra, A. (2014). Gliotransmitters travel in time and space. *Neuron* 81, 728–739. doi: 10.1016/j.neuron.2014.02.007

Arias, C., Arrieta, I., and Tapia, R. (1995). β-Amyloid peptide fragment 25–35 potentiates the calcium-dependent release of excitatory amino acids from depolarized hippocampal slices. *J. Neurosci. Res.* 41, 561–566. doi: 10.1002/jnr.490410416

Bartolomucci, A., Possenti, R., Mahata, S. K., Fischer-Colbrie, R., Loh, Y. P., and Salton, S. R. J. (2011). The extended granin family: structure, function, and biomedical implications. *Endocr. Rev.* 32, 755–797. doi: 10.1210/er.2010-0027

Brito-Moreira, J., Paula-Lima, A. C., Bomfim, T. R., Oliveira, F. F., Sepúlveda, F. J., De Mello, F. G., et al. (2011). Aβ oligomers induce glutamate release from hippocampal neurons. *Curr. Alzheimer Res.* 8, 552–562. doi: 10.2174/156720511796391917

Cawley, N. X., Rathod, T., Young, S., Lou, H., Birch, N., and Loh, Y. P. (2016). Carboxypeptidase E and secretogranin III coordinately facilitate efficient sorting of proopiomelanocortin to the regulated secretory pathway in AtT20 cells. *Mol. Endocrinol.* 30, 37–47. doi: 10.1210/me.2015-1166

Cawley, N. X., Wetsel, W. C., Murthy, S. R. K., Park, J. J., Pacak, K., and Loh, Y. P. (2012). New roles of carboxypeptidase E in endocrine and neural function and cancer. *Endocr. Rev.* 33, 216–253. doi: 10.1210/er.2011-1039

Chen, Z.-Y., Jing, D., Bath, K. G., Ieraci, A., Khan, T., Siao, C.-J., et al. (2006). Genetic variant BDNF (Val66Met) polymorphism alters anxiety-related behavior. *Science* 314, 140–143. doi: 10.1126/science.1129663

Cheng, Y., Cawley, N. X., and Loh, Y. P. (2014). Carboxypeptidase E (NF-α1): a new trophic factor in neuroprotection. *Neurosci. Bull.* 30, 692–696. doi: 10.1007/s12264-013-1430-z

Cheng, Y., Cawley, N. X., Yanik, T., Murthy, S. R. K., Liu, C., Kasikci, F., et al. (2016). A human carboxypeptidase E/NF-α1 gene mutation in an Alzheimer's disease patient leads to dementia and depression in mice. *Transl. Psychiatry* 6:e973. doi: 10.1038/tp.2016.237

Cool, D. R., Normant, E., Shen, F., Chen, H. C., Pannell, L., Zhang, Y., et al. (1997). Carboxypeptidase E is a regulated secretory pathway sorting receptor: genetic obliteration leads to endocrine disorders in Cpe(fat) mice. *Cell* 88, 73–83. doi: 10.1016/s0092-8674(00)81860-7

Crippa, D., Schenk, U., Francolini, M., Rosa, P., Verderio, C., Zonta, M., et al. (2006). Synaptobrevin2-expressing vesicles in rat astrocytes: insights into molecular characterization, dynamics and exocytosis. *J. Physiol.* 570, 567–582. doi: 10.1113/jphysiol.2005.094052

Dahlgren, K. N., Manelli, A. M., Stine, W. B. Jr., Baker, L. K., Krafft, G. A., and LaDu, M. J. (2002). Oligomeric and fibrillar species of amyloid-β peptides differentially affect neuronal viability. *J. Biol. Chem.* 277, 32046–32053. doi: 10.1074/jbc.M201750200

Decker, H., Lo, K. Y., Unger, S. M., Ferreira, S. T., and Silverman, M. A. (2010). Amyloid-β peptide oligomers disrupt axonal transport through an NMDA receptor-dependent mechanism that is mediated by glycogen synthase kinase 3β in primary cultured hippocampal neurons. *J. Neurosci.* 30, 9166–9171. doi: 10.1523/JNEUROSCI.1074-10.2010

DeKosky, S. T., and Scheff, S. W. (1990). Synapse loss in frontal cortex biopsies in Alzheimer's disease: correlation with cognitive severity. *Ann. Neurol.* 27, 457–464. doi: 10.1002/ana.410270502

De Strooper, B., and Karran, E. (2016). The cellular phase of Alzheimer's disease. *Cell* 164, 603–615. doi: 10.1016/j.cell.2015.12.056

Encalada, S. E., and Goldstein, L. S. B. (2014). Biophysical challenges to axonal transport: motor-cargo deficiencies and neurodegeneration. *Annu. Rev. Biophys.* 43, 141–169. doi: 10.1146/annurev-biophys-051013-022746

Fagan, A. M., and Perrin, R. J. (2012). Upcoming candidate cerebrospinal fluid biomarkers of Alzheimer's disease. *Biomark. Med.* 6, 455–476. doi: 10.2217/bmm.12.42

Ferreira, S. T., Lourenco, M. V., Oliveira, M. M., and De Felice, F. G. (2015). Soluble amyloid-β oligomers as synaptotoxins leading to cognitive impairment in Alzheimer's disease. *Front. Cell. Neurosci.* 9:191. doi: 10.3389/fncel.2015.00191

Fisher, J. M., Sossin, W., Newcomb, R., and Scheller, R. H. (1988). Multiple neuropeptides derived from a common precursor are differentially packaged and transported. *Cell* 54, 813–822. doi: 10.1016/s0092-8674(88)91131-2

Gan, K. J., and Silverman, M. A. (2015). Dendritic and axonal mechanisms of Ca^{2+} elevation impair BDNF transport in Aβ oligomer-treated hippocampal neurons. *Mol. Biol. Cell* 26, 1058–1071. doi: 10.1091/mbc.e14-12-1612

Ghidoni, R., Benussi, L., Paterlini, A., Missale, C., Usardi, A., Rossi, R., et al. (2007). Presenilin 2 mutations alter cystatin C trafficking in mouse primary neurons. *Neurobiol. Aging* 28, 371–376. doi: 10.1016/j.neurobiolaging.2006.01.007

Gondré-Lewis, M. C., Park, J. J., and Loh, Y. P. (2012). Cellular mechanisms for the biogenesis and transport of synaptic and dense-core vesicles. *Int. Rev. Cell. Mol. Biol.* 299, 27–115. doi: 10.1016/B978-0-12-394310-1.00002-3

Hascup, K. N., and Hascup, E. R. (2016). Soluble amyloid-β42 stimulates glutamate release through activation of the α7 nicotinic acetylcholine receptor. *J. Alzheimers Dis.* 53, 337–347. doi: 10.3233/JAD-160041

Hosaka, M., Watanabe, T., Sakai, Y., Kato, T., and Takeuchi, T. (2005). Interaction between secretogranin III and carboxypeptidase E facilitates prohormone

sorting within secretory granules. *J. Cell Sci.* 118, 4785–4795. doi: 10.1242/jcs.02608

Hur, Y. S., Kim, K. D., Paek, S. H., and Yoo, S. H. (2010). Evidence for the existence of secretory granule (dense-core vesicle)-based inositol 1,4,5-trisphosphate-dependent Ca^{2+} signaling system in astrocytes. *PLoS One* 5:e11973. doi: 10.1371/journal.pone.0011973

Jan, A., Adolfsson, O., Allaman, I., Buccarello, A.-L., Magistretti, P. J., Pfeifer, A., et al. (2011). Aβ42 neurotoxicity is mediated by ongoing nucleated polymerization process rather than by discrete Aβ42 species. *J. Biol. Chem.* 286, 8585–8596. doi: 10.1074/jbc.M110.172411

Joshi, G., Chi, Y., Huang, Z., and Wang, Y. (2014). Aβ-induced Golgi fragmentation in Alzheimer's disease enhances Aβ production. *Proc. Natl. Acad. Sci. U S A* 111, E1230–E1239. doi: 10.1073/pnas.1320192111

Koss, D. J., Jones, G., Cranston, A., Gardner, H., Kanaan, N. M., and Platt, B. (2016). Soluble pre-fibrillar tau and β-amyloid species emerge in early human Alzheimer's disease and track disease progression and cognitive decline. *Acta Neuropathol.* 132, 875–895. doi: 10.1007/s00401-016-1632-3

Lee, S., Zemianek, J., and Shea, T. B. (2013). Rapid, reversible impairment of synaptic signaling in cultured cortical neurons by exogenously-applied amyloid-β. *J. Alzheimers Dis.* 35, 395–402. doi: 10.3233/JAD-122452

Lleó, A., Cavedo, E., Parnetti, L., Vanderstichele, H., Herukka, S. K., Andreasen, N., et al. (2015). Cerebrospinal fluid biomarkers in trials for Alzheimer and Parkinson diseases. *Nat. Rev. Neurol.* 11, 41–55. doi: 10.1038/nrneurol.2014.232

Llorens-Martín, M., Jurado, J., Hernández, F., and Avila, J. (2014). GSK-3β, a pivotal kinase in Alzheimer disease. *Front. Mol. Neurosci.* 7:46. doi: 10.3389/fnmol.2014.00046

Lou, H., Kim, S.-K., Zaitsev, E., Snell, C. R., Lu, B., and Loh, Y. P. (2005). Sorting and activity-dependent secretion of BDNF require interaction of a specific motif with the sorting receptor carboxypeptidase e. *Neuron* 45, 245–255. doi: 10.1016/j.neuron.2004.12.037

Lue, L. F., Kuo, Y. M., Roher, A. E., Brachova, L., Shen, Y., Sue, L., et al. (1999). Soluble amyloid-β peptide concentration as a predictor of synaptic change in Alzheimer's disease. *Am. J. Pathol.* 155, 853–862. doi: 10.1016/s0002-9440(10)65184-x

Moreth, J., Kroker, K. S., Schwanzar, D., Schnack, C., von Arnim, C. A. F., Hengerer, B., et al. (2013). Globular and protofibrillar aβ aggregates impair neurotransmission by different mechanisms. *Biochemistry* 52, 1466–1476. doi: 10.1021/bi3016444

Mucke, L., and Selkoe, D. J. (2012). Neurotoxicity of amyloid β-protein: synaptic and network dysfunction. *Cold Spring Harb. Perspect. Med.* 2:a006338. doi: 10.1101/cshperspect.a006338

Nagahara, A. H., Merrill, D. A., Coppola, G., Tsukada, S., Schroeder, B. E., Shaked, G. M., et al. (2009). Neuroprotective effects of brain-derived neurotrophic factor in rodent and primate models of Alzheimer's disease. *Nat. Med.* 15, 331–337. doi: 10.1038/nm.1912

Paco, S., Hummel, M., Plá, V., Sumoy, L., and Aguado, F. (2016). Cyclic AMP signaling restricts activation and promotes maturation and antioxidant defenses in astrocytes. *BMC Genomics* 17:304. doi: 10.1186/s12864-016-2623-4

Paco, S., Margelí, M. A., Olkkonen, V. M., Imai, A., Blasi, J., Fischer-Colbrie, R., et al. (2009). Regulation of exocytotic protein expression and Ca^{2+}-dependent peptide secretion in astrocytes. *J. Neurochem.* 110, 143–156. doi: 10.1111/j.1471-4159.2009.06116.x

Paco, S., Pozas, E., and Aguado, F. (2010). Secretogranin III is an astrocyte granin that is overexpressed in reactive glia. *Cereb. Cortex* 20, 1386–1397. doi: 10.1093/cercor/bhp202

Palop, J. J., and Mucke, L. (2016). Network abnormalities and interneuron dysfunction in Alzheimer disease. *Nat. Rev. Neurosci.* 17, 777–792. doi: 10.1038/nrn.2016.141

Parodi, J., Sepúlveda, F. J., Roa, J., Opazo, C., Inestrosa, N. C., and Aguayo, L. G. (2010). β-amyloid causes depletion of synaptic vesicles leading to neurotransmission failure. *J. Biol. Chem.* 285, 2506–2514. doi: 10.1074/jbc.M109.030023

Plá, V., Paco, S., Ghezali, G., Ciria, V., Pozas, E., Ferrer, I., et al. (2013). Secretory sorting receptors carboxypeptidase E and secretogranin III in amyloid β-associated neural degeneration in Alzheimer's disease. *Brain Pathol.* 23, 274–284. doi: 10.1111/j.1750-3639.2012.00644.x

Potokar, M., Stenovec, M., Kreft, M., Kreft, M. E., and Zorec, R. (2008). Stimulation inhibits the mobility of recycling peptidergic vesicles in astrocytes. *Glia* 56, 135–144. doi: 10.1002/glia.20597

Prada, I., Marchaland, J., Podini, P., Magrassi, L., D'Alessandro, R., Bezzi, P., et al. (2011). REST/NRSF governs the expression of dense-core vesicle gliosecretion in astrocytes. *J. Cell Biol.* 193, 537–549. doi: 10.1083/jcb.201010126

Rama Rao, K. V., Curtis, K. M., Johnstone, J. T., and Norenberg, M. D. (2013). Amyloid-β inhibits thrombospondin 1 release from cultured astrocytes: effects on synaptic protein expression. *J. Neuropathol. Exp. Neurol.* 72, 735–744. doi: 10.1097/NEN.0b013e31829bd082

Rönicke, R., Mikhaylova, M., Rönicke, S., Meinhardt, J., Schröder, U. H., Fändrich, M., et al. (2011). Early neuronal dysfunction by amyloid β oligomers depends on activation of NR2B-containing NMDA receptors. *Neurobiol. Aging* 32, 2219–2228. doi: 10.1016/j.neurobiolaging.2010.01.011

Russell, C. L., Semerdjieva, S., Empson, R. M., Austen, B. M., Beesley, P. W., and Alifragis, P. (2012). Amyloid-β acts as a regulator of neurotransmitter release disrupting the interaction between synaptophysin and VAMP2. *PLoS One* 7:e43201. doi: 10.1371/journal.pone.0043201

Saito, T., Iwata, N., Tsubuki, S., Takaki, Y., Takano, J., Huang, S.-M., et al. (2005). Somatostatin regulates brain amyloid-β peptide Aβ42 through modulation of proteolytic degradation. *Nat. Med.* 11, 434–439. doi: 10.1038/nm1206

Scheltens, P., Blennow, K., Breteler, M. M. B., de Strooper, B., Frisoni, G. B., Salloway, S., et al. (2016). Alzheimer's disease. *Lancet* 388, 505–517. doi: 10.1016/s0140-6736(15)01124-1

Selkoe, D. J., and Hardy, J. (2016). The amyloid hypothesis of Alzheimer's disease at 25 years. *EMBO Mol. Med.* 8, 595–608. doi: 10.15252/emmm.201606210

Son, S. M., Nam, D. W., Cha, M.-Y., Kim, K. H., Byun, J., Ryu, H., et al. (2015). Thrombospondin-1 prevents amyloid β-mediated synaptic pathology in Alzheimer's disease. *Neurobiol. Aging* 36, 3214–3227. doi: 10.1016/j.neurobiolaging.2015.09.005

Stenovec, M., Trkov, S., Lasič, E., Terzieva, S., Kreft, M., Rodríguez Arellano, J. J., et al. (2016). Expression of familial Alzheimer disease presenilin 1 gene attenuates vesicle traffic and reduces peptide secretion in cultured astrocytes devoid of pathologic tissue environment. *Glia* 64, 317–329. doi: 10.1002/glia.22931

Talantova, M., Sanz-Blasco, S., Zhang, X., Xia, P., Akhtar, M. W., Okamoto, S.-I., et al. (2013). Aβ induces astrocytic glutamate release, extrasynaptic NMDA receptor activation, and synaptic loss. *Proc. Natl. Acad. Sci. U S A* 110, E2518–E2527. doi: 10.1073/pnas.1306832110

van den Pol, A. N. (2012). Neuropeptide transmission in brain circuits. *Neuron* 76, 98–115. doi: 10.1016/j.neuron.2012.09.014

Verkhratsky, A., Matteoli, M., Parpura, V., Mothet, J.-P., and Zorec, R. (2016). Astrocytes as secretory cells of the central nervous system: idiosyncrasies of vesicular secretion. *EMBO J.* 35, 239–257. doi: 10.15252/embj.201592705

Vilijn, M. H., Das, B., Kessler, J. A., and Fricker, L. D. (1989). Cultured astrocytes and neurons synthesize and secrete carboxypeptidase E, a neuropeptide-processing enzyme. *J. Neurochem.* 53, 1487–1493. doi: 10.1111/j.1471-4159.1989.tb08542.x

Viola, K. L., and Klein, W. L. (2015). Amyloid β oligomers in Alzheimer's disease pathogenesis, treatment, and diagnosis. *Acta Neuropathol.* 129, 183–206. doi: 10.1007/s00401-015-1386-3

Willis, M., Leitner, I., Jellinger, K. A., and Marksteiner, J. (2011). Chromogranin peptides in brain diseases. *J. Neural Transm.* 118, 727–735. doi: 10.1007/s00702-011-0648-z

Winsky-Sommerer, R., Benjannet, S., Rovère, C., Barbero, P., Seidah, N. G., Epelbaum, J., et al. (2000). Regional and cellular localization of the neuroendocrine prohormone convertases PC1 and PC2 in the rat central nervous system. *J. Comp. Neurol.* 424, 439–460. doi: 10.1002/1096-9861(20000828)424:3<439::AID-CNE4>3.0.CO;2-1

Yang, Y., Kim, J., Kim, H. Y., Ryoo, N., Lee, S., Kim, Y., et al. (2015). Amyloid-β oligomers may impair SNARE-mediated exocytosis by direct binding to syntaxin 1a. *Cell Rep.* 12, 1244–1251. doi: 10.1016/j.celrep.2015.07.044

Yang, T., Li, S., Xu, H., Walsh, D. M., and Selkoe, D. J. (2017). Large soluble oligomers of amyloid β-protein from Alzheimer brain are far less neuroactive than the smaller oligomers to which they dissociate. *J. Neurosci.* 37, 152–163. doi: 10.1523/JNEUROSCI.1698-16.2016

Zhang, L., Fang, Y., Lian, Y., Chen, Y., Wu, T., Zheng, Y., et al. (2015). Brain-derived neurotrophic factor ameliorates learning deficits in a rat model of Alzheimer's disease induced by aβ1–42. *PLoS One* 10:e0122415. doi: 10.1371/journal.pone.0122415

Zhang, Z., Wu, Y., Wang, Z., Dunning, F. M., Rehfuss, J., Ramanan, D., et al. (2011). Release mode of large and small dense-core vesicles specified by different synaptotagmin isoforms in PC12 cells. *Mol. Biol. Cell* 22, 2324–2336. doi: 10.1091/mbc.E11-02-0159

Zurita, M. P., Muñoz, G., Sepúlveda, F. J., Gómez, P., Castillo, C., Burgos, C. F., et al. (2013). Ibuprofen inhibits the synaptic failure induced by the amyloid-β peptide in hippocampal neurons. *J. Alzheimers Dis.* 35, 463–473. doi: 10.3233/JAD-122314

Conflict of Interest Statement: The authors declare that the research was conducted in the absence of any commercial or financial relationships that could be construed as a potential conflict of interest.